A

MATHEMATICAL STUDY OF CONTROLLED RELEASE DRUG DELIVERY TO BIOLOGICAL TISSUES

KOYEL CHAKRAVARTY

DEPARTMENT OF MATHEMATICS

INDIAN INSTITUTE OF TECHNOLOGY GUWAHATI

GUWAHATI 781039, INDIA

JULY, 2018

A MATHEMATICAL STUDY OF CONTROLLED RELEASE DRUG DELIVERY TO BIOLOGICAL TISSUES

A thesis submitted

in partial fulfillment of the requirements

for the degree of

DOCTOR OF PHILOSOPHY

by

Koyel Chakravarty

(Roll No. 136123013)

DEPARTMENT OF MATHEMATICS

INDIAN INSTITUTE OF TECHNOLOGY GUWAHATI

GUWAHATI - 781039, INDIA

JULY, 2018

Dedication

To

my "Gosai"

Sadguru Shree Shree Bijoy Krishna Goswami,

the source of my strength and on His wings only have I soared.

To

the precious memory of my "Maa" (Dida)

Karunamoyee Chattopadhyay,

the reason of my existence, my storyteller, my first teacher, a gift from the Almighty.

To

my "Mummum"

Latika Chattopadhyay (Chakravarty)

&

my "Baba"

Santabrata Chakravarty,

who are my confidant problem solvers, my idols, my motivation, my sunshine and my best friends.

Declaration

I hereby declare that the work presented in the current dissertation entitled "***A Mathematical Study of Controlled Release Drug Delivery to Biological Tissues***" is entirely mine. Proper acknowledgement is provided in the text for the information derived from the published work of others and corresponding references are supplied in the bibliography. The copyright of the dissertation rests with the author. The present dissertation has not been previously submitted for another degree in any other institution.

July, 2018

Koyel Chakravarty

Department of Mathematics

Indian Institute of Technology Guwahati

Certificate

It is certified that the work contained in this thesis entitled "***A Mathematical Study of Controlled Release Drug Delivery to Biological Tissues***" by **Koyel Chakravarty,** a research scholar of Department of Mathematics, Indian Institute of Technology Guwahati, for the award of the degree of Doctor of Philosophy, has been carried out under my supervision and that this work has not been submitted elsewhere for a degree.

July, 2018

Dr. Durga Charan Dalal

Professor

Department of Mathematics

Indian Institute of Technology Guwahati

ACKNOWLEDGEMENTS

The path toward this dissertation has been circuitous. It is my pleasure to acknowledge the special people who challenged, supported and stuck with me along the way. I would like to express my sincere gratitude to my thesis supervisor, Prof. D. C. Dalal, for introducing me to a new way of looking at Biomathematics and for having a confidence in my ability to participate in it. Without his readings of my inchoate thoughts that were both careful and encouraging, I could not have found my way to this end. I take this opportunity to thank the Head, Department of Mathematics, IIT Guwahati for providing me the necessary facilities during my research work. I am indebted to the members of my doctoral committee, Prof. R. K. Sinha, Prof. S. N. Bora, and Dr. B. Deka for their generous time, advice, encouragement, support and for persevering with me through the completion of this work. I would also like to express my sincere thanks to all the faculty members of the Department of Mathematics for their help and cooperation. I also thank MHRD, Govt. of India, for offering me financial assistance to carry out my research work. I extend my thanks to Sridhar Da, Phatik Da and Saurav Da for their assistance in all official matters and also to our technical assistants Santanu Da, Pranpratim Da and Pranab Da for their help.

I would like to express my heartfelt thanks to Prof. P. K. Mandal, Visva-Bharati, Santiniketan, for motivating me to pursue my research and for helping me in all possible ways. I am grateful to Mr. Kaushik Roy and Mr. Sunil Sinha Roy, teachers of my school, for their blessings and encouragement. Whatever knowledge in English I have is because of them. Special thanks to my childhood drawing teacher, Mr. Chandan Samanta, whose brush strokes motivated me to draw artistic schematic diagrams of my mathematical problems. I would like to take this opportunity to thank all my teachers of East West Model School (Burdwan), M.U.C Women's College (Burdwan) and Indian School of Mines (IIT Dhanbad), whose names I could not mention since it will be a long list.

My years at the institute could not have been joyful and colourful without the group of my colleagues. I must thank Giri (Kaushik) Dada, Chitralekha Di, Gayatri Di, Debopam Da, Arnab Da, Abhishek Da, Sougata Da, Swapnendu Da, Aniruddha Da, Swarup Da, Ankur Da, Balasubramani, Biswajit, Devanand, Madhu, Tamal, Sonjoy, Ramesh, Papri, Popi, Nilay, Abhijit, Shantiram, Rakesh and Koushik

Kanti. My time in Subansiri Hostel was made enjoyable because of my hostel-mates – many thanks to Chitrita Di, Ramyani, Pratibha, Rima, Ishita Di, Ruma, Srijita, Sharmistha, Camelia and Swapna for having long-lasting chats at the dinner table. I cherish the time spent with all my friends in Guwahati whose names I have missed. Thank you all for the fond memories and for the feelings I'll always treasure.

I am deeply indebted to my parents for their affection, encouragement and everything in my life. I express my sincere and deepest sense of gratitude towards my extended family members for staying beside me all the time. I do thank my uncles and aunts—- Masimoni, Meso, Baro Meso, Kaka, Jethi, Baro Pisi, Pisemosai, Mejo Pisi, Chhoto Pisi, Baro Mama, Baro Mamima, Chhoto Mama, Chhoto Mamima. Heartfelt thanks are due to my cousins—— Barda, Boudimoni, Mejda, Sejda, Sejo Boudi, Chhorda, Chhoto Boudi, Phul Dada, Phul Bou, Chhotochhorda, Chhoto Bou, Bardi, Mejdi, Chhordi, Dustu Dada, Mona Didi, Jnui Didi, Sonai, Piya and Riku. Thanks are also tendered to my nephews and nieces—Prithviraj, Ujjayini, Yubaraj, Rishiraj, Praneel, Pranusha, Srijan and Raj. No words in English can ever be strong enough to express my gratitude to you for your unconditional love. I am highly grateful to those who have blessed me from Heaven—- my Dida (Karunamoyee Chattopadhyay), my Dadu (Nanigopal Chattopadhyay), my Thakurda (Sasadhar Chakravarty), my Thakuma (Malati Chakravarty), my Jethu (Debabrata Chakravarty) and my Baro Masi (Aparajita Bandopadhyay). Thank you for blessing me much more than I deserve.

At the very end, I express my deepest sense of gratitude to Gurudev Rabindranath Tagore for conveying the peace of the soul in harmony with nature during my solitary struggles, for teaching me the power of free thinking and the essence of happiness. I owe my gratitude to Swami Vivekananda for awaking me to chase my dreams and for uplifting my self confidence. I praise Shree Shree Bijoy Krishna Goswami, my Gosai, the merciful, for being the ultimate remedy to all my struggles and complications. I am blessed and thank you for everyday for everything that happens to me.

These words may not express my feelings properly,
But they carry the sound from the strings of my heart

!!!!!Thank you!!!!!

July, 2018

With regards,

(**Koyel Chakravarty**)
Department of Mathematics
Indian Institute of Technology Guwahati

ABSTRACT

Studies on controlled drug release and drug transport are important in the realm of pharmacokinetics for the development of medical treatment. Pharmacotherapy using medicines differs considerably from many other classical therapies involving surgery, radiation or other invasive methods. The appropriate use of pharmacotherapy through drugs / vaccines in the treatment largely helps the prevention and sometimes eradication of fatal diseases. The drug delivery system helps controlling the therapeutic effect of the drug as it can influence the pharmacokinetic profile of the drug, drug release rate, target regions, duration of drug action and consequently the toxicity including side effects as well. Controlled drug release involves drug encapsulating devices from which drug or therapeutic compounds may be released at controlled rates for prolonged span of time. Mathematical models and simulations appear to have their importance in the design of drug delivery systems for an effective drug release and drug bioavailability. Thus, the use of mathematical modelling, by and large, helps the conventional and novel drug delivery systems to be much more therapeutically efficient for improved patient compliance.

The present dissertation aims to begin with a comprehensive mathematical model for drug release from microparticles to the adjacent tissues. In the elucidation of drug release mechanisms, the role of mathematical modelling has been depicted thereby facilitating the development of new therapeutic drug by a systematic approach, rather than expensive experimental trial-and-error methods. In order to study the whole process, a two-phase mathematical model describing the dynamics of drug transport in two coupled media is presented. Drug release is described taking into consideration both solubilisation dynamics of drug crystallites and diffusion of the solubilised drug through the microparticle. In the coupled media, reversible dissociation / recystallization processes are considered. The proposed model has led to a system of partial differential equations that are solved analytically. The advocated model points out the influences of the diffusion, mass-transfer and reaction parameters, which are the main architects behind drug kinetics across two layers.

The second work provides an appropriate mathematical model for drug release from a porous polymeric matrix to biological tissues through endocytosis. Drug release phenomenon is described by taking into account both solubilisation dynamics of solid drug and diffusion of solubilised drug through porous

polymeric matrix unlike that of the previous model. In the tissue medium, reversible dissociation / association together with internalization processes of drug are involved. The present model is also solved analytically with the appropriate choice of the initial, boundary and interface conditions as well. In order to establish the potency of the model, the simulated results are compared with the existing experimental data. A quantitative analysis is carried out through numerical simulations in order to illustrate the behaviour of drug concentrations with time under various situations. The dependency of most of the model parameters on drug concentrations and drug masses is also put on record for the purpose of applicability of the drug release model under consideration.

The next work is concentrated on the formulation of mathematical model elucidating degradation of drug loaded polymeric matrix followed by drug release to the adjacent biological tissues. Polymeric degradation is modelled with mass conservation equations. Drug release phenomenon is mathematized by considering solubilisation dynamics of drug particles, diffusion of the solubilised drug through polymeric matrix along with reversible dissociation / recrystallization process. In the tissue phase, processes similar to those considered in previous model are taken into account. In order to reflect the validity of the advocated model, the simulated results are analogized with corresponding experimental data available in the literature. This model seems to foster the delicacy of the mantle enacted by important drug kinetic parameters, such as diffusion coefficients, mass transfer coefficients, particle binding and internalization parameters, which is illustrated through local sensitivity analysis.

Subsequently, the fourth study leads to another updated mathematical model illustrating the integrated kinetics of drug release in a polymeric matrix and its ensuing drug transport to the encompassing biological tissue. The model embodies drug diffusion, dissolution, solubilisation, polymer degradation and dissociation / recrystallisation phenomena in the polymeric matrix accompanied by diffusion, advection, reaction, internalization and specific / non-specific binding in the biological tissue. Unlike those of the previous models, the present updated model is solved numerically using suitable finite difference scheme. After spatial discretization, the system of nonlinear partial differential equations is reduced to a system of nonlinear ordinary differential equations, which is subsequently solved by the fourth order Runge-Kutta method. The model simulations deal with the comparison between a drug delivery from a biodegradable polymeric matrix and that from a biodurable one. Besides, simulated results are compared with corresponding existing experimental data to manifest the efficaciousness of the advocated model. A quantitative analysis is performed through numerical computation relied on model parameter values. The numerical results obtained reveal an estimate of the effects of biodegradable and biodurable polymeric matrices on drug release rates. Additionally, through graphical representations, the sensitized impact of the model parameters on the drug kinetics are illustrated so as to assess the model parameters of significance.

Furthermore, the fifth endeavour is to include liposomal drug delivery in order to wisely modulate the targeted drug delivery system. Temperature-sensitive liposomes function as a prospective weapon to combat toxic side effects corresponding to direct infusion of anticancer drugs. The main objective of the present study is to model liposomal drug release, subsequent drug transport in solid tumour along with integrated actions of tumour cell surface and endosomal events. Generalized mathematical model

for liposomal drug delivery is proposed through a series of physical phenomena, such as kinetics of liposome-encapsulated drug, free drug release from liposomes, transport of both liposomal drug and free drug into the tumour compartment, plasma clearance, protein-drug interactions, drug-tumour cell receptor interactions, internalization of drug through endocytosis along with corresponding endosomal events. The model is expressed through a system of coupled partial differential equations along with appropriate set of initial, interface and boundary conditions, which is solved numerically. Simulated results are compared with respective existing experimental data to demonstrate the potency and reliability of the proposed model. The proposed model and the simulated results act as a tool in designing a more effective drug delivery system for cancerous tumours.

Finally, the present dissertation ends with a concluding study of stability analysis for a mathematical model of drug release from polymeric matrix and consequent intracellular drug transport. Modelling of drug release is done through solubilisation dynamics of drug particles, diffusion of the solubilised drug through the polymeric matrix in addition to reversible dissociation / recrystallization process. The interaction between drug-receptor, drug-plasma proteins along with other intracellular endosomal events are modelled. These lead to a mixed system of partial and ordinary differential equations with associated pertinent set of initial and boundary conditions. Furthermore, besides the stability of the proposed model, several sub-models are also studied for their stability criteria. Prominence is provided to the reduced model system having requisite relevance to the original system, where Quasi Steady State Approximation (QSSA) theory is utilized. For the model to be potent enough to generate appropriate predictive results for drug delivery, the stability properties of equilibrium of the system are analysed both analytically and numerically. Numerical simulations in the embodiment of graphical representations speak about various vital characteristics of the underlying physical phenomena along with the importance and sensitized impact of the model parameters controlling significant biological functions. The underlying study confirms the necessity of stability analysis so that advocated mathematical model can effectively complement the real physiological behaviour of pharmacokinetics.

"Knowing does not mean simply intellectual assent, it means realisation."

Swami Vivekananda

CONTENTS

LIST OF FIGURES

LIST OF TABLES

1 INTRODUCTION

You can't cross the sea merely by standing and staring at the water.

Rabindranath Tagore

1.1 Motivation

Disease is a general term used to describe an irregular health condition that is not caused by direct impact of a physical injury. The causes of disease are many and diseases differ in individual susceptibility, severity, exposure, age and predisposing factors. The most vital feature of a disease is that the normal functionality of a living body is disordered. Proper medicinal and surgical treatment of the body's disorders is the basis of an advanced civilization. The objective of drug therapy is to correct the imbalances in body's system and subtly adjust the physiological challenges. The impressive advances in the physical, chemical, biological and mathematical sciences and parallel innovations in the field of engineering have led to novel ideas in modern drug discovery and development.

A drug is a substance that brings a physiological change for the betterment of health condition and has a reproducible effect on the body which can be measured. Drug delivery systems refer to the formulations or devices that introduce a therapeutic substance in the body according to its need for a specific time period and thus improves the efficacy of the therapeutic compound. There are several anatomical routes of drug administration, namely, oral, parenteral, transdermal, transmucosal, nasal, pulmonary or controlled release implants. While developing and formulating a drug delivery system, care must be given to the rate-controlling mechanism of drug release in order to get rid of toxicity and adverse side effects. Moreover, it is also important to have optimal bioavailability of the therapeutic compound in the diseased site over an appropriate time period. There is constant advancement in the drug delivery methods, which comprises reforming the conventional methods and innovating new devices to deliver optimal drug dose and affect the availability of drugs. Based on the technologies related to drug release and its bioavailability, a classification may be made as follows:

Drug formulations

Sustained release

Drug delivery system that is formulated and designed to deliver the therapeutic compound over an extended time period after a single dose administration in order to achieve a prolonged therapeutic effect is termed as sustained release drug delivery system. The sustained release preparations are also referred to as "long-acting" or "delayed-release" in comparison to "conventional" release preparations. The main objectives behind such formulation are to reduce the dosing frequency and to achieve steady state plasma level that is therapeutically effective and non-toxic for the extended duration of the action of the drug.

Controlled release

Controlled release drug delivery system is such a system which delivers drug at a pre-determined rate for a stipulated time period either locally or systemically. These systems are developed to improve the temporal and spatial availability of drug in the body, to preserve drug from physiological elimination and to enhance patient compliance. Furthermore, they are devised to assist drug in crossing the physiological barriers and to target drug at the desired diseased site while minimizing drug exposure elsewhere in the body, that is, the drug concentration must be within the therapeutic window. In order to achieve such diverse and complex objectives, several mechanisms may work simultaneously or at different stages of a delivery process.

Prodrugs

A prodrug is an active drug in its dormant and inert stage. These drugs transform to their therapeutically active stage *in vivo* due to some chemical or enzymatic reactions. Prodrugs should have enough opportunity to interact with the pharmacological receptors. The chemical or enzymatic reactions responsible for activating the drug must be operational only at the target site. Moreover, the enzymes should be in adequate supply in order to produce desired therapeutic effect and also the prodrugs must retain at the target site without diffusing into the systemic circulation.

Antibody-targeted systems

Immunoglobulins are used as macromolecules for delivering drug through macromolecular attachment, that is, through the attachment of drugs with immunoglobulins. The main advantages are that drugs can be targeted to the site of antibody specificity and the required drug amount is less along with reduced side effects. Drugs are linked to the antibodies through covalent or non-covalent bonds and sometimes drugs are placed in vesicles such as liposomes or microparticles so that these drug encapsulated liposomes or microparticles are targeted by the antibodies.

Gene therapy

It is the targeted transfer of a defined genetic material with the motive of disease prevention. Moreover, gene therapy is also purposed to modify a particular diseased state [65]. This is a very effective method of drug delivery. Cell-mediated gene therapy involves the transformation of genetically mutated cells which are injected into the target tissues. Sometimes, certain natural tumour-specific bacteria are treated as gene vectors for transporting the genetic products into the tumour environment through intravenous administration.

Drug delivery devices

Though the idea of drug delivery devices is not new, but recently, latest technologies are supplementing drug delivery devices to evolve into their advanced and effective embodiment. For implantation of these devices, surgical and injection procedures are required. The polymeric implants must be biocompatible for prevention of patient health hazards. The detailed discussion regarding polymeric drug delivery devices are given in the next section.

The study of drugs and their actions is named as pharmacology which is broadly divided into pharmacokinetics and pharmacodynamics. Pharmacokinetics deals with how the living body affects a drug whereas pharmacodynamics deals with how drug affects a living body. Since ages, most of the medicines available in market are taken orally. This administration route is effective if the drug is well absorbed providing minimum inconvenience to the patient. Therefore, pharmaceutical research has been focussed on the development of oral dosage forms so that the drug gets delivered efficiently to the systemic circulation in appropriate time. In order to concentrate on the physicochemical properties of drug, effect of formulation of drug delivery systems and the physiology of drug absorption, the study of biopharmaceutics comes to the fore. The main aim of this section of pharmacology is to bridge the gap between *in vivo* character of the pharmaceutical formulation and *in vitro* data collected in the laboratory. Though historically, drug administration through oral route has been the most used mode for both conventional and novel drug delivery, yet, there are certain serious limitations to it. The absorption rate and serum concentrations are unpredictable for various drugs orally taken in order to have the required effects in systemic circulation. The digestive enzymes of the gastrointestinal tract along with its high acid content often degrades some drugs before they reach their targeted site through bloodstream. Some drugs get inactivated by the liver in their transport pathway to the systemic circulation. Furthermore, certain target-specific drugs may not even reach their target sites. These constraints lead to the development of various drug delivery devices with sustained release and controlled release modes.

Whatever discussed till now regarding new innovative ways of drug delivery, have limited studies due to heavy dependency on trial-and-error experiments. Even for *in vitro* study of drug release, an in-depth understanding of the inherent governing mechanisms controlling the drug release is necessitated. The situation is more complex for localised targeted drug delivery due to various interactions between drug and physiological environment of the diseased site. In order to understand and evaluate the efficiency

of these novel drug delivery methods, information about drug release and intracellular drug uptake are significant but difficult to acquire. Mathematical models and simulations come to facilitate in this situation. These are the only possible approaches through which such information may be gathered and thus smoothens the process of drug delivery. Mathematical modelling plays a significant role in the design of a drug delivery system. It helps in assessing the key parameters controlling the drug release phenomenon. Furthermore, it supports to help out the researchers doing experiment in pharmaceutical industries in the formulation and design of drug delivery systems to have an effective drug release and drug bioavailability. The befitting use of mathematical models in the field of medical and pharmaceutical science can reduce the frequency of trial-and-error experiments needed to have an optimal drug delivery technique, thereby saving time and money. It is high time to develop and upgrade the mathematical models so that much more biological complexities can be dealt with. Since the mathematical aspect of pharmaceutical science is not utterly focussed in the past, there is an inordinate scope for the researchers in mathematical biology to bridge the gap between experimental findings and the theoretical standpoint. Therefore, mathematical modelling by and large helps the conventional and novel drug delivery systems to be much more therapeutically efficient and thus improving patient compliance in the long run. The predictive characteristics of mathematical models are too potent to be ignored.

1.2 Background concepts

This section provides an overview of the drug delivery systems, underlying phenomena of drug release and subsequent drug transport to the biological tissues. In the following section, different types of drug delivery systems are discussed, with special emphasis laid on those considered in the current dissertation.

1.2.1 Polymeric drug delivery systems

In the construction of controlled release drug delivery systems, polymeric materials are the obvious choice to make use of due to their highly developed technology. Moreover, desired polymers with required properties can be synthesized in chemical laboratories. Appropriate choice of polymers is responsible for the release rate, pattern and the time duration of drug release, according to the requirements of a particular drug. There are two types of polymer systems, namely, matrix systems and reservoir systems. Drug is uniformly distributed in the matrix systems whereas in case of reservoir systems, a drug core is embedded within a polymeric coating. Drug is released from polymeric matrix through drug diffusion or due to combined effect of drug diffusion and polymeric erosion. Actually, the drug delivery matrices are coated with specific polymers. These polymeric matrices are employed for local drug delivery.

In controlled release drug delivery systems, polymeric matrices may be either biodurable or biodegradable. Biodurable polymers are non-erodible and stay intact leading to the permanent presence of the polymeric coatings in biological tissues. Hence, the drug diffusivity in the biodurable polymeric matrix remains unchanged at the initial polymeric drug diffusivity. Biodurable polymers are generally used

in drug delivery systems where prolonged medication is necessary and these systems can be removed after the drug release . The main application of such drug delivery system lies in transdermal drug delivery systems in the form of transdermal patches and others. Biodegradable polymers are designed to dissolve slowly in the physiological system itself after a stipulated time without surgical removal or retrieval of the implant. These systems are observed to be able to release drug at a controlled and uniform rate. Some examples of biodegradable polymers used in biomedical devices are polylactic-co-glycolic acid (PLGA), polyanhydrides, poly (orthoesters) and polyphosphazenes. Biodegradable polymers are synthesized in such a way that no undesirable and harmful tissue responses are induced and the degradation by-products are non-toxic and biocompatible.

1.2.2 Particulate drug delivery systems

The idea of particulate drug delivery systems lies behind using particles as the carriers of drug to the targeted disease sites evolved from their use as radiodiagnostic agents to investigate the reticuloendothelial system. It has been proposed that particles of size $20-300\ \mu m$ can be used for drug targeting. Since these particles are smaller in size, they are injected into the systemic circulation or diseased compartment of the body. These particles are the carriers of drug where the drug may be dispersed as an emulsion or it may be encapsulated within the carrier material. The examples of particulate drug carrier systems are microparticles or microspheres, nanoparticles, liposomes, cellular particles such as resealed erythrocytes, leukocytes and platelets along with glass-like sugar matrices. Some of them are taken into account in the present thesis and elaborated as follows:

Microparticles

The drug is embedded in the microparticle matrix. Due to the potential for the microparticles to spend an extended time in the body relative to that for naked drug, good biocompatibility and biodegradability of the microparticles particularly those with polymeric coating such as polylactic acid (PLA), polyglycolic acid (PGA) and polylactic-co-glycolic acid (PLGA), they are reliably used in recent years as potential drug delivery devices. Since these are long circulating particles, they have the ability to circulate for a prolonged duration of time in the vicinity of the organ at which they are targeted either by injecting or through some other targeting mechanisms.

Liposomes

Liposomes, the injectable particulate drug delivery systems, are vesicles of phospholipid molecules enclosing an aqueous interior, specially formed as carriers of drugs and other substances, into biological tissues. The lipid bilayers of liposomes are comparable to the living cell membranes' lipid bilayer. Moreover the process of drug transport adopted by liposomes is also similar to that of cell membranes. The therapeutic properties of liposomes depend on the composition of lipid bilayer along with its fluidity and permeability. The present trend is to categorize liposomes into a class of pharmaceutical devices in the nanoscale range contrived by chemical and physical approaches, thus referring as nanomedicines. Liposomes are the first generation nanomedicines accepted for cancer treatment.

Liposomal encapsulation of anticancer drugs has overshadowed the conventional free drug delivery systems by diminishing cytotoxicity and also by targeting tumour sites due to enhanced permeability and retention (EPR) effect.

1.2.3 Drug release mechanisms

The term "release" is a collective term used to describe the underlying governing phenomena helping to transfer drug from the drug delivery system to the specific sites such as gastrointestinal fluids, systemic plasma or diseased biological tissues. Various mathematical models are developed to illustrate drug release from controlled release dosage forms. The controlled release drug delivery systems are of three types depending on the drug release mechanisms, namely, diffusion-controlled, chemically-controlled and swelling-controlled drug delivery systems. Till now, diffusion is considered as the most vital release mechanism compared to both chemically-controlled and swelling-controlled drug delivery systems and occurs at varying rates. The mathematical modelling of drug release primarily depends on Fick's laws, the details of which are provided in the next chapter.

As the drug encapsulated in the polymeric matrix is mainly present in solid state, it is immobile to diffuse out of the matrix. Hence, it is transformed into free state. Dissolution is the main process behind the transformation of solid drug into its free form. The initial step in drug dissolution is the reaction of the solid drug with the body fluids. Dissolution kinetics is dependent on three factors, namely the flow rate of dissolution medium, reaction at the solid-liquid interface and the diffusion of the dissolved drug particles away from the interface. These factors vary according to drug properties and surrounding physiological environment. It is possible to imagine how complicated the study of drug dissolution is when one compares the *in vivo-in vitro* conditions due to limited knowledge of the *in-vivo* hydrodynamical condition.

1.2.4 Drug transport mechanisms

The released drug enters into the biological tissue directly or through systemic circulation or through gastrointestinal tract. It is also important to observe the route of drug into the intracellular domain. Targeting drug particles to individual intracellular compartment has developed in advantages to therapies associated with the suborganalles. Endocytosis, a phenomenon common to all cells in the body, internalizes macromolecules, drug particles proteins etc. and perpetuates them in transport vesicles which gets transported along the endolysosomal scaffold. Pharmaceutical scientists have manifested a huge interest in the process. The endocytosis pathway is studied [79] and explained how ligands interact with cytomembrane, enter cells and move in different pathways. There are many unexplored portions about endocytosis which are still to be investigated and understood properly, so it is inevitable to study further and the new discoveries may be bestowed on the emerging local drug delivery systems. For endocytosis to take place, cell surface receptors interact with free drug particles to form complexes, that is bound drug. These receptor-drug complexes can activate various intracellular reactions leading to several events such as internalization, recycling, lysosomal degradation and synthesis which are collectively known as trafficking.

1.3 Current status and objectives of drug delivery

During the past decade, considerable success has been achieved in drug delivery systems. Some common medicines are now available in extended release, controlled release and once-a-day dosage forms. Gene therapy and protein therapeutics have experienced considerable advances. Innovative and advanced drug delivery technologies have improved cancer treatment a great deal. In the coming decade, the use of new drug delivery systems will depend on the interdisciplinary collaborative work among material scientists, biologists, chemists, physicists, biotechnological engineers, pharmaceutical scientists and mathematicians. Nanotechnology and microelectronics are currently the great revolutionaries of drug delivery. The current scenario is that though there is noteworthy advancement in the field of pharmaceutical and medical science, yet the pharmaceutical industry is facing some serious problems enlisted below.

- The pharmaceutical industries need to have up-to-date drug delivery technologies, so that their products can be redesigned from time to time in order to keep pace with the developing new drug design methods and new biotechnology products.
- A simultaneous research must be carried out to make the drugs cost effective. As the drug cost is getting higher and higher day by day, improving bioavailability of drugs will reduce the cost of drugs due to minimum drug intake.
- Till date it is difficult to medicate certain vital parts of the living body crossing some physiological barriers such as blood-brain barrier. Fundamental research needs to be carried out to characterize and modulate such barriers so that drug particles can easily pass through them.
- Consistently new therapeutic compounds are being discovered and launched in medical world, such as various types of nanoparticles. These products must undergo thorough safety studies and should have regulatory approval.
- Most of the experiments carried out in different laboratories are not implemented in practical application due to various reasons. Hence, more advanced and effective mathematical models along with computer simulations need to be set up to reduce the number of unnecessary experiments thereby making the whole process cost effective and resource effective.

Whatever is discussed above depicts an apparent sketch illustrating the current status of the domain of pharmaceutical sciences. Mathematicians have a lot to contribute in this field to have a better and healthy world, provided they gain updated knowledge of biology, physiology and pharmacology. The interdisciplinary research only can lead to the most advanced and effective drug delivery systems.

1.4 Research objectives

The present dissertation work is intended to develop mathematical modelling of pharmacokinetics, focussing mainly on controlled drug release from a local drug delivery and subsequent drug transport

into the biological tissues. Development of the model requires understanding of drug release kinetics and underlying physiological phenomena governing the drug transport. Any approach used in the present work may be of application in other parts of the human body provided the system does not have major clinical complexity. The outcomes of the models under study will certainly be of some assistance for evolution of future models through the introduction of more biological complexities and different modes of drug administration depending on the objectives of the drug release phenomena adhere to the real situation.

Here, the following six research objectives with pertinent improvement at every stages of the dissertation are illustrated and discussed in details.

- ✓ **Objective 1:**
  To mathematically model drug release from microparticles with combined effects of solubilisation and recrystallization.
  This study aims to provide a comprehensive mathematical model of drug release from microparticles to the adjacent tissues. In the elucidation of drug release mechanisms, the role of mathematical modelling has been proposed thereby facilitating the development of new therapeutic drug by a systematic approach, rather than expensive experimental trial-and-error methods. In order to study the whole process, a two-phase mathematical model describing the dynamics of drug transport in two coupled media is proposed. Drug release may be described by taking into consideration both solubilisation dynamics of drug crystallites and diffusion of the solubilised drug through the microparticles. In the coupled media, reversible dissociation / recrystallization processes take place. The model seems to point out the important roles played by the diffusion, mass-transfer and reaction parameters, which are the main architects behind drug kinetics across two layers.

- ✓ **Objective 2:**
  To mathematically model drug release from polymeric matrix and subsequent drug transport to the biological tissue through endocytosis.
  The purpose of the current study is to frame primarily an appropriate mathematical model for drug release from a porous polymeric matrix to biological tissues through endocytosis. Drug release phenomenon needs to be described by taking into account both solubilisation dynamics of solid drug and diffusion of solubilised drug through porous polymeric matrix. In the tissue medium, reversible dissociation / association together with internalization processes of drug are also involved. In order to establish the potency of the proposed model, the simulated results are to be compared with corresponding experimental data to look for any remarkable agreement so as to validate the applicability of the model considered. A quantitative analysis is also planned to be carried out through numerical simulations in order to understand the temporal behaviour of drug concentrations under various situations.

- ✓ **Objective 3:**
  To mathematically model drug release kinetics from a degradable polymeric matrix and to carry

out local sensitivity analysis.

The work undertaken is to concentrate on the formulation of mathematical model elucidating degradation of drug-loaded polymeric matrix followed by drug release to the adjacent biological tissues. Drug release phenomenon is to put forward by considering solubilisation dynamics of drug particles, effective diffusion of the solubilised drug through polymeric matrix along with reversible dissociation / recrystallization process. In the tissue phase, reversible dissociation / association along with internalization processes of drug are to be taken into account. This model is likely to propound the sensitivity of important drug kinetic parameters, such as diffusion coefficients, mass transfer coefficients, particle binding and internalization parameters, which may be illustrated through local sensitivity analysis.

✓ **Objective 4:**

To have a nonlinear mathematical model of drug delivery from polymeric matrix incorporating more biological complexities.

The objective of the present study is to mathematically model the integrated kinetics of drug release in a polymeric matrix and its ensuing drug transport to the encompassing biological tissue. The model embodies drug diffusion, dissolution, solubilisation, polymer degradation and dissociation / recrystallisation phenomena in the polymeric matrix accompanied by diffusion, advection, reaction, internalization and specific / non-specific binding in the biological tissue. The model simulations should deal with the comparison between a drug delivery from a biodegradable polymeric matrix and that from a biodurable polymeric matrix. Furthermore, simulated results are to be examined and compared with corresponding existing experimental data to manifest the efficaciousness of the advocated model. A quantitative analysis is also in mind to be performed through numerical computation relied on model parameter values. The numerical results obtained are expected to reveal an estimate of the effects of biodegradable and biodurable polymeric matrices on drug release rates. Furthermore, through graphical representations, the sensitized impact of the model parameters on the drug kinetics are to be illustrated so as to assess the model parameters of significance.

✓ **Objective 5:**

To mathematically model the liposomal drug release to tumour.

The main objective of this study is to model liposomal drug release, subsequent drug transport in solid tumour along with integrated actions of tumour cell surface and endosomal events. Generalized mathematical model for liposomal drug delivery is proposed in which vital physical phenomena, such as kinetics of liposome-encapsulated drug, free drug release from liposomes, transport of both liposomal drug and free drug into the tumour compartment, plasma clearance, protein-drug interactions, drug-tumour cell receptor interactions, internalization of drug through endocytosis along with corresponding endosomal events are taken into account. Simulated results are to be examined and compared with respective existing experimental data to demonstrate the potency and reliability of the proposed model. Graphical representations of time variant con-

centration profiles are to be illustrated to understand the underlying phenomena in details. Moreover, the model should speak for the sensitized impact of important drug kinetic parameters, such as advection coefficients, drug release coefficient, plasma clearance rate and internalization parameters through graphical portrayals. The proposed model and the simulated results should act as a tool in designing a more effective drug delivery system for cancerous tumours.

✓ **Objective 6:**

To study stability analysis of drug dynamics model.

Here, a mathematical model of drug release from polymeric matrix and consequent intracellular drug transport is proposed and needs to be analysed. Modelling of drug release is done through solubilisation dynamics of drug particles, diffusion of the solubilised drug through the polymeric matrix in addition to reversible dissociation / recrystallization process. The interaction between drug-receptor, drug-plasma proteins along with other intracellular endosomal events are to be modelled. Furthermore, besides the stability of the proposed model, several sub-models are also proposed to study for their stability criteria. Prominence may be provided to the reduced model system having requisite relevance to the original system where Quasi Steady State Approximation (QSSA) theory is utilized. For the model to be potent enough to generate appropriate predictive results for drug delivery, the stability properties of equilibrium in the mathematical model are to be analysed both analytically and numerically. Numerical simulation in the embodiment of graphical representations should speak about various vital characteristics of the underlying physical phenomena along with the importance and sensitized impact of the model parameters controlling significant biological functions.

1.5 Thesis structure

The dissertation is organised as follows.

- In Chapter 2, a brief literature review of pharmocokinetics study and its corresponding modelling efforts are provided.
- In Chapter 3, the model framework of drug release from microparticles and subsequent drug transport to biological tissue (Objective 1) is developed and analysed.
- In Chapter 4, the model framework of drug release from polymeric matrix and subsequent drug transport to biological tissue through the endocytosis phenomenon (Objective 2) is developed and studied.
- In Chapter 5, the more advanced model framework of drug release from degradable polymeric matrix and subsequent drug transport to biological tissue is developed and studied. Furthermore, local sensitivity of the vital parameters is studied (Objective 3).
- In Chapter 6, a nonlinear mathematical model of drug release from polymeric matrix to biological tissue is advocated and studied where more physiological complexities are taken into consideration (Objective 4).

- In Chapter 7, the model framework of liposomal drug delivery (Objective 5) is developed and analysed.
- In Chapter 8, stability analysis of drug dynamics model (Objective 6) is carried out analytically as well as numerically.
- In Chapter 9, overall conclusions for the complete dissertation work are discussed. Moreover, a comprehensive schematic diagram connecting all the mathematical models portrayed in the thesis is presented.
- In the present dissertation, both dimensional and non-dimensional parameter values are provided wherever necessary, for the sake of clarity.
- Towards the end of the dissertation, glossary, nomenclature and index are provided for readers' ease.

2 LITERATURE REVIEW

Everything changes and nothing stands still

Heraclitus of Ephesus

In this chapter, a comprehensive review of the literature on topics related to drug release from local drug delivery device and consequent drug transport to the biological tissues is discussed. The key processes in pharmacokinetics are dealt with separately in the form of review of previous studies. The entire clinical, experimental and mathematical modelling aspects are covered in the literature survey with special emphasis on modelling efforts. The discussion of governing processes involved in the pathway drug transport serves as an introduction to the realm of pharmacokinetics.

2.1 Drug release phenomenon

Drug release has been the most vital process in the field of drug delivery for decades. In order to maximize bioefficacy, both naturally derived and synthetic macromolecules are used extensively in controlled drug release. This also facilitates clinical applicability and improve patient compliance. 'Drug release' is the phenomenon through which drug particles migrate from the initial position in the polymeric matrix to the outer boundary of the matrix and then to the release medium [78]. The physicochemical properties of the drug particles, the structural characteristics of the matrix, the release domain, and various types of interactions in between these factors are collectively responsible for drug release. The evolution of a new therapeutically efficient drug is based on experimental research in pharmaceutical companies to obtain a particular drug release profile.

2.1.1 Polymeric matrix and its degradation

The governing phenomena dealing with drug transport through controlled drug release include diffusion, swelling, dissolution and erosion. In order to accomplish such assignment, pharmacists had

incepted the utilization of nonbiodegradable polymers [112] as drug carriers which were generally represented as polymeric matrices. These are widely used in the pectoral dosage forms, for implantation purpose and in transdermal films. Some examples of such polymers are polyurethanes, silicone rubber, poly(ethylene vinyl acetate) (PEVA). These are mainly utilized for long-term use as in case of orthopedic and dental implants. They are characterized with water repellent surfaces to avoid degradation or erosion process [74]. Nowadays, pharmacists are utilizing both non-biodegradable and biodegradable polymers together. Biodegradable polymers are generally responsible for the progress of controlled release drug delivery systems leading to improved patient compliance and curtailment of toxic side effects through extended dosing and targeting [81]. Food and Drug Administration (FDA) have approved various biodegradable delivery systems based pharmaceutical products which include hormones, antitumour drugs and antibiotics [33]. Biodegradable polymers contain labile bonds of ester, amide and anhydride bonds that usually undergo hydrolytic or enzymatic degradation. Modes of degradation are two-fold, namely, surface degradation and bulk degradation. As the name suggests, surface degradation refers to the confined degradation of the outer surface of the device [57]. Homogeneous degradation throughout the material is referred as bulk degradation [105]. Due to the importance of water during hydrolysis, water intrusion into the drug delivery device is noteworthy in view of studying degradation and drug release kinetics. Semicrystalline polymers degrade in two stages, firstly, water is infused into amorphous regions to have random hydrolytic scission of ester bonds. Second stage starts when already major portion of the amorphous region is degraded [73]. The outcome of degradation in the form of polymer chain scission leads to average molecular mass change of the polymer which quantifies degradation process over time. In order to demonstrate degradation kinetics, the following two equations are widely used.

$$\text{Zero-order: } M_{r(t)} = M_{r0}\, k_{deg}\, t, \tag{2.1.1}$$

$$\text{Pseudo-first order: } M_{r(t)} = M_{r0}\, exp\, (-k_{deg}\, t), \tag{2.1.2}$$

where the average polymer molecular mass at time t and time zero are represented by M_{rt} and M_{r0} respectively. k_{deg} depicts the polymer degradation rate constant. The second equation was applied to denote the degradation process in poly(lactide-co-glycolide) (PLGA), microparticles [20, 76]. Siepmann and Göpferich defined polymer degradation as the chain scission process such that polymer chains are broken to form oligomers and monomers, whereas loss of material from bulk erosion or surface erosion after coming in contact with a biological system was termed as bioerosion [129].

Polyester represents a class of polymers having ester linkages in their backbone, such as poly(lactic acid) (PLA), poly(glycolic acid) (PGA), poly(lactide-co-glycolide) (PLGA), to name a few. PLGA is widely used as biodegradable polymer in developing particulate drug delivery systems [134] which is synthesized by ring-opening copolymerization of two different monomers, the cyclic dimers (1,4-dioxane-2,5-diones) of glycolic acid and lactic acid [4]. The degradation of PLGA is initiated through hydrolysis of its ester linkages in the presence of water. Since PLGA is hydrophobic, PLGA nano / microparticles with core-shell structures are synthesized through several emulsification processes.

The hydrophilic drugs may be embedded in the hydrophilic core of the nano / microparticles [71]. On the other hand, hydrophobic drugs are encapsulated in their hydrophobic shell [122]. Polyanhydrides represent the class of surface erosion-based biodegradable polymers. A study of drug release conducted on a polyanhydride (poly (fatty acid dimer-sebacic acid), p (FAD-SA), 50:50 w / w)-based implant for local drug delivery claimed that the release kinetics was dependent on the drug solubility and the intrinsic dissolution rate [104]. Manoharan and Singh [94] probed the study of poly-1,3-bis-(p-carboxyphenoxy)propane-co-sebacic acid (p (CPP : SA)) microspheres for controlled release drug delivery of basal insulin. Insulin was released within a timespan of three days from microspheres composed of SA (sebacic acid) only. On the other hand, a meagre amount of insulin was released from microspheres composed of CPP only over a time period of one month due to the slow degradation in CPP polymers. By adjusting the CPP : SA ratios of the copolymer, initial burst release got reduced and insulin release was optimally prolonged and uniformity is maintained over a month with 67% cumulative drug release at the thirty-fifth day [94].

Stimuli triggered biodegradable polymeric drug delivery systems are designed to achieve controlled release targeted drug delivery *in vivo* on specific stimuli, namely, pH, enzyme substrate, magnetic, electrical, thermal, ultrasound, ionic strength [75]. Drug release from pH- and enzyme-sensitive polymeric delivery devices is initiated when degradation gets triggered by the respective stimulus. Aimetti and co-workers [2] innovated a poly(ethylene glycol) hydrogel platform with human neutrophil elastasesensitive peptide crosslinks where a zero-order release of bovine serum albumin (BSA) in the stimulus of human neutrophil elastase was noticed. Dissolution of polymers in solvents is a vital process undergoing in polymer science and has been applied largely in microlithography, controlled drug release and membrane science to name a few [99]. Solvent diffusion and chain disentanglement are the two transport processes involved in polymer dissolution [97]. Polymer dissolution results in the the loss of bulk material. Polysaccharides such as hydroxypropyl methylcellulose (HPMC), cyclodextrin, dextran and gellan gum are widely used in pharmaceutical industry due to their low toxicity, biocompatibility, availability. Those remain stable under normal body pH and temperature and undergo hydrolysis at extreme pH and temperatures. These polysaccharides undergo dissolution in the aqueous medium as a combined action of solvent penetration effect, swelling and polymer chain disentanglement [12]. Hence, drug transport from polysaccharides based drug delivery systems is mainly governed by diffusion and dissolution phenomena.

2.1.2 Release mechanism from matrices

It is a known fact by now that drug release kinetics is controlled by polymer swelling, polymer erosion, drug dissolution / diffusion characteristics, drug distribution inside the matrix, drug-polymer ratio and system geometry [25, 23]. Ophthalmic matrices are exceptional since matrices are stored in dry, shrunken state without any liquid phase inside, due to optimal dosage form and for physical and chemical stability of the system. As a result, the solid drug present in the polymeric matrices in the form of microcrystals, nanocrystals or amorphous state, cannot diffuse through the meshes of the polymeric matrix [80]. Upon contact with the biofluids, the polymer swells to transform from the glassy dry state

to the rubbery swollen one and drug dissolution prevails. When the infused biofluid concentration exceeds a threshold value, polymeric chains unfold to undergo glassy-rubbery polymer transition and a gel like layer begins to appear encompassing the matrix dry core [68, 85]. This transition results into a molecular rearrangement of polymeric chains on interaction with the incoming biofluid [53].

Due to glassy - rubbery transition the motility of polymer chains increase enormously leading to network mesh enlargement so that the drug can dissolve and diffuse through the gel layer. Dissolution of nanocrystals and amorphous drug, unlike to microcrystals, exhibit a peculiar behaviour. Since, solubility depends on crystal size [1], both of them, due to their small size are highly soluble in aqueous medium. Nanocrystals and amorphous state are thermodynamically unstable and hence while interacting with the incoming biofluid, they tend to merge to form the original macrocrystal. Thus, the dissolved drug undergoes a recrystallisation with reduction in solubility and slow down of the dissolution process. Dissolved drug recrystallisation may prevail within the matrix or in the release environment which are characterised by different recrystallisation constants [51]. Drug diffusion through polymeric matrix depends on the physical and chemical characteristics of polymer / drug [135, 136, 137] in addition to the ratio between diffusant and mesh size [111, 118].

2.1.3 Mathematical modelling efforts formulating drug release

There are two types of mathematical models for the formulation of drug release mechanism, namely, empirical / semi-empirical and mechanistic. Empirical / semi-empirical mathematical models are mainly descriptive in nature and does not depend on real physical, chemical or biological phenomena. Hence, this leads to limited understanding of the underlying drug release mechanisms and low predictive potential of these models. These empirical mathematical models are useful in the investigation of different types of drug release profiles with respect to a specific parameter. On the other hand, mechanistic mathematical models depend on physical phenomena such as diffusion, dissolution, swelling, erosion, precipitation and degradation. System-specific parameters are determined in mechanistic mathematical models through the comprehension of underlying drug release mechanisms. Thus, during product development, realistic and mechanistic mathematical models are responsible for predicting the significant parameters and for optimizing the formulation of drug release kinetics. Therefore, one may theoretically predict the required size, shape, preparation methodology and composition of therapeutically efficient unique drug dosage form.

Mathematical modelling of drug release from matrix systems was developed from empirical to semi-empirical and later attained advanced stage after entering into the realm of mechanistic mathematical models. In the year 1961, Higuchi [60] proposed a very popular mathematical model, which is referred till today. The model was to describe the drug release rate from matrix systems in the following way.

$$\frac{M_t}{A} = \sqrt{D\,(2\,c_0 - c_s)\,c_s\,t}, \qquad \text{for} \quad c_0 > c_s, \tag{2.1.3}$$

where M_t is the cumulative absolute amount of drug released at time t, A represents the surface area of the controlled release device exposed to the release medium, D is the drug diffusion coefficient in the

polymeric carrier, c_0 and c_s depict the initial drug concentration and the drug solubility in the polymer, respectively. It is noteworthy that this model shows an M_t square root dependence on time which is similar to what Fick's solution predicts when the released amount is less than sixty percent [29]. In order to quantify diffusional mass transport, Fick's laws of diffusion are usually used [29]: Fick's first law of diffusion:

$$F = -D\frac{\partial c}{\partial x}, \tag{2.1.4}$$

where F is the rate of transfer per unit area of section which is termed as flux, c denotes diffusing species concentration and D is the diffusion coefficient, also termed as diffusivity. Fick's second law of diffusion which can be derived from Fick's first law, is as follows:

$$\frac{\partial c}{\partial t} = D\left(\frac{\partial^2 c}{\partial x^2} + \frac{\partial^2 c}{\partial y^2} + \frac{\partial^2 c}{\partial z^2}\right), \tag{2.1.5}$$

where c is diffusing species concentration, t denotes time, D is the diffusivity and x, y and z are spatial Cartesian coordinates. In 1963, Higuchi [61] carried out theoretical analysis of mathematical relationships controlling the drug release rate from solid matrices where solid drugs were randomly dispersed. Fu et al. [43] in 1976, derived a unified mathematical model for drug release estimation and validated with experimental findings. Moreover, an analytical solution for Fick's second law [29] for cylindrical geometry was also provided. Peppas et al. [109] in 1980, proposed and solved a moving boundary diffusion problem due to swelling in which the drug was uniformly distributed throughout the polymeric matrix.

With passage of time, empirical mathematical model got improved to semi-empirical model which was more comprehensive, yet simple, in order to describe drug release from polymeric matrices. The newly evolved semi-empirical mathematical model was the so-called power law:

$$\frac{M_t}{M_\infty} = k\, t^n \tag{2.1.6}$$

where, M_t and M_∞ are the absolute cumulative amount of drug released at time t and infinite time respectively, k represents the constant incorporating structural and geometric characteristics of the matrix and n depicts the exponent which indicates the drug release mechanism. The above-mentioned power law based semi-empirical model was first introduced during the period 1985-86 by Peppas and his co-workers [108, 110]. In 1988, Cohen and Erneux [21, 22] used free boundary problems to model swelling-controlled drug release which was achieved by diffusion through a penetrated solvent. The drug release rate was calculated considering the diffusion rate of the solvent into the polymer. In this study, theoretical analysis was done for the thin films. In 1994, the idea of power law was utilized by Conte et al. [26] to formulate drug release from HPMC (hydroxypropyl methylcellulose)-based multi-layer matrix tablets. Ju with his co-workers [68, 70, 69] during the time period 1995-97 formulated the swelling / dissolution behaviour and drug release from HPMC matrices through a comprehensive mathematical model. The model incorporated important physical properties of the polymer and matrix

dissolution was considered similar to the dissolution of an object immersed in a fluid, thereby introducing a diffusion layer separating the matrix from the bulk solution. Furthermore, an anisotropic expansion model was derived for formulating the anisotropic expansion of the matrix. Colombo and his co-workers [23] also validated the suitability of the power law model for drug release problems by comparing their experimental results of a water-soluble drug, buflomedil pyridoxal phosphate released from HPMC-based matrix tablets in 1999. In 2000, a noteworthy mathematical model of drug release from HPMC-based matrix tablets was proposed by Siepmann and Peppas [130], considering diffusion of water and drug, non-constant diffusivities, moving boundary conditions, swelling of the system, drug dissolution, radial and axial mass transfer in cylindrical geometries.

Mathematical model of drug dissolution is mainly based on the work of Noyes and Whitney, carried out in 1897 [101] and they published the first article based on quantitative study of a dissolution process. They used the dissolution medium as water. Then they rotated cylinders of benzoic acid and lead chloride and lastly conducted an analysis of resulting solutions at several temporal points. It was found that the rate of change of concentration $c(t)$ of the dissolved species was proportional to the difference between the saturation solubility c_s and the instantaneous concentration of the dissolved species. Applying k as the constant of proportionality, the above criteria was mathematically formulated as follows:

$$\frac{dc}{dt} = k\,[c_s - c(t)], \qquad c(0) = 0. \tag{2.1.7}$$

Development of a mathematical model by taking into account drug dissolution, diffusion with non-constant diffusivities, moving boundary conditions and polymer erosion on the basis of Monte-Carlo simulation was introduced by Siepmann et al. [128] in 2002. Another study was conducted by Siepmann et al. [127] in 2005 in order to apprehend the importance of autocatalysis in PLGA-based microparticle that was implemented as a controlled release drug delivery device. An unified model was developed in 2009 by Rothstein et al. [120] for the prediction of drug release from bulk and surface eroding systems in addition to drug release prediction regarding matrices that undergo transition from surface eroding to bulk eroding behaviour during the course of degradation. Frasch and Barbero [39] reviewed the study of numerical methods to solve a mechanistic, diffusion based mathematical model for skin permeation in 2013. In some polymeric matrices, both diffusion and drug dissolution occur simultaneously and govern the drug release mechanism. Casaslini et al. [18] in 2013 studied experimentally as well as theoretically the drug release kinetics from polymeric microparticles. Moreover, polymer degradation was represented by considering the autocatalytic effect due to acidic environment within the device. Drug release mechanism was mathematically modelled by taking into account solubilisation of encapsulated solid drug and eventually diffusion of solubilised drug from the microparticle. It was assumed in their study that no significant recrystallization of solubilised drug occurred. Furthermore, Casaslini et al. [18] accomplished the complex assignment of validating their proposed mathematical model with corresponding experimental findings.

2.1.4 Drug delivery devices

Some examples of drug delivery devices are drug-eluting stents for reducing the extent of restenosis maximally (cf. [138, 139, 55, 91, 16, 147]), therapeutic contact lenses to intensify ocular bioavailability (cf. [13, 5]) along with dermal and transdermal drug delivery (cf. [93, 114, 119]). The first application demonstrating the restenosis process after stent implantation, used for treating coronary arterial disease, involves the interaction between vascular biology, pharmacology, polymer chemistry, mathematical modelling and engineering techniques. The work of Bozsak et al. [16] dealt with the development of a computational model to illustrate the drug transport phenomena of two drugs, Paclitaxel and Sirolimus, used in drug-eluting stents in the arterial wall. It was ultimately concluded that the transport of Paclitaxel was dominated by convection whereas that of Sirolimus was dominated by the binding process. The second application is concerned with the ailment of the anterior segment of the eye which is usually medicated by topical ocular administration. The bioavailability of such medicines tends to be low and it depends on precorneal fluid dynamics. In order to increase the ocular bioavailability of ophthalmic drug, the use of therapeutic contact lens has come to play. The work of Avtar and Tandon [5] was the formulation of a simple mathematical model in order to understand the time variant concentration profiles of ophthalmic drugs administered topically in the anterior chamber aqueous humor. Moreover, analysis of the effects of various model parameters based on the chemical nature of drugs, was carried out. The main concern from medical view point is to predict the ophthalmic drug concentration in the inferior fornix of the conjunctiva. These issues are resolved only through mathematical modelling and numerical simulations since they are the only equipments to do such predictions. The third application deals with transdermal drug delivery which has flourished as a mode of drug administration, but it still needs to be improved to act as a potential substitute for oral and parenteral administrations. Various studies were conducted to model transdermal diffusion of drugs so that the knowledge of permeation of molecules through the stratum corneum being the main barrier to percutaneous permeation, is grasped. Multiscale modelling of multicomponent transdermal diffusion was proposed by Rim et al [119]. It considered the microstructure of the stratum corneum. The different length scales taken into account in the transdermal diffusion phenomenon were examined and the effect of each length scale was merged into the macroscopic permeation barrier of the stratum corneum. The above-mentioned proposed model can be applied to any general transport problem through heterogeneous composite media. All these techniques of drug delivery deal with homologous model fabrication, that is, drug release from a polymeric matrix. The significant therapeutic effect of the drug-eluting stents is ascribed to the extended, targeted and appropriate discharge of anti-inflammatory or antiproliferative drugs into the arterial wall which was well described by Costa and Simon [27].

Liposomes are the first generation nanomedicines accepted for cancer treatment. Liposomal encapsulation of anticancer drugs has overshadowed the conventional free drug delivery systems by diminishing cytotoxicity and also by targeting tumour sites due to enhanced permeability and retention (EPR) effect [92]. Doxorubicin (DOX) is an anticancer drug widely used in the treatment of cancer varieties like genitourinary, thyroid, lymphoma and stomach cancer [48], however its clinical efficacy is restricted by

inadequate local DOX concentration. Moreover, DOX interacts with DNA in cells which can hamper the DNA replication process. Thus, high DOX concentration in normal tissues may cause lethal side effects such as cardiomyopathy [124, 133]. In order to enhance therapeutic efficacy thereby reducing toxicity of DOX in the normal tissues, liposome-mediated DOX is developed. Various attempts are made to design liposomes in such a way that they are able to target tumour sites and release embedded therapeutic agents quickly following specific stimulus such as temperature [141]. Drug-loaded temperature-sensitive liposomes pass through the vasculature wall due to their small size after administration and accumulate in the extracellular space in the tumour. These liposomes are anticipated to remain stable at body temperature. Upon localised heating, the encapsulated drug gets released from the temperature-sensitive liposomes rapidly when the temperature reaches phase transition point [148, 154].

2.2 Drug transport mechanisms

For drug dispersion throughout the biological environment, drug diffusion is a vital mechanism. Therapeutic compounds have different sizes and shapes and hence it is difficult to predict the varied diffusion coefficients. Molecular diffusion is also hindered by various resistances presented by the biological tissues. Drugs diffusing through a tissue interact with tissue elements which may be non-specific as binding with extracellular matrix (ECM) sites or highly specific such as ligand-receptor interactions. Binding of ligand to cell surface receptors was on focus in direct experimental research for the past two decades which was mainly based on equilibrium binding properties. After that recognition of highly dynamic property of receptor binding phenomena instigated interest in binding kinetics. Some background texts may be studied to get the details of experimental research on cell surface binding events [84, 64]. Binding of ligands such as drugs with cell surface receptors lead to internalization of both receptors and drugs by endocytosis. Endocytosis results in accumulation of ligand in lysosomes which lead to drug degradation. Endocytosis helps the cells to internalize a variety of compounds such as serum proteins, viruses, growth factors and many others, as observed by Mukherjee et al. [98]. Ligand-receptor complexes formed as a result of interaction between ligand and receptors at the cell surface, are internalized into the cell intracellular region and stored into common endosomes (cf. [95]). It is an accepted fact that trafficking plays an important part in receptor-mediated cell response. Internalization of receptors can lead to cellular response generation as observed by Bretcher [17] or attenuation of a response as remarked by Zigmond [159]. Cell surface receptor generation may get enhanced on exposure to stimuli which demonstrates that receptor concentration regulation may be significant in cellular responses. Thus, in order to increase drug efficacy and its therapeutic efficiency, the endocytic trafficking cycle should be studied and investigated in details. Two levels of mathematical models are mainly used to deal with endocytic trafficking cycle, firstly, the models that demonstrate the kinetics of receptor / drug interactions throughout the whole cellular region and secondly, the models dealing with specific endocytic mechanism. Whole-cell kinetic mathematical models predict receptor and drug states in connection to cell behavorial functions. On the other hand, mechanistic mathematical models deal with trafficking parameters in accordance with biophysical and biochemical properties of endo-

cytic cycle components. A combined apprehension of both types of mathematical models can relate molecular properties and cell functions effectively. The chemical interactions between a drug and a binding site lead to drug response, which can be observed from the work conducted by Salahudeen and Nishtala [123]. Their work focussed on modelling of drug binding phenomenon, where it was concluded that drug response was dependent on the receptor occupancy by the drug particles, but deterministic modelling was not done by them. The basic fundamental mathematical models of drug diffusion in the biological tissue, specific and non-specific interactions of drug with cell receptors and ECM sites were well illustrated by Lauffenburger, Linderman and Saltzman [79, 125]

2.2.1 Drug transport in solid tumour

Transport within blood vessel

Drug particles begin to circulate in systemic plasma throughout the body just after the initial dose is injected. Drug properties along with *in vivo* body environment regulate the process of drug transport within blood stream. During their transport through blood, drugs may get discharged into the tissues while passing by. Moreover, various organs of the body can take active part in filtering plasma, thereby eliminating drugs from systemic circulation, biologically termed as plasma clearance. The drug dosage, way of its administration into the circulatory system and plasma clearance together determine the plasma drug concentration. This function of renal excretion may vary according to the drug type [77].

Transport through blood vessels

While transported in systemic plasma, some drugs get dispersed into tumour plasma via blood perfusion due to advective and diffusive transport. These drugs can be extravasated into the interstitial fluid due to high permeability of tumour vasculature. Across the vessel wall, drug transport by fluid flux follows advection which is the outcome of hydrostatic and osmotic pressure difference between lumen and interstitium. On the other hand, diffusive drug transport is the outcome of concentration gradient between blood and interstitial fluid along with vasculature permeability and area for drug exchange. Hence, if the gradient alters in opposite direction, drug may get discharged back into the plasma. Here, the main modes of transport are diffusion and advection. Drug uptake by endothelial cells, that is, transcytosis is having negligible effect in comparison to diffusion and advection [67]. Deen [30] presented a review work based on studies conducted by various researchers on hindered transport through pores available on membranes.

Transport in interstitial fluid

The extracellular matrix and intense non-uniformity in vasculature distribution generate a complicated tumour interstitial space [125]. The tumour pressure may go beyond the atmospheric pressure [125, 15], which is the result of inefficient lymphatics, increased tumour vasculature permeability and cell proliferation in a restricted tumour volume leading to vasculature collapse [66]. An effec-

tive mathematical model was derived by Baxter and Jain [8] for transvascular exchange in addition to extravascular fluid and macromolecular transport in tumour. Moreover, in the study of Baxter and Jain, interstitial space was considered as a porous medium where Darcy's law was utilized. In order to reach the targeted tumour cells, the drugs pass through the interstitial fluid by advection and diffusion depending on interstitial fluid pressure and interstitial fluid velocity within tumour. The extracellular space composition affects the diffusivity of drugs due to the presence of proteins. Diffusivity is also affected by the tissue geometry which leads to the difference in diffusion coefficient of a particular drug in tumour and normal tissue [125].

In this chapter, general literature survey is carried out and underlying physical phenomena are discussed so that the readers get an overview of the advancement of study of drug release and drug transport with time. In the following chapters where various problems are focussed and elucidated, problem specific literature reviews are provided at the beginning of the chapters for readers' ease.

3 DRUG RELEASE FROM MICROPARTICLES

3.1 Introduction

Sometimes patients consciously or unconsciously change their prescribed drug dosage schedules and many a time physicians are not informed of this. Forgetfulness is one of the major reasons behind this non-compliance by the patients, which leads to serious consequences in their treatment. New drug delivery systems certainly offer the opportunity to reduce patient non-compliance by tailoring some of the conventional dosage forms. Not only non-compliance by the patients, but also drug distribution, absorption and metabolism vary among individuals. Controlled drug release mechanism provides much relief to these problems. It increases patient's comfort by reducing the frequency of doses. A major advantage of controlled drug release is that besides prolonging the action of the drug, it maintains drug levels within the therapeutic windows (range of drug dosages that can treat diseases effectively while staying within the safety range) of the drug. One of the most common practices to get controlled release is to encapsulate a drug in microparticles or any matrix to enhance or reduce the kinetics behind drug release mechanism depending on the anticipated healing target.

Drug encapsulating microparticles have the potential to spend an extended time in the body relative to that for naked drug. Hence, they have the ability to circulate for a prolonged duration of time in the vicinity of the organ at which they are targeted. Due to biocompatibility and biodegradability of the microparticles, particularly those with polymeric coating such as polylactic acid (PLA), polyglycolic acid (PGA) and polylactic-co-glycolic acid (PLGA), they are reliably used in recent years as potential drug delivery devices. There are several advantages of using microparticles as controlled drug release devices [102]. First, particle size and the characteristics of the surface can be varied according to the necessity to have both passive and active self-programmed controlled release system. In passively programmed system, the release rate of drug is predetermined and it does not depend on any external biological stimuli. In actively programmed system, the release rate can be controlled by some external mechanism. Secondly, since microparticles have biodegradable polymeric coating, they are particu-

larly attractive for use in drug delivery, as once introduced into the body the microparticle matrix is degraded into non-toxic by-products leading to reduction of side effects. Thirdly, encapsulation of drug in a polymeric matrix is done in such a way that the drug and its polymeric coating are mutually inert, thus preserving the chemical stability of the drug and its biological activities. Moreover, these microparticles can be used through various paths of administration, including oral, nasal etc.

Mathematical modelling of drug release process is a subject of recent medical progress. Due to the advancement in computational science, the models have become easier to apply. Theoretical results should predict the effects of processing parameters, not only on the pharmacokinetic aspect, but also on the resulting pharmacodynamics. An extremely helpful, yet challenging aspect is to have such type of mathematical modelling for formulating drug transport in the living cells [132]. Besides, controlled drug release is also an important part of the recent medical research, many attempts have been made to control drug release through various approaches and different theories. An important work is done by Pontrelli and Monte [113], where drug association / dissociation aspect is taken into account while dealing with transdermal drug delivery. A work of Casalini et al. [18] on drug release process is described as —water penetrates inside the polymeric microparticle and wets drug crystals, allowing solubilisation of the drug, which diffuses through the microparticle. There is an assumption that no significant recrystallization of solubilised drug occurs during its release. In the present study, an improved model of controlled drug release is proposed. In this improved model, some of the simplifying assumptions made in the works of Pontrelli and Monte [113] and Casalini et al. [18] are not taken into account which make the model a more realistic one. The process of drug release is described by taking into account the solubilisation dynamics of drug crystallites and diffusion of the solubilised drug through the microparticle. The reversible drug binding process both in the microparticle and in tissue is also addressed. An important aspect of this type of modelling is to have correct judgement of the main parameters, such as diffusion coefficient, mass transfer coefficient, drug association and dissociation rates. A significant perspective of the present work is that the model is solved analytically. The numerical results and their graphical representations provide trustworthy predictions about various aspects of controlled drug release kinetics, which can be utilised by pharmacists to revive their ideas and make few tweaks to the prevailing drug delivery technique.

3.2 Formulation of the problem

In order to model the release kinetics of drug from a microparticle, a two layered system composed of —— (a) the matrix (microparticle) and (b) the tissue (the collection of living cells, which is acted upon by the drug) is considered. The drug is encapsulated in the matrix coated with some biodegradable polymer. The polymeric microparticles are assumed to be in perfect spherical shape having a fixed volume with only radial variations in concentration. It is assumed that all the particles are of same dimensions. It is also assumed that there is uniform distribution of drug concentration inside the microparticle. Lastly, it is presumed that there is no re-distribution of drug back into the tissue from the systemic circulation.

Water enters into the polymeric matrix and wets the solid drug (C_L) loaded inside it, allowing solubilisation of the drug crystals that diffuse through the microparticle. When the drug diffuses through the microparticle, it is the outcome of an unbinding process (solubilisation). Initially, the drug is present inside the microparticle at maximum concentration, being in bound phase, it cannot be transferred to the biological tissue. Then a fraction of this drug ($\beta_0\, C_L$) is converted to an unbound (free) drug particles (C_0), which has the ability to diffuse into the tissue. Conversely, by a recrystallization process, a fraction of the free drug ($\delta_0\, C_0$) is again back to the bound state. At the same instant, a portion of the free drug (C_1) diffuses into the tissue. In the tissue also, a fraction of the free drug ($k_a\, C_1$) is bound by the cell receptors and converted into bound phase (C_b) (this is due to the absorption phenomena by the cells in the tissue). From the bound state (C_b), a portion ($k_d\, C_b$) is transferred into the unbound state. The diffusion of the free drug is assumed to follow Fick's law. The dissolution of the drug is described by the aid of Noyes-Whitney equation [101, 52]. Since the density of binding sites is much higher than the local free drug concentration, the use of a linear relationship is quite reasonable. The whole process is described using the schematic diagram 3.1.

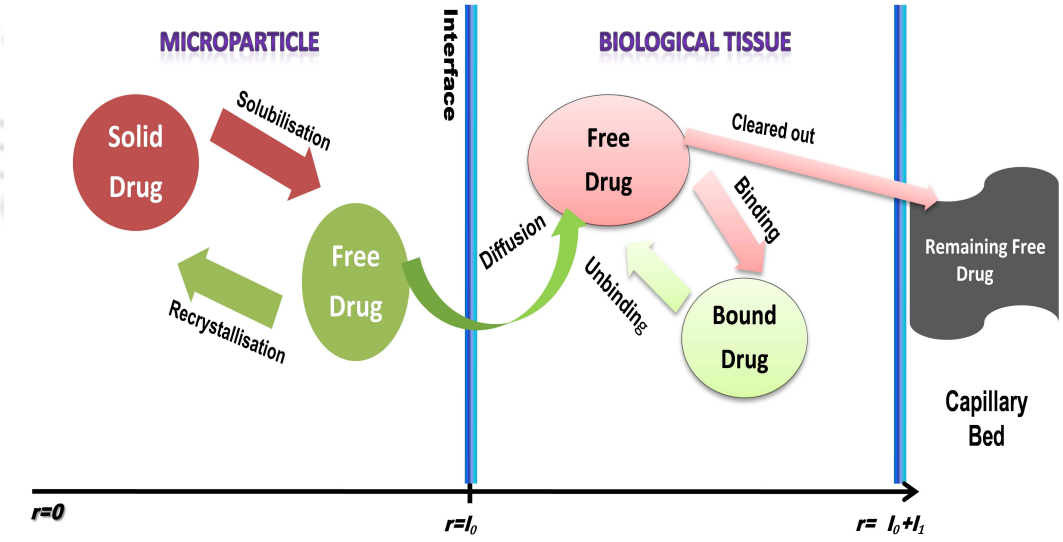

Figure 3.1: Schematic diagram of drug transport to biological tissue from microparticle

Modelling drug dynamics in the microparticle

The equations represent modelling of drug dynamics in the first layer, i.e., microparticle in the following manner:

$$\frac{\partial C_L}{\partial t} = -k_m(C_{lim} - C_0) - \beta_0\, C_L + \delta_0\, C_0, \qquad r \in (0, l_0), \tag{3.2.1}$$

$$\frac{\partial C_0}{\partial t} = \frac{1}{r^2}\frac{\partial}{\partial r}\left(D_0\, r^2 \frac{\partial C_0}{\partial r}\right) + k_m(C_{lim} - C_0) + \beta_0\, C_L - \delta_0\, C_0, \qquad r \in (0, l_0), \tag{3.2.2}$$

where C_L and C_0 are the molar concentrations of the loaded (bound) and free (unbound) drug respectively, k_m is the mass transfer coefficient related to drug crystals inside the microparticle, C_{lim} is the drug solubilisation limit, β_0 and δ_0 are the dissociation and association rate constants respectively in the microparticle, D_0 is the diffusion coefficient of the free drug in the microparticle and l_0 is the radius of the microparticle.

Modelling drug dynamics in the biological tissue

Similarly, in the second layer (tissue) modelling of drug dynamics is done in the following manner:

$$\frac{\partial C_1}{\partial t} = \frac{1}{r^2}\frac{\partial}{\partial r}\left(D_1\, r^2 \frac{\partial C_1}{\partial r}\right) - k_a\, C_1 + k_d\, C_b, \qquad r \in (l_0, l_1), \tag{3.2.3}$$

$$\frac{\partial C_b}{\partial t} = k_a\, C_1 - k_d\, C_b, \qquad r \in (l_0, l_1), \tag{3.2.4}$$

where C_b and C_1 are the molar concentrations of the bound and free (unbound) drug respectively in the tissue, k_a and k_d are the association and dissociation rate constants respectively in the tissue, D_1 is the diffusion coefficient of the free drug in the tissue and $l_0 + l_1$ is the radius of the tissue.

Initial, interface and boundary conditions

A flux continuity condition at the interface of the microparticle and the tissue must be dealt with: $-D_0 \frac{\partial C_0}{\partial r} = -D_1 \frac{\partial C_1}{\partial r}$ at $r = l_0$.
At $r = l_0$, a concentration jump also may occur: $-D_1 \frac{\partial C_1}{\partial r} = P_1(C_0 - C_1)$,
where P_1 is the overall mass transfer coefficient.
A condition is chosen on the tissue-capillary boundary where the clearance of drug is assumed to take place through capillary system:
$K_{cl}\, C_1 + D_1 \frac{\partial C_1}{\partial r} = 0$ at $r = l_0 + l_1$, where K_{cl} is the tissue-capillary clearance per unit area.
The initial conditions are as follows:
$C_L(r,0) = M$, $C_0(r,0) = 0$, $C_1(r,0) = 0$, $C_b(r,0) = 0$,
where M is the maximum value of loaded solid drug concentration. Moreover, regulatory conditions, that both C_L and C_0 are finite, at $r = 0$, are imposed.

3.2.1 Model solutions

All the variables and parameters are now made dimensionless to obtain well-behaved computations.

$$\bar{r} = \frac{r}{l_1}, \quad \bar{t} = \frac{D_1\, t}{l_1^2}, \quad \bar{l_i} = \frac{l_i}{l_1}, i = 0, 1, \quad \gamma = \frac{D_0}{D_1}, \quad \overline{C_j} = \frac{C_j}{M}, j = L, 0, 1, b, lim, \quad K_{cl} = \frac{K_{cl}\, l_1}{D_1}$$

$$\overline{\beta_0} = \frac{\beta_0\, l_1^2}{D_1}, \quad \Pi = \frac{P_1 l_1}{D_1}, \quad \overline{k_a} = \frac{k_a\, l_1^2}{D_1}, \quad \overline{\delta_0} = \frac{\delta_0\, l_1^2}{D_1}, \quad \overline{k_d} = \frac{k_d\, l_1^2}{D_1}, \quad \overline{k_m} = \frac{k_m\, l_1^2}{D_1}.$$

Bars over the parameters are omitted for convenience, so the aforementioned equations along with

initial, interface and boundary conditions are as follows:

$$\frac{\partial C_L}{\partial t} = -k_m(C_{lim} - C_0) - \beta_0\, C_L + \delta_0\, C_0, \qquad r \in (0, l_0), \tag{3.2.5}$$

$$\frac{\partial C_0}{\partial t} = \frac{1}{r^2}\frac{\partial}{\partial r}\left(\gamma\, r^2 \frac{\partial C_0}{\partial r}\right) + k_m(C_{lim} - C_0) + \beta_0\, C_L - \delta_0\, C_0, \qquad r \in (0, l_0) \tag{3.2.6}$$

$$\frac{\partial C_1}{\partial t} = \frac{1}{r^2}\frac{\partial}{\partial r}\left(r^2 \frac{\partial C_1}{\partial r}\right) - k_a\, C_1 + k_d\, C_b, \qquad r \in (l_0, 1), \tag{3.2.7}$$

$$\frac{\partial C_b}{\partial t} = k_a\, C_1 - k_d\, C_b, \qquad r \in (l_0, 1), \tag{3.2.8}$$

$$-\gamma \frac{\partial C_0}{\partial r}\Big|_{r=l_0} = -\frac{\partial C_1}{\partial r}\Big|_{r=l_0}, \quad -\frac{\partial C_1}{\partial r}\Big|_{r=l_0} = \Pi(C_0 - C_1)\Big|_{r=l_0}, \tag{3.2.9}$$

$$K_{cl}\, C_1 + \frac{\partial C_1}{\partial r} = 0 \text{ at } r = l_0 + 1, \tag{3.2.10}$$

$$C_L(r,0) = 1, \quad C_0(r,0) = C_1(r,0) = C_b(r,0) = 0. \tag{3.2.11}$$

The governing equations are solved by using the process of separation of variables and the individual solutions are as follows:

$$C_L = \frac{(k_m + \delta_0)\sin\frac{ar}{\sqrt{\gamma}}}{r(\beta_0 - m_1)(\beta_0 - m_2)}\Big((\beta_0 - m_2)e^{-m_1 t} - (\beta_0 - m_1)e^{-m_2 t} + (m_2 - m_1)e^{-\beta_0 t}\Big)$$

$$-\frac{k_m\, C_{lim}}{\beta_0}(1 - e^{-\beta_0 t}) + e^{-\beta_0 t}, \tag{3.2.12}$$

$$C_0 = \frac{1}{r}(e^{-m_1 t} - e^{-m_2 t})\sin\frac{ar}{\sqrt{\gamma}}, \tag{3.2.13}$$

$$C_1 = \frac{E_2}{r}(e^{-\widehat{m_1} t} - e^{-\widehat{m_2} t})\sin br, \tag{3.2.14}$$

$$C_b = \frac{E_2\, k_a}{r(k_d - \widehat{m_1})(k_d - \widehat{m_2})}\Big((k_d - \widehat{m_2})e^{-\widehat{m_1} t} - (\delta_1 - \widehat{m_1})e^{-\widehat{m_2} t} + (\widehat{m_2} - \widehat{m_1})e^{-\delta_1 t}\Big)\sin br, \tag{3.2.15}$$

where a and E_2 are to be determined from the following relations obtained from (3.2.9):

$$\frac{\Pi\, \tan\frac{a\, l_0}{\sqrt{\gamma}}}{\gamma\, l_0\, (\frac{-1}{l_0^2}\, \tan\frac{a\, l_0}{\sqrt{\gamma}} + \frac{a}{l_0\, \sqrt{\gamma}})} = \frac{(\Pi/l_0 + 1/l_0^2)\, \tan b\, l_0 + b/l_0}{\frac{-1}{l_0^2}\, \tan b\, l_0 + \frac{b}{l_0}}, \tag{3.2.16}$$

$$E_2 = \frac{\Pi\, (m_2 - m_1)\, \widehat{m_1}\, \widehat{m_2}\, \sin\frac{a\, l_0}{\sqrt{\gamma}}}{l_0\, m_1\, m_2\, (\widehat{m_2} - \widehat{m_1})\, [(\Pi/l_0 + 1/l_0^2)\, \sin b\, l_0 + (b/l_0)\, \cos b\, l_0]}. \tag{3.2.17}$$

Other parameters are given by

$$m_1 = \frac{A - \sqrt{A^2 + 4B}}{2}, \quad m_2 = \frac{A + \sqrt{A^2 + 4B}}{2}, \quad A = \beta_0 + \delta_0 + k_m - \lambda, \quad B = \beta_0 \lambda,$$

$$\widehat{m_1} = \frac{A_1 - \sqrt{A_1^2 + 4B_1}}{2}, \quad \widehat{m_2} = \frac{A_1 + \sqrt{A_1^2 + 4B_1}}{2}, \quad A_1 = k_a + k_d - \lambda_1,$$

$$B_1 = k_d\lambda_1, \quad \lambda = -a^2, \quad \lambda_1 = -b^2, \quad b = \frac{3.14}{2\,(l_0+l_1)}.$$

a is obtained by approximating trigonometric function having small argument.

Table 3.1: Simulated values of the model parameters

Parameters	Values	References
β_0	$10^{-4}\ s^{-1}$	[113]
δ_0	$10^{-4}\ s^{-1}$	[113]
D_0	$5*10^{-7}\ cm^2/s$	[113]
l_0	$0.01\ cm$	Estimated from [113]
l_1	$0.1\ cm$	[113]
D_1	$7*10^{-8}\ cm^2\ s^{-1}$	[113]
k_m	$5.6*10^{-5}\ s^{-1}$	[18]
C_{lim}	$2.79*10^{-5}\ mol/cm^3$	[18]
k_a	$1.5*10^{-4}s^{-1}$	[113]
k_d	$2*10^{-5}\ s^{-1}$	Estimated from [79]
P_1	$10^{-6}\ cm/s$	[113]

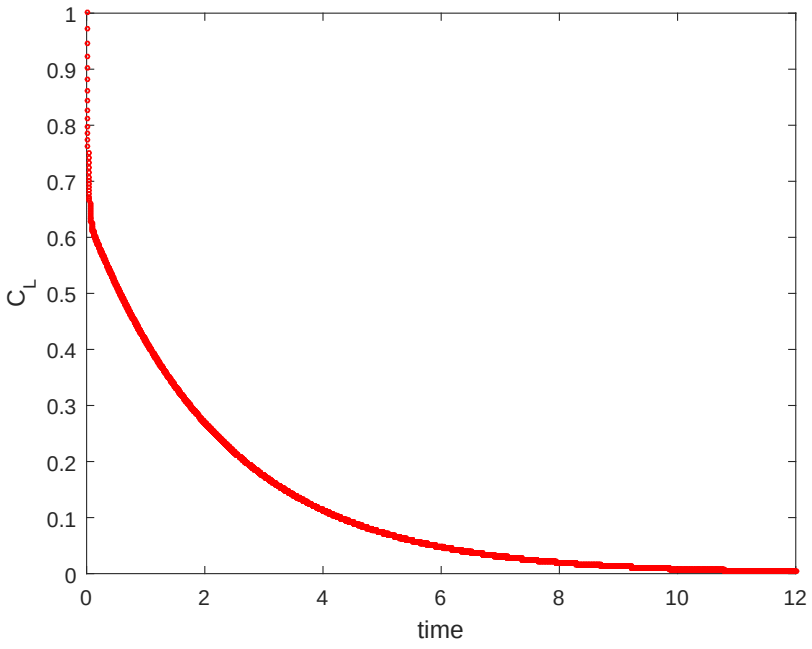

Figure 3.2: Time variant concentration profile of C_L.

3.3 Numerical results and discussion

For the purpose of carrying out a quantitative analysis of a drug release system for better understanding of the drug kinetics, one must need the appropriate values of the parameters involved. The arbitrary choice of the model parameters may not always help in achieving the objectives. Hence, the values of the relevant parameters of the present study are tabulated in Table 3.1. Based on numerical values of the model parameters, an extensive quantitative analysis is performed through graphical representations of the results presented in Figs. 3.2 - 3.16. All the time-variant concentration profiles are plotted for a fixed position, both in the microparticular phase ($r = 0.001\ cm$) and in the biological tissue ($r = 0.05\ cm$).

The time-variant concentration profiles for bound (solid loaded) and free drug particles in the first phase of transport in the microparticle are shown in Figs. 3.2 and 3.3. As the drug is being solubilised, the solid drug C_L gets dissociated which is on the process of transformation into free drug C_0. So, C_0 increases and attains up to a certain limit (maximum) corresponding to a specific instant of time. Following that critical instant of time, some portion of C_0 gets transformed back again into the solid drug in the process of association while some portion of it (C_1) enters into the second phase of the tissue from the microparticle through the process of diffusion. Eventually, C_0 appears to diminish with passage of time, which is shown in Fig. 3.3. In Fig. 3.2, the reason for continuous declination is the concentration of the solid drug C_L continuing to decrease as the amount of recrystallized solid drug becomes smaller compared to that of the unbounded free drug.

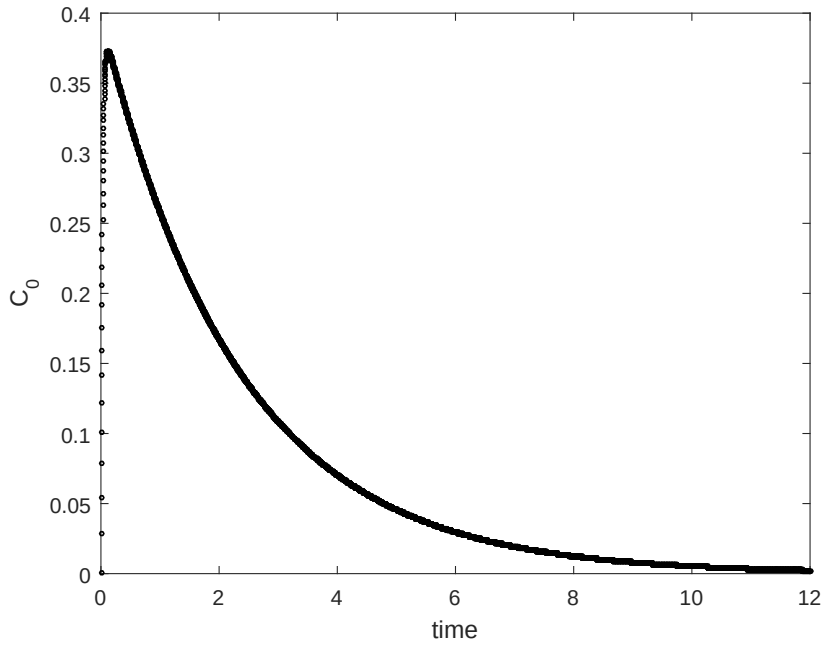

Figure 3.3: Time variant concentration profile of C_0.

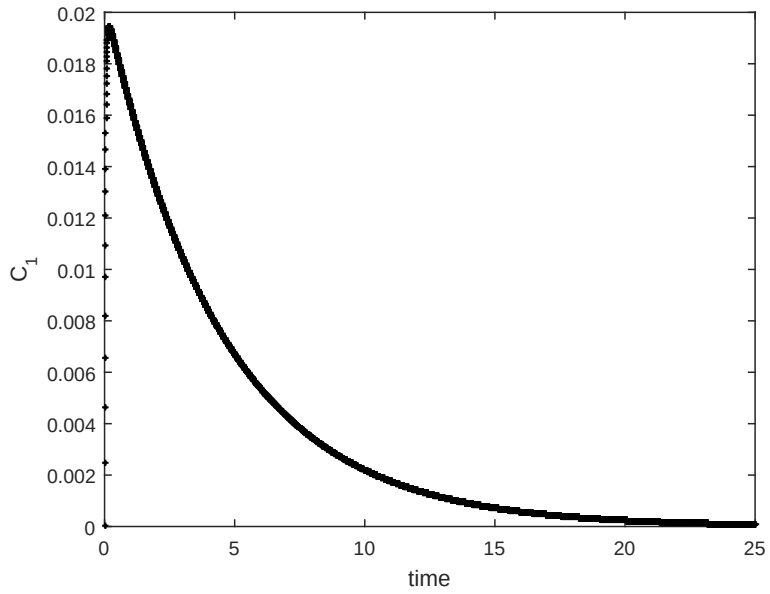

Figure 3.4: Time variant concentration profile of C_1.

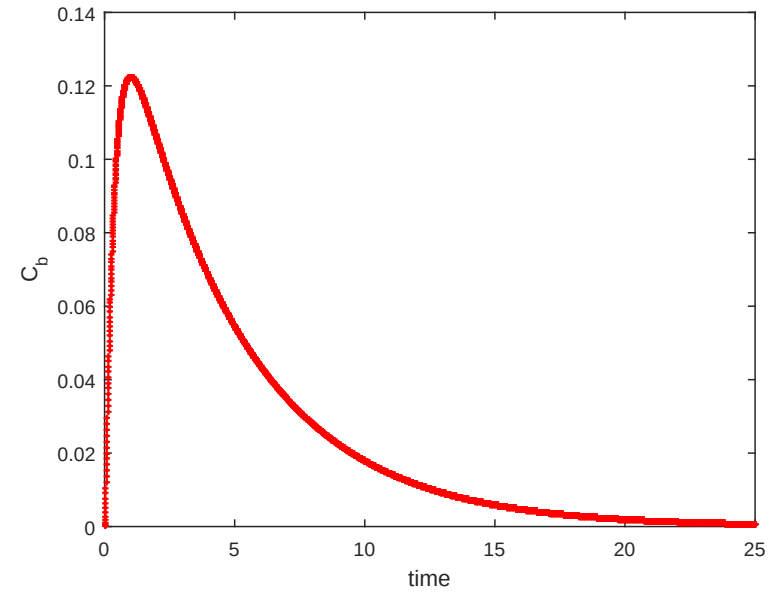

Figure 3.5: Time variant concentration profile of C_b.

The results shown in Figs. 3.4 and 3.5 represent the respective time-dependent concentration profiles for free (C_1) and bound (C_b) drug particles in the second phase of tissue transport, that is in the biological tissue. The characteristics of both the graphs are found to be quite similar as anticipated because in the second phase of the tissue, binding and unbinding processes take place simultaneously. If both the plots are observed minutely, one may notice that C_b attains its peak concentration afterwards in

comparison to that of C_1. This authenticates the validity of the model as it depicts graphically that C_b is formed from C_1 and a minimum time is required for its formation.

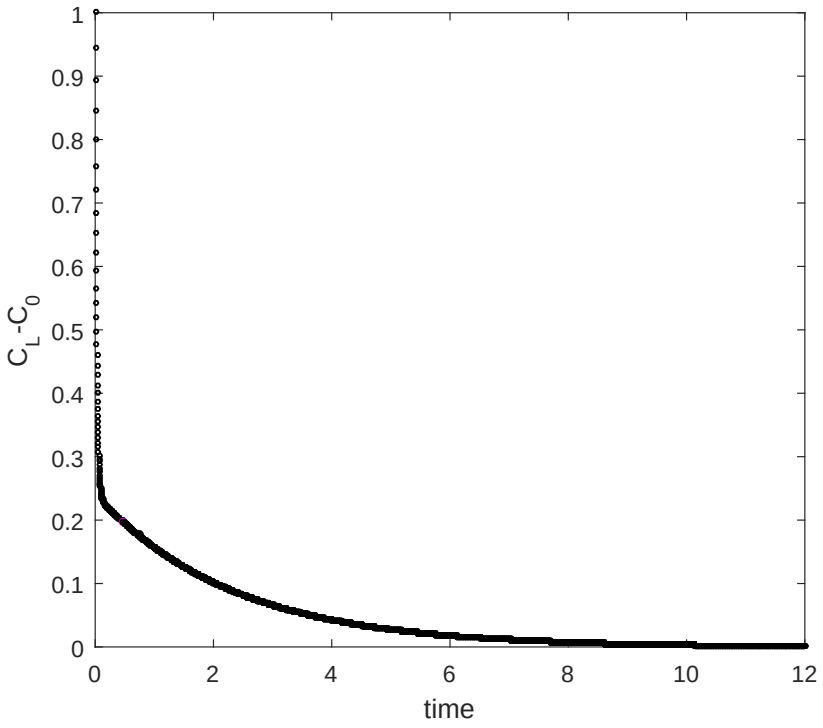

Figure 3.6: Time variant concentration deviation profile of $C_L - C_0$.

The deviation of the drug concentration for solid and free drug $(C_L - C_0)$ in the microparticular phase as well as that of bound and free drug $(C_b - C_1)$ in the tissue phase with time are plotted in Figs 3.6 and 3.7. The former deviation shows the process by means of which the solid loaded drug first unbinds to form free drug through dissociation and then it exhibits how some fraction of free drug binds again to form solid drug through association in the microparticle. The latter one shows that the free drug from the microparticle enters into the tissue through diffusion and after some time, a portion of it gets associated to form bound drug. This ongoing binding / unbinding process is well-established in Fig. 3.8, which emphasizes on the deviation towards the onset since it is not clearly visible from Fig. 3.7.

The influence of unbinding rate constant of drug (β_0) on the solid loaded drug concentration in the microparticular phase is displayed in Fig. 3.9 over a stipulated period of time. It is observed that with decreasing binding rate, the solid drug concentration C_L increases. This may be clearly understood if the internal process behind it is observed critically. First, solid drug solubilises to free drug and some portion of the free drug recrystallizes to form solid drug again. As, solubilisation process takes some time, before the next fraction of drug solubilises, some portion of recrystallized drug gets unbound due to its chemical property. When β_0 decreases, certain bulge is noticed in the contour.

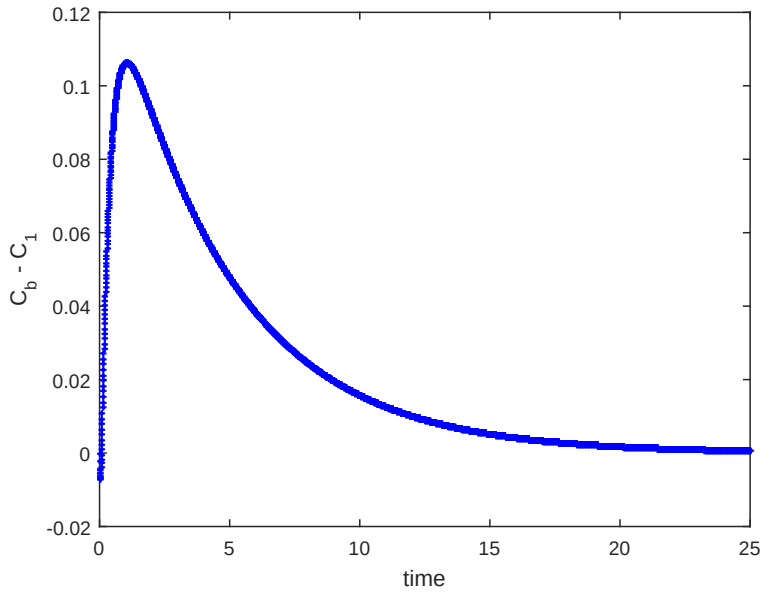

Figure 3.7: Time variant concentration deviation profile of $C_b - C_1$.

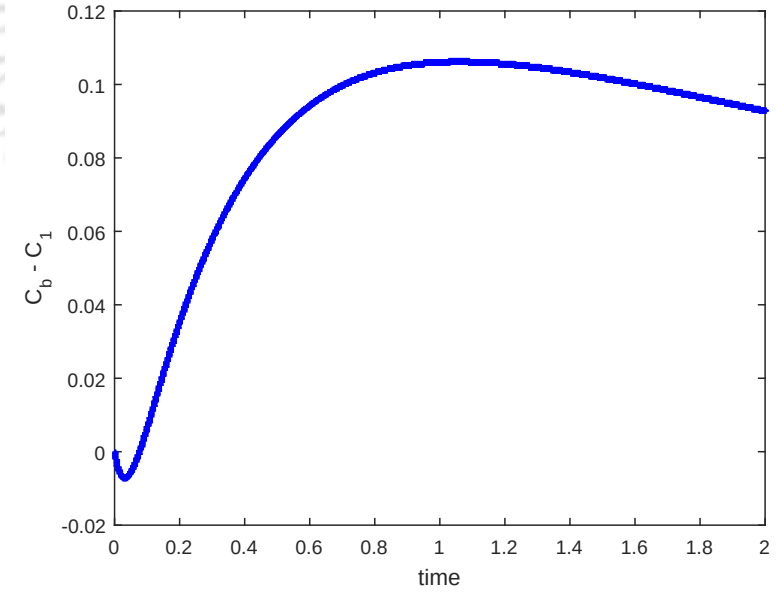

Figure 3.8: Time variant concentration deviation profile of $C_b - C_1$ at the initial stage.

In order to understand the reason behind such behaviour, some factors must be considered. First, solubilisation is a comparatively slow process in comparison to dissociation / recrystallization phenomenon. Hence, before the next fraction of solid drug gets solubilised, recrystallization of free drug to solid drug occurs with very slow dissociation of solid drug (due to lower β_0). The effect of bind-

ing rate constant of drug (δ_0) on the drug concentration C_L in the microparticle over the entire period of time is depicted in Fig. 3.10. If the binding rate decreases, the solid bound drug C_L decreases, which is indeed quite natural as it is just the reverse phenomenon with respect to the previous one (Fig. 3.9). In this figure also, certain bulge is observed for increased binding rate, which leads to increased recrystallization. Thus, this situation becomes similar to that for Fig. 3.9, which is already discussed.

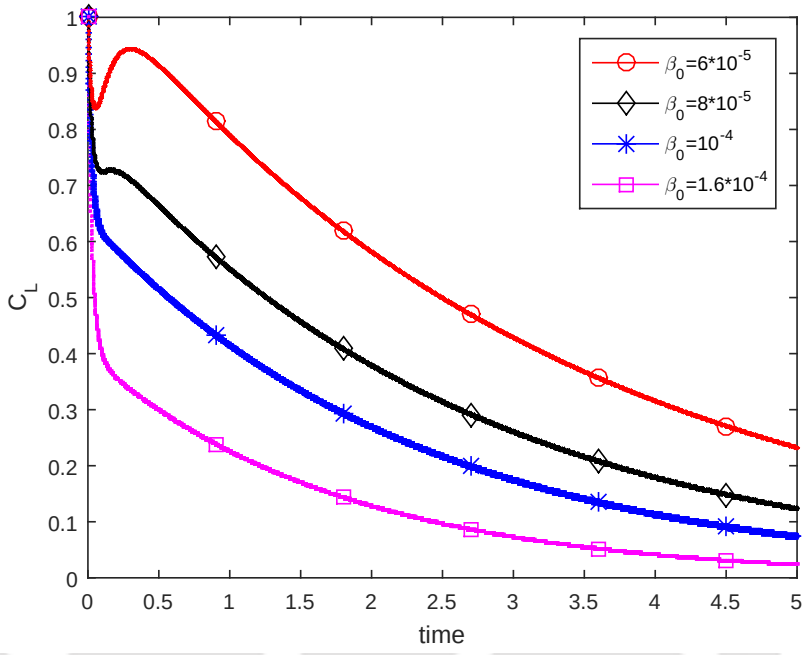

Figure 3.9: Time variant concentration profile of C_L at different β_0.

Before discussing about the next two plots, Figs. 3.11 and 3.12, certain aspects of drug encapsulation in microparticle need to be considered. Solid loaded drug is dispersed in the microparticle in such a way that when transformation of solid drug to free drug occurs, solid and free phases of drug occurs in intermingled state throughout the microparticle. Thus, increased free drug concentration in comparison to that of solid drug leads to higher rate of diffusion due to less hindrance provided by the solid phase. The influence of unbinding rate constant of drug (β_0) on the free drug concentration in the microparticular phase is displayed in Fig. 3.11 over a stipulated period of time. It is observed that with decreasing β_0, the free drug concentration C_0 increases. In the event of smaller rate of dissociation (β_0), both solid and free drugs are present in comparable amount in the system. So, the rate of diffusion of free drug lessens and C_0 increases. The influence of binding rate constant (δ_0) on the free drug concentration in the microparticle phase is presented in Fig. 3.12. With decreasing binding rate, the free drug C_0 decreases. The reason behind it is that recrystallization of free drug into bound drug lessens and maximum amount of free drug diffuses out of the microparticle. One may remark in this connection that, when the association rate is allowed to be minimum, most of the drug in the microparticle is in the form of free drug and consequently, the diffusion of the drug becomes maximum.

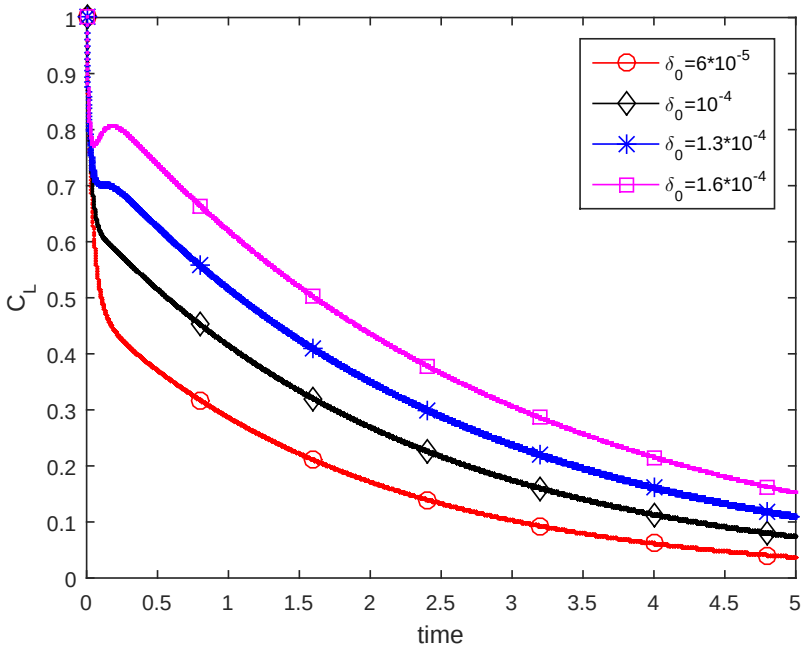

Figure 3.10: Time variant concentration profile of C_L at different δ_0.

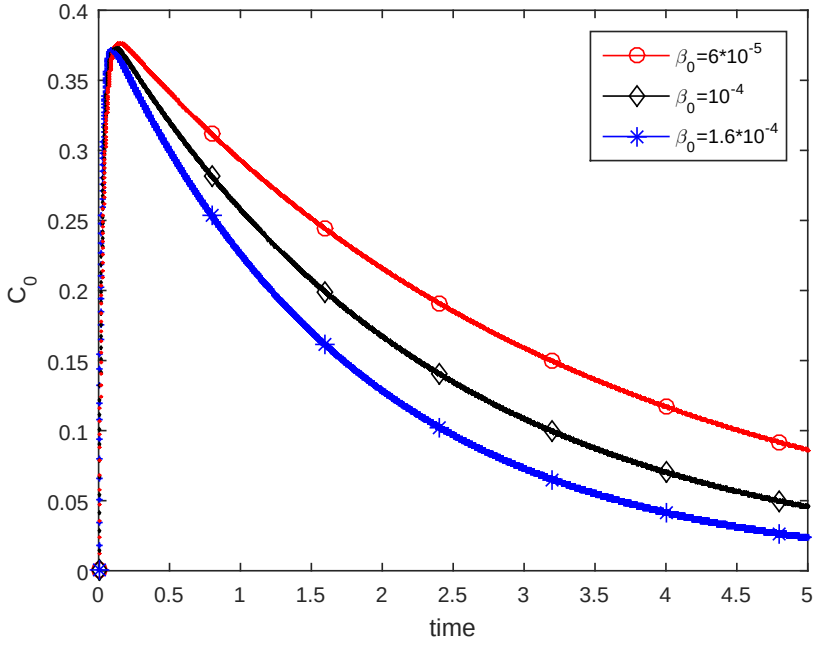

Figure 3.11: Time variant concentration profile of C_0 at different β_0.

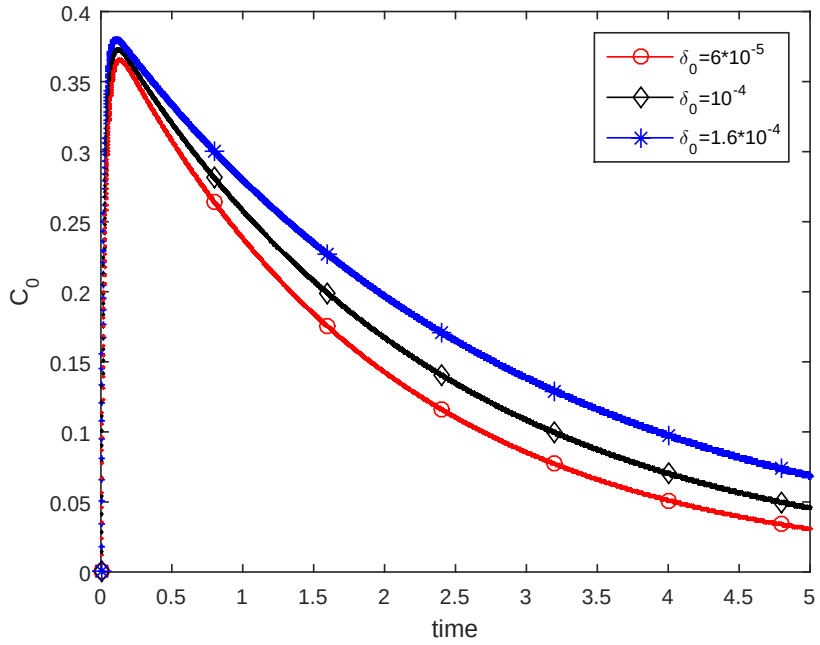

Figure 3.12: Time variant concentration profile of C_0 at different δ_0.

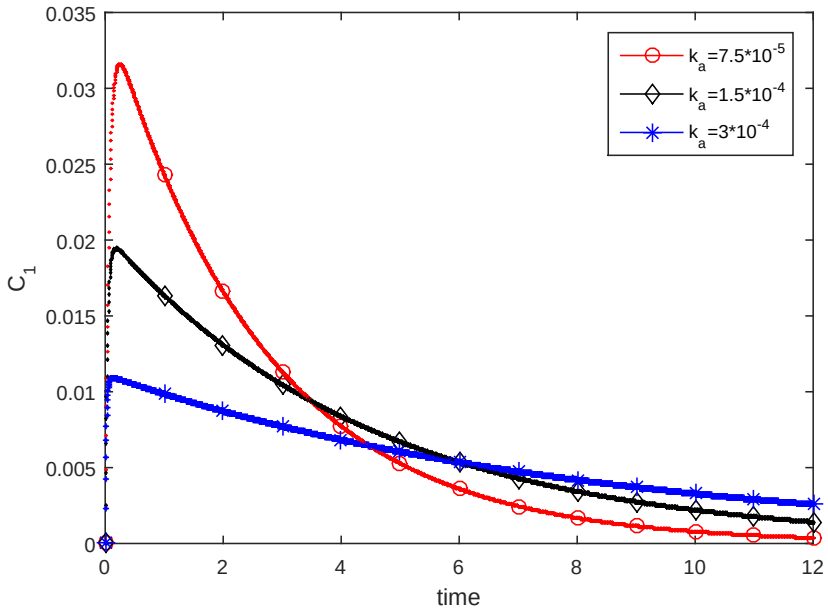

Figure 3.13: Time variant concentration profile of C_1 at different k_a.

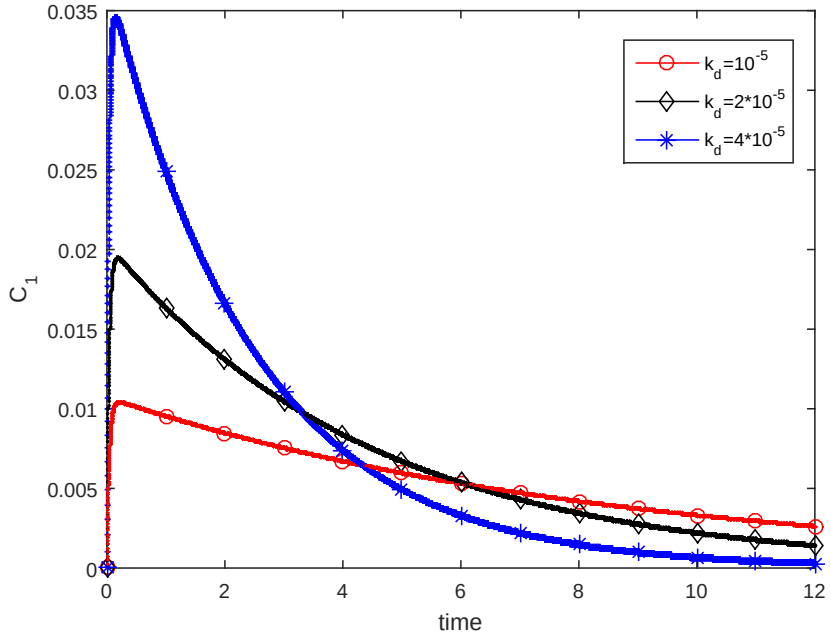

Figure 3.14: Time variant concentration profile of C_1 at different k_d.

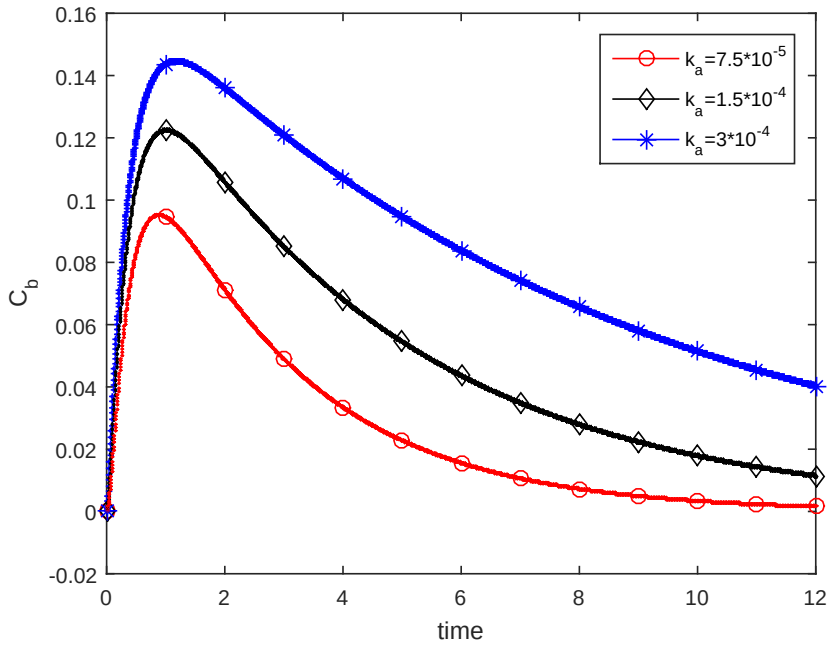

Figure 3.15: Time variant concentration profile of C_b at different k_a.

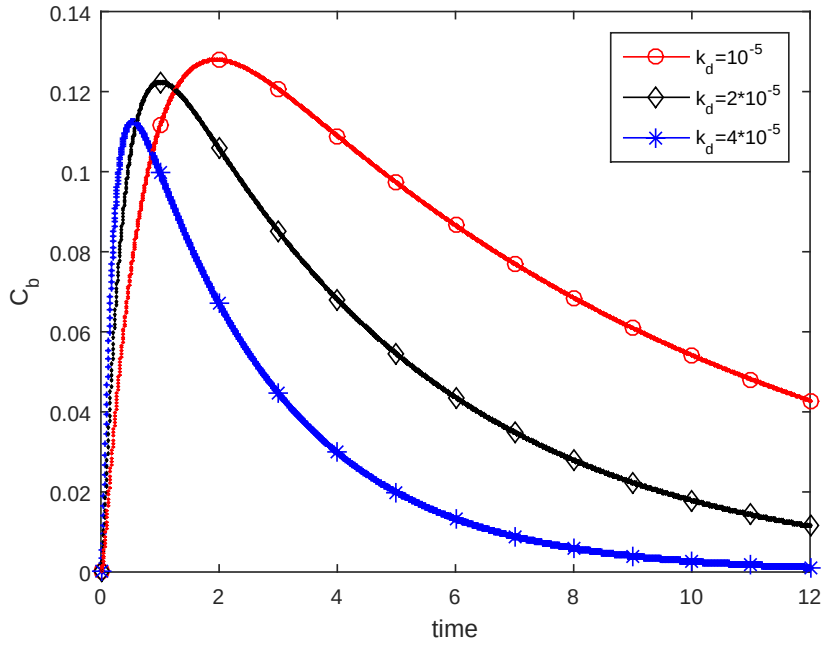

Figure 3.16: Time variant concentration profile of C_b at different k_d.

The next couple of graphical representations (Figs. 3.13 and 3.14) reveal the time variant concentration profiles of free drug (C_1) in the biological tissue for different values of association (k_a) and dissociation (k_d) rate constants. It must be kept in mind that when association rate constant gets increased, greater fraction of free drug (C_1) gets transformed into bound drug (C_b) leading to higher concentration of bound drug and lower concentration of free drug. Since the dissociation rate constant is unaltered and C_b concentration is higher, dissociation of bound drug leads to the formation of free drug. This re-transformation of free drug suffices the contour of C_1 to decline slowly. The present discussion is graphically illustrated in Fig. 3.13, which exhibits the influence of binding rate constant (k_a) on the drug concentration C_1 in the tissue phase. The influence of unbinding rate constant (k_d) on the free drug concentration C_1 in the tissue is shown in Fig. 3.14. With decreasing unbinding rate constant, C_1 decreases as lesser fraction of bound drug re-transforms back to free drug.

The slow degradation of C_1 contours, which are having lower peaks, is due to the fact that flux of free drug (C_1) into the biological tissue depends also on the concentration difference between those in microparticle and tissue respectively. Thus, when C_1 contour peak is less, there is more influx of free drug into the tissue leading to its slow decline. On the other hand, for higher C_1, there is less influx of free drug from the microparticle into the biological tissue. Hence, the corresponding C_1 contour declines quickly.

The effects on the C_b contours due to the influence of the binding rate constant (k_a), in the tissue phase, are shown in Fig. 3.15. It is an obvious observation that if the binding rate decreases then C_b decreases. On the other hand, in Fig. 3.16, the effects on the C_b contours due to the influence of the unbinding

rate constant (k_d), in the tissue phase, are visualized. This is also quite obvious that with decreasing unbinding rate constant, the bound drug concentration C_b increases. This is because as the dissociation phenomenon slows down, there is less re-transformation of bound drug back to free drug. Therefore, it may be inferred that with increasing binding rate constant and decreasing unbinding rate constant, the drug assimilation in the biological tissue takes prolonged time.

It is verified that the variation of concentration with space is meagre for all time compared to all other substantial variations shown and hence any discussion on this is considered insignificant.

3.4 Conclusions

The present work is dedicated to the development of a mathematical model by taking into account some physical phenomena of drug transportation to describe the dynamical behaviour of a microparticle with drug embedded in it. The significant influence of model parameters on different drug concentrations are shown graphically, which establishes the strong fact that by altering the parameters various means of drug release control can be achieved according to the patient's needs. Various conclusions are drawn from the dynamical behaviour of the present model study, such as the drug diffusion rate and the drug assimilation rate in the tissue are inversely proportional to the binding rate. It is worth mentioning that as the drug needs prolonged time in the tissue to get absorbed completely, its effect will certainly persist for a long time before the same drug is administered subsequently. This approach may be applied to other parts of the human body provided the system does not have major clinical complexity. Based upon the present model validation, the model can be evolved further with the incorporation of several factors depending on the objectives of the drug release phenomena in various situations for future research in this direction by utilizing the present knowledge of the system.

4 DRUG TRANSPORT THROUGH ENDOCYTOSIS

This chapter is devoted to study drug delivery with the introduction of endocytosis phenomenon through mathematical model, keeping in view the second objective in succession mentioned in Chapter 1.

4.1 Introduction

It is a well-established fact that pharmacotherapy claims to be an important therapy for medical treatment using pharmaceutical drugs (medicines), which differs significantly from many other therapies involving surgery, radiation or other invasive methods. Pharmacotherapy is no way inferior to other important modes of medical treatment. Its history is quite impressive concerning the use of medicine (or drugs) and vaccines in the treatment, prevention and sometimes eradication of fatal diseases. It is the formulation of drug into a dosage form or drug delivery system that, in reality, transforms the research comprising discovery of drugs and other pharmacological aspects into clinical practice. The drug delivery system involved plays a critical role in controlling the therapeutic effect of the drug as it can influence the pharmacokinetic profile of the drug, rate of drug release, target regions, duration of drug action and consequently the toxicity along with side-effect profile as well. The quintessential drug delivery should not only be inert, biocompatible, but also at the same time provide patient compliance, capable of attaining high drug loading. However, it should also have preventive measures for the accidental release of drug and at the same time it should be simple to administer and to remove from the body. Controlled release drug delivery involves drug-encapsulating devices from which drug or therapeutic compounds may be released at controlled rates for prolonged span of time. The most stirring openings in controlled drug delivery lie in the realm of responsive delivery system, with which it is possible to release drugs from its encapsulating device in reaction to a measured drug level in blood or to release the therapeutic agent to the localized target site.

Though many new as well as old therapeutics are considered patient-friendly, numerous compounds are in requirement of localized advanced drug delivery technologies to reduce toxicity level, enhance therapeutic efficacy and potentially recast biodistribution. Local drug delivery is the manifestation of drug delivery in which drugs are delivered at a specific site inside the body to a particular diseased organ or tissue. Though drug delivery, in principle, may be monitored, but the most important hazard is that the design of drug delivery system. This is because there exists complex interaction among biology, polymer chemistry and pharmacology [132] to develop controlled release drug delivery system. Mathematical modelling of drug delivery and predictability of drug release is a steadily growing subject with respect to its importance in academic and industrial areas due to its estimation potential. Homologous to other scientific disciplines, computer simulations are likely to be an integral part in future research in the field of pharmacy. Various studies have already been taken up by researchers in the past on drug delivery devices regarding its release phenomenon, therapeutic efficiency and optimal design [129, 28, 99, 16, 150, 49].

In the present study, a generalized mathematical model of release of drug from a local drug delivery device and its transport to the biological tissue is proposed. The model is comprised of drug release phenomena where the drug undergoes solubilisation, recrystallisation and internalization through a porous membrane. Porosity of the polymeric matrix and internalization process are such facets of drug release kinetics that devise its mathematical model in a much more naturalistic, convincing and practical fashion strengthening the thoroughfare between mathematical modelling and pharmacokinetics. It is important to study the drug transport through endosomal events. This is because targeting nanomedicine complexes to endolysosomal pathway improves the drug uptake for the treatment of lysosomal storage diseases, cancer and Alzheimer's disease. The system of partial differential equations in the present model depicts solid-liquid transfer, solubilisation phenomenon, and diffusion processes in the polymeric matrix as well as binding / unbinding process and internalization phenomena in the tissue. An important aspect of the aforementioned model is to appropriately judge governing parameters of significance, such as diffusion coefficient, solid-liquid mass transfer coefficient, mass-transfer parameter, drug association / dissociation rate constants, membrane permeability and internalization rate constant. A significant sweep of the present work is that an analytical approach is adopted to solve the partial differential equations supplemented with the appropriate choice of the conditions having relevance to the physical situation. The numerical results based on the parameter values and their graphical representations provide reliable insights on different properties of drug release kinetics.

4.2 Formulation of the problem

In a model of local drug delivery device, a two-phase system is usually considered that is made of: (a) a polymeric matrix, which operates as a reservoir and where the drug is loaded initially, along with (b) the biological tissue, where the drug is transported as target region. The first phase, that is, the polymeric matrix, is framed as a planar slab, encompassed on one side with an impermeable backing

and the other side of the matrix is in contact with layer (b). A rate-controlling membrane protecting the polymeric matrix is present at the interface of the coupled layers. Generally, mass transport prevails in the direction normal to the tissue, which may be the reason behind the modelling confined to one-dimensional case. In the present study, x-axis is considered to be normal to the layer and aligned with the positive direction outwards.

4.2.1 Some preliminary concepts

In the continuum approach, in general, a porous medium is thought of as a homogeneous material by defining averaged variables over a large enough volume, the representative elementary volume V_{rev}. The length scale of V_{rev} is assumed to be much larger than the size scale of the pores and lesser than the model length scale of the phenomenon. Porosity, ε_0 is generally described as the ratio of void volume (V_{rev}^f) to total volume $(V_{rev} = V_{rev}^f + V_{rev}^s)$, where f and s stand for fluid and solid phases respectively [11]. As a part of the void space is accessible to the drug particles, a new parameter, the partition coefficient (k) is introduced, such that $k\varepsilon_0$ becomes the available void volume. The volume-averaged drug concentrations in fluid and solid phase are designated respectively by the relationship $C = k\varepsilon_0 C^f$ and $C_L = (1-\varepsilon_0)C^s$, where C^f and C^s represent the intrinsic volume-averaged drug concentration in accessible fluid and solid phase respectively.

4.2.2 Drug release mechanism and its transport phenomena

Initially, the drug occurs completely in a solid phase embraced within the polymeric matrix (for example, in crystalline form) (C_L) at its maximum concentration. Being in a bound state, it cannot be transferred to the tissues directly. As time elapses, water enters into the polymeric matrix and wets the drug encapsulated inside it, permitting solubilisation of the loaded drug crystals into free state (C_0), which diffuses out of the matrix into the tissue. The rate of transfer of drug from solid state to free state depends not only on solubilisation phenomenon but is also proportional to the difference between C_L and C_0. Again, a fraction of solid drug $(\beta_0 C_L)$ is transformed into its free state, that is competent to diffuse. Conversely, through a recrystallisation process, another fraction of free drug $(\delta_0 C_0)$ is transferred back to its bound state. Simultaneously, a part of free drug (C_1) diffuses into the tissue. In the similar way, in tissue, a portion of free drug $(k_a C_1)$ is metabolised into bound phase (C_b), which also unbinds $(k_d C_b)$ to form free drug. Now, the bound drug is engulfed (internalized) $(k_i C_b)$ by the cell in the tissue through the process of endocytosis. Endocytosis is an active energy-using transport phenomenon in which molecules (proteins, drugs etc.) are transported into the cell. Thus bound drug gets transformed into internalized drug particles (C_{int}). These internalized drug particles, after a span of time, get degraded by the lysosomes and the drug remnants after degradation $(k_{id} C_{int})$ are expelled out of the cell into the extracellular fluid. The complete drug transport process is schematically demonstrated in Fig. 4.1. The diffusion of free drug is expected to emanate from Fick's law [29]. The dissolution of the drug is formulated with the help of Noyes-Whitney equation [101].

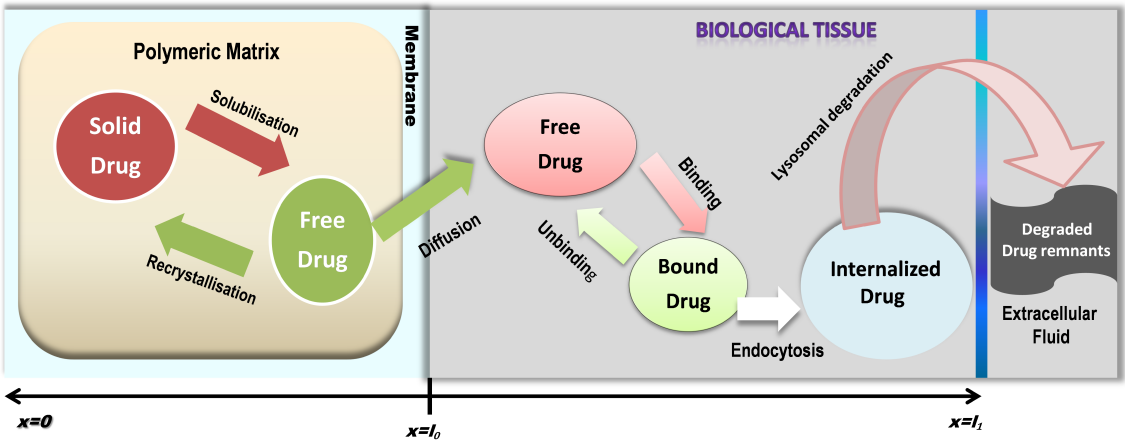

Figure 4.1: Schematic diagram of drug transport

Table 4.1: Simulated values of the model parameters

Parameters	Values	References
β_0	$10^{-4}\ s^{-1}$	[113]
δ_0	$10^{-4}\ s^{-1}$	[113]
D_0	$6*10^{-8}\ cm^2/s$	[79]
l_0	$0.01\ cm$	Estimated from [113]
l_1	$0.1\ cm$	[113]
D_1	$7*10^{-5}\ cm^2\ s^{-1}$	–
α_0	$7.5*10^{-4}\ s^{-1}$	Estimated from [96]
k_m	$5.6*10^{-5}\ s^{-1}$	[18]
C_{lim}	$2.79*10^{-5}\ mol/cm^3$	[18]
ε_0	0.71	–
k_a	$1.5*10^{-4}s^{-1}$	[113]
k_d	$4.55*10^{-4}\ s^{-1}$	[79]
k_i	$0.69*10^{-4}\ s^{-1}$	[79]
P_1	$10^{-6}\ cm/s$	[113]
k_{id}	$4.55*10^{-4}\ s^{-1}$	[79]
k	1	[11]

Modelling drug dynamics in the polymeric matrix

The governing equations describing the dynamics of drug release in the polymeric matrix phase are

$$\frac{\partial C_L}{\partial t} = -\alpha_0(\Phi_0 C_L - C_0) - k_m(C_{lim} - C_0) - \beta_0 C_L + \delta_0 C_0, \qquad x \in (0, l_0), \tag{4.2.1}$$

$$\frac{\partial C_0}{\partial t} = D_0\frac{\partial^2 C_0}{\partial x^2} + \alpha_0(\Phi_0 C_L - C_0) + k_m(C_{lim} - C_0) + \beta_0 C_L - \delta_0 C_0, \qquad x \in (0, l_0), \tag{4.2.2}$$

where $\Phi_0(=\frac{k\varepsilon_0}{1-\varepsilon_0})$ is the ratio of accessible void volume to solid volume, C_L denotes available molar concentration of solid drug, C_0 is the available molar concentration of free drug, k stands for partition coefficient, ε_0 denotes porosity, l_0 is the length of the polymeric matrix, k_m is mass transfer coefficient, C_{lim} stands for drug solubilisation limit, β_0 is the dissociation rate constant, δ_0 is the association rate constant, α_0 denotes solid-liquid mass transfer coefficient and D_0 is the diffusion coefficient of free drug in the matrix.

Modelling drug dynamics in the biological tissue

The corresponding equations governing the dynamics of drug in the tissue are

$$\frac{\partial C_b}{\partial t} = k_a C_1 - k_d C_b - k_i C_b, \qquad x \in (l_0, l_1), \tag{4.2.3}$$

$$\frac{\partial C_1}{\partial t} = D_1 \frac{\partial^2 C_1}{\partial x^2} - k_a C_1 + k_d C_b, \qquad x \in (l_0, l_1), \tag{4.2.4}$$

$$\frac{\partial C_{int}}{\partial t} = k_i C_b - k_{id} C_{int}, \qquad x \in (l_0, l_1), \tag{4.2.5}$$

where C_1 is the molar concentration of free drug in the tissue, C_b is the molar concentration of bound drug in the tissue, C_{int} denotes the molar concentration of internalized drug particles, $l_1 - l_0$ is the length of the tissue, k_a depicts the binding rate coefficient, k_d is the dissociation rate coefficient, k_i stands for internalization rate coefficient, k_{id} denotes degradation rate constant in the lysosome and D_1 is the diffusion coefficient of free drug in the biological tissue.

Initial, interface and boundary conditions

The initial conditions are as follows:
$C_L(x,0) = M$, $C_0(x,0) = 0$, $C_b(x,0) = 0$, $C_1(x,0) = 0$, $C_{int}(x,0) = 0$, where M is the maximum value of loaded solid drug concentration.
A flux continuity must be assigned at the interface, i.e., at $x = l_0$, $-D_0 \frac{\partial C_0}{\partial x} = -D_1 \frac{\partial C_1}{\partial x}$.
At $x = l_0$, a concentration jump may occur: $-D_1 \frac{\partial C_1}{\partial x} = P_1(C_0 - C_1)$,
where P_1 is the overall mass transfer coefficient.
No mass flux can pass to exterior environment due to the presence of impermeable backing and hence no flux condition arises. At $x = 0$, $D_0 \frac{\partial C_0}{\partial x} = 0$.
Lastly, at $x = l_1$, $C_1(l_1, t) = 0$, since the free drug (C_1) gets converted into bound drug (C_b) completely before it reaches the boundary.

4.3 Dimensionless equations

All the variables and parameters are now made dimensionless in order to make simplified computations in the following way:

$$\bar{x} = \frac{x}{l_1}, \quad \bar{t} = \frac{D_1 t}{l_1^2}, \quad \bar{l_i} = \frac{l_i}{l_1}, i = 0, 1, \quad \gamma = \frac{D_0}{D_1}, \quad \overline{C_j} = \frac{C_j}{M}, j = L, 0, b, 1, int, lim,$$

$$\overline{\beta_0} = \frac{\beta_0 l_1^2}{D_1}, \quad \overline{\alpha_0} = \frac{\alpha_0 l_1^2}{D_1}, \quad \overline{\delta_0} = \frac{\delta_0 l_1^2}{D_1}, \quad \overline{k_y} = \frac{k_y l_1^2}{D_1}, y = d,a,i,id,m, \quad \Pi = \frac{P_1 l_1}{D_1} \quad .$$

Bars over the parameters are omitted for convenience, so the aforementioned equations are as follows:

$$\frac{\partial C_L}{\partial t} = -\alpha_0(\Phi_0 C_L - C_0) - k_m(C_{lim} - C_0) - \beta_0 C_L + \delta_0 C_0, \qquad x \in (0, l_0), \tag{4.3.1}$$

$$\frac{\partial C_0}{\partial t} = \gamma \frac{\partial^2 C_0}{\partial x^2} + \alpha_0(\Phi_0 C_L - C_0) + k_m(C_{lim} - C_0) + \beta_0 C_L - \delta_0 C_0, \qquad x \in (0, l_0), \tag{4.3.2}$$

$$\frac{\partial C_b}{\partial t} = k_a C_1 - k_d C_b - k_i C_b, \qquad x \in (l_0, 1), \tag{4.3.3}$$

$$\frac{\partial C_1}{\partial t} = \frac{\partial^2 C_1}{\partial x^2} - k_a C_1 + k_d C_b, \qquad x \in (l_0, 1), \tag{4.3.4}$$

$$\frac{\partial C_{int}}{\partial t} = k_i C_b - k_{id} C_{int}, \qquad x \in (l_0, 1). \tag{4.3.5}$$

The initial, interface and boundary conditions in dimensionless approach are the following:

$$C_L(x,0) = 1, \quad C_0(x,0) = 0, \quad C_b(x,0) = 0, \quad C_1(x,0) = 0, \quad C_{int}(x,0) = 0, \tag{4.3.6}$$

$$-\gamma \frac{\partial C_0}{\partial x}\Big|_{x=l_0} = -\frac{\partial C_1}{\partial x}\Big|_{x=l_0}, \tag{4.3.7}$$

$$-\frac{\partial C_1}{\partial x}\Big|_{x=l_0} = \Pi(C_0 - C_1)\Big|_{x=l_0}, \tag{4.3.8}$$

$$\frac{\partial C_0}{\partial x}\Big|_{x=0} = 0, \quad C_1(1,t) = 0. \tag{4.3.9}$$

4.3.1 Method of solution

The governing equations are solved with the help of separation of variables technique. The individual solutions are as follows:

$$C_0 = (e^{-m_1 t} - e^{-m_2 t}) \cos ax, \tag{4.3.10}$$

$$C_L = \frac{(\alpha_0 + k_m + \delta_0)\cos ax}{(m_1 - (\alpha_0\Phi_0 + \beta_0))(m_2 - (\alpha_0\Phi_0 + \beta_0))} \Big[(m_1 - (\alpha_0\Phi_0 + \beta_0))e^{-m_2 t}$$

$$-(m_2 - (\alpha_0\Phi_0 + \beta_0))e^{-m_1 t} + (m_2 - m_1)e^{-(\alpha_0\Phi_0 + \beta_0)t}\Big]$$

$$-\frac{k_m C_{lim}}{(\alpha_0\Phi_0 + \beta_0)}\Big[1 - e^{-(\alpha_0\Phi_0 + \beta_0)t}\Big] + e^{-(\alpha_0\Phi_0 + \beta_0)t}, \tag{4.3.11}$$

$$C_1 = E_2(e^{-n_1 t} - e^{-n_2 t}) \cos bx, \tag{4.3.12}$$

$$C_b = \frac{E_2 k_a \cos bx}{(k_d+k_i-n_1)(k_d+k_i-n_2)}\Big[(k_d+k_i-n_2)e^{-n_1 t} - (k_d+k_i-n_1)e^{-n_2 t}$$

$$+ (n_2-n_1)e^{-(k_d+k_i)t}\Big], \tag{4.3.13}$$

$$C_{int} = \frac{E_2 k_a k_i \cos bx}{(k_d+k_i-n_1)(k_d+k_i-n_2)}\Big[\frac{(k_d+k_i-n_2)}{(k_{id}-n_1)}(e^{-n_1 t} - e^{-k_{id}t}) - \frac{(k_d+k_i-n_1)}{(k_{id}-n_2)}$$

$$(e^{-n_2 t} - e^{-k_{id}t}) + \frac{(n_2-n_1)}{(k_{id}-k_d-k_i)}(e^{-(k_d+k_i)t} - e^{-k_{id}t})\Big], \tag{4.3.14}$$

where a (obtained by approximating trigonometric function) and E_2 are determined from the following relations obtained from (4.3.7) - (4.3.8) respectively:

$$\frac{\Pi}{\gamma a}\cot al_0 = 1 + \frac{\Pi}{b}\cot bl_0, \tag{4.3.15}$$

$$E_2 = \frac{n_1 n_2 \gamma a \sin(al_0)(m_2-m_1)}{m_1 m_2 b \sin(bl_0)(n_2-n_1)}, \tag{4.3.16}$$

$$m_1 = \frac{A-\sqrt{A^2+4B}}{2}, \quad m_2 = \frac{A+\sqrt{A^2+4B}}{2}, \quad A = \alpha_0(\Phi_0+1)+k_m+\beta_0+\delta_0-\lambda\gamma,$$

$$B = \lambda\gamma(\alpha_0\Phi_0+\beta_0), \quad \lambda = -a^2, \quad n_1 = \frac{P-\sqrt{P^2-4Q}}{2}, \quad n_2 = \frac{P+\sqrt{P^2-4Q}}{2},$$

$$P = k_d+k_i+k_a-\mu, \quad Q = k_i k_a - \mu(k_d+k_i), \quad \mu = -b^2, \quad b = 3.14/2l_1.$$

The corresponding drug masses in the dimensionless form can be calculated as follows:

$$M_j = \int_c^d C_j(x,t)dx, \qquad c = 0, l_0,\ d = l_0, l_1,\ j = L, 0, b, 1, int. \tag{4.3.17}$$

4.4 Numerical simulation and discussion

A thorough quantitative analysis for the present drug release system is carried out based on the values of the parameters of the model under consideration in order to characterize the pharmacokinetic aspects in detail. The goal of the study may not always be attained through arbitrary selection of the parameters. The data for the present model parameters are provided in Table 4.1.

4.4.1 Model validation

Generally, a drug (in the form of solid oral products, like tablets and capsules) gets absorbed into the blood stream so that the therapeutic product may reach its target site. Hence, it is very much necessary that the drug should be present in solution form in the GI tract, particularly in the intestinal tissue. The *in vitro* dissolution testing is carried out by Qureshi [115] to anticipate dissolution of the medicine in

the GI tract or in *in vivo*. The experimental study is conducted based on *in vitro-in vivo* co-relationship (IVIVC) to develop a dissolution test. This type of experimental study amplifies the potency of an *in vitro* test together with some advantages, such as reduction of the necessitated number of *in vivo* studies in humans. The intent of dissolution testing in the work of Qureshi [115] is to appraise or balance the dissolution results from a test in a significant manner depicting its *in vivo* or physiological activities. The dissolution tests are carried out using DISTEK 2100C system and the medium (900 mL) utilized is distilled water. The dissolution sampling is procured using an automated sampling system attached with an online UV diode-spectrophometer (Agilent 8453). Here, depiction is through drug concentration-time profiles. In order to demonstrate the practicality of the present mathematical model, focus is given to its validation with experimental results. The experimental set-up of 120 mg extended-released (ER) Diltiazem capsule products is contemplated and harmonized with the time-variant concentration profile of free drug, which is procured from the present simple mathematical model. The experiment [115] is restricted to a specific product, which is not having recrystallization property. In contrast to that, the present mathematical model is general enough to subsume all other varieties of polymeric pharmaceutical compounds, where recrystallization is an imperative process. Hence, the experimental data is compared with the present results, both in the absence (recrystallization parameter is made zero) and presence of recrystallization phenomenon (Figs. 4.2 & 4.3 respectively). It is observed that in both the cases, there is well agreement between the experimental data and the present theoretical results. It may be visualized in Fig. 4.3, there is much dissimilitude at the extremity of the contour with respect to the experimental data, in comparison to that of Fig. 4.2. This is due to the fact that with recrystallization phenomenon taken into account, the drug concentration takes longer time to melt away completely as anticipated, since transformation of free drug back into solid drug reduces the rate of free drug diffusion out of the polymeric matrix.

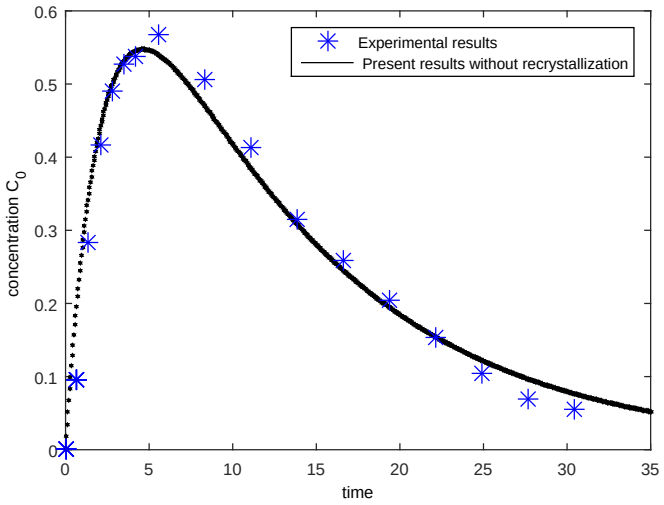

Figure 4.2: Agreement of the present results with experimental data in the absence of recrystallization [115].

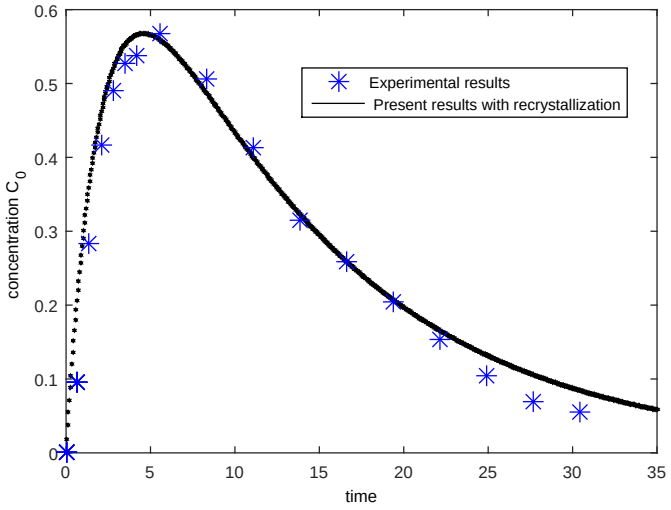

Figure 4.3: Agreement of the present results with experimental data in the presence of recrystallization [115].

Discussion

Graphical representations of the time-variant concentration profiles of the drug in its different states together with drug masses for both the facets are well illustrated through Figs. 4.4 - 4.21 in order to have accomplished understanding of the drug release phenomena.

The time-variant concentration profiles for solid (loaded) and free drug particles in the polymeric matrix phase at four different axial locations disseminating the entire domain are demonstrated in Figs. 4.4 and 4.5. It appears that the concentration of loaded drug C_L decays from its maximum at the initial stage, which gradually depletes with time advancement. The rate of decrease of concentration becomes higher as one proceeds away from the impermeable backing of the polymeric matrix towards the interface resulting in early disappearance. When the loaded drug gets exposed to water, solubilisation process is initiated causing drug release from the matrix, which is on the process of transformation of free drug C_0. One may note on the other hand that C_0 grows to its peak in accordance to a specific instant of time followed by a gradual descend for rest of the times. The reduction of the peak concentration subject to the location towards the interface occurs due to the reason that the drug gets diffused faster in the vicinity of the interface than all other preceding locations away from the interface.

Figures 4.6 - 4.8 represent the time-variant concentration profiles for free, bound and internalized drug particles respectively in the biological tissue for different axial locations stretched over the entire domain. It is important to observe that C_1 heightens hastily compared to other two C_b and C_{int} towards the inception. This observation, as anticipated, reflects in the realm of drug kinetics that free drug (C_1) gets transformed into bound drug (C_b) and subsequently the bound drug is metabolised into internalized drug (C_{int}) after a short passage of time. Ultimately, it is further noted that the internalized drug takes

more time to get absorbed completely in the tissue than the time taken by both bound and free drug particles. In addition to the present findings, one may append that the extended time span distinctly reveals that both loaded and free drug particles in polymeric matrix melt away in a comparatively small span of time than those in the tissue, where they need to take time lengthened to get the drug absorbed completely.

All the following time-variant concentration profiles are plotted for a fixed position in the polymeric matrix ($x = 0.005\ cm$) and in the biological tissue ($x = 0.05\ cm$). The influence of unbinding rate constant (β_0) on both free (C_0) and loaded drug (C_L) concentrations in the polymeric matrix phase are shown in Figs. 4.9 and 4.10 over a specified period of time. With the increase in the unbinding rate, the free drug concentration enhances rapidly at first to reach its zenith and on that account, the rate of diffusion increases. As a result, the concentration profile declines faster than those corresponding to lower values of β_0. As discussed in Chapter 3, just like microparticle, the drug is dispersed in the polymeric matrix in such a way that the solid and free phases remain in intermingled state after the initiation of dissolution and dissociation phenomena. As a result, increased concentration of free drug C_0 in comparison to that of solid drug C_L leads to higher rate of drug diffusion out of the polymeric matrix due to less hindrance by the solid phase. On the other hand, the loaded drug concentration diminishes from its extremity with increasing β_0 as anticipated.

The effect of binding rate constant (δ_0) on both the free (C_0) and loaded drug (C_L) concentrations in the same phase is depicted in Figs. 4.11 and 4.12 over the entire period of time. When the binding rate is allowed to increase, the free drug concentration increases owing to the reason that recrystallisation of free drug into loaded drug augments and minimum amount of free drug diffuses out of the matrix. One may remark in this context that in the event of minimum binding rate, most of the drug in the polymeric matrix is in the form of free drug and accordingly the diffusion of the drug becomes maximum. The usual behaviour of the enhancement of loaded drug concentration with increasing δ_0 is also perceived in the matrix phase under consideration. In Fig. 4.12, a shallow bulge is observed when the binding rate constant rises above a threshold value. Binding-unbinding are synchronous phenomena and hence, enhanced binding rate constant hinders loaded drug to diminish smoothly after a specified time, outshining the upshots of unbinding and solubilisation phenomena.

As porosity of the polymeric matrix is one of the significant components, its impact on drug concentration in the drug kinetics cannot be ruled out. The profiles of Fig. 4.13 exhibit how the time-variant free drug concentration C_0 increases to attain its peak and thereafter declines over the entire passage of time. In the event of decreasing porosity (ε_0), the free drug concentration becomes higher due to lower rate of diffusion. On the other hand, the solid drug concentration C_L drops down faster from its fixed initial value for higher permeability and takes smaller time to dissipate than those with lower permeability as evident from Fig. 4.14. Moreover, in Fig. 4.14, a similar bulge is discerned at low porosity value. The basis of this slight distortion is that low porosity value allows reduced accessible void volume for solid drug to transform into free drug.

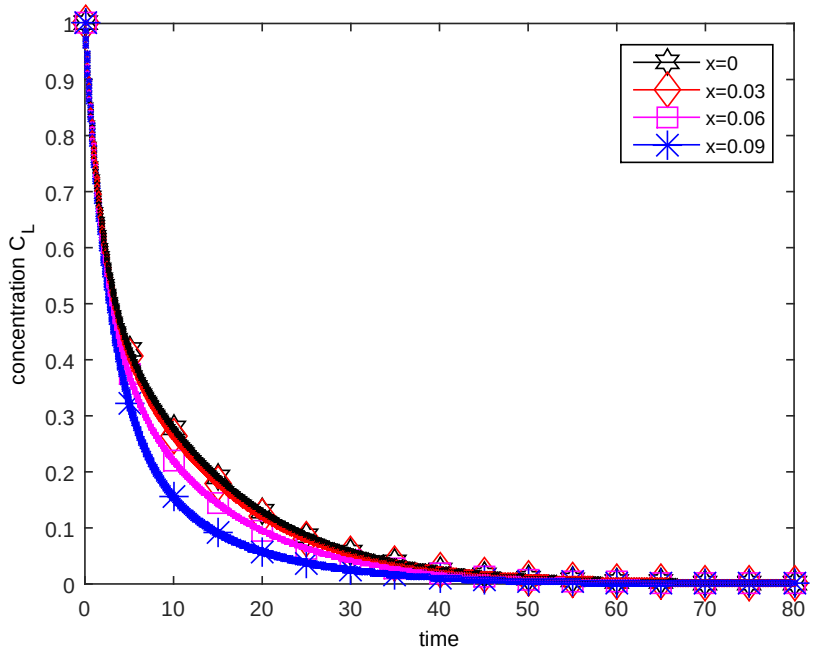

Figure 4.4: Time variant concentration profile of C_L at different locations.

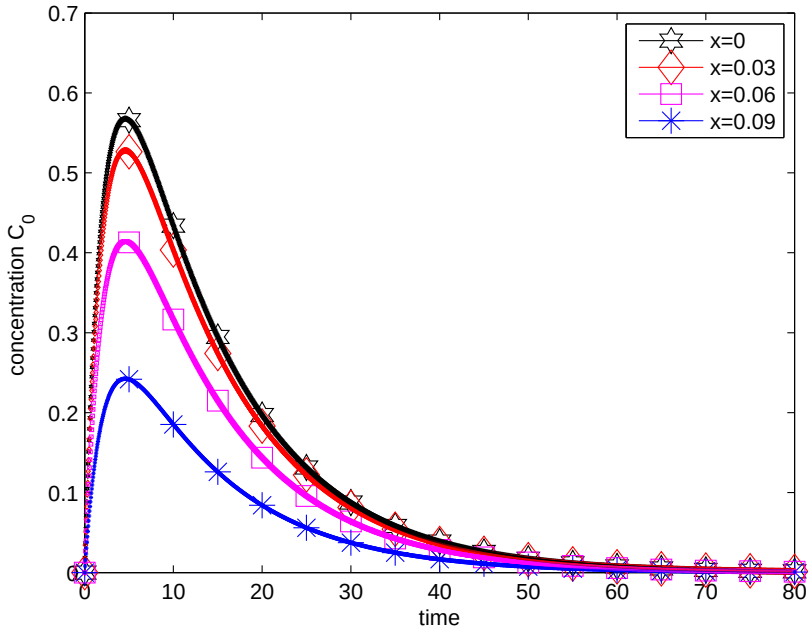

Figure 4.5: Time variant concentration profile of C_0 at different locations.

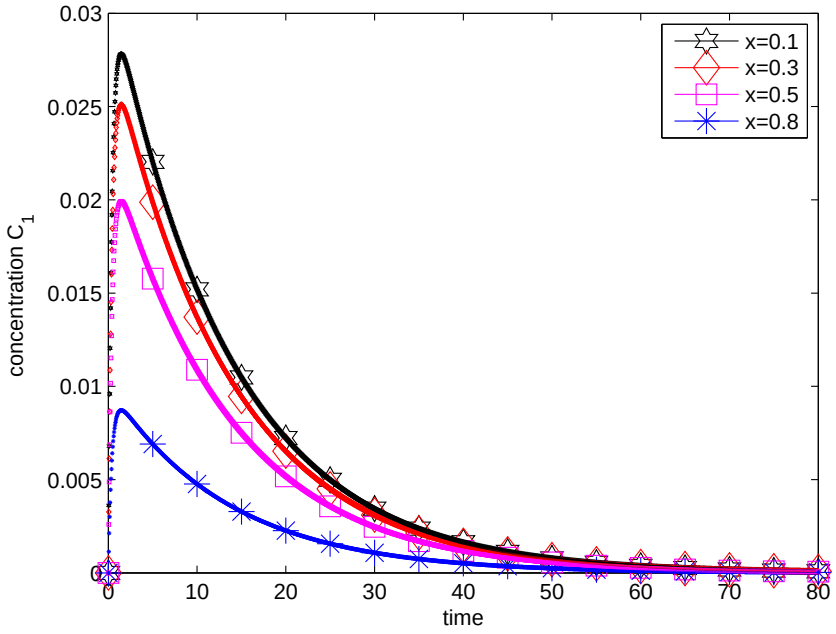

Figure 4.6: Time variant concentration profile of C_1 at different locations.

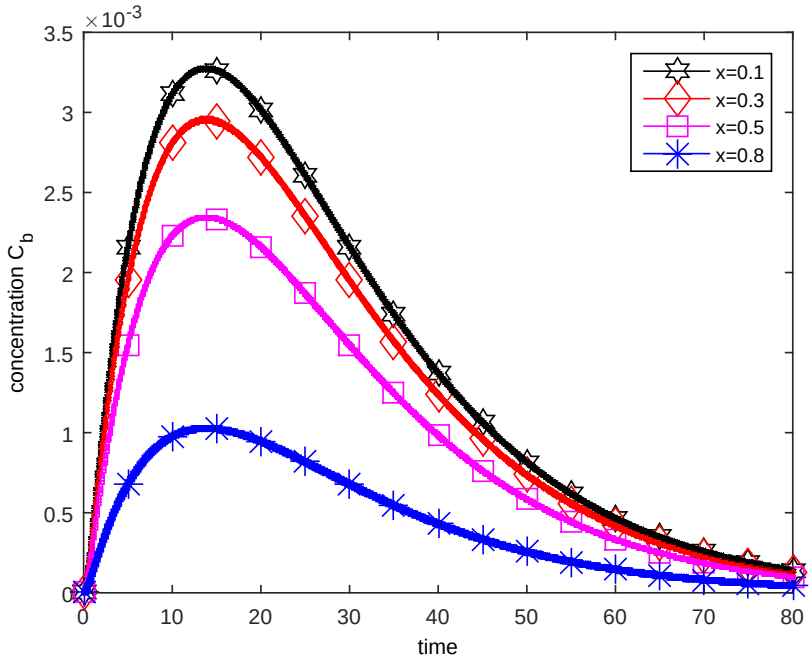

Figure 4.7: Time variant concentration profile of C_b at different locations.

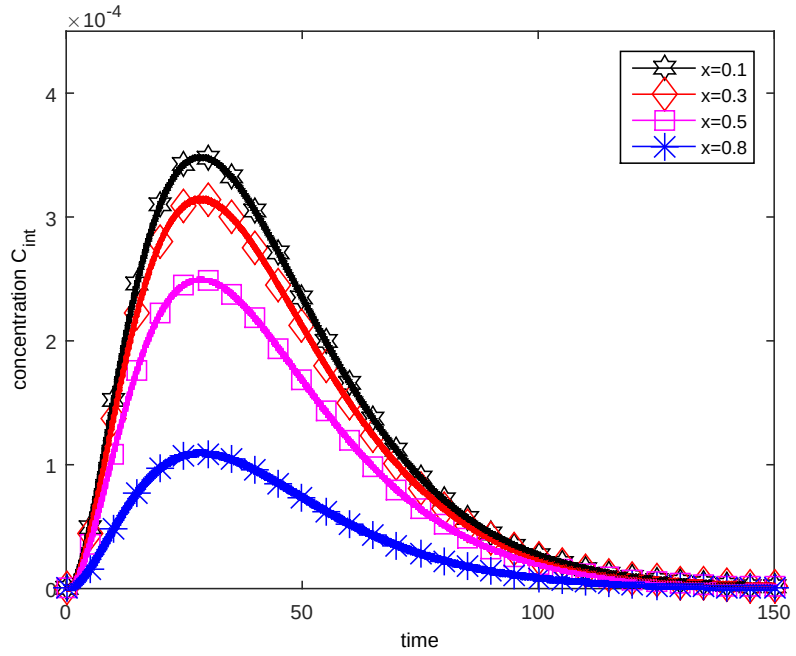

Figure 4.8: Time variant concentration profile of C_{int} at different locations.

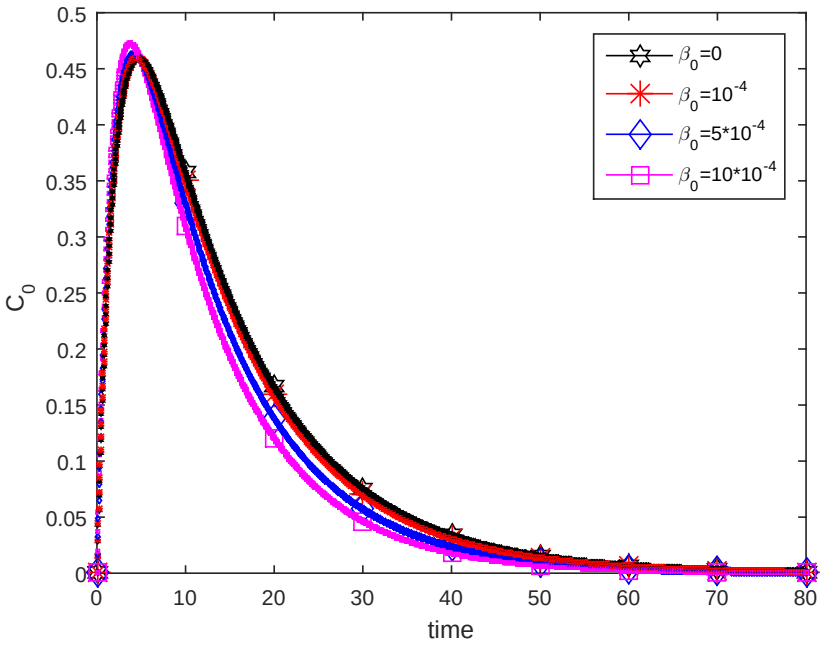

Figure 4.9: Time variant concentration profile of C_0 for different β_0 .

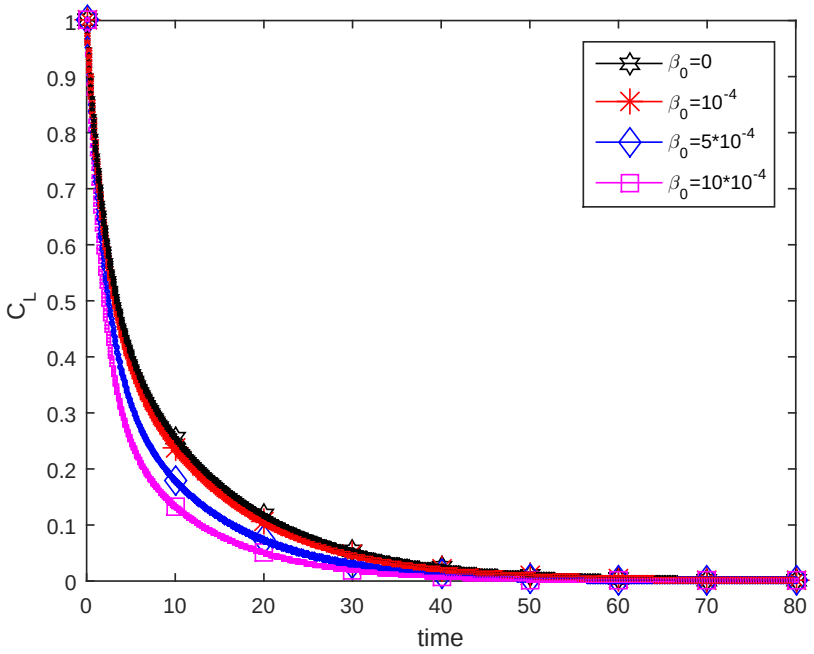

Figure 4.10: Time variant concentration profile of C_L for different β_0 .

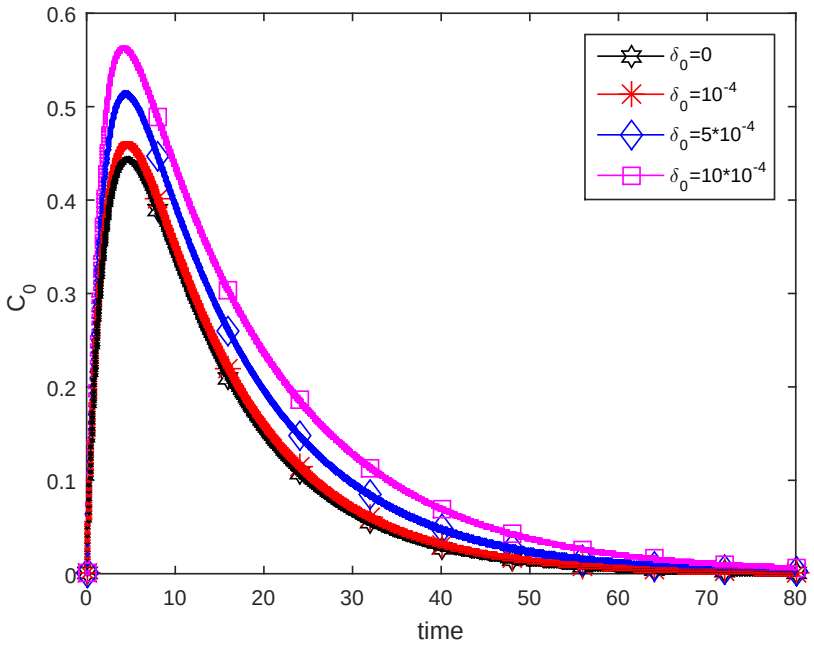

Figure 4.11: Time variant concentration profile of C_0 for different δ_0 .

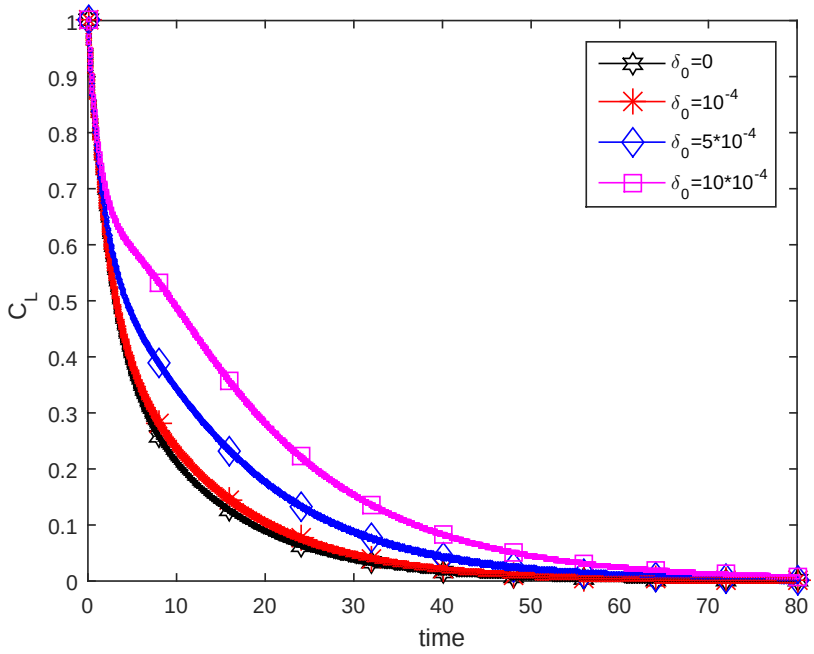

Figure 4.12: Time variant concentration profile of C_L for different δ_0 .

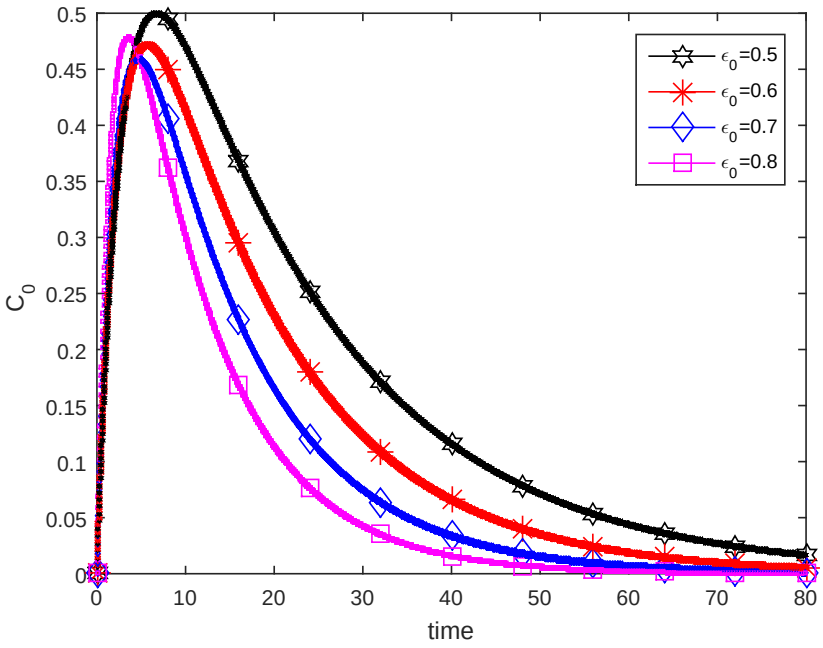

Figure 4.13: Time variant concentration profile of C_0 for different ε_0 .

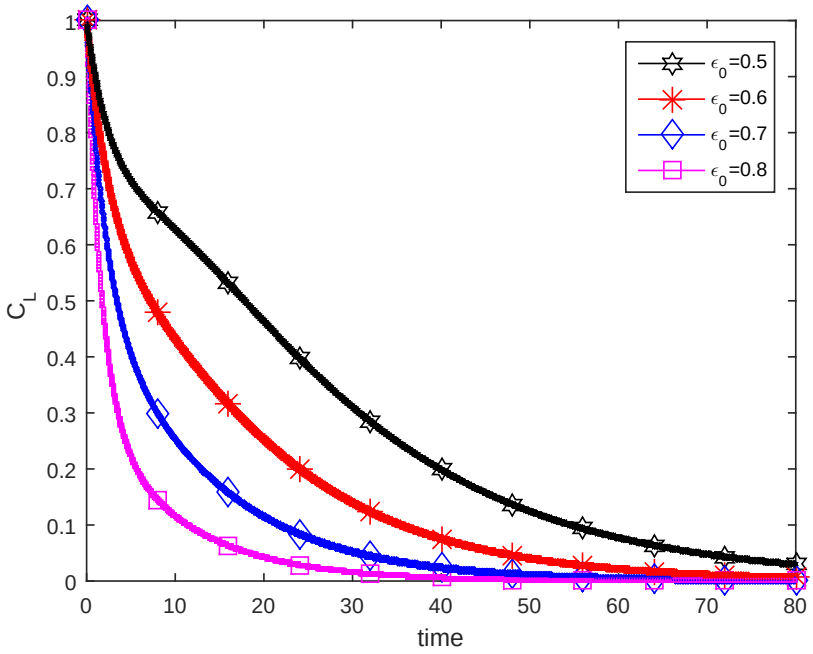

Figure 4.14: Time variant concentration profile of C_L for different ε_0 .

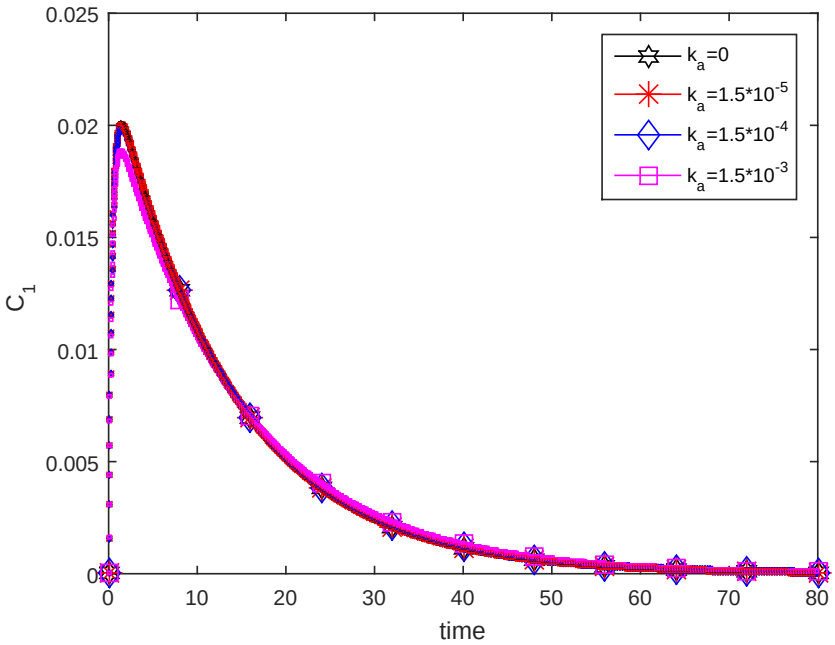

Figure 4.15: Time variant concentration profile of C_1 for different k_a .

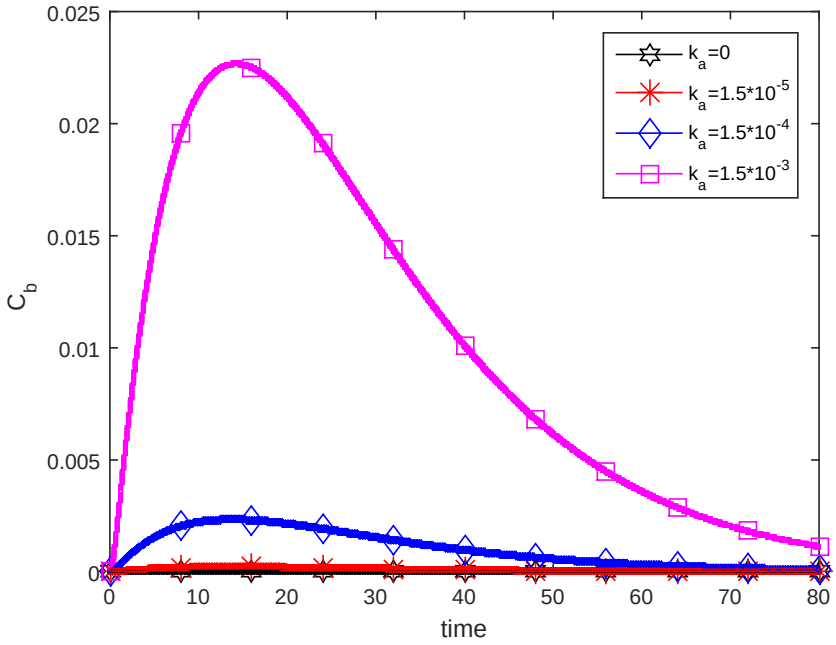

Figure 4.16: Time variant concentration profile of C_b for different k_a .

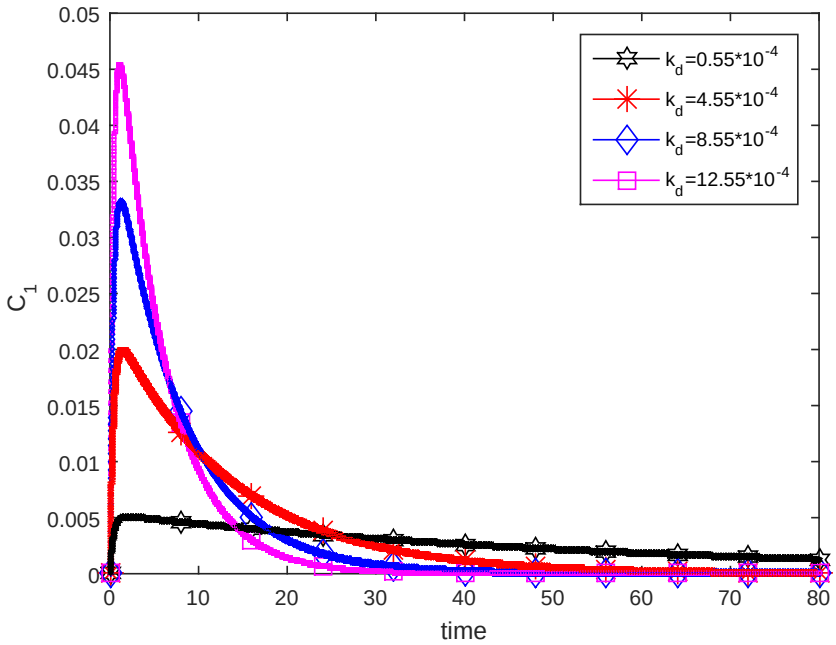

Figure 4.17: Time variant concentration profile of C_1 for different k_d .

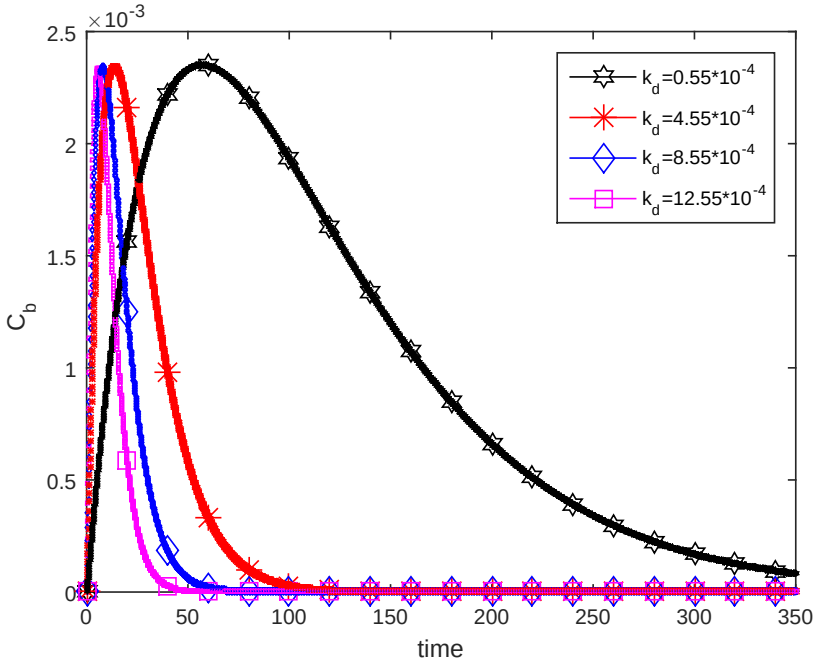

Figure 4.18: Time variant concentration profile of C_b for different k_d .

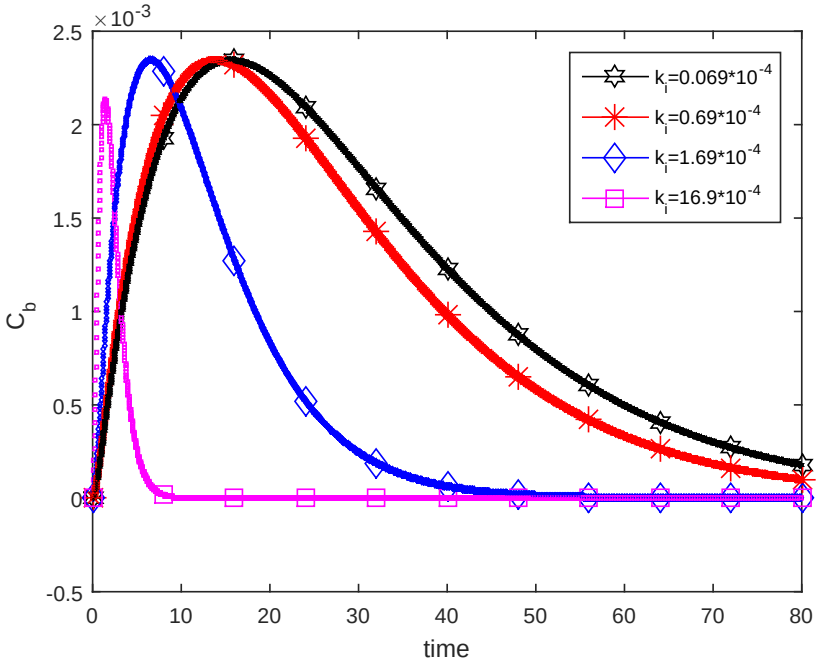

Figure 4.19: Time variant concentration profile of C_b for different k_i .

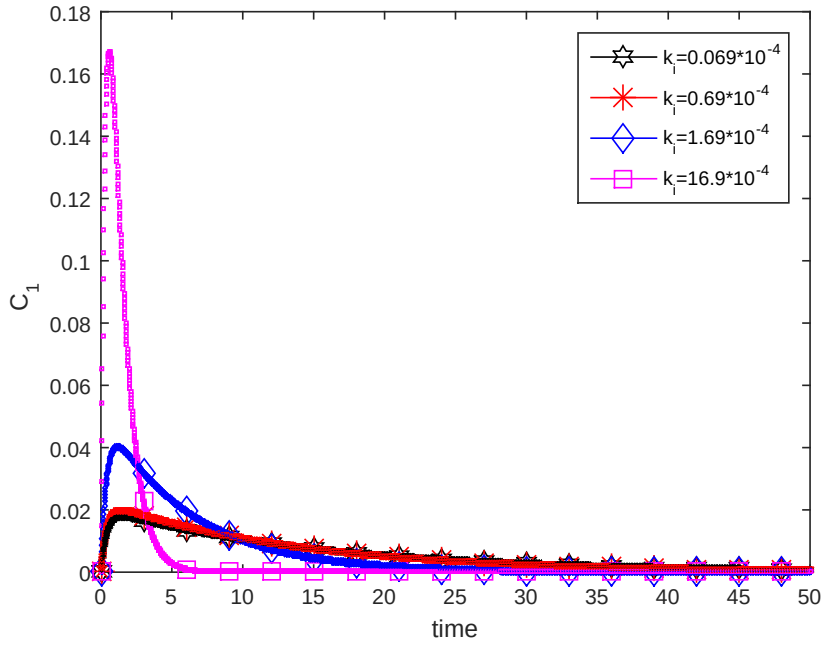

Figure 4.20: Time variant concentration profile of C_1 for different k_i .

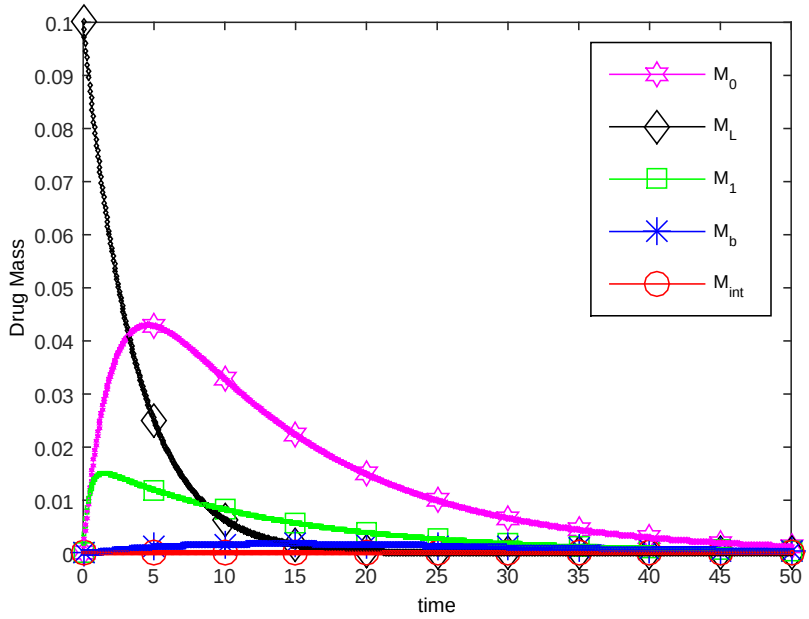

Figure 4.21: Time variant profile of drug masses.

Figures 4.15 and 4.16 record the respective concentration profiles of both free (C_1) and bound drug (C_b) in the tissue phase with various values of association rate constant (k_a) over a span of time. While meagre variation of the free drug concentration is observed even if one varies k_a from 0 to $1.5 * 10^{-3}$, there is substantial deviation of bound drug concentration subject to association rate constant. When association rate increases, the amount of bound drug concentration enhances appreciably over the entire period of time but in the absence of drug binding rate ($k_a = 0$), no bound drug is formed from free drug at all, which is clearly evident from the graph.

The time variant drug concentration profiles in the tissue get largely perturbed by the dissociation rate parameter (k_d) as displayed in Figs. 4.17 and 4.18. When the dissociation rate is allowed to increase in phases, both the free (C_1) and bound drug (C_b) concentration profiles appear to diminish significantly in subsequent phases. When the dissociation rate constant is large, the bound drug formed from free drug takes minimal time to transform back to free drug. As a consequence, free drug concentration increases rapidly to reach its zenith, but after attaining the maximum value it diminishes rapidly. This is because the presence of abundant free drug in the tissue particularly in the vicinity of the rate controlling membrane, retards heavily the rate of diffusion of free drug into the tissue. Moreover, since bound drug is getting internalized with time, very small amount of bound drug is left to get back to free drug. On the other hand, when k_d is small, bound drug is being re-transformed into free drug nominally lead to the well balanced rate of diffusion of free drug into the tissue, allowing the stable free drug concentration before it vanishes completely. Since binding and unbinding phenomena in the tissue occur synchronously and as it is observed that with lower k_d, free drug concentration peak is less, bound drug concentration takes enhanced time to attain its pinnacle in addition to prolonged time to eventually vanish. On the contrary, with increased dissociation rate, due to higher free drug concentration, bound drug concentration attains its maximum value in less time due to unchanged association rate constant.

Internalization is the penultimate step of the drug transport under consideration, where the bound drug is engulfed by the cell of the biological tissue through the process of endocytosis. Effect of variation of internalization rate constant (k_i) on bound (C_b) and free drug (C_1) concentrations in the tissue is demonstrated in Figs. 4.19 and 4.20. With increasing k_i, the bound drug rapidly diminishes to zero, which is quite natural. If it is observed minutely, then one may notice that with increasing k_i, bound drug concentration reaches its pinnacle quickly at the very onset. This is due to the fact that k_a and k_d are unchanged and all the undergoing phenomena are well synchronised and instantaneous, eventually the combined effects of binding / unbinding overshadows the internalization process at the beginning, which is a little late runner in the race. Though the free drug concentration is not directly related to the internalization phenomenon, yet one may observe an overwhelming effect especially when k_i is increased from $1.69 * 10^{-4}$ to $16.9 * 10^{-4}$. This is due to the fact that with escalated internalization parameter, bound drug gets internalized too hastily to accelerate the diffusion rate of free drug into the tissue.

Finally, the behaviour of all the drug masses for both the phases of polymeric matrix and the tissue with time is depicted in Fig. 4.21. It appears that the solid drug mass in the matrix declines asymptotically with time from its initial value while its free counterpart increases initially, rises to a maximum at a

particular instant of time and thereafter diminishes gradually for rest of the time. In addition to these, the drug mass of free, bound and internalized drugs in the tissue increases initially by a smaller amount and continues to follow small variations with time. Their behaviour further reveals that both the free and solid drug masses in the matrix melt away in a comparatively small span of time than those in the tissue where they demand much longer period of time to get the drug masses absorbed completely. Thus, one may infer from these observations that monotony in the profiles of drug masses in the tissue elucidates that uniform concentration of drug is accessible to the tissue, which abates side-effects appreciably.

4.5 Conclusions

Of concern, the work undertaken is the characterization of concentration of drug in its different states through the process of solubilisation, recrystallisation, binding / unbinding and internalization in order to release drug from polymeric matrix to the biological tissue. The study ventured speaks volumes about its merits and upgradation. First, the model formulated is very general and more realistic since it takes into account those relevant, imperative and vital phenomena whose domination in the environs of drug kinetics are too significant to neglect. Secondly, the obtained closed form analytical solutions of the governing equations add spice to the present undertaking. The previous accomplishments in this domain of research are predominantly based on either numerical methods or semi-analytical approaches. Thirdly, drug internalization is one of the governing processes for drug metabolism in the physiological environment [157], hence its incorporation in the mathematical model is necessary. In the present study, lysosomal degradation is also incorporated along with internalization, which connect the rift between mathematical modelling and pharmacology in a much better fashion. Fourthly, notwithstanding the amenity of nonlinear models in drug kinetics, the current advocated model depicts outcomes in the embodiment of graphical representations reasonably akin to that of nonlinear models proposed in the work of Zhu and Braatz [157]. This manifests the fidelity of the postulated linear portrayal. Lastly, comparison of the proposed model with experimental evidence reveals the gravity of the proffered model in apprehending the pragmatic physical phenomena of drug kinetics. The sensitivity of the model parameters poses challenges to the applicability of drug administration for treatment of patients at large through pharmacotherapy. The salient observations of the present investigation reveal to draw various conclusions, like drug diffusion and drug assimilation rates are inversely proportional to the drug binding rate. It may also be highlighted that as both loaded and free drug particles in polymeric matrix melt away in comparatively small span of time than those in the tissue. Hence, the drug influence in the tissue will certainly persist for a long time before repeated medication occurs and hence care needs to be exercised for maintaining appropriate time-gap before redispensation in order to avoid toxicity by the presence of excess drug. The fact that membrane permeability of the polymeric matrix, together with association / dissociation rate, affects the drug concentration significantly in the first phase while the drug concentration in the second phase is largely influenced by the binding / unbinding and internalization rates as well, depicts the significance of the model parameters. Any approach of the present one may be of use in other parts of the human body provided the system does

not have major clinical complexity. The outcomes of the model under study will certainly be of some assistance for evolution of future models through the introduction of several important components not addressed here depending on the objectives of the drug release phenomena adhere to the real situation.

5 DRUG RELEASE FROM DEGRADABLE POLYMERIC MATRIX

The foregoing treatment of this chapter is focussed on drug release mechanism from degradable polymeric matrix through mathematical model with the objectives as enlisted in Chapter 1.

5.1 Introduction

The first stride of pharmacometrics is the classical pharmacokinetic analysis. There are two principal perspectives in the classical pharmacokinetic analysis, namely, compartmental and non-compartmental analyses. The compartmental analysis is based on mass balance equations on various interacting compartments, whereas for non-compartmental one, it is the statistical moments, playing pivotal role, derived from time course of the drug concentration data. The compartmental models are commonly applied to simulate concentration profiles from one dosage form to another. The major limitation of compartmental modelling is that the unrevealed physiology of the model and the proposed model presentation is based on the analyst's exposition. The physiologically based pharmacokinetic model is unfolded to subdue the restrictions of the compartmental modelling. The structure of the model, characteristics of the compartments and the parameters are rooted in accordance with the physiological and biological processes that are accountable for drug release and disposition.

In order to victoriously sail across the applied field of transport in biological media, the comprehension of the theoretical and the computational facets of transport modelling is a necessity. Moreover, this endeavour needs a basic perception of the physiological essence of the biological media in which the transport phenomena are prevalent. Empirical considerations, though vital in discerning the actuality and the action of transport phenomena inside the living biological tissue, do not inevitably grant direct apprehension of the physics concealed in the phenomena. Likewise, empirical models, that are competent to anticipate the upshots of transport in order to exactly match controlled experimental environment, do not necessitate to represent the physical laws dominating the transport. In recent times, there has been a shove in research circle to dump empirical modelling entirely in order to advocate

mechanistic physics-based postulations of transport mechanism. The present investigation is to nurture the comprehension of amalgamated accomplishment of the physics, the mathematical modelling and the biological physiology for the sake of bridging the gap between biological perspectives and transport modelling.

Biodegradable polymers are generally used as coatings for the polymeric matrix. These polymers are suitable for effective drug release as an outcome of the coupled action of degradation and erosion. Although degradation and erosion are entangled, they represent non-identical processes. Degradation is a chemical phenomenon, which breaks the chemical bonds in the polymers, resulting into monomers and oligomers. On the other hand, erosion supervises the loss of material followed up with the monomers and oligomers vacating the polymeric matrix [50]. Degradation and erosion blend in order to synchronize drug release rate in the polymeric coatings [40]. For designing and studying poly(D,L-lactic-*co*-glycolic acid) (PLGA) stent coatings, trial-and-error experimental studies are conducted [146, 153, 103, 37]. Modelling degradation and erosion is a necessity for formulating drug release kinetics, where mechanistic approaches are generally used [121, 129]. A favourable viewpoint for describing degradation is through first-order degradation models [131, 116, 20, 35]. The exploration conducted successfully by Zhu and Braatz [158] in the recent past is pedestalled on polymer degradation and erosion in a biodegradable stent along with consequent drug release by overlooking the minute details of drug release phenomena without illumining the hazy and misty arena of drug transport.

In the current study, proposal of a general but, a simple mathematical model of polymer degradation and drug release from a local drug delivery device to the adjacent biological tissue is accorded. Polymer degradation is sketched with mass conservation equations. The method of moments is utilized for formulating polymer degradation. Additionally, a two-phase drug release model is advocated mathematically considering solubilisation and recrystallisation phenomena in the polymeric matrix phase along with binding, unbinding and internalization phenomena in the biological tissue. Besides, variable diffusivity of drug (that diffuses out of polymeric matrix) is proposed using the combined action of change-in-porosity, change-in-molecular weight of the polymer coating plus drug partitioning. The target of the present study is to solve the system of governing differential equations analytically and to have a thorough sensitivity analysis of key parameters producing phenomenal brush strokes in the canvas of drug release kinetics. Moreover, the aspired objectives lead to comparison of the proposed model with experimental evidence proclaiming the gravity of the present model in perceiving the realistic physical phenomena of drug kinetics.

5.2 Formulation of the problem

The advocated mathematical model of local drug delivery device, a two-phase system, is constituted of a polymeric matrix regarded as a chamber, where drug is loaded at the beginning, and the edging biological tissue, where the therapeutic compound is being delivered. The polymeric matrix is regarded as a biodegradable polymeric coating that is being degraded gingerly and it is enclosed on one side with

an impermeable backing while the other one merges with the tissue. In the tissue part, the reversible unbinding / binding and internalization processes of drug are spotlighted. Customarily, mass transport prevails in the direction normal to the tissue leading to the restraint of the propounded model to one dimensional only.

Mechanisms of polymer degradation, drug release and drug transport

In accomplishing the pertinence in complete drug release phenomenon, degradation and erosion of a polymeric matrix with one accord plays a pivotal role. Degradation may be defined as a chemical process by means of which polymer backbones are chopped to form monomers and oligomers while, the erosion denotes a physical phenomenon portraying the loss of materials processed from monomers and oligomers. The degradation and erosion are generally quantified by polymer molecular weight (MW) change and mass loss correspondingly. In the current study, the familiar degradation model is chosen for procuring the weight-average MW change as $M_w = M_{w,0}\ e^{-k_w t}$, $M_{w,0}$, being the initial weight-average MW and k_w is the degradation rate constant corresponding to weight-average MW decay. The drug release rate is synchronized mutually through the combined effect of both degradation and erosion. At the outset of erosion in the companionship of polymer degradation, as the smaller products (monomers and oligomers) diffuse out of the matrix, pores are produced and unfolded within the coating to invigorate drug diffusion. With the furtherance of drug diffusion and consequential reduction of polymer chain length, the activity of drug release boosts up.

The drug materializes absolutely in a solid phase rooted within the polymeric matrix (e.g. in crystalline form) (C_L) at its maximum concentration initially. Being in a bound state, it cannot be transported straight to the tissues. Water penetrates into the polymeric matrix and moistens the drug, leading to its solubilisation into free state (C_0) that ultimately diffuses out of the matrix into the tissue. A portion of solid drug ($\beta_0 C_L$) is re-transformed into its free state. Conversely, through a recrystallisation process, another fraction of free drug ($\delta_0 C_0$) is remoulded back to its bound state and a part of free drug (C_1) diffuses into the tissue. In tissue, a portion of free drug ($k_a C_1$) is metabolised into bound phase (C_b), which also dissociates ($k_d C_b$) to form free drug. Now, the bound drug is swallowed up (internalized) ($k_i C_b$) by the cells in the tissue through the process of endocytosis. Endocytosis is an active energy-using transport phenomenon in which molecules (proteins, drugs etc.) are transported into the cell. Thus bound drug gets turned into internalized drug particles (C_{int}). These internalized drug particles, after a spell of time, get degraded by the lysosomes and the drug remnants after degradation ($k_{id} C_{int}$) are voided out of the cell into the extracellular fluid. The complete process is schematically illustrated in Fig. 5.1.

Polymer degradation

The governing equations depicting polymer degradation (into oligomers and monomers) and erosion by diffusion reaction are given by

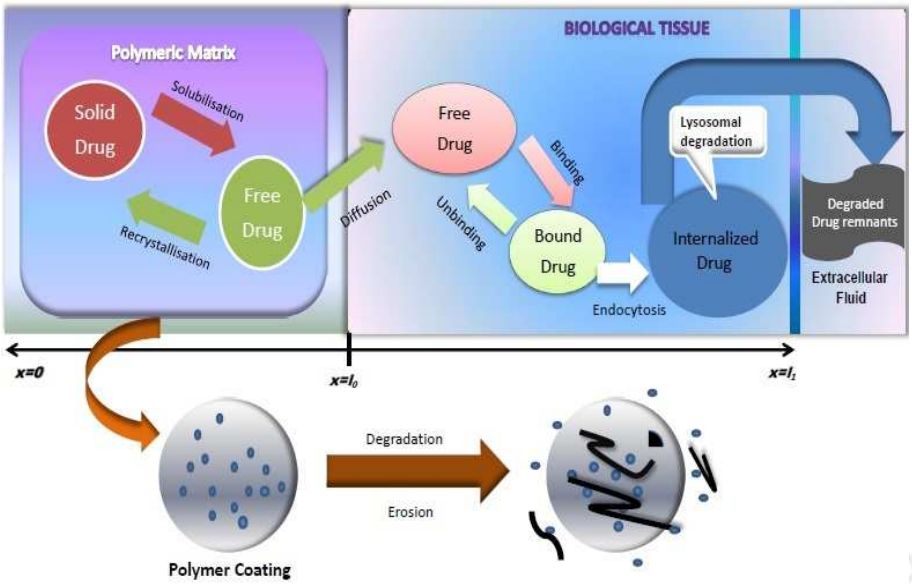

Figure 5.1: Schematic diagram of drug transport along with polymer degradation

Monomers:

$$\frac{\partial C_M}{\partial t} = \frac{\partial}{\partial x_p}\left[D_M(M_w,\phi)\frac{\partial C_M}{\partial x_p}\right] + 2k_{dd}(x_p)\Sigma_{j=2}^{\infty}C_j, \tag{5.2.1}$$

Oligomers: For $2 \leq i \leq 9$

$$\frac{\partial C_i}{\partial t} = \frac{\partial}{\partial x_p}\left[D_i(M_w,\phi)\frac{\partial C_i}{\partial x_p}\right] + 2k_{dd}(x_p)\Sigma_{j=i+1}^{\infty}C_j - k_{dd}(x_p)(i-1)C_i, \tag{5.2.2}$$

Polymers: For $n > 9$

$$\frac{\partial C_n}{\partial t} = 2k_{dd}(x_p)\Sigma_{j=n+1}^{\infty}C_j - k_{dd}(x_p)(n-1)C_n, \tag{5.2.3}$$

where C_M and C_n are the concentrations of the monomers and polymers while C_i represents that of oligomers, i and n depict the length of the polymer, D_i and D_M are the effective diffusivities and x_p is the horizontal coating thickness. M_w and ϕ designate the average molecular weight of the polymer and matrix porosity respectively while k_{dd} represents the degradation rate constant corresponding to number-average molecular weight change. The above model is based on the following assumptions [158]:

- The pH gradient inside the polymer coating is assumed to be insignificant on account of the fast diffusion of monomers at the length scale of the polymeric matrix. This follows to homogeneous degradation all through the coating.

- The monomers diffuse out of the coating much faster than the oligomers. Hence, it is supposed that only monomers play pivotal role to erosion initially before disintegration of the polymeric matrix. The diffusion terms in the above equations can be isolated from degradation reaction in accordance with the aforementioned assumption.

Drug release

The governing equations bespeaking the dynamics of drug release in the polymeric matrix are given by

$$\frac{\partial C_L}{\partial t} = -k_m(C_{lim} - C_0) - \beta_0 C_L + \delta_0 C_0, \qquad x \in (0, l_0), \tag{5.2.4}$$

$$\frac{\partial C_0}{\partial t} = D_0 \frac{\partial^2 C_0}{\partial x^2} + k_m(C_{lim} - C_0) + \beta_0 C_L - \delta_0 C_0, \qquad x \in (0, l_0), \tag{5.2.5}$$

where C_L denotes available molar concentration of solid drug, C_0 is the available molar concentration of free drug, l_0 is the length of the polymeric matrix, k_m is mass transfer coefficient, C_{lim} stands for drug solubilisation limit, β_0 is the dissociation rate constant, δ_0 is the association rate constant, D_0 is the effective diffusion coefficient of free drug (C_0) in the matrix, defined by, as in [158]

$$D_0 = \frac{(1-\phi)D_s + k\phi D_l}{1 - \phi + k\phi}, \tag{5.2.6}$$

where D_s is the diffusivity in the polymer phase, D_l is the diffusivity in liquid-filled pores, ϕ is the porosity and k is the drug partitioning between the liquid-filled pores and solid phase. Now, D_s and ϕ are defined as

$$D_s = D_{s0}\left(\frac{M_w}{M_{w,0}}\right)^{-1.714}, \tag{5.2.7}$$

$$\phi = \phi_i + (1 - \phi_i)(1 + e^{-2k_{dd}t} - 2e^{-k_{dd}t}), \tag{5.2.8}$$

where D_{s0} is the initial diffusivity of the solid phase and ϕ_i is the initial porosity.

Drug transport

The corresponding equations governing the dynamics of drug in the tissue are

$$\frac{\partial C_b}{\partial t} = k_a C_1 - k_d C_b - k_i C_b, \qquad x \in (l_0, l_1), \tag{5.2.9}$$

$$\frac{\partial C_1}{\partial t} = D_1 \frac{\partial^2 C_1}{\partial x^2} - k_a C_1 + k_d C_b, \qquad x \in (l_0, l_1), \tag{5.2.10}$$

$$\frac{\partial C_{int}}{\partial t} = k_i C_b - k_{id} C_{int}, \qquad x \in (l_0, l_1), \tag{5.2.11}$$

where C_1 is the molar available concentration of free drug in the tissue, C_b is the molar available concentration of bound drug in the tissue, C_{int} denotes the molar concentration of internalized drug

particles, $l_1 - l_0$ is the length of the tissue, k_a depicts the binding rate coefficient, k_d is the dissociation rate coefficient, k_i stands for internalization rate coefficient, k_{id} denotes degradation rate constant in the lysosome, and D_1 is the diffusion coefficient of free drug in the biological tissue.

Initial, interface and boundary conditions

The set of partial differential equations (5.2.1) - (5.2.3) are reduced to a set of ordinary differential equations which are solved using the method of moments [158]. The method of moments may be used as the first approximation to the solution. The main advantage of this method is that the lower-order moments can be traced directly without knowing the details of the distribution. The initial conditions for monomers and oligomers are considered as null concentration and hence the initial conditions for statistical moments are referred to non-degraded polymers.

The initial conditions for the remaining set of equations are as follows:
since the solid loaded drug is prevalent initially without any of its transformed forms, so
$C_L(x,0) = G$, $C_0(x,0) = 0$, $C_b(x,0) = 0$, $C_1(x,0) = 0$, $C_{int}(x,0) = 0$, where G is the maximum value of loaded solid drug concentration.
A flux continuity must be assigned at the interface, that is at $x = l_0$, $-D_0 \frac{\partial C_0}{\partial x} = -D_1 \frac{\partial C_1}{\partial x}$.
At $x = l_0$, a concentration jump may occur: $-D_1 \frac{\partial C_1}{\partial x} = P_1(C_0 - C_1)$,
where P_1 is the overall mass transfer coefficient.
No mass flux can pass to exterior environment due to the presence of impermeable backing and hence no flux condition at $x = 0$, becomes $D_0 \frac{\partial C_0}{\partial x} = 0$.
Lastly, at $x = l_1$, $C_1(l_1,t) = 0$, $t > 0$.

5.3 Model solutions

The moment method is utilized to solve equations (5.2.1) - (5.2.3) analytically in terms of μ_n as the nth order moment of polymers as

$$\mu_0 = \mu_1 + \mu_1 \left(\frac{1}{X_{n,0}} - 1 \right) e^{-k_{dd}t}, \tag{5.3.1}$$

$$C_M = \mu_1 + \mu_1 \left(1 - \frac{2}{X_{n,0}} \right) e^{-2k_{dd}t} + 2\mu_1 \left(\frac{1}{X_{n,0}} - 1 \right) e^{-k_{dd}t}, \tag{5.3.2}$$

where $X_{n,0}$ is the initial number-average degree of polymerization. The number-average degree of polymerization is defined as the fraction of total number of monomer units (μ_1) to the total concentration of polymer chains (μ_0),

$$X_n = \frac{\mu_1}{\mu_0} = \frac{1}{1 + \left(\frac{1}{X_{n,0}} - 1 \right) e^{-k_{dd}t}}. \tag{5.3.3}$$

As $t \to \infty$, $X_n \to 1$ which designates complete degradation of the polymer into monomers.

The degradation of biodegradable polymers is affected by numerous factors comprising chemical composition, molecular structure, morphology and many more processing conditions of the polymers. Cor-

relating the degradation rate with all these afore-mentioned factors and harmonizing it with drug release quantitatively is an intimidating job. However, the present study paves the way to develop a phenomenological framework based on the understanding of the underlying biodegradation mechanisms, in a simple, yet, general approach.

All the remaining equations (5.2.4) - (5.2.11) together with the stated conditions are made dimensionless for their tractability.

5.3.1 Dimensionless equations

All the variables and parameters are now made dimensionless in order to make simplified computations in the following way:

$$\bar{x}=\frac{x}{l_1},\quad \bar{t}=\frac{D_1 t}{l_1^2},\quad \overline{l_i}=\frac{l_i}{l_1},\ i=0,1,\quad D=\frac{D_0}{D_1},\quad \overline{C_j}=\frac{C_j}{G}, j=L,0,1,b,int,lim,$$
$$\overline{\beta_0}=\frac{\beta_0 l_1^2}{D_1},\quad \overline{\delta_0}=\frac{\delta_0 l_1^2}{D_1},\quad \overline{k_y}=\frac{k_y l_1^2}{D_1},\ y=w,dd,d,a,m,i,id,\quad \Pi=\frac{P_1 l_1}{D_1}.$$

Bars over the parameters are omitted for convenience, so the aforementioned equations are as follows:

$$\frac{\partial C_L}{\partial t}=-k_m(C_{lim}-C_0)-\beta_0 C_L+\delta_0 C_0,\qquad x\in(0,l_0), \tag{5.3.4}$$
$$\frac{\partial C_0}{\partial t}=D\frac{\partial^2 C_0}{\partial x^2}+k_m(C_{lim}-C_0)+\beta_0 C_L-\delta_0 C_0,\qquad x\in(0,l_0), \tag{5.3.5}$$
$$\frac{\partial C_b}{\partial t}=k_a C_1-k_d C_b-k_i C_b,\qquad x\in(l_0,1), \tag{5.3.6}$$
$$\frac{\partial C_1}{\partial t}=\frac{\partial^2 C_1}{\partial x^2}-k_a C_1+k_d C_b,\qquad x\in(l_0,1), \tag{5.3.7}$$
$$\frac{\partial C_{int}}{\partial t}=k_i C_b-k_{id} C_{int},\qquad x\in(l_0,1). \tag{5.3.8}$$

The initial, interface and boundary conditions in dimensionless approach are the following:

$$C_L(x,0)=1,\quad C_0(x,0)=0,\quad C_b(x,0)=0,\quad C_1(x,0)=0,\quad C_{int}(x,0)=0, \tag{5.3.9}$$
$$-D\frac{\partial C_0}{\partial x}\Big|_{x=l_0}=-\frac{\partial C_1}{\partial x}\Big|_{x=l_0}, \tag{5.3.10}$$
$$-\frac{\partial C_1}{\partial x}\Big|_{x=l_0}=\Pi(C_0-C_1)\Big|_{x=l_0}, \tag{5.3.11}$$
$$\frac{\partial C_0}{\partial x}\Big|_{x=0}=0,\qquad C_1(1,t)=0. \tag{5.3.12}$$

The analytical solutions of these equations in their dimensionless form are thus obtained with the help of separation of variables technique as follows:

$$C_0=(e^{-d_1 t}-e^{-d_2 t})\cos ax, \tag{5.3.13}$$

$$C_L = \frac{(k_m+\delta_0)\cos ax}{(d_1-\beta_0)(d_2-\beta_0)}\left[(d_1-\beta_0)e^{-d_2t}-(d_2-\beta_0)e^{-d_1t}+(d_2-d_1)e^{-\beta_0 t}\right]$$

$$-\frac{k_m C_{lim}}{\beta_0}\left[1-e^{-\beta_0 t}\right]+e^{-\beta_0 t}, \tag{5.3.14}$$

$$C_1 = E_2(e^{-m_1t}-e^{-m_2t})\cos bx, \tag{5.3.15}$$

$$C_b = \frac{E_2 k_a \cos bx}{(k_d+k_i-m_1)(k_d+k_i-m_2)}\left[(k_d+k_i-m_2)e^{-m_1t}-(k_d+k_i-m_1)e^{-m_2t}\right.$$

$$\left.+(m_2-m_1)e^{-(k_d+k_i)t}\right], \tag{5.3.16}$$

$$C_{int} = \frac{E_2 k_a k_i \cos bx}{(k_d+k_i-m_1)(k_d+k_i-m_2)}\left[\frac{(k_d+k_i-m_2)}{(k_{id}-m_1)}(e^{-m_1t}-e^{-k_{id}t})\right.$$

$$\left.-\frac{(k_d+k_i-m_1)}{(k_{id}-m_2)}(e^{-m_2t}-e^{-k_{id}t})+\frac{(m_2-m_1)}{(k_{id}-k_d-k_i)}(e^{-(k_d+k_i)t}-e^{-k_{id}t})\right], \tag{5.3.17}$$

where a (obtained by approximating trigonometric function having small argument) and E_2 are determined from the following relations obtained from (5.3.10) - (5.3.11) respectively:

$$\frac{\Pi}{Da}\cot(al_0) = 1+\frac{\Pi}{b}\cot(bl_0). \tag{5.3.18}$$

$$E_2 = \frac{m_1\ m_2\ D\ a\ \sin(al_0)\ (d_2-d_1)}{d_1\ d_2\ b\ \sin(bl_0)\ (m_2-m_1)}. \tag{5.3.19}$$

The quantities involved in the above expressions could be systematically defined as follows:

$$d_1 = \frac{A-\sqrt{A^2-4B}}{2}, \quad d_2 = \frac{A+\sqrt{A^2-4B}}{2}, \quad A = k_m+\beta_0+\delta_0-\lambda$$

$$B = -\lambda\beta_0, \quad \lambda = -a^2D, \quad m_1 = \frac{P-\sqrt{P^2-4Q}}{2}, \quad m_2 = \frac{P+\sqrt{P^2-4Q}}{2},$$

$$P = k_d+k_i+k_a-\mu, \quad Q = k_ik_a-\mu(k_d+k_i), \quad \mu = -b^2, \quad b = 3.14/2l_1.$$

5.4 Experimental validation

Paclitaxel is an anti-cancer ("antineoplastic" or "cytotoxic") chemotherapy drug. Paclitaxel is categorized as a "plant alkaloid," a "taxane" and an "antimicrotubule agent." Mechanisms behind the release of Paclitaxel (PTX)from poly(ethylene glycol/poly(lactic-*co*-glycolic acid)) (PEG / PLGA) blend films are probed by coherent anti-Stokes Raman scattering (CARS) microscopy through the experimental study [72].

In their investigation, HPLC (High Performance Liquid Chromatography) is utilized to analyse the amount of PTX released from the (8:2) PLGA/PEG blend film and the PLGA film, where PBS (phosphate-buffered saline, pH 7.4) acts as the releasing medium. The short-term (24 hours) release profile is illustrated in Fig. 5A of [72]. In contradistinction to PTX release from the PLGA matrix, addition of 20% PEG stimulates the initial burst release of PTX in the first 8 hours and afterwards a quite stable pattern is followed (Fig. 5A of [72]).

To elucidate the practicality of the present mathematical model, focus is given to its experimental validation. The experimental set-up [72] of Paclitaxel distribution in poly(ethylene glycol)/ poly(lactide-co-glycolic acid) blend films is probed and harmonized with the drug released percentage-time profile (here, non-dimensionalised parameters are used), which is procured from the proposed mathematical model (Fig. 5.2). It can be noticed that the agreement of experimental data [72] with the theoretical drug released percentage profile is quite worthy of mention. When observed meticulously the results of Fig. 5.2, it can be visualized that towards the onset, the experimental data matches quite exactly, while towards the termination, there is a small deviation between the profile of present mathematical model and its experimental counterpart [72]. The rationale behind this consequence is that the current model deals with the free drug being transported to the biological tissue whereas the experimental framework [72] lacks in drug transport.

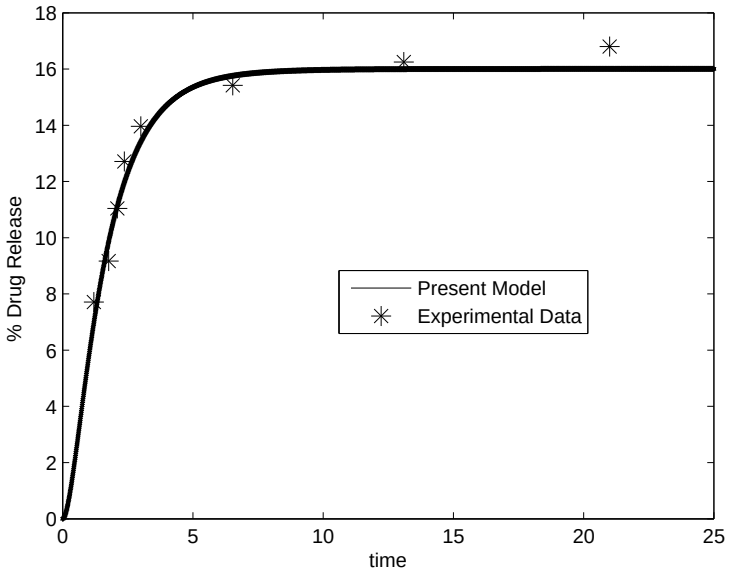

Figure 5.2: Agreement of the present theoretical results with existing experimental data [72].

5.5 Sensitivity analysis

For the purpose of characterization of the influences of the perturbations of the model parameters on the outcomes of the model, a sensitivity analysis is carried out. Of several approaches available at the

present time that have been applied to pharmacokinetic systems, the partial derivative-based method is found to be most fundamental one that requires varying parameter values one-at-a-time, known as local sensitivity analysis. Mathematically, the sensitivity of the drug concentration function with respect to model parameters is characterized to the partial derivative of the concentration function with respect to those parameters. The term 'local' refers to the fact that all partial derivatives are evaluated at a point. Local method involves the partial derivatives of the drug concentration function $C_k(X_{p,t})$ with respect to model input parameters X_p , defined by $\left[\frac{\partial C_k}{\partial X_p}\right]_{X^0}$, where X^0 indicates that the derivative is evaluated at a fixed point in the space of input model parameters and X_p designates a particular model parameter whose sensitivity is to be estimated. Here, C_k represents various drug concentrations in both the phases.

The partial derivatives of the drug concentrations corresponding to both the phases of polymeric matrix and biological tissue with respect to the perturbed parameters do accord a measure of model sensitivity to each parameter of significance. The primary goals for performing sensitivity analysis for the present model study are (i) to gain insight in how patterns and emergent properties are generated, (ii) to quantify the variability in the outcomes of the model resulting from model parameters, (iii) to examine the robustness of the model with respect to changes of the parameter values and finally, (iv) to quantify the uncertainty of the model outcomes caused by parameter perturbations. A series of illustrations are carried out with various model parameters which are made to vary on the lower and higher sides of their respective base values. Each illustration is administered by altering one parameter at a time by keeping all the remaining parameters unaltered. The quantitative representations of these illustrations are included in the following section.

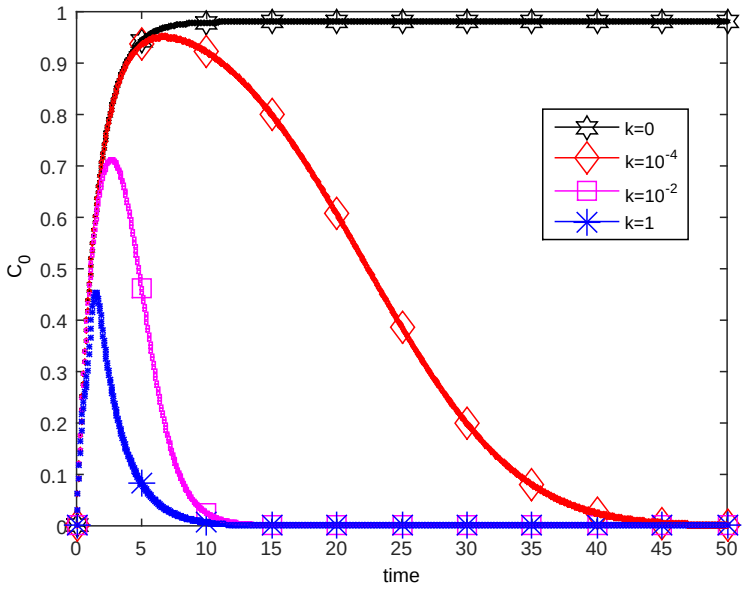

Figure 5.3: Time variant concentration profile of C_0 at different k.

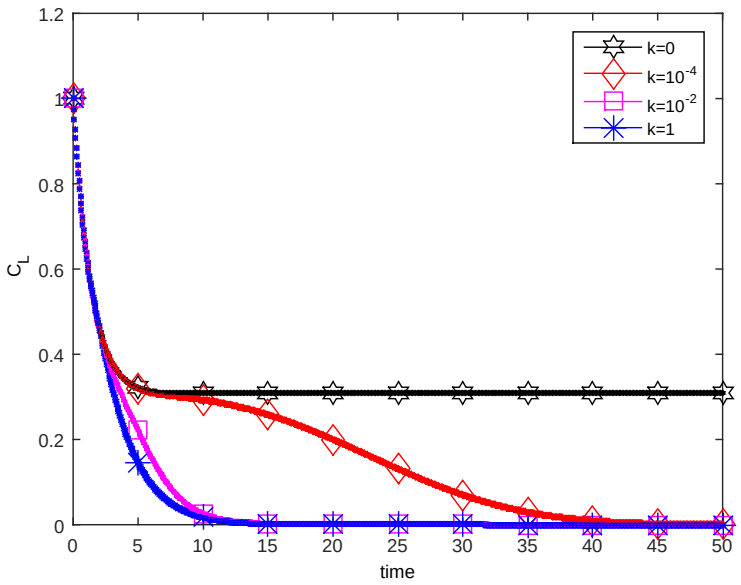

Figure 5.4: Time variant concentration profile of C_L at different k.

Table 5.1: Simulated values of the model parameters

Parameters	Values	References
β_0	$3.5 * 10^{-4}\ s^{-1}$	Estimated from [113]
δ_0	$10^{-4}\ s^{-1}$	[113]
D_{s0}	$10^{-13}\ cm^2/s$	[158]
D_l	$50\ cm^2/s$	–
l_0	$0.01\ cm$	Estimated from [113]
l_1	$0.1\ cm$	[113]
D_1	$7 * 10^{-6}\ cm^2\ s^{-1}$	[79]
k_{dd}	$0.55 * 10^{-7}\ s^{-1}$	Estimated from [7]
k_m	$10^{-5}\ s^{-1}$	Estimated from [18]
C_{lim}	$2.79 * 10^{-5}\ mol/cm^3$	[18]
k_w	$7.5 * 10^{-7}\ s^{-1}$	[7]
k_a	$1.5 * 10^{-5} s^{-1}$	Estimated from [113]
k_d	$4.55 * 10^{-5}\ s^{-1}$	Estimated from [113]
k_i	$0.69 * 10^{-5}\ s^{-1}$	[79]
P_1	$10^{-7}\ cm/s$	Estimated from [113]
k_{id}	$4.55 * 10^{-5}\ s^{-1}$	[79]
k	10^{-4}	[36]

5.6 Numerical simulation and discussion

Numerical simulation for the present drug release phenomenon is carried out based on the existing data as provided in Table 5.1 for various parameters of relevance for the purpose of characterization of the pharmacokinetic features of drug release.

At the polymeric matrix phase, the graphical representations of the time-variant concentration profiles for both the free and bound drug are displayed in Figs. 5.3 and 5.4 in order to have a complete understanding of the drug release kinetics and the impact of drug hydrophobicity on it. These profiles corresponding to different drug partitioning between the liquid-filled pores and solid polymer coating phase are plotted for the purpose of making an estimation of its effect on drug release. Smaller values of k reduce the effective drug diffusivity so that the concentration profiles remain invariant towards their initial variations with time while the enhanced effective diffusivity corresponding to larger values of k results in quicker outflow of free drug out of the polymeric matrix. Hence, as an indirect consequence, solid drug also gets faded away hastily.

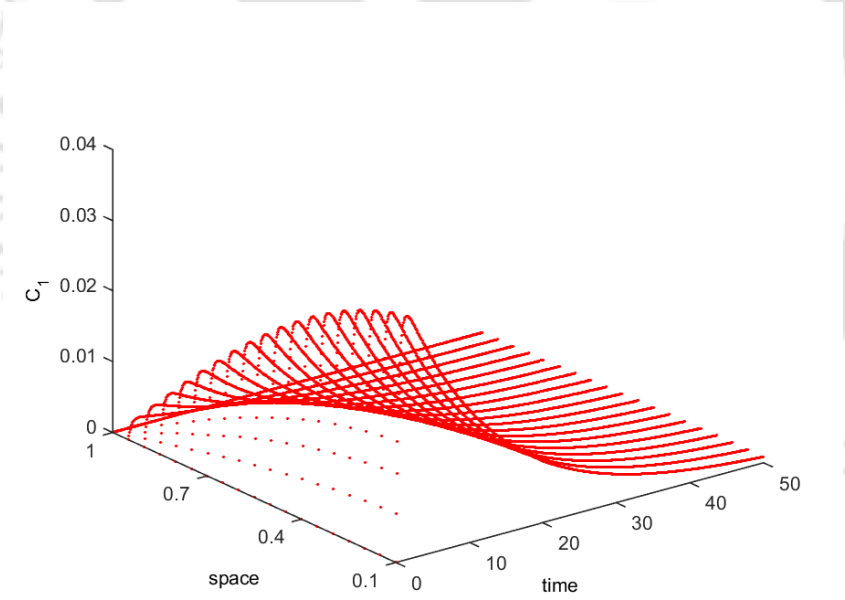

Figure 5.5: Space-time variant concentration profile of C_1.

The subsequent phase of biological tissue over the entire axial domain of reference experiences space time-variant concentration profiles for free, bound and internalized drug particles whose responses are outlined in the respective Figs. 5.5 - 5.7. The responses of all these 3D profiles are homologous with the exception of the characteristics towards the onset of drug transport. It is consequential to perceive that the free drug concentration rises rapidly compared to that of both bound and internalized drugs towards the inception. This observation undoubtedly reflects in the domain of drug kinetics that free drug gets transformed into bound drug followed by the metabolisation of bound drug into internalized

drug after a short period of time. It may be noted further that the internalized drug needs more time to get absorbed completely in the tissue than the time taken by other drug particles.

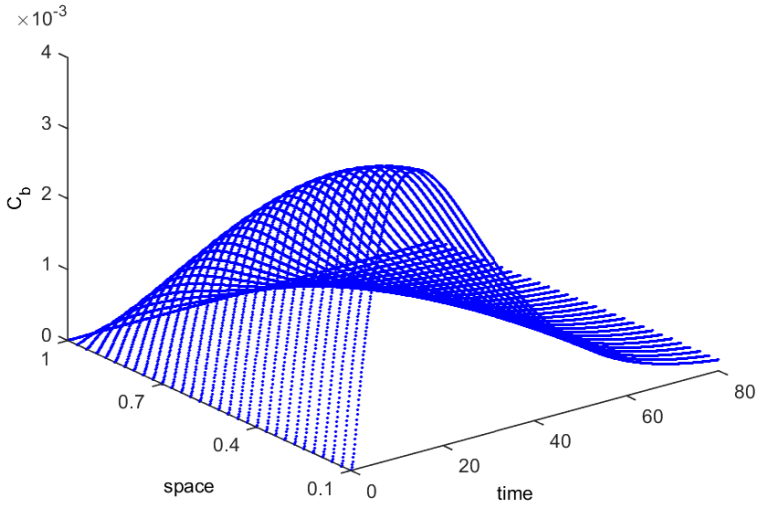

Figure 5.6: Space-time variant concentration profile of C_b.

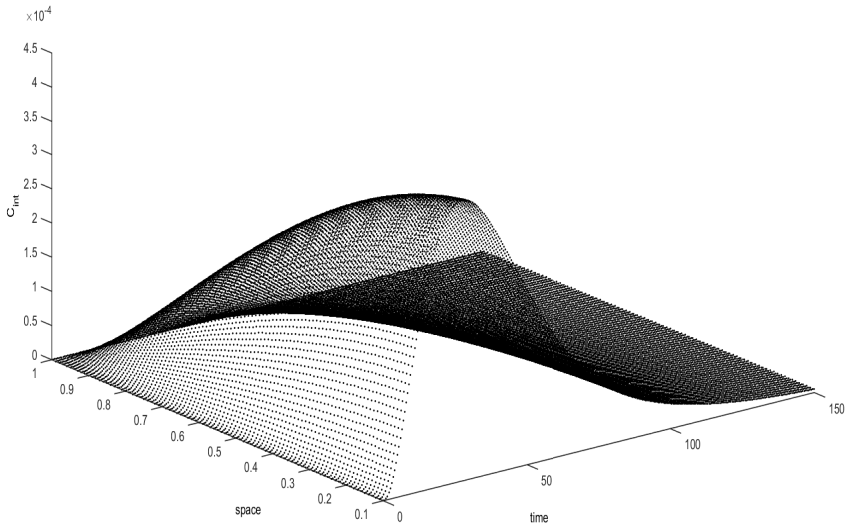

Figure 5.7: Space-time variant concentration profile of C_{int}.

Figures 5.8 - 5.10 represent the time-variant measure of sensitivity of free drug concentration in the

polymeric matrix with respect to the non-dimensional parameters of diffusivity (D), dissociation rate constant (β_0) and the association rate constant (δ_0) respectively at a specific location ($x = 0.005\ cm$) in the polymeric matrix. It appears from the behaviour of D-variant curves (Fig. 5.8) that the maximum deviation of the results in the event of decreasing value of D from its base value occurs during the time $t = 40$, which eventually dies out for time $t = 100$. However, smaller deviation is recorded at $t = 10$ for ten-fold increasing value of D from its base one. One may argue that in order to estimate the parameter D precisely, one must have proper measurements at later times where all the curves approach to dissipate. The considerable variation of the outcomes adds credibility of the model regarding the significance of diffusivity in the system. It is evident from Fig. 5.9 that the β_0-variant curves shift towards the origin as β_0 increases by ten-fold over its base value but they move away from origin for smaller β_0 . Here too, the outcome of the profile does not get perturbed for larger passage of time even if the parameter is perturbed by many-fold. Although appreciable variations of the output profiles with respect to the increasing parameter δ_0 of the model as exhibited in Fig. 5.10 are recorded at two specific instants of time ($t = 2$ and $t = 25$), but they all merge together after certain period of time. Hence non-perturbation characteristics of the output profile of drug concentration subject to variations of the model parameters towards larger span of time enable the choice of model parameters effectively which may augment insight into the overall behaviour of the system. The patterns and emergent properties of these curves subject to variability of the parameters under examination can help to understand the dynamics of the drug release system effectively because the influence of parameter changes on the model outcomes contains clues of the model dynamics.

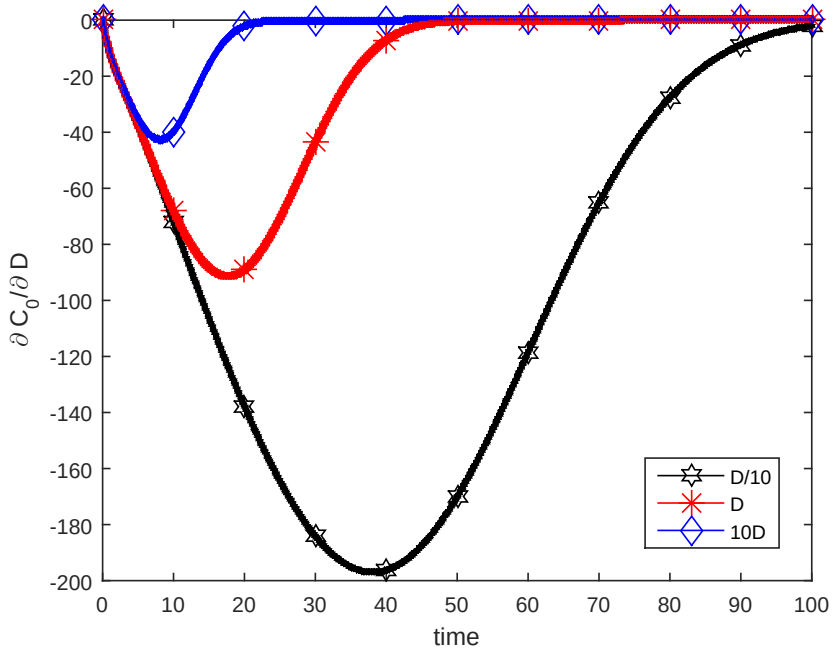

Figure 5.8: *D*-variant local sensitivity of C_0.

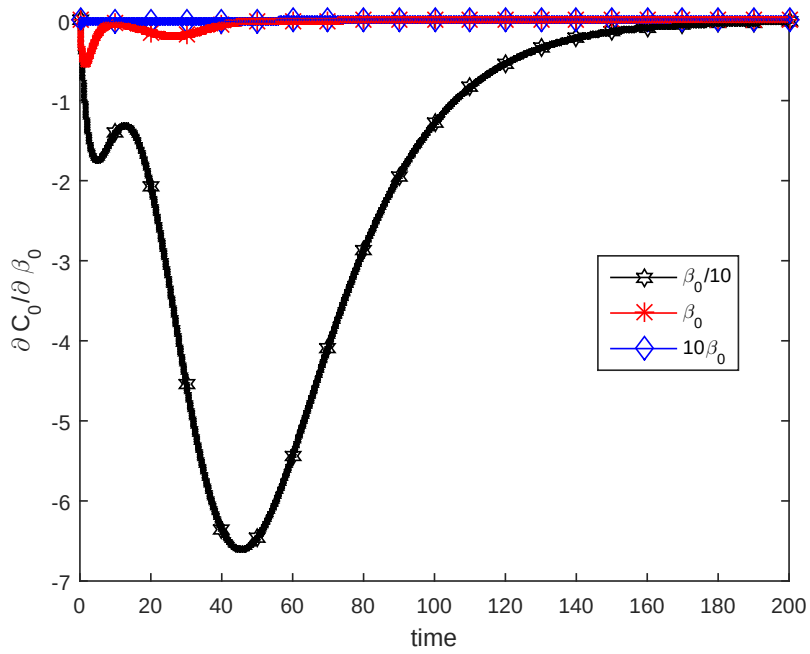

Figure 5.9: β_0-variant local sensitivity of C_0.

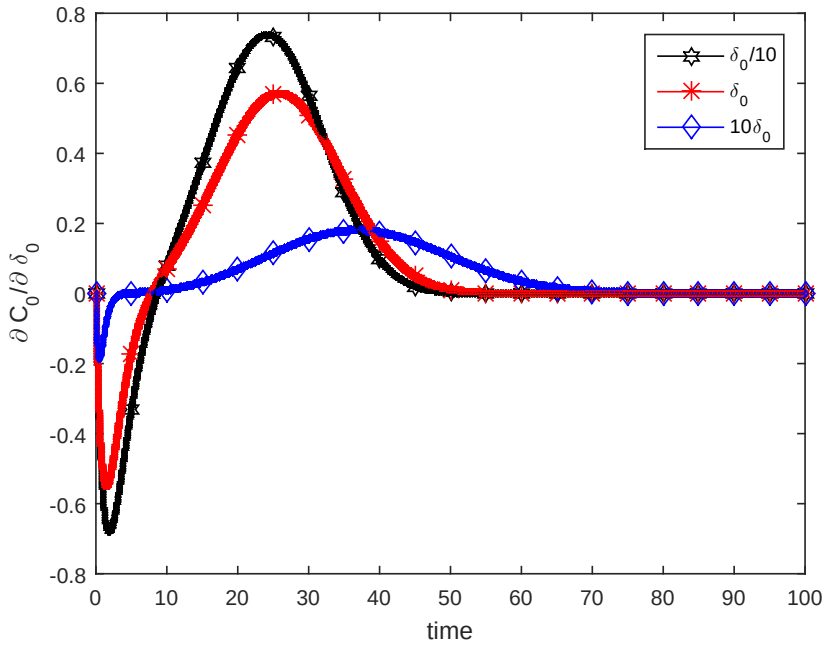

Figure 5.10: δ_0-variant local sensitivity of C_0.

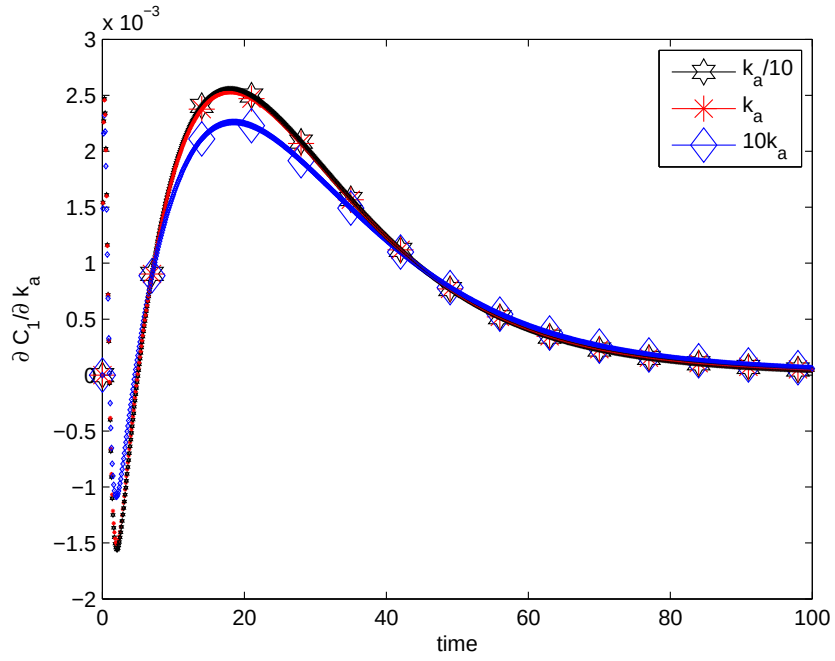

Figure 5.11: k_a-variant local sensitivity of C_1.

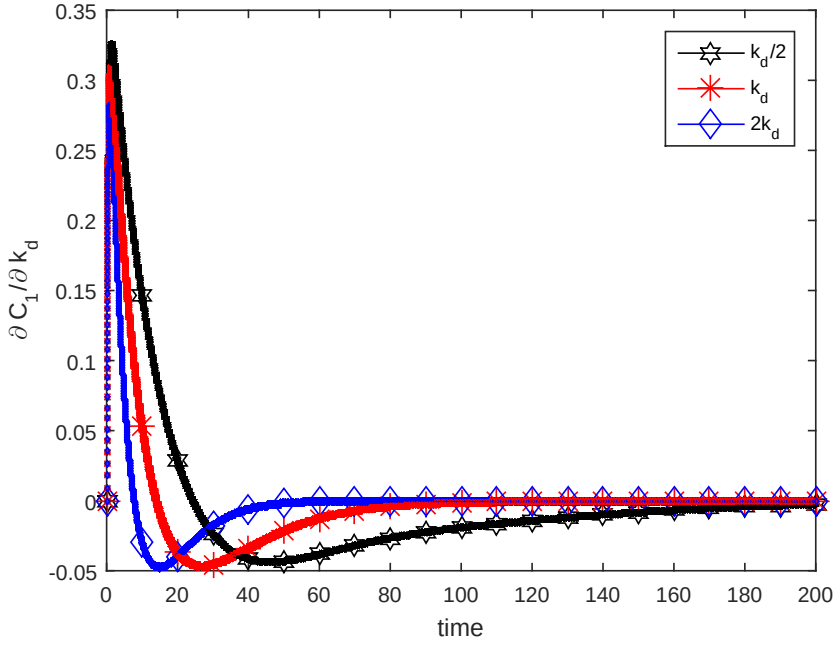

Figure 5.12: k_d-variant local sensitivity of C_1.

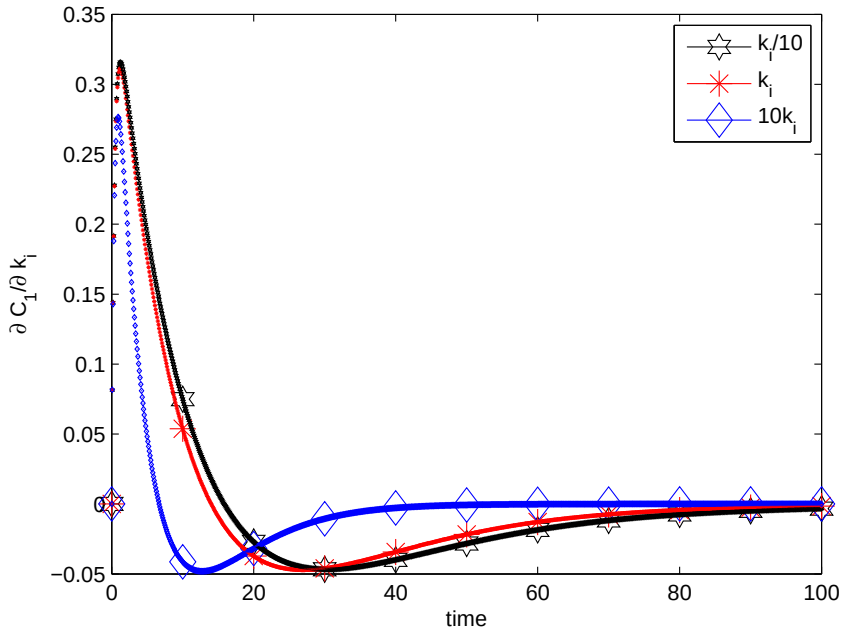

Figure 5.13: k_i-variant local sensitivity of C_1.

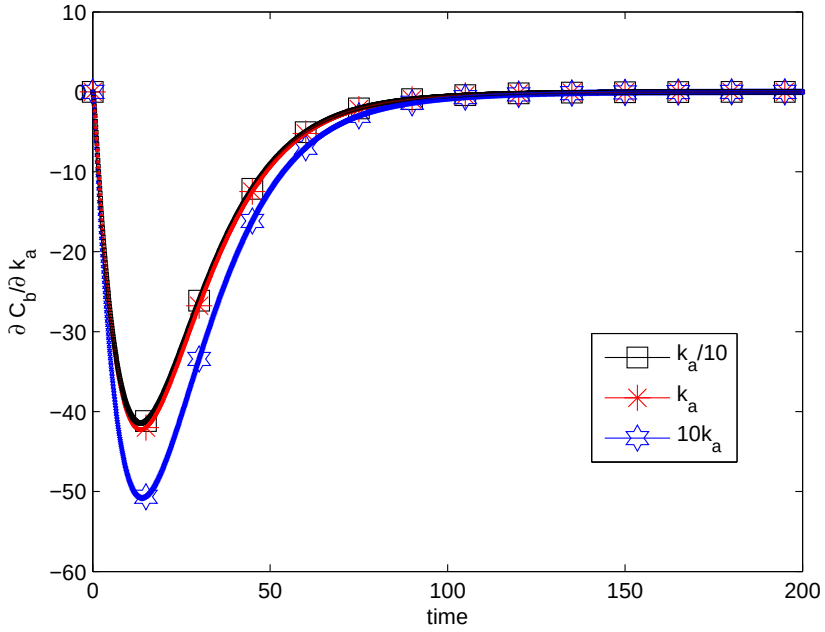

Figure 5.14: k_a-variant local sensitivity of C_b.

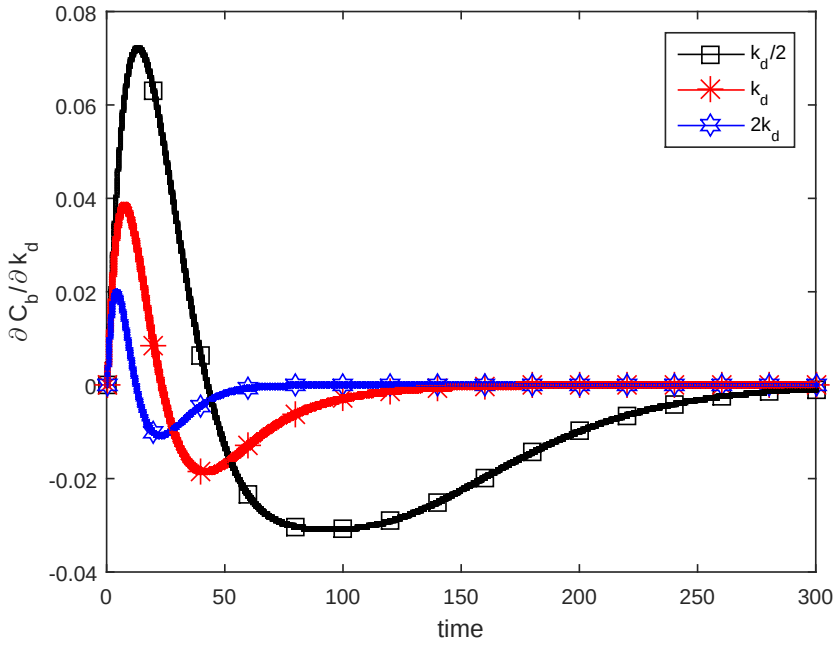

Figure 5.15: k_d-variant local sensitivity of C_b.

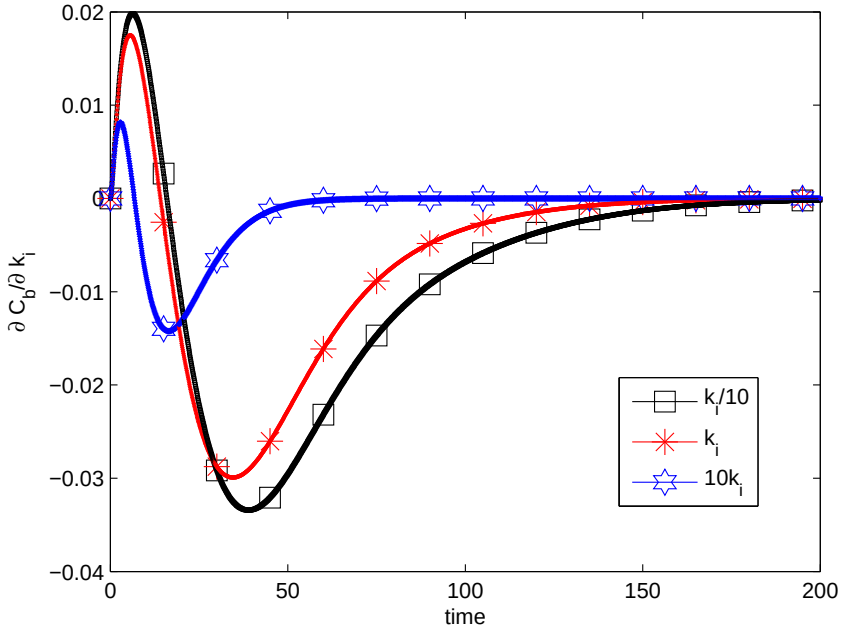

Figure 5.16: k_i-variant local sensitivity of C_b.

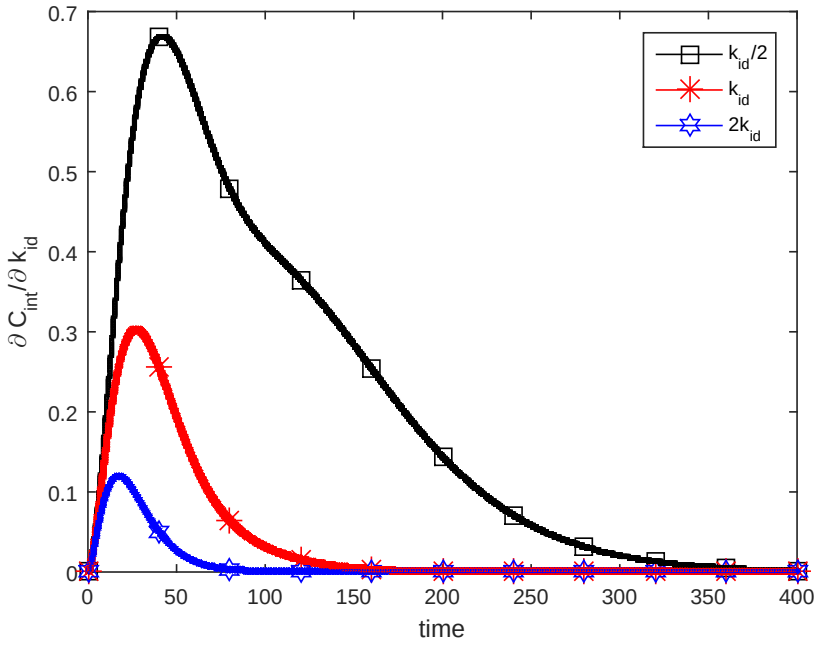

Figure 5.17: k_{id}-variant local sensitivity of C_{int}.

The sensitivity analyses corresponding to different set of model parameters for free drug, bound drug and internalized drug concentrations in the biological tissue are, however, not ruled out from the present quantitative study. Here, the time-variant profiles are plotted at $x = 0.05\ cm$. Simulated outcomes of the partial derivative of the free drug concentration profile for perturbations in the binding rate coefficient (k_a) are provided in Fig. 5.11 over a large span of time. The deviation of the results is smaller for ten-fold perturbation of the parameter k_a than that for one-tenth of its base value, which precisely indicates the sensitivity of the parameter under consideration. One may note that near $t = 40$, all the curves do merge completely and they gradually advance to die out in the long run. It emerges from Fig. 5.12 that the k_d-variant curves in accordance with the perturbation of the dissociation rate coefficient (k_d) deviate almost uniformly over the entire period of time with larger magnitudes in the event of reduction of the parameter value and smaller magnitudes for increasing value of the parameter. Two-fold enhanced value of k_d leads the corresponding contour to die out early than that for reduced parameter one, although they all approach zero level towards the larger course of time. Almost analogous behaviour to those of Fig. 5.12 excepting an amalgamation of the profile with respect to smaller internalization rate coefficient (k_i) can be observed in Fig. 5.13. The results are less disturbed for smaller k_i and substantially influenced by larger parameter value. It appears that the free drug concentration is not that sensitive to parameter k_a relative to other significant parameters k_d and k_i of the present model and hence proper attention needs to be paid on the dynamics of the drug release phenomena. On the other hand, the profiles of the bound drug in the biological tissue subject to the respective perturbed parameters of binding rate, dissociation rate and internalization rate as well are depicted in Figs. 5.14 -

5.16 over a large span of time. Smaller binding rate causes insignificant deviation while ten-fold larger binding rate yields maximum deviation at $t = 20$ but this eventually dies out completely near $t = 100$ as observed in Fig. 5.14. Similar behaviour of those profiles corresponding to Figs. 5.12 and 5.13 may be attributed from the curves of the respective Figs. 5.15 and 5.16 and hence their descriptions are not repeated here for the sake of brevity. Finally, the results of the concluding graph Fig. 5.17 represent the variation of the partial derivative of the internalized drug concentration in the biological tissue with respect to degradation rate constant parameter (k_{id}) over a stipulated period of time for three different perturbed values of the parameter. The observation of smaller the degradation rate larger is the deviation of the outcomes and vice-versa ensures the sensitivity of the degradation rate parameter in the drug release system under study. The sensitivity analysis carried out here quantifies variability in the outcomes and decomposes it into terms that are attributed to different model parameters and no output uncertainty corresponding to variable input model parameters is perceived.

5.7 Conclusions

The present work deals with a simple mathematical model of polymer degradation and drug release from a local drug delivery device to the adjacent biological tissue. The solubilisation and recrystallisation characteristics in the polymeric matrix phase together with association, dissociation and internalization phenomena in the biological tissue are well adopted mathematically. Moments method is made use of for the purpose of formulating polymer degradation.

The study undertaken is of adequate merit on several counts. First, the model formulated is quite realistic since it takes into account those relevant, imperative and important characteristics whose roles in the domain of drug kinetics are too significant to discard. Secondly, the closed form analytical solutions of the governing equations describing the physical phenomena is an added advantage of the present pursuit. Thirdly, a comparison of the proposed model with the experimental evidence reveals the validity as well as reliability of the model undertaken and its applicability in the domain of pharmacokinetics. Lastly, by performing local sensitivity analysis subject to parameter perturbations, the present study claims to possess a better understanding of the model characteristics. The sensitivity of drug concentration to the model parameters poses challenges to the applicability of drug administration for treatment of patients at large through pharmacotherapy. Several conclusions can well be drawn right from the simulations undertaken to measure sensitivity of various parameters of relevance regarding the applicability and accuracy of the model parameters of the system. The investigation of the behaviour of drug release model is conducted in some region around the base parameter values. In biology, input parameters are often very uncertain and cover large ranges which is difficult to investigate using local sensitivity technique.

Local techniques are limited to ponder changes to one parameter at a time keeping all other parameters fixed to their base values. In the biological system, it is likely that interactions between parameters are significant. Therefore, the present study can be updated further with an incorporation of global sensitivity approach by altering multiple parameters simultaneously instead of a single parameter at

a time in the case of local sensitivity analysis. It would then be of much use for an estimation of parameter interactions within the model system.

6 DRUG DELIVERY WITH SPECIFIC / NON SPECIFIC BINDING PHENOMENA

Having the objectives underlined in Chapter 1, an attempt is made here to carry out a thorough study on drug delivery with the introduction of specific / non specific binding phenomena in biological tissue through mathematical models.

6.1 Introduction

A strong aspiration of modern cell biologists, of molecular biologists, of biotechnologists, and of bioengineers is to perceive the characteristics of a living cell taking its molecular properties into consideration. Great progress has been made towards this target by the usage of tools from molecular cell biology. Notwithstanding the colossal headway in understanding the phenomena behind cell functions at the molecular level, which is just the dawn of comprehension procedure from the point of view of complex cellular activities. Studying component molecules by themselves will not suffice until it is figured out how they work jointly. In order to analyse complicated systems quantitatively, mathematical modelling is a very useful tool. Mathematical modelling can be regarded as a language, which solely narrates hypotheses and speaks about their inferences. It is aimed in the present study to speak up the objective that the mathematical models can accompany, that is, understanding the cellular functions in a simplified way with the help of mathematical models.

This work of concern presents a mathematical model that elucidates the integrated process of drug release from a polymeric matrix and consequent transport of drug particles into the biological tissue. The integrated model incorporates polymer degradation, diffusion kinetics, solubilisation dynamics and recrystallisation phenomena that govern the process of drug release from the polymeric matrix. In addition, the proposed model also incorporates tissue diffusion, advection, binding / unbinding and internalisation phenomena that occur in the biological tissue. The model includes two phases of drug (free and bound) in the tissue. The bound drug is formed from two types of binding: binding to spe-

cific receptors (SR), i.e., specific binding and non-specific binding that happens to occur as a result of binding of drug with membrane constituents or due to confinement of the drug particles in the extracellular matrix (ECM). Furthermore, the advocated mathematical model elucidates the complex process of drug release from the polymeric matrix as an outcome of the coupled action of polymer degradation and erosion. Fick's laws state that concentration gradients are the driving forces behind diffusion mass transport. Moreover, the porous structure of the biological tissue controls the ability of free drug to diffuse into the tissue. Hence, an effective diffusivity within the porous biological tissue is responsible for free drug concentration in the tissue phase, which may be highly influenced by compression of the porous wall. The propounded model is a deterministic mathematical model, which takes into account all the significant underlying phenomena that govern the drug release and drug transport processes. Whereas in the literature, it is easy to observe that all the above-mentioned physical processes are not considered simultaneously, though they work conjointly to perform the physiological functions. Even though the advocated generalised mathematical model includes various significant as well as complex physiological and biochemical functions, it is very simple to comprehend and apply in the field of pharmaceutical sciences. The purpose of the present theoretical investigation is to establish the reliability and accuracy of the proposed model through fruitful comparison of the results obtained with those of the existing experimental ones. Another important objective of the current study is to visualize drug concentration profiles in case of biodegradable and biodurable polymeric matrices.

6.2 Model development

The proposed mathematical model for controlled release drug delivery, from a local drug delivery device, deals with a two-phase system. The first phase consists of a polymeric matrix, which acts as the reservoir where the drug is encapsulated. The second phase is the edging biological tissue, which is the delivery site of drug. The polymeric matrix is contemplated as a biodegradable polymeric coating that is degraded gradually and it is enclosed on one side with an impermeable backing while, the other one faces the tissues. In the tissue phase, the reversible unbinding / binding (specific and non-specific) and internalization processes of drug are focussed on. Mass transport occurs in the direction normal to the tissue since the coating layer is generally thin in relation to its lateral dimensions for which it is assumed that transverse diffusion is negligible and only longitudinal diffusion is taken into account. This is the reason for which the proposed model is considered to be one dimensional. Since the thickness of cells and the tissue at large is extremely small in comparison with the length of tissue, it is sensible to use Cartesian coordinate system.

Drug transport in polymer coating

Degradation and erosion are customarily calculated by the indices as measures of polymer molecular weight (MW) change and mass loss respectively. In the present study, the first-order degradation model (cf. [35, 116, 20]) is chosen in order to obtain the weight-average MW change as $M_w = M_{w,0}e^{-k_w t}$, $M_{w,0}$ being the initial weight-average MW and k_w is the degradation rate constant corresponding to weight-

average MW decay. The drug release rate is tuned mutually by coupling the effects of both degradation and erosion. Degradation and erosion together play a pivotal role in drug molecule diffusion, as reduction in molecular weight leads to gradual disentanglement of the polymer chains and the resulting mass loss leads to formation of pore space. In the work of Zhu and Braatz [158], a model is propounded for drug release from stents where they considered the contribution of effective diffusivity due to the combined effect of diffusion and erosion. In our study, effective diffusivity of the polymeric matrix is utilized to elucidate the drug release kinetics from the polymeric matrix to the biological tissue due to the synchronized action of polymer degradation and erosion. The diffusion of drug molecules through the polymeric mass with decreasing molecular weight and the pore space in the matrix, whose volume fraction is being increased, is illustrated by embracing an effective diffusivity.

Drug release mechanism and its transport to the biological tissue

Initially, the drug remains in solid and bound phase (C_L), i.e., in crystalline form, encapsulated in the polymeric matrix at its maximum concentration. This bound drug cannot be transferred into the tissues directly, so it needs to be converted into a free drug. With time, water permeates into the polymeric matrix and the solid drug embedded inside it gets moistened leading to solubilisation of the loaded drug particles into a free drug (C_0). The free drug (C_0) only diffuses out of the matrix following the effective diffusivity of polymeric constituent of the matrix and enters into the biological tissue as C_1. In the Noyes-Whitney approach (cf. [101, 52]), the rate of dissolution tends to be proportional to the difference between the drug solubilisation limit and solubilised drug concentration at that instant, following a linear relation. Later on, the nonlinear model of dissolution was attempted in the work of Hixson and Crowell [62], where it was experimentally proved that Noyes-Whitney's assumption of constant surface condition was not fully rationalized. The nonlinear relation demonstrated by Hixson and Crowell [62] expressed a mathematical relation between the rate of transformation of solid into liquid, surface and concentration factors. In solid-liquid dissolution system, the most bothersome factors were shape and specific surface of solid particles, whereas the abrasive effects of temperature and heat transfer were not very significant. In the work of Hixson and Crowell [62], it was assumed that if the factors other than concentration and surface can be held constant, then the solid-liquid transformation may be modelled properly. Through experimental research work, Hixson and Crowell were successful in making a strong confirmation regarding the generalized viewpoint of having nonlinear relation depicting the dissolution phenomenon. Furthermore, the approach discussed above has been utilized in [42] in the context of drug delivery and later in [38] in the context of a complex 2D model formulation having the effect of polymer degradation.

Moreover, a fraction of solid drug ($\beta_0 C_L$) is converted into free drug depending on its chemical properties and through recrystallization process, a portion of free drug ($\delta_0 C_0$) is transformed back into bound state (β_0 and δ_0 are the dissociation and association rate constants respectively). The free drug (C_1) in the tissue experiences diffusion and advection. Also, the drug (C_1) binds reversibly to the non-specific ECM sites and specific receptors (SR) (C_{b1} and C_{b2} respectively) forming corresponding bound drugs b_1 and b_2. The bound drugs are swallowed up (internalized) by the cells in the tissue through endo-

cytosis. Endocytosis is an active energy-based transport process of transporting molecules (proteins, drugs etc.) into the cell. Thus bound drugs get converted into internalized drug (C_{int}). The internalized drug particles get degraded by the lysosomes after some time and the drug remnants after degradation ($k_{id}C_{int}$) are emptied out of the cell into the extracellular fluid (k_{id} is the lysosomal degradation rate constant). Description of the present work is schematically illustrated in Fig. 6.1.

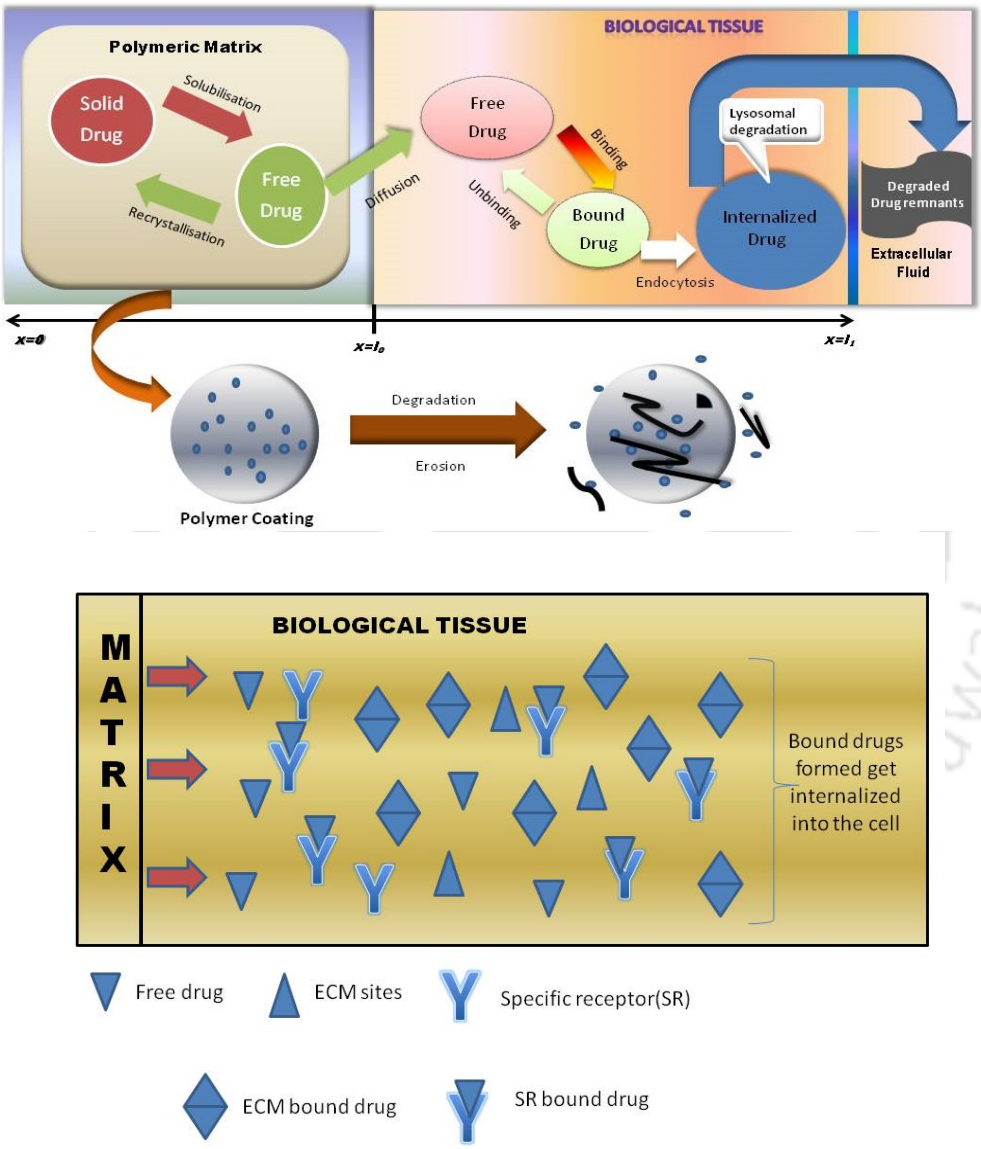

Figure 6.1: Schematic diagram of drug transport along with polymer degradation

6.3 Mathematical formulation

Modelling drug dynamics in the polymeric matrix

Initially, the encapsulated drug is immobile to diffuse out of the polymeric matrix. In exposition to biofluid, the bound drug gets converted into a free drug after the initiation of dissolution process. Subsequently, association phenomenon of the free drug to the bound drug and dissociation phenomenon of the bound drug to the free drug go on simultaneously. Hence, accumulation of bound drug and free drug at any instant in the polymeric matrix depends on bound drug dissolution (cf. [62, 42]), effective free drug diffusion, dissociation rate of bound drug and recrystallisation rate of free drug. Based on the discussion of their work in the previous section, the nonlinear model of the dissolution term (e.g. $C_L^{2/3}$) developed by Hixson and Crowell [62] is taken into account to make the present model more realistic. The solubilisation process depends on the rate of dissolution and the solubility limit of the drug in the release medium. The governing equations manifesting the dynamics of a drug release in the polymeric matrix are given by

$$\frac{\partial C_L}{\partial t} = -k_n C_L^{2/3}(C_{lim} - C_0) - \beta_0 C_L + \delta_0 C_0, \qquad x \in (0, l_0), \tag{6.3.1}$$

$$\frac{\partial C_0}{\partial t} = D_0 \frac{\partial^2 C_0}{\partial x^2} + k_n C_L^{2/3}(C_{lim} - C_0) + \beta_0 C_L - \delta_0 C_0, \qquad x \in (0, l_0), \tag{6.3.2}$$

where C_L denotes available molar concentration of solid drug, C_0 is the available molar concentration of free drug, l_0 is the length of the polymeric matrix, k_n is rate of dissolution, C_{lim} stands for drug solubilisation limit, β_0 is the dissociation rate constant, δ_0 is the association rate constant, D_0, the effective diffusion coefficient of free drug, as outlined in [158] in a matrix, is defined as

$$D_0 = \frac{(1-\phi)D_s + k\phi D_l}{1 - \phi + k\phi}, \tag{6.3.3}$$

where D_s is the diffusivity in the polymer phase, D_l is the diffusivity in liquid-filled pores, ϕ is the porosity and k is the drug partitioning between the liquid-filled pores and solid phase as depicted in [158] such that D_s and ϕ are defined as

$$D_s = D_{s0}\left(\frac{M_w}{M_{w,0}}\right)^{-1.714}, \tag{6.3.4}$$

$$\phi = \phi_i + (1-\phi_i)(1 + e^{-2k_{dd}t} - 2e^{-k_{dd}t}), \tag{6.3.5}$$

where D_{s0} is the initial diffusivity of the solid phase, k_{dd} is the degradation rate constant corresponding to number-average molecular weight change and ϕ_i is the initial porosity. The association / dissociation process involved in equations (6.3.1) - (6.3.2) is represented by linear terms. This is because here, association (recrystallisation) is treated to take place due to chemical nature of the drug only, instead of the formation of a chemical complex while dissociation is merely the first order breakdown of solid

drug.

Modelling drug dynamics in the biological tissue

The free drug, ensued from the solubilisaton phenomenon, diffuses through the polymeric matrix into the biological tissue as an outcome of the mass flux across the interface. It is assumed that the biological tissue layer is single and homogeneous, and exhibits isotropic diffusion characteristics. The free drug in the tissue undergoes diffusion, binding with specific receptors and ECM sites to form two types of bound drug. The bound drugs undergo internalization phenomenon to form internalised drug, which ultimately gets degraded by the lysosomes. Hence, accumulation of free drug at any instant depends on diffusion, advection and binding rates of specific receptors and non-specific binding sites. Moreover, accumulation of receptors and bound drugs at any instant depends on the binding rates and internalization rates. Furthermore, the accumulation of internalized drug at any instant of time in the biological tissue depends on the internalization rates and lysosomal degradation rate. Based upon the primary understanding of the model formulation as illustrated by Lauffenburger and Linderman [79], the present model equations demonstrating the dynamics of a drug in the tissue are

$$\frac{\partial C_1}{\partial t} = D_1 \frac{\partial^2 C_1}{\partial x^2} - \gamma_1 \frac{\partial C_1}{\partial x} - k_1^f C_1 C_{b1} + k_1^r b_1 - k_2^f C_1 C_{b2} + k_2^r b_2, \qquad x \in (l_0, l_1), \tag{6.3.6}$$

$$\frac{\partial C_{b1}}{\partial t} = -k_1^f C_1 C_{b1} + k_1^r b_1 + k_{i1} b_1, \qquad x \in (l_0, l_1), \tag{6.3.7}$$

$$\frac{\partial b_1}{\partial t} = k_1^f C_1 C_{b1} - k_1^r b_1 - k_{i1} b_1, \qquad x \in (l_0, l_1), \tag{6.3.8}$$

$$\frac{\partial C_{b2}}{\partial t} = -k_2^f C_1 C_{b2} + k_2^r b_2 + k_{i2} b_2, \qquad x \in (l_0, l_1), \tag{6.3.9}$$

$$\frac{\partial b_2}{\partial t} = k_2^f C_1 C_{b2} - k_2^r b_2 - k_{i2} b_2, \qquad x \in (l_0, l_1), \tag{6.3.10}$$

$$\frac{\partial C_{int}}{\partial t} = k_{i1} b_1 + k_{i2} b_2 - k_{id} C_{int}, \qquad x \in (l_0, l_1), \tag{6.3.11}$$

where C_1 is the molar available concentration of free drug in the tissue, C_{b1} is the molar concentration of available binding sites on extracellular matrix (ECM), b_1 is the molar concentration of drug bound to non-specific extracellular matrix binding sites, C_{b2} is the molar concentration of available specific binding receptors (SR), b_2 is the molar concentration of drug bound to specific binding receptors, C_{int} denotes the molar concentration of internalized drug particles, $l_1 - l_0$ is the length of the tissue, γ_1 is the magnitude of advection (defined by the velocity field of the free drug), k_1^f depicts the association rate constant, which denotes the velocity of second-order interaction between ECM sites and free drug in the tissue, k_1^r is the dissociation rate coefficient denoting the first-order breakdown velocity of ECM sites-free drug complex, k_2^f depicts the association rate constant, which denotes the velocity of second-order interaction between SR and free drug in the tissue, k_2^r is the dissociation rate coefficient denoting the first-order breakdown velocity of SR receptors-free drug complex, k_{i1} stands for internalization rate coefficient for b_1, k_{i2} stands for internalization rate coefficient for b_2, k_{id} denotes degradation

rate constant in the lysosome, and D_1 is the effective diffusion coefficient of free drug in the porous biological tissue, depicted as follows:

$$D_1 = \frac{\varepsilon}{\tau} \times D_{free}. \tag{6.3.12}$$

Here, ε, τ and D_{free} are the porosity of the biological tissue, tortuosity of its pore path and free diffusivity of the biological tissue respectively. The above concepts are discussed in details by Saltzman [125]. The porosity of the biological tissue is used only to determine the effective diffusivity of the free drug in the tissue.

Initial, interface and boundary conditions

The initial conditions for the above set of equations are as follows:
Since the solid loaded drug is prevalent at the onset without any of its transformed forms,

$$C_L = M, \quad C_{b1} = b^1_{max}, \quad C_{b2} = b^2_{max}$$

and rest are all zero at $t = 0$, where M is the maximum value of loaded solid drug concentration and b^1_{max} along with b^2_{max} bespeak the local density of ECM sites and SR respectively.
A flux continuity must be assigned at the interface,

$$-D_0 \frac{\partial C_0}{\partial x} = -D_1 \frac{\partial C_1}{\partial x} + \gamma_1 C_1, \qquad x = l_0.$$

At the interface, a concentration jump may occur because of a different drug partitioning between polymeric matrix and tissue. Such situation may be tackled through a suitable mass transfer coefficient. Thus

$$-D_1 \frac{\partial C_1}{\partial x} = P_1 (C_0 - C_1), \qquad x = l_0,$$

where P_1 is the mass transfer coefficient.
No mass flux can leave outward into external domain due to the presence of impermeable backing and hence no flux condition emerges.

$$-D_0 \frac{\partial C_0}{\partial x} = 0, \qquad x = 0.$$

Lastly, at the extreme boundary of the tissue, as there is a feeble possibility of the existence of the free drug (due to its binding with specific receptors and ECM sites, it is assumed to be completely transformed into other forms),

$$C_1 = 0, \qquad x = l_1.$$

6.3.1 Nondimensionalization

All the variables and parameters are nondimensionalized in order to proceed towards converting the equations in simple form for performing computation in a systematic approach. In the process of getting rid of dimension in a system of reaction-diffusion-advection equations, pertinent numbers such as Peclet (Pe) and Damkohler (Da) numbers are obtained. The variables and parameters are made dimensionless in the following way:

$$x' = \frac{x}{l_1}, \quad t' = \frac{D_1 t}{l_1^2}, \quad b_1' = \frac{b_1}{M}, \quad b_2' = \frac{b_2}{M}, \quad C_i' = \frac{C_i}{M}, i = L, 0, 1, b1, b2, lim, \quad \beta_0' = \frac{\beta_0\, l_1^2}{D_1},$$

$$\delta_0' = \frac{\delta_0\, l_1^2}{D_1}, \quad b_{max}^{1'} = \frac{b_{max}^1}{M}, \quad b_{max}^{2'} = \frac{b_{max}^2}{M}, \quad D = \frac{D_0}{D_1}, \quad L = \frac{l_0}{l_1}, \quad D_{a0} = \frac{k_n\, M^{-1/3}\, C_{lim}\, l_1^2}{D_1},$$

$$k_{dd}' = \frac{k_{dd} l_1^2}{D_1}, \quad Pe = \frac{\gamma_1 l_1}{D_1}, \quad D_{a1} = \frac{k_1^f\, l_1^2\, b_{max}^1}{D_1}, \quad D_{a2} = \frac{k_2^f\, l_1^2\, b_{max}^2}{D_1}, \quad k_{id}' = \frac{k_{id}\, l_1^2}{D_1},$$

$$K_{d1} = \frac{k_1^r}{k_1^f}, \quad K_{d2} = \frac{k_2^r}{k_2^f}, \quad B_{p1} = \frac{b_{max}^1}{K_{d1}}, \quad B_{p2} = \frac{b_{max}^2}{K_{d2}}, \quad B_{i1} = \frac{b_{max}^1}{\frac{k_{i1}}{k_f^1}}, \quad B_{i2} = \frac{b_{max}^2}{\frac{k_{i2}}{k_f^2}},$$

$$k_w' = \frac{k_w\, l_1^2}{D_1}, \quad \Pi = \frac{P_1\, l_1}{D_1}.$$

Dimensionless equations

In the sequel, primes($'$) are dropped from all the nondimensional variables and parameters for the sake of convenience. The succeeding equations are in nondimensionalized manifestation, given by

$$\frac{\partial C_L}{\partial t} = -D_{a0} C_L^{2/3}(1 - \frac{C_0}{C_{lim}}) - \beta_0 C_L + \delta_0 C_0, \qquad x \in (0, L), \tag{6.3.13}$$

$$\frac{\partial C_0}{\partial t} = D\frac{\partial^2 C_0}{\partial x^2} + D_{a0} C_L^{2/3}(1 - \frac{C_0}{C_{lim}}) + \beta_0 C_L - \delta_0 C_0, \qquad x \in (0, L), \tag{6.3.14}$$

$$\frac{\partial C_1}{\partial t} = \frac{\partial^2 C_1}{\partial x^2} - Pe\frac{\partial C_1}{\partial x} - \frac{D_{a1}}{b_{max}^1} C_1 C_{b1} + \frac{D_{a1}}{B_{p1}} b_1 - \frac{D_{a2}}{b_{max}^2} C_1 C_{b2} + \frac{D_{a2}}{B_{p2}} b_2, \quad x \in (L, 1), \tag{6.3.15}$$

$$\frac{\partial C_{b1}}{\partial t} = -\frac{D_{a1}}{b_{max}^1} C_1 C_{b1} + \frac{D_{a1}}{B_{p1}} b_1 + \frac{D_{a1}}{B_{i1}} b_1, \qquad x \in (L, 1), \tag{6.3.16}$$

$$\frac{\partial b_1}{\partial t} = \frac{D_{a1}}{b_{max}^1} C_1 C_{b1} - \frac{D_{a1}}{B_{p1}} b_1 - \frac{D_{a1}}{B_{i1}} b_1, \qquad x \in (L, 1), \tag{6.3.17}$$

$$\frac{\partial C_{b2}}{\partial t} = -\frac{D_{a2}}{b_{max}^2} C_1 C_{b2} + \frac{D_{a2}}{B_{p2}} b_2 + \frac{D_{a2}}{B_{i2}} b_2, \qquad x \in (L, 1), \tag{6.3.18}$$

$$\frac{\partial b_2}{\partial t} = \frac{D_{a2}}{b_{max}^2} C_1 C_{b2} - \frac{D_{a2}}{B_{p2}} b_2 - \frac{D_{a2}}{B_{i2}} b_2, \qquad x \in (L, 1), \tag{6.3.19}$$

$$\frac{\partial C_{int}}{\partial t} = \frac{D_{a1}}{B_{i1}} b_1 + \frac{D_{a2}}{B_{i2}} b_2 - k_{id} C_{int}, \qquad x \in (L, 1). \tag{6.3.20}$$

The dimensionless embodiment of initial, interface and boundary conditions comes next as

$$C_L(x,0) = 1, \qquad C_{b1}(x,0) = b^1_{max}, \qquad C_{b2}(x,0) = b^2_{max},$$
$$C_0(x,0) = C_1(x,0) = b_1(x,0) = b_2(x,0) = C_{int}(x,0) = 0,$$
$$-D\frac{\partial C_0}{\partial x} = -\frac{\partial C_1}{\partial x} + PeC_1 \quad \text{along with} \quad -\frac{\partial C_1}{\partial x} = \Pi(C_0 - C_1) \quad \text{at} \quad x = L,$$
$$-D\frac{\partial C_0}{\partial x} = 0 \quad \text{at} \quad x = 0 \quad \text{and lastly} \quad C_1 = 0 \quad \text{at} \quad x = 1.$$

6.4 Numerical solution

The system of nondimensional equations (6.3.13) - (6.3.20) are solved numerically using finite difference approximations for the spatial derivatives. In each layer, the diffusive terms are discretized by second order accurate three-point central difference formula at the internal nodes. Since the reaction terms lack any derivative, they are discretized at each of the nodal points. An important criteria of the layered geometry is the flux continuity and concentration jump conditions at the interface due to the fact that the interface is the common boundary between the two layers. It is assumed that only one grid-point is present on the interface for spatial discretizaton in case of flux continuity condition. On the other hand, for concentration jump condition, an assumption that no grid-point lies in the interface is taken into account. Moreover, at the left boundary ($x = 0$) of the present system, no flux condition is imposed, where it is also supposed that only one grid-point lies at that position. The other boundary condition is of Dirichlet type ($C_1 = 0$), which is too simple to tackle. In order to address the flux continuity and concentration jump conditions at the interface along with no flux condition at the boundary, Taylor series approximations are considered around the neighbouring nodal points of the specific grid-point on the interface and boundary. This type of modified finite difference scheme is outlined in the work of Hickson et al. [59], where numerical results are validated with exact solutions in order to bespeak the potency and accuracy of the scheme. After spatial discretization, the proposed system of partial differential equations reduces to a system of nonlinear ordinary differential equations. The new emanated system is solved using fourth order Runge-Kutta method having an adaptive time step. While these advocated models are applicable in general recognition, the model parameters may alter, based on diverse types of drugs. For simulation purpose, the model parameters are rooted in data collected from available literature. The dimensional numerical values demonstrating the model parameters are tabulated through the portrayal of Table 6.1.

6.5 Model validation

One of many applications of local drug delivery is the transdermal drug delivery as spotted from the work of Prausnitz and Langer [114]. Drug delivery through the skin, is a simple and non-intrusive mode of drug administration. For the patients who are too critical to get admitted into the intensive care unit (ICU), transdermal drug delivery provides a vital choice in addition to oral and parenteral approaches, which is studied in details by Liu and Xu [87]. An experimental work was conducted by Argemí et

Table 6.1: Parameter values

	Values	Ref.
C_{lim}	$10^{-5} mol\ cm^{-3}$	[18]
k_n	$1 s^{-1} (mol\ cm^{-3})^{-2/3}$	[42]
β_0	$10^{-4} s^{-1}$	[113]
δ_0	$10^{-4} s^{-1}$	[113]
M	$10^{-4} mol\ cm^{-3}$	[16]
l_0	$0.001 cm$	—
P_1	$10^{-6} cm\ s^{-1}$	[113]
γ_1	$5.8 \times 10^{-6} cm\ s^{-1}$	[142]
l_1	$0.045 cm$	[90]
ϕ_i	0	[158]
k_{dd}	$2.5 \times 10^{-7} s^{-1}$	[7]
k_w	$7.5 \times 10^{-7} s^{-1}$	[7]
k	10^{-4}	[36]
D_{s0}	$10^{-13} cm^2\ s^{-1}$	[158]
D_l	$50 cm^2\ s^{-1}$	—
D_{free}	$2.5 \times 10^{-6} cm^2\ s^{-1}$	[16, 142]
ε	0.611	[24]
τ	1.232	[24]
k_1^f	$2 \times 10^6 (mol\ cm^{-3} s)^{-1}$	[144]
k_1^r	$5.20 \times 10^{-3} s^{-1}$	[144]
b_{max}^1	$3.63 \times 10^{-7} mol\ cm^{-3}$	[144]
k_2^f	$8 \times 10^8 (mol\ cm^{-3} s)^{-1}$	[142]
k_2^r	$1.6 \times 10^{-4} s^{-1}$	[142]
b_{max}^2	$3.3 \times 10^{-9} mol\ cm^{-3}$	[142]
k_{i1}	$10^{-4} s^{-1}$	[79]
k_{i2}	$10^{-5} s^{-1}$	[79]
k_{id}	$4.55 \times 10^{-5} s^{-1}$	[79]

al. [3] where a polymeric patch impregnated with Naproxen was developed. Their study dealt with the preparation and characterization of a transdermal patch with the help of pressurized CO_2 as a processing medium to act as a model system of sustained release, where the drug used was Naproxen. Naproxen is the member of the 2-arylpropionic acid family of nonsteroidal anti-inflammatory drugs, which is generally prescribed for reducing mild-to-moderate pain, fever, inflammation, and stiffness. The materials used for their experiments and the techniques adopted are discussed at length in the article of Argemí et al. [3]. The primary objective of the present study is to validate the applicability of the model through a direct comparison of experimental results based on transdermal drug delivery. Due

to non-availability of all the model parameter values relevant to transdermal drug, several articles are consulted to keep the parameter values within the pharmacological range of the order of magnitudes as indicated in Table 6.1. All the model parameter values used in the present study are enlisted in the table.

Study of drug release

In the experimental article of Argemí et al. [3], Figure $5(b)$ (of [3]) demonstrates the cumulative released amount of Naproxen as the function of $\sqrt{\text{time}}$. Due to a mechanism kinetics guided by the polymeric matrix, there has been an inter-connection between drug delivery and the $\sqrt{\text{time}}$. Naproxen concentration in the polymeric matrix slowly melted away and drug release was its immediate outcome.

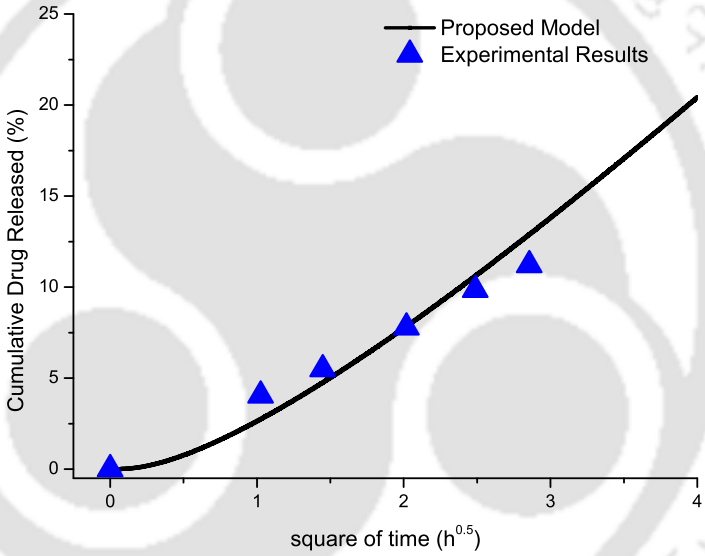

Figure 6.2: Comparison of the present results with experimental data (cf. [3]).

In order to bespeak the potency of the advocated mathematical model, validation of the theoretical results with that of the experimental study of Argemí et al. [3] is in the center-stage of the current study. The experimental set-up of polymeric patch impregnated with Naproxen is scrutinized and matched with the cumulative drug released percentage-time profile (here, non-dimensionalised parameters are converted back to dimensionalised ones), which is obtained from the present generalised mathematical model (Fig. 6.2). It can be observed that experimental data accorded well with the theoretical drug released percentage profile, which speaks volumes about the authenticity of the proposed model. The reason behind slight difference between the experimental and theoretical results, may be argued that the present model deals with the free drug being transported to the biological tissue and there is intermingled processes of specific / non-specific drug binding along with internalization phenomenon, but the experimental setting of Argemí et al. [3] lacked such considerations in drug transport.

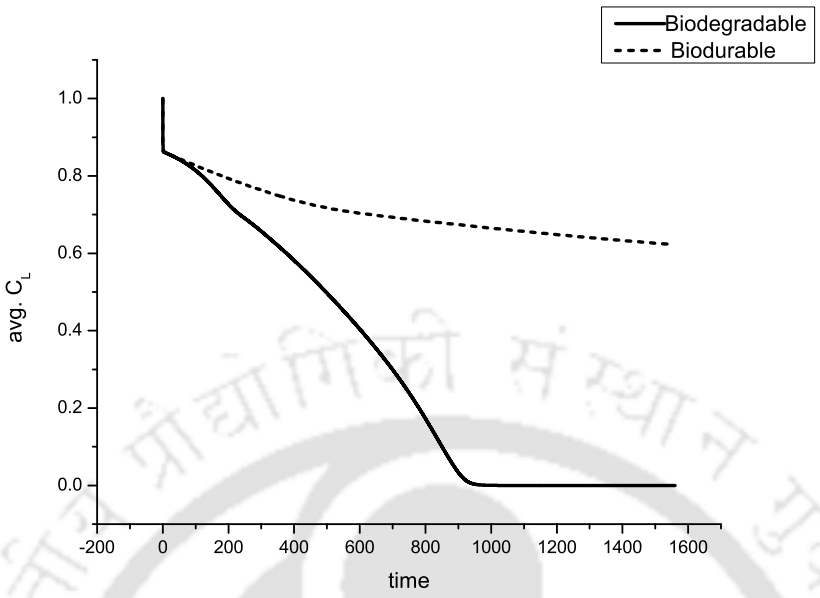

Figure 6.3: Time variant spatially averaged C_L for biodegradable and biodurable polymer coating cases.

6.6 Results and discussion

A systematic quantitative analysis for the proposed drug release system is accomplished based on the model parameters described in Table 6.1, with the objective of characterizing the pharmacokinetic aspects. Graphical representations of time-variant concentration profiles of the drug in its different mutated forms for both the layers (at $x = 0.0005\ cm$ in the polymeric matrix and $x = 0.023\ cm$ in the biological tissue respectively) are well illustrated in Figs. 6.3 - 6.17 so that one may elucidate the physical phenomena governing the drug release kinetics.

In model simulations for local drug delivery, the biodegradable coating of the polymeric matrix is compared with the biodurable one. Biodurable polymers are non-erodible and stay intact leading to the permanent presence of the polymeric coatings in biological tissues. Hence, the drug diffusivity in the biodurable polymeric matrix remains unchanged at the initial polymeric drug diffusivity (D_{s0}). All the remaining model parameters are considered identical for both biodurable and biodegradable polymeric coatings. In order to envisage the probable status of the drug assimilation in biological tissues in presence of biodurable / biodegradable polymeric matrix at the fullness of time, the results of the present study are analysed with graphical portrayals.

Figure 6.3 represents the spatially averaged concentration profile for solid (loaded) drug (C_L) in polymeric matrix in the presence of biodegradable as well as biodurable coatings. It is noticed that the concentration of loaded drug dwindles from its peak at its beginning which gradually depletes with time. The present graphical representation manifests the sign of dissimilitude when biodegradable and biodurable polymer coatings are taken into consideration. Moreover, it can be observed that the

depletion rate of solid drug is higher in biodegradable polymeric matrix in comparison to biodurable polymeric matrix. The reason behind this behaviour is that the diffusivity of the biodegradable polymeric coating increases with time leading to higher diffusion rate of the free drug (C_0) out of the matrix and higher diffusion rate of tissue fluid into the matrix, accelerating solubilisation phenomenon, resulting in a faster rate of transformation of the solid drug into a free drug.

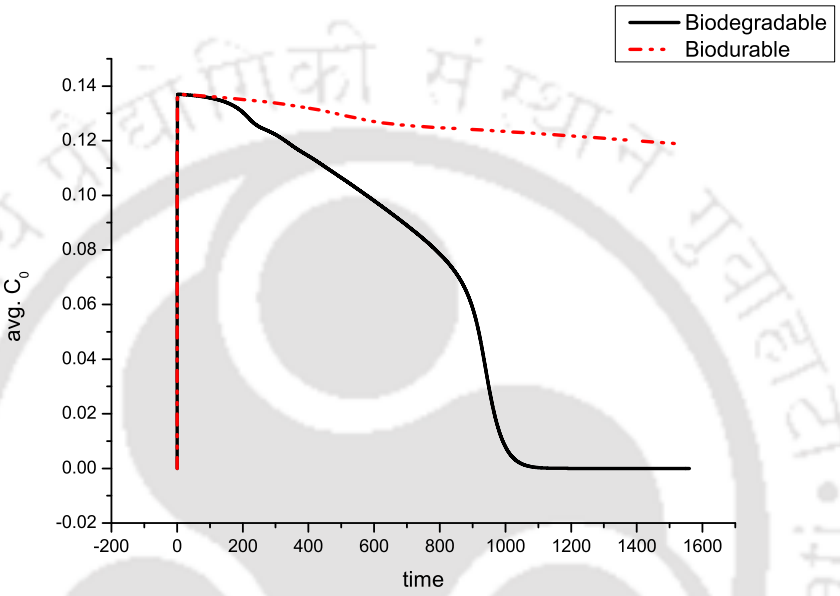

Figure 6.4: Time variant spatially averaged C_0 for biodegradable and biodurable polymer coating cases.

The results of Fig. 6.4 illustrate the characteristics of the spatially averaged concentration profile for free drug (C_0) in polymeric matrix in the presence of both biodegradable and biodurable coatings. It can be easily observed that both the frameworks initiate with indistinguishable drug release rates upto nondimensionalized time $t = 100$ (about 2 days) due to inconsequential polymer degradation and subsequent erosion at that time. Subsequently, the drug release due to biodegradable polymer transcends that of biodurable polymer as a consequence of augmented polymer degradation and erosion. In the simulation contrast, the total drug release is attained by biodegradable polymeric coating in around 20 days, whereas by that time a meagre amount of drug is released from biodurable polymeric coating. It is very interesting to perceive the gradual downward slope until time $t = 900$ followed by a sharp decline for rest of the times. This is due to the fact that till time $t = 900$, there is simultaneous solubilisation / dissociation of loaded drug into free drug and again recrystallisation of free drug back to its bound form, but after that stipulated time period, rate of recrystallizaton of the free drug diminishes as multiple recrystallization does not occur, as a result the solid drug gets converted totally into free form, which is depicted by the drastic decline in the concentration profile.

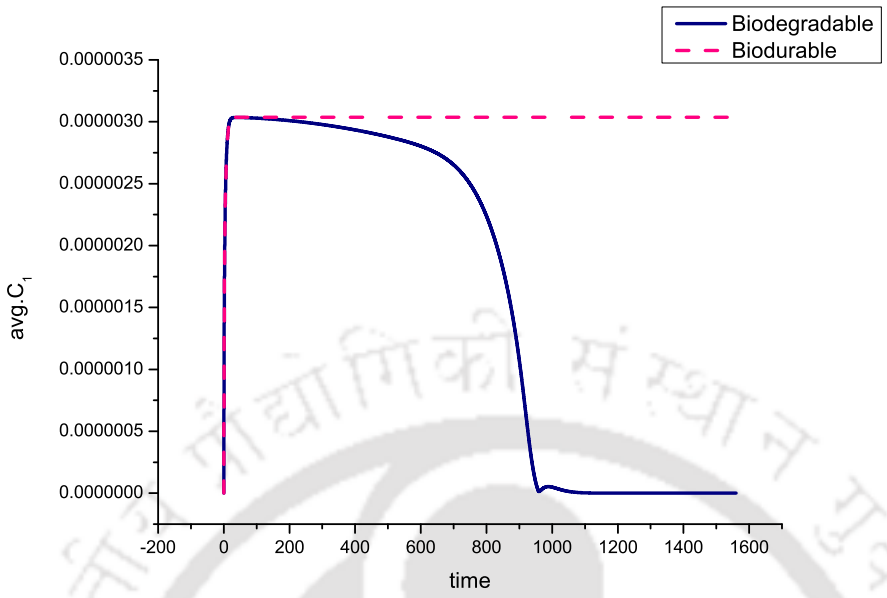

Figure 6.5: Time variant spatially averaged C_1 for biodegradable and biodurable polymer coating cases.

The concentration profiles of Figs. 6.5 and 6.6 demonstrate that the temporal variations of the spatially averaged concentration profile of free drug (C_1) and that of the bound drug (b_1) in biological tissue. It is observed that there is distinct difference between the concentration profiles (each of C_1 and b_1 independently) when the drug gets released from a biodegradable and a biodurable polymer coatings. On the other hand, as a whole, the concentration profiles of C_1 and b_1 are analogous to each other. It is quite interesting to note that at around time $t = 950$, both free and bound drug concentrations reduce to zero, but immediately after that instant, there is slight enhancement in concentration before getting faded away completely. This is just a visualization of the underlying phenomena of association / dissociation between the free drug particles and the ECM sites to form bound drug or break apart to transform back to free drug. At time $t = 950$, the concentration profiles fade away apparently but due to dissociation of bound drugs (b_1 and b_2) there is again some formation of free drug in the tissue. On the other hand, the newly formed free drug gets associated with ECM sites afresh to form bound drug.

Figure 6.7 represents the spatially averaged concentration profile against time for bound drug (b_2) in biological tissue in the presence of biodegradable and biodurable coatings. This concentration profile is quite distinct from the other previously examined graphical representations. Furthermore, it is worth notifying that the present graphical representation shows analogous behaviour until time $t = 800$ (in comparison to other plots) between the bound drug concentration profiles when the drug gets released from a biodegradable polymeric matrix or from a biodurable one. The pharmacological effect of a drug is determined by the duration of time in which the drug-receptor complex persists (residence time). The duration of the drug-receptor complex is influenced by dynamic processes (conformation changes) that regulate the rate of drug association and dissociation. Regarding the uniformity of the

b_2 profile over a long period of time, it may be concluded that there is a prolonged therapeutic effect in the biological tissue. Receptors' binding ability is regulated not only by external factors but also by intracellular regulatory mechanisms. Baseline receptor density and the efficiency of stimulus-response mechanisms vary from tissue to tissue. Drugs, ageing, genetic mutations, and disorders can enhance or diminish the binding affinity of receptors.

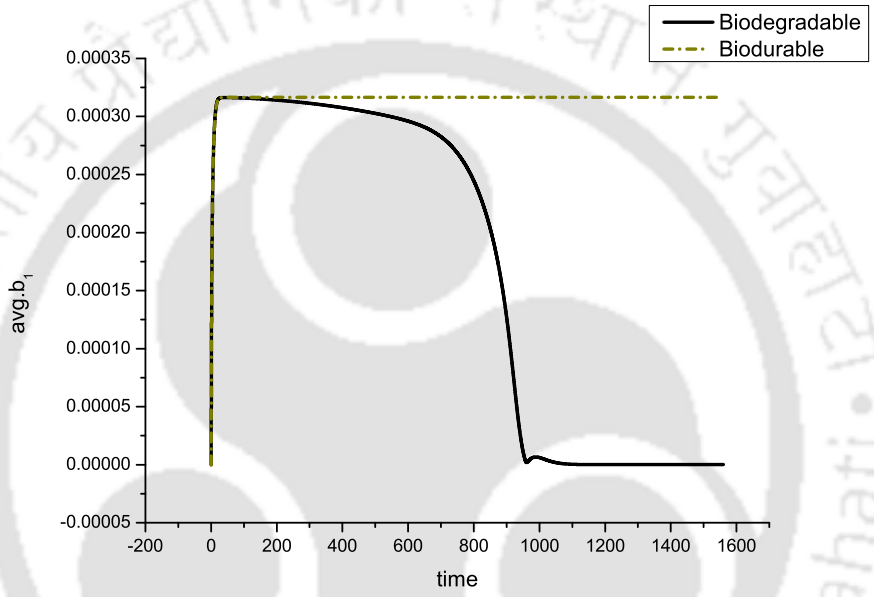

Figure 6.6: Time variant spatially averaged b_1 for biodegradable and biodurable polymer coating cases.

Fig. 6.8 depicts the temporal variations of the spatially averaged concentration profile for internalized drug (C_{int}) in biological tissue in the presence of biodegradable and biodurable coatings. The drug internalization is an important mechanism in the domain of drug metabolism, which deals with cellular uptake of drug molecules after being coupled with specific or non-specific binding sites (cf. [19, 32]). The graphical portrayals show build-up for bound drug at the initial stage, which reaches its pinnacle and melts away as an outcome of bound drug internalization. In the fullness of time, it can be perceived that both free and bound drugs are transformed into internalized drug. Lastly, the internalized drug concentration declines due to lysosomal degradation and it is important to note that it takes prolonged time in comparison to that of the other drug embodiments to fade away, which is obvious as all drug-forms ultimately get converted into internalized drug.

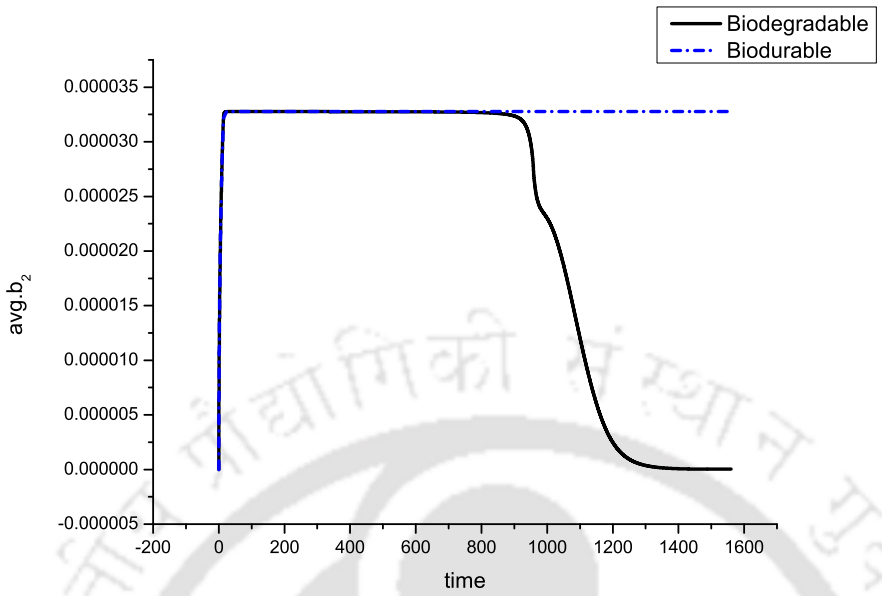

Figure 6.7: Time variant spatially averaged b_2 for biodegradable and biodurable polymer coating cases.

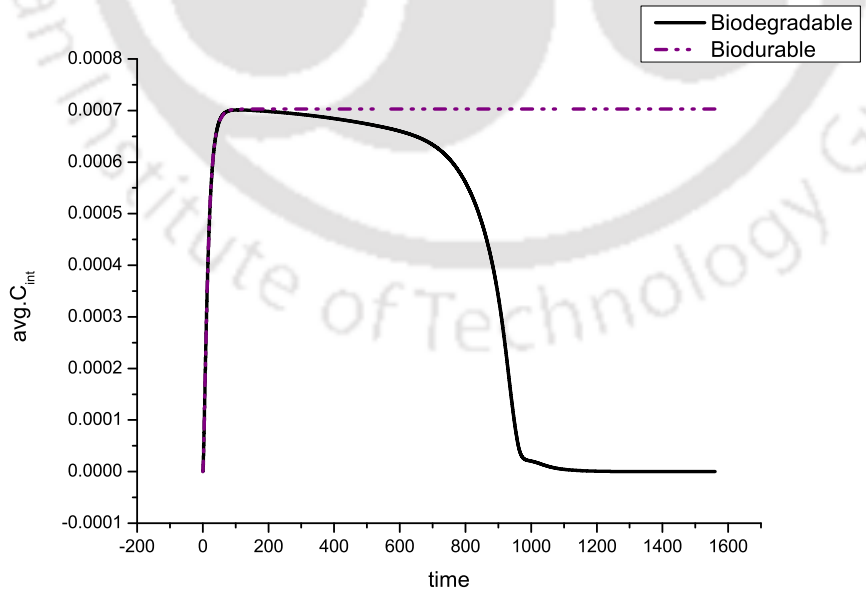

Figure 6.8: Time variant spatially averaged C_{int} for biodegradable and biodurable polymer coating cases.

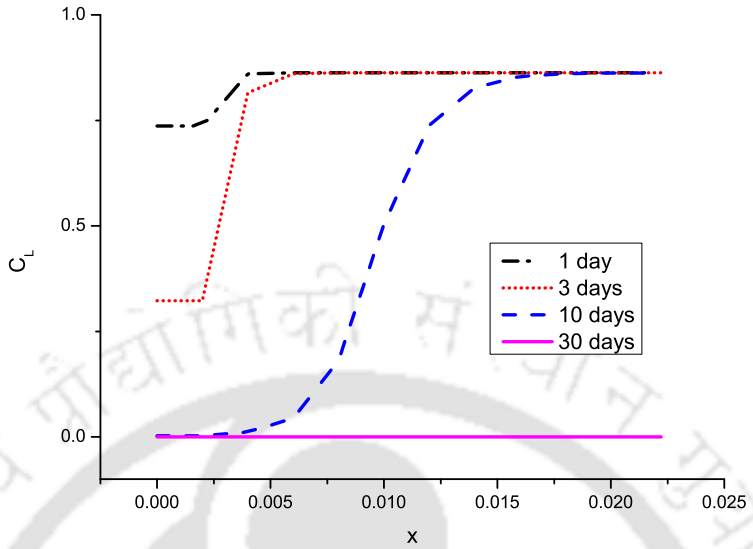

Figure 6.9: Space variant concentration profile of C_L in biodegradable polymeric matrix at four times.

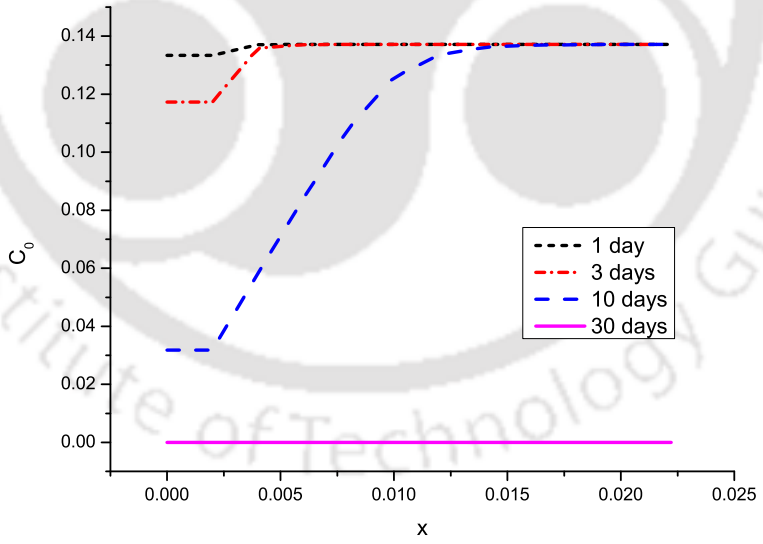

Figure 6.10: Space variant concentration profile of C_0 in biodegradable polymeric matrix at four times.

Figures 6.9 and 6.10 represent the space variant concentration profiles of both the solid drug (C_L) and free drug (C_0) for four different time spans. The trends in both the profiles are quite analogous. When observed minutely, it may be visualized that with increasing time duration, the graph is shifting towards the interface where concentrations get stabilized. This is due to the fact that with increasing

time duration, diffusivity of the polymeric matrix is enhancing with the loosening of polymer chains and as an outcome, concentrations towards the impermeable backing is getting diminished and drug particles are accumulating towards the interface. These two graphical representations are proofs of the fact that solubilisation of solid drug starts from the neighbourhood of impermeable backing and it is quite noteworthy that at the interface, there is availability of drug to have its non-interrupted sustained supply to the tissues.

The effects of association rate constant (δ_0) on both solid drug (C_L) and free drug (C_0) in the polymeric matrix are illustrated in Figs. 6.11 and 6.12 respectively. It is observed in Fig. 6.11 that with decrease in the association rate constant, the decline of C_L from its maximum loaded concentration rapidly increases. This behaviour is the result of low recrystallization due to decreased δ_0. On the other hand, in Fig. 6.12, with decrease in the association rate constant, the peak of C_0 heightens considerably since there is lower transformation of free drug back to solid drug.

The consequences of dissociation rate constant (β_0) on both solid drug (C_L) and free drug (C_0) in the polymeric matrix are illustrated in Figs. 6.13 and 6.14 respectively. As β_0 increases, the solid drug dissociates much faster to form free drug as anticipated. Hence, it is worthwhile to notice a sharp decline of the concentration profile C_L coupled with a stiff increase of C_0 in the event of the enhancement of dissociation rate constant.

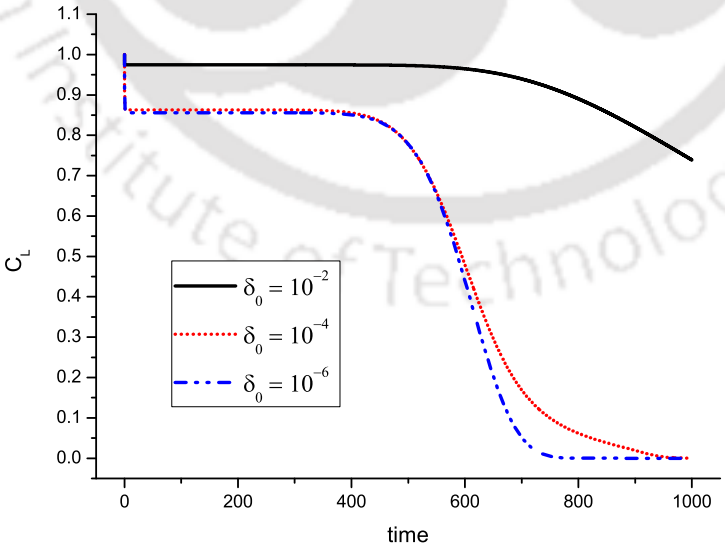

Figure 6.11: Time variant concentration profile of C_L in biodegradable polymeric matrix for different δ_0.

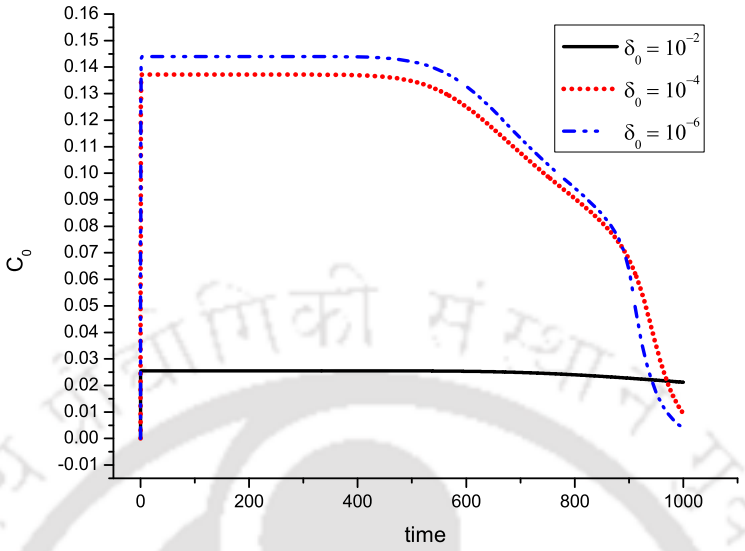

Figure 6.12: Time variant concentration profile of C_0 in biodegradable polymeric matrix for different δ_0.

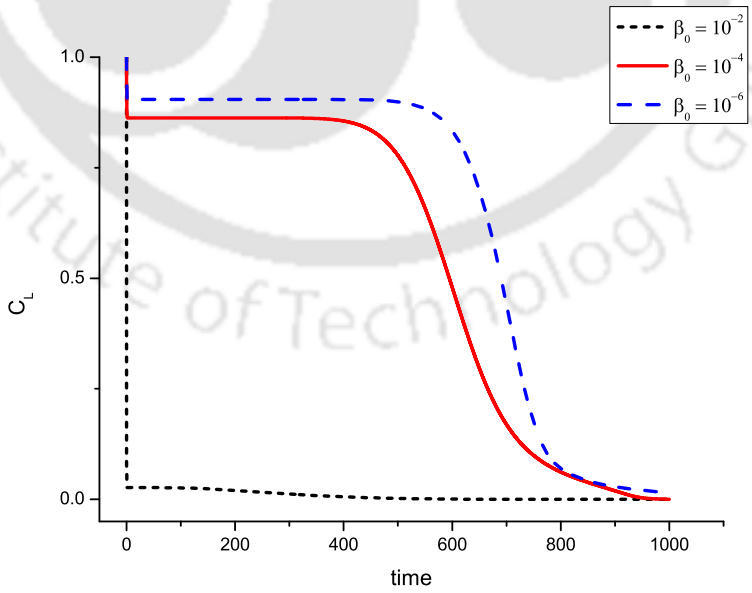

Figure 6.13: Time variant concentration profile of C_L in biodegradable polymeric matrix for different β_0.

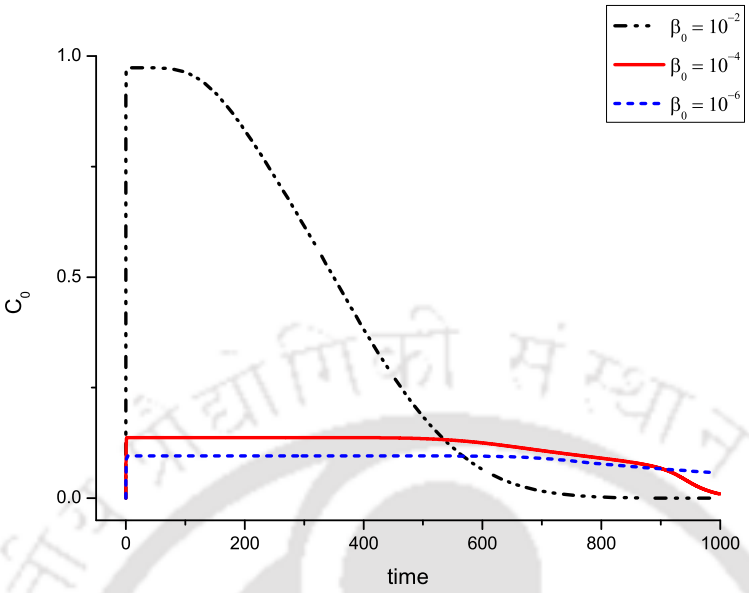

Figure 6.14: Time variant concentration profile of C_0 in biodegradable polymeric matrix for different β_0.

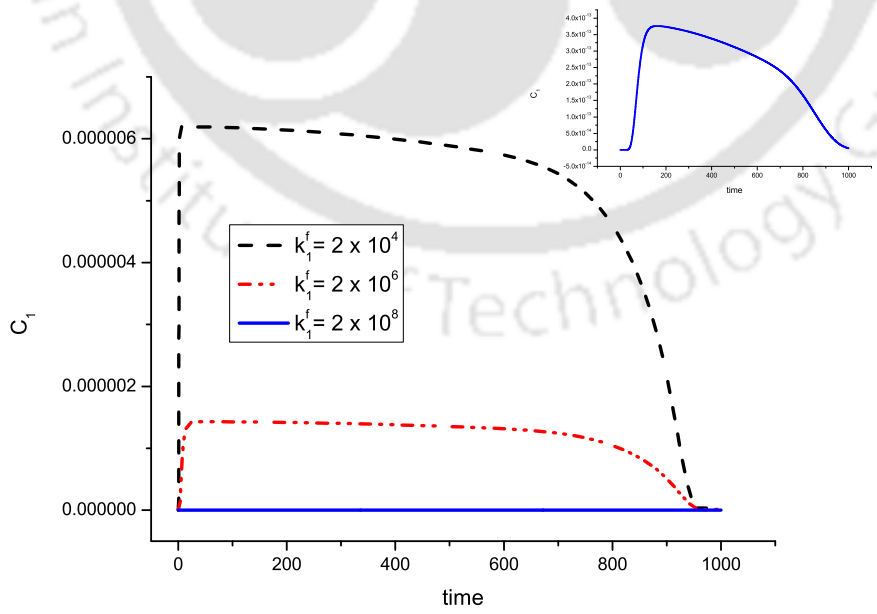

Figure 6.15: Time variant concentration profile of C_1 in biological tissue for different k_1^f.

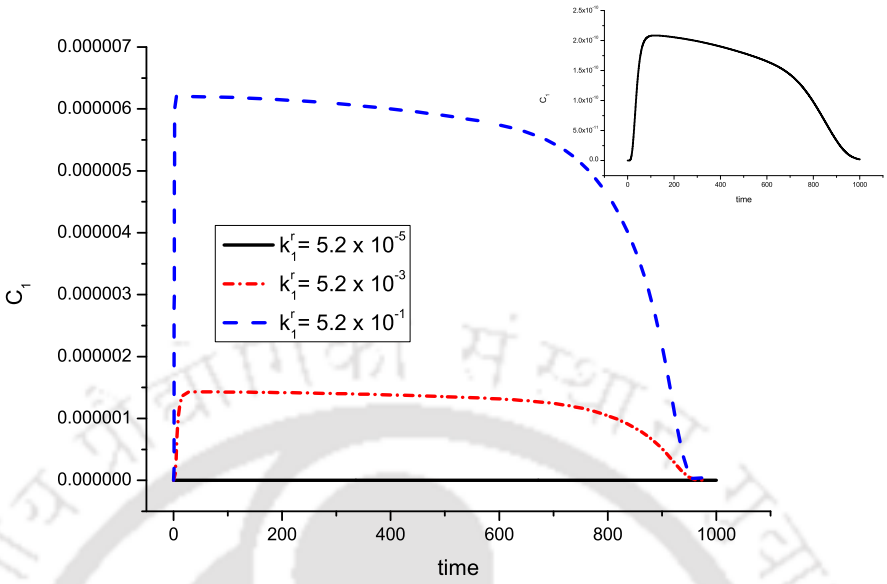

Figure 6.16: Time variant concentration profile of C_1 in biological tissue for different k_1^r.

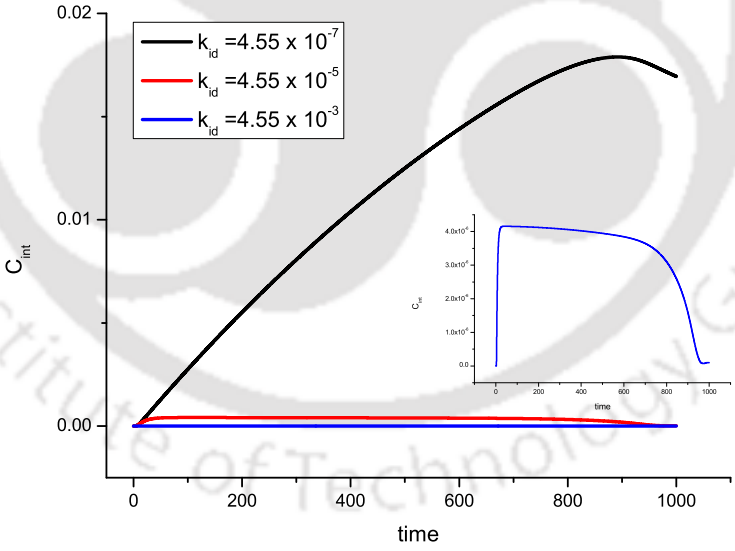

Figure 6.17: Time variant concentration profile of C_{int} in biological tissue for different k_{id}.

Figs. 6.15 and 6.16 represent the effects of association rate constant (k_1^f) and dissociation rate constant (k_1^r) respectively due to interaction between free drug and ECM sites on free drug concentration (C_1) in the biological tissue. One may observe in Fig. 6.15 that with increasing k_1^f, free drug concentration decreases as rate of transformation of free drug into bound drug increases. In Fig. 6.16, it is observed that with increasing k_1^r, the free drug concentration profile in the biological tissue increases. This is

due to the fact that if the dissociation rate increases, then the bound drug formed as an outcome of the interaction between free drug and ECM sites unbinds to transform into free drug again and therefore, free drug concentration in the biological tissue increases.

Lastly, the concluding plot Fig. 6.17 represents the influence of lysosomal degradation rate constant (k_{id}) on the internalized drug (C_{int}). The lysosomal degradation rate constant depicts the degradation rate of drug particles in the lysosomes of the cell. Thus, with increasing k_{id}, the internalized drug concentration decreases and this is also evident from Fig. 6.17. The inset plots are provided just to indicate that the concentration profiles, which seemed to be null in main plots, are actually having lower order of magnitude. Thus, all the above-mentioned graphical representations help in understanding the underlying drug kinetics in more details. Moreover, the influence of the model parameters are also well perceived through the graphical portrayals.

6.7 Conclusions

The present study proposes a simplified yet general mathematical model of polymer degradation and drug release from a local drug delivery device along with its subsequent transport to the biological tissue. The diffusion, dissolution and association / recrystallisation processes in the polymeric matrix phase along with specific / non-specific binding, dissociation and internalization phenomena in biological tissues are well embraced mathematically. The novelty of the present study is to examine the combined effects of biodegradable polymeric matrix and nonlinear biological processes on drug delivery to the biological tissues. Special emphasis is also laid to the drug release kinetics subject to biodurable polymeric matrix. The work undertaken speaks volumes about its accomplishments. First, the proposed model is realistic as it takes into consideration those apposite, imperative and vital physical phenomena. Secondly, nonlinear model is adopted to deal with biological complexities with minute details, yet in a simplified approach. Thirdly, a comparison of the proposed model with the experimental findings [3] reveals its authenticity as well as reliability in addition to the potency of the model undertaken and its pharmacokinetic applicability. Lastly, the numerical quantitative analysis is carried out in the embodiment of graphical representations for both biodegradable and biodurable polymeric coatings. These graphical portrayals reveal the difference in drug release rates corresponding to biodegradable and biodurable polymers. Additionally, the significant impacts of model parameters on drug kinetics are also well demonstrated through graphical representations, which illustrate the underlying governing physical phenomena of drug release and transport in great details. The improved model proposed in this study can form the basis for an upgraded and optimized drug delivery system. Moreover, the results obtained through this model can be utilized to delve deep into underlying kinetics of drug release and its transport. This also helps to comprehend the potential impacts of various model parameters of significance that control the therapeutic efficacy of the drug delivery system.

7 LIPOSOMAL DRUG DELIVERY

This chapter is completely designated by the model framework of liposomal drug delivery to solid tumour with the fulfilment of the objectives outlined in Chapter 1.

7.1 Introduction

In the last decade, in depth understanding of pathological behaviour of cancer cells through underlying molecular processes has developed noticeably [54]. With respect to cancer targeting, it is now a known fact that the number of receptors, especially growth factor receptors are detected to be overexpressed in tumour cells. Thus, these receptors enact as catalysts of growth in addition to as potential weak points for targeting specific ligands, antibodies or drugs [14]. Moreover, the pathophysiology of tumour neovasculature along with tumour-stroma interaction are detected as the backbone of tumour development. The conversion of normal cell into malignant tumour cell as an outcome of somatic gene mutations causes cancer. In the last two decades, implantable and injectable drug delivery systems have developed enormously for applications in the treatment of cancer. The reasons behind the development of such systems are to provide trouble-free vehicles for poorly soluble drug administration and to ameliorate the efficacy of anti-cancer drugs through the reduction of their side effects. The main purpose is to modify the biodistribution and bioavailability profiles of anti-cancer drugs so that the pharmacokinetics gets altered thereby having a positive influence on drug pharmacodynamics.

Drug-loaded temperature-sensitive liposomes after administration pass through the vasculature wall due to their small size and accumulate in the extracellular space in the tumour. These liposomes are anticipated to remain stable at body temperature. The current research trend in temperature-sensitive liposomes is to formulate their design so that their drug release kinetics, with respect to local hyperthermia, is maintained in a rapid but controlled manner. Drug release kinetics is not the only centre of attraction with regard to liposome-mediated drug delivery. All the stages in drug transport through systemic circulation to tumour intracellular compartment are equally vital in apprehending the underlying

biological phenomena.

A number of mathematical models have been proposed by various researchers [56, 45, 46, 58] in order to elucidate the underlying biological processes governing liposome-mediated drug transport. The work of Harashima et al. [56] dealt with liposomal drug delivery, which are temperature independent. The interaction between proteins in blood plasma and interstitial fluid with the drug particles was not considered in their work. The complexities of heat-based cancer treatment, such as thermal ablation via low temperature sensitive liposomes were studied computationally by Gasselhuber et al. [45]. Gasselhuber and his group developed a computational model that illustrates heat-based treatment with high intensity focused ultrasound (HIFU) [46]. Predictions regarding distributions of temperature and that of drug concentration due to hyperthermia-mediated drug delivery from temperature-sensitive liposomes were made, where hyperthermia was generated through HIFU heating. A generalised model proposed by Zhan and Xu [156] involves most of the prominent biochemical phenomena, such as drug transport through blood, lymphatic vessels and tumour compartments. The model also incorporated processes like drug binding with proteins, lymphatic drainage and drug uptake by tumour cells. Comparisons were done between Doxorubicin delivery to solid tumour by direct intravenous administration and temperature-sensitive liposomal drug delivery through mathematical modelling in order to measure their therapeutic efficacy. In a significant work, Liu and Xu [86] proposed a multi-compartment model for temperature-sensitive liposomal delivery of Doxorubicin. A detailed sensitivity analysis was made in order to have a glimpse of the significance of the input parameters playing vital roles on peak intracellular drug concentration. In all the above-mentioned studies, none has lightened up the fate of the drug particles after binding with the cell surface receptors and undergoing various complicated biological processes before being internalized into the cell. These complex processes play crucial role in transporting the drug from the extracellular space into the intracellular space.

In the present study, an improved compartmentalized mathematical model is proposed, which takes into account the important biological, physiological and biochemical phenomena, such as drug release in systemic plasma from the injected liposomes along with subsequent drug transport in the tumour compartment. It also includes plasma clearance, protein-drug interactions and transcapillary exchange of drugs. Moreover, the tumour compartment is subdivided into tumour plasma, tumour interstitial fluid and tumour intracellular phases respectively. Additionally, the tumour intracellular compartment is illustrated in details in order to interpret the path of drug particles from extracellular space into intracellular space, where vital processes like internalization through endocytosis and lysosomal degradation are given utmost importance. Thus, the complex interplay between free drug particles with surface and internalized cell receptors along with related endosomal events are well demonstrated with the help of a simple comprehensive mathematical model. A total of fifteen variables are used to describe the whole process, which is formulated as a system of partial differential equations with appropriate initial, interface and boundary conditions. The work of concern is a generalization of the models discussed so far.

7.2 Formulation of the problem

7.2.1 Physical background

Drug particles begin to circulate in systemic plasma throughout the body just after the initial dose is injected. Drug properties along with *in vivo* body environment regulate the process of drug transport within blood stream. During their transport by means of blood, drugs may get discharged into the tissues while passing by. Moreover, various organs of the body can take active part in filtering plasma thereby eliminating drugs from systemic circulation, biologically termed as plasma clearance. Being transported in systemic plasma, some drugs get dispersed into tumour plasma via blood perfusion due to advective and diffusive transport. These drugs can be extravasated into the interstitial fluid due to high permeability of tumour vasculature. Across the vessel wall, drug transport by fluid flux follows advection, which is the outcome of hydrostatic and osmotic pressure difference between lumen and interstitium. On the other hand, diffusive drug transport results from concentration gradient between blood and interstitial fluid along with vasculature permeability and area for drug exchange. Drug uptake by endothelial cells, i.e., transcytosis is having negligible effect in comparison to diffusion and advection [67]. The extracellular matrix and intense non-uniformity in vasculature distribution generate a complicated tumour interstitial space [125]. The tumour pressure may go beyond the atmospheric pressure by 4200 Pa [125, 15], which is the result of inefficient lymphatics, increased tumour vasculature permeability and cell proliferation in a restricted tumour volume leading to vasculature collapse [66]. An effective mathematical model is derived by Baxter and Jain [8] for transvascular exchange in addition to extravascular fluid and macromolecular transport in tumour.

In order to formulate the liposomal drug release mechanism from the initial administration of liposomes and subsequent drug transport to the tumour compartment, two compartments namely, systemic plasma compartment and tumour compartment are considered. The tumour compartment consists of three sub-compartments: tumour plasma, interstitial fluid and tumour cells. Drug transport is mainly governed by advection-diffusion equations, mass transfer equations and binding / unbinding equations. Before illustrating the complete process of liposomal drug release and consequent drug transport compartment-wise, some well-known equations are described, which are utilized in the primary governing equations. In accordance with Starling's law, the transvascular flux per tumour volume from blood to interstitium is defined as,

$$F_v = K_v \frac{S}{V} [\, p_v - p_i - \sigma_T \, (\pi_v - \pi_i) \,], \tag{7.2.1}$$

where K_v denotes the hydraulic conductivity of the wall of blood vessels, S/V is blood vessels' surface area per unit volume of tumour tissue, p_v and p_i are the respective pressures of blood vessels and interstitial fluid, σ_T is the average osmotic reflection coefficient (a measure of the relative permeability of a particular membrane to a particular solute) for plasma proteins and lastly, π_v and π_i denote the respective osmotic pressures of plasma and that of interstitial fluid.

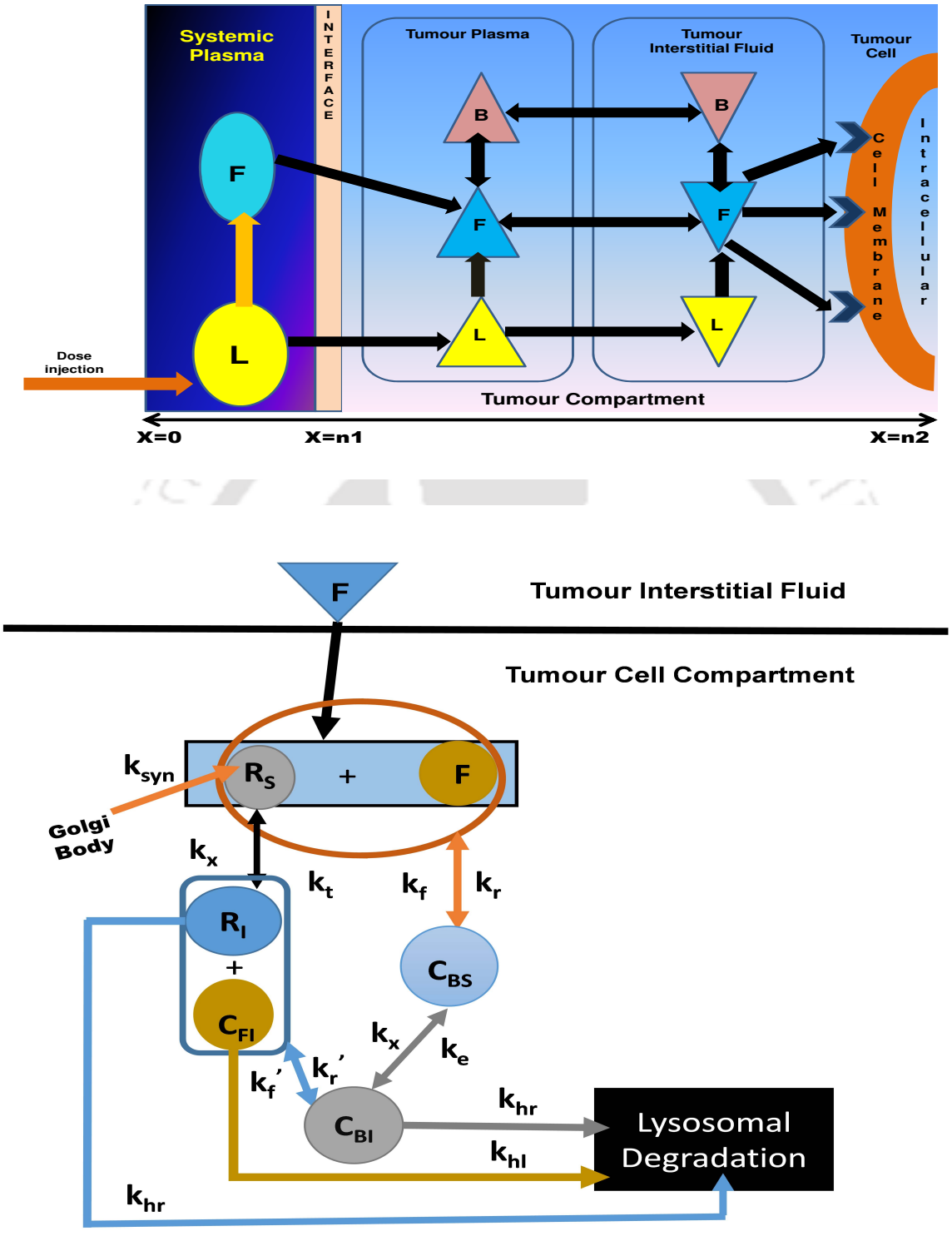

Figure 7.1: Schematic diagram of liposomal drug release and drug transport to tumour compartment

In order to elucidate the drug release and drug transport mechanism to the targeted tumour cells, the physical, biological and biochemical phenomena are discussed in details separately for all compart-

ments and sub-compartments. Besides theoretical narration, its mathematical representation in the form of models is also propounded. The self-explanatory schematic diagram for the compartmentalized mathematical modelling is provided in Fig. 7.1.

7.2.2 Mathematical modelling of drug release

Systemic plasma compartment

The pharmacokinetics of injected temperature-sensitive liposomes (C_L^S) is described in systemic plasma compartment. Following intravenous injection, the liposomes get distributed in the systemic plasma through the modes of diffusion and advection. Moreover, due to tortuous, elongated and usually dilated tumour vasculature, liposomes directly enter into the tumour plasma. Additionally, drugs encapsulated in the liposomes are released into the systemic plasma as free drugs (C_F^S). These free drugs also get distributed in systemic plasma through diffusion and advection, and subsequently enter into the tumour plasma. Hence, accumulation of liposomal drug at any instant in the systemic plasma depends on liposomal drug diffusion, advection and the rate of drug release from the liposomes. Similarly, accumulation of free drug at any instant in the systemic plasma, depends on free drug diffusion, advection and drug release rate of liposomes. So, the governing equations manifesting the dynamics of drug release in the systemic plasma can be written as follows:

Liposome-encapsulated drug concentration $[C_L^S]$

$$\frac{\partial C_L^S}{\partial t} = D_L^S \frac{\partial^2 C_L^S}{\partial x^2} - \gamma_1 \frac{\partial C_L^S}{\partial x} - k_1 C_L^S, \tag{7.2.2}$$

where D_L^S is the diffusion coefficient of liposome-encapsulated drug in the systemic plasma, γ_1 is the magnitude of advection and k_1 represents the drug release rate constant from liposomes at the systemic plasma.

Free drug concentration$[C_F^S]$

$$\frac{\partial C_F^S}{\partial t} = D_F^S \frac{\partial^2 C_F^S}{\partial x^2} - \gamma_2 \frac{\partial C_F^S}{\partial x} + k_1 C_L^S, \tag{7.2.3}$$

where D_F^S is the diffusion coefficient of free drug in the systemic plasma, γ_2 is the magnitude of advection and k_1 represents the drug release rate constant from liposomes at the systemic plasma.

7.2.3 Mathematical modelling of drug transport

Tumour compartment

As time elapses, the liposomal as well as free drug enter into the tumour compartment from the systemic plasma compartment. As mentioned earlier, the tumour compartment is sub-categorized into

tumour plasma, tumour interstitial fluid and tumour intracellular. Drug exchange between tumour plasma and tumour interstitial fluid goes on simultaneously, however in this study, a specific path of drug transport is taken into consideration. The liposomes having drug encapsulation move from the systemic plasma into the tumour plasma as C_L^{TP}. Similarly, the free drug in the systemic plasma enters into the tumour plasma as C_F^{TP}.

The accumulation of liposomal drug at any instant in the tumour plasma depends on liposomal drug diffusion, advection, rate of drug release from the liposomes and the net loss of liposomes due to transcapillary exchange of liposomes between plasma and interstitial fluid compartments of tumour. Thus, the governing equation denoting the dynamics of liposome-encapsulated drug concentration in tumour plasma is the following:

Liposome encapsulated drug concentration in tumour plasma $[C_L^{TP}]$

$$\frac{\partial C_L^{TP}}{\partial t} = D_L^{TP}\frac{\partial^2 C_L^{TP}}{\partial x^2} - \gamma_3\frac{\partial C_L^{TP}}{\partial x} - F_{lp} - k_{rel}C_L^{TP}, \tag{7.2.4}$$

where D_L^{TP} and γ_3 denote the diffusion coefficient and magnitude of advection of liposomal drug in tumour plasma respectively. F_{lp} is the liposome encapsulated drug loss due to the movement of liposome-encapsulated drugs into the interstitial fluid through capillary wall. k_{rel} stands for the drug release rate of liposome. Thus, F_{lp} is defined as

$$F_{lp} = F_v\,(1-\sigma_l)\,C_L^{TP} + P_l\,\frac{S}{V}\,(C_L^{TP} - C_L^{TIF})\,\frac{Pe_l}{e^{Pe_l}-1}, \tag{7.2.5}$$

where σ_l is the osmotic reflection coefficient for liposomal drug particles, P_l the vasculature wall permeability to liposomes and $Pe_l = \frac{F_v\,(1-\sigma_l)}{P_l\,(S/V)}$ represents the transcapillary Péclet number.

An exchange of liposomal drug occurs between tumour plasma and tumour interstitial fluid. Thus, the accumulation of liposomal drug at any instant in the tumour interstitial fluid depends on diffusion, advection of liposome-encapsulated drug particles in the interstitial fluid, net rate of liposomal drug gained from the tumour plasma and the rate of drug release from the liposomes. Hence, the dynamics of liposome-encapsulated drug may be modelled as follows:

Liposome encapsulated drug concentration in interstitial fluid $[C_L^{TIF}]$

$$\frac{\partial C_L^{TIF}}{\partial t} = D_L^{TIF}\frac{\partial^2 C_L^{TIF}}{\partial x^2} - \gamma_4\frac{\partial C_L^{TIF}}{\partial x} + F_{lp} - k_{rel}C_L^{TIF}, \tag{7.2.6}$$

where D_L^{TIF} and γ_4 denote the diffusion coefficient and the magnitude of advection of liposomal drug in the tumour interstitial fluid respectively. F_{lp} is the liposome encapsulated drug gained from transcapillary exchange in tumour sub-compartments with k_{rel} being the release rate of liposome.

The drug released from the liposomes in the interstitial fluid is depicted as free drug (C_F^{TIF}). This free drug gets disseminated throughout the interstitial fluid, binds with the proteins available there. Moreover, the free drug interacts with the surface receptors of the tumour cells and enters into the tumour intracellular space. No other forms of drug, whether it is liposomal drug or bound drug, can enter into the tumour cells. Accordingly, the accumulation of free drug at any instant in the interstitial fluid is influenced by diffusion, advection, rate of drug release from the liposomes, exchange of free drug from tumour plasma, association with proteins, dissociation of protein-free drug complex (i.e. bound drug C_B^{TIF}). Furthermore, free drug concentration in the interstitial fluid also depends on association with tumour cell surface receptors (R_S^{TC}) and dissociation of free drug-surface receptor complex (i.e. cell surface bound drug C_{BS}^{TC}). Hence, the dynamics of free drug in the interstitial fluid is demonstrated as follows:

Free drug concentration in the interstitial fluid $[C_F^{TIF}]$

$$\frac{\partial C_F^{TIF}}{\partial t} = D_F^{TIF}\frac{\partial^2 C_F^{TIF}}{\partial x^2} - \gamma_5\frac{\partial C_F^{TIF}}{\partial x} + F_{fp} + k_{rel}C_L^{TIF} + k_d C_B^{TIF} - k_a C_F^{TIF} C_P^{TIF} - k_f C_F^{TIF} R_S^{TC} + k_r C_{BS}^{TC}, \tag{7.2.7}$$

where D_F^{TIF} and γ_5 are the diffusion coefficient and the magnitude of advection of free drug in the interstitial fluid, respectively. F_{fp} is the free drug crossing the capillary wall into the interstitial fluid which may be defined as

$$F_{fp} = F_v(1-\sigma_d)C_F^{TP} + P_{fe}\frac{S}{V}(C_F^{TP} - C_F^{TIF})\frac{Pe_f}{e^{Pe_f}-1}, \tag{7.2.8}$$

where σ_d is the osmotic reflection coefficient for drug particles, C_F^{TP} is free drug concentration in tumour plasma, P_{fe} denotes the vasculature wall permeability to free drug particles and $Pe_f = \frac{F_v(1-\sigma_d)}{P_{fe}(S/V)}$ represents the transcapillary Péclet number. k_{rel} is the release rate of liposome, whereas, k_d , k_r and k_a, k_f are the dissociation and association rate constants, respectively.

Free drug (C_F^{TIF}) binds with the proteins (C_P^{TIF}) in the interstitial fluid to form a free drug-protein complex, i.e. bound drug (C_B^{TIF}). Therefore, the accumulation of proteins and bound drug at any instant in the interstitial fluid depends on the association and dissociation rate constants respectively. Moreover, bound drug concentration also depends on its diffusion, advection and transcapillary exchange of bound drug into tumour interstitial fluid. Hence, the governing equations manifesting the dynamics of proteins and bound drug in the interstitial fluid are the following:

Protein concentration in the interstitial fluid $[C_P^{TIF}]$

$$\frac{\partial C_P^{TIF}}{\partial t} = k_d C_B^{TIF} - k_a C_F^{TIF} C_P^{TIF}, \tag{7.2.9}$$

where k_d and k_a are described earlier.

Bound drug concentration in the interstitial fluid $[C_B^{TIF}]$

$$\frac{\partial C_B^{TIF}}{\partial t} = D_B^{TIF}\frac{\partial^2 C_B^{TIF}}{\partial x^2} - \gamma_6\frac{\partial C_B^{TIF}}{\partial x} - k_d C_B^{TIF} + k_a C_F^{TIF} C_P^{TIF} + F_{be}, \tag{7.2.10}$$

where D_B^{TIF} and γ_6 are the diffusion coefficient and magnitude of advection of bound drug respectively in the interstitial fluid. F_{be} depicts the amount of bound drug gained from transcapillary exchange into the interstitial fluid, defined as,

$$F_{be} = F_v(1-\sigma_d)C_B^{TP} + P_{be}\frac{S}{V}(C_B^{TP} - C_B^{TIF})\frac{Pe_b}{e^{Pe_b}-1}, \tag{7.2.11}$$

where P_{be} denotes the vasculature wall permeability to bound drug particles and $Pe_b = \frac{F_v\,(1-\sigma_d)}{P_{be}\,(S/V)}$ represents the transcapillary Péclet number.

Free drug in the systemic plasma enters into tumour plasma as C_F^{TP}. Furthermore, liposomes in the tumour plasma also discharge free drug particles. In addition to that, there is simultaneous exchange of free drug between tumour plasma and tumour interstitial fluid. Besides, the free drug particles in the tumour plasma interact with proteins present there. Therefore, the accumulation of free drug at any instant in the tumour plasma depends on liposomal drug release rate, inter-exchange of drug particles between tumour plasma and interstitial fluid, plasma clearance of free drug, binding with the tumour plasma proteins and dissociation of the free drug-protein complex (i.e., bound drug C_B^{TP}). Thus, the dynamics of free drug in tumour plasma may be mathematically portrayed as follows:

Free drug concentration in tumour plasma $[C_F^{TP}]$

$$\frac{\partial C_F^{TP}}{\partial t} = k_{rel}C_L^{TP} - v^{TP}F_{fp} - ke_1 C_F^{TP} - k_a C_F^{TP} C_P^{TP} + k_d C_B^{TP}, \tag{7.2.12}$$

where, k_{rel} is liposomal drug release rate, v^{TP} is the volume fraction of tumour plasma, F_{fp} is the free drug crossing the capillary wall into the interstitial fluid, ke_1 is the plasma clearance rate, k_a and k_d are association and dissociation rates with proteins, respectively.

Free drug (C_F^{TP}) in the tumour plasma binds with the plasma proteins (C_P^{TP}) to form a free drug-protein complex, i.e. bound drug (C_B^{TP}). Therefore, the accumulation of proteins and bound drug at any instant in the tumour plasma depend on both association and dissociation rate constants. Moreover, bound drug concentration also depends on the exchange of bound drug between tumour plasma and interstitial fluid. Hence, the governing equations manifesting the dynamics of proteins and bound drug in the tumour plasma are the following:

Protein concentration in tumour plasma $[C_P^{TP}]$

$$\frac{\partial C_P^{TP}}{\partial t} = -k_a C_F^{TP} C_P^{TP} + k_d C_B^{TP}, \tag{7.2.13}$$

where k_a and k_d are association and dissociation rates with proteins.

Bound drug concentration in tumour plasma $[C_B^{TP}]$

$$\frac{\partial C_B^{TP}}{\partial t} = -v^{TP} F_{be} + k_a C_F^{TP} C_P^{TP} - k_d C_B^{TP}, \tag{7.2.14}$$

where F_{be} depicts the amount of bound drug lost due to transcapillary exchange into the interstitial fluid.

The free drug particles of the tumour interstitial fluid (C_F^{TIF}), being eligible to enter into the intracellular space, interact with the cell surface receptors (R_S^{TC}) to form free drug-receptor complex, i.e., cell surface bound drug (C_{BS}^{TC}). The accumulation of cell surface receptors at any instant in the tumour cell compartment depends on its binding with the free drug, unbinding of the bound drug, synthesis rate of new surface receptors in the Golgi body, constitutive internalization rate and recycle rate of internalized cell receptors. Therefore, the governing equation manifesting the dynamics of cell surface receptors can be written as

Cell surface receptor concentration $[R_S^{TC}]$

$$\frac{\partial R_S^{TC}}{\partial t} = -k_f R_S^{TC} C_F^{TIF} + k_r C_{BS}^{TC} - k_t R_S^{TC} + k_x R_I^{TC} + k_{syn} R_S^{TC}, \tag{7.2.15}$$

where k_f and k_r are the association and dissociation rate constants respectively. k_t is the constitutive internalization rate constant, k_x denotes the receptor recycling rate constant and k_{syn} represents the synthesis rate of surface receptors.

The accumulation of cell surface bound drug at any instant in the tumour cell compartment depends on free drug-surface receptor interaction, rate of its internalization into the cell and the rate of recycling of internalized bound drug back to the cell surface. Hence, the dynamics of cell surface bound drug may be mathematically represented as follows:

Cell surface bound drug concentration $[C_{BS}^{TC}]$

$$\frac{\partial C_{BS}^{TC}}{\partial t} = k_f R_S^{TC} C_F^{TIF} - k_r C_{BS}^{TC} - k_e C_{BS}^{TC} + k_x C_{BI}^{TC}, \tag{7.2.16}$$

where k_e represents the internalization rate constant.

The cell surface bound drug gets internalized into the cell as C_{BI}^{TC}. This internalized bound drug dissociates into free drug (C_{FI}^{TC}) in the intracellular space and the free drug (C_{FI}^{TC}) interacts with the internalized cell receptors (R_I^{TC}) to again form internalized free drug-receptor complex, i.e., internalized bound drug (C_{BI}^{TC}). The internalized bound drug may get degraded by the lysosomes or recycle back to

the cell surface. Thus, accumulation of internalized bound drug at any instant depends on the rate of internalization of cell surface bound drug, rate of its dissociation into free drug, rate of association of the free drug with the internalized receptors, its recycle rate and lysosomal degradation rate. Accordingly, the dynamics of internalized bound drug may be manifested as follows:

Internalized bound drug concentration $[C_{BI}^{TC}]$

$$\frac{\partial C_{BI}^{TC}}{\partial t} = k_e C_{BS}^{TC} + k_f^{'} R_I^{TC} C_{FI}^{TC} - k_r^{'} C_{BI}^{TC} - (k_{hr} + k_x) C_{BI}^{TC}, \tag{7.2.17}$$

where $k_f^{'}$ and $k_r^{'}$ are the association and dissociation constants respectively. k_{hr} denotes the lysosomal degradation rate constant.

The internalized free drug is formed as an outcome of dissociation of internalized bound drug. The accumulation of internalized free drug at any instant depends on dissociation of bound drug, association with internalized receptors and lysosomal degradation rate. Thus, dynamics of internalized free drug may be modelled as follows:

Internalized free drug concentration $[C_{FI}^{TC}]$

$$\frac{\partial C_{FI}^{TC}}{\partial t} = -k_f^{'} R_I^{TC} C_{FI}^{TC} + k_r^{'} C_{BI}^{TC} - k_{hl} C_{FI}^{TC}, \tag{7.2.18}$$

where k_{hl} denotes the lysosomal degradation rate constant of internalized free drug.

The accumulation of internalized receptors at any instant depends on their interactions with internalized free drug particles, dissociation of internalized bound drug, internalization of cell surface receptors, their recycling back to the cell surface and finally their lysosomal degradation. Hence, all the physical phenomena are summed up in the following equation:

Internalized receptor concentration $[R_I^{TC}]$

$$\frac{\partial R_I^{TC}}{\partial t} = -k_f^{'} R_I^{TC} C_{FI}^{TC} + k_r^{'} C_{BI}^{TC} + k_t R_S^{TC} - (k_{hr} + k_x) R_I^{TC}. \tag{7.2.19}$$

Initial, interface and boundary conditions

Initially at time $t = 0$, only the injected dose of liposome-encapsulated drug is available. Moreover, since plasma and interstitial fluid in the tumour compartment contain proteins, so initially they are having non-zero concentration. The receptor concentrations in the tumour intracellular compartment are also having non-null concentrations initially. All the other drug embodiments taken into consideration are initially have null concentration. Therefore, the initial conditions are as follows:

$$C_L^S(x,0) = M, \quad C_F^S(x,0) = 0, \quad C_L^{TP}(x,0) = 0, \quad C_L^{TIF}(x,0) = 0, \quad C_F^{TIF}(x,0) = 0,$$
$$C_P^{TIF}(x,0) = P_0^{TIF}, \quad C_B^{TIF}(x,0) = 0, \quad C_F^{TP}(x,0) = 0, \quad C_P^{TP}(x,0) = P_0^{TP}, \quad C_B^{TP}(x,0) = 0,$$
$$R_S^{TC}(x,0) = R_{S0}^{TC}, \quad C_{BS}^{TC}(x,0) = 0, \quad C_{BI}^{TC}(x,0) = 0, \quad C_{FI}^{TC}(x,0) = 0, \quad R_I^{TC}(x,0) = R_{I0}^{TC};$$

in which M, P_0^{TIF}, P_0^{TP}, R_{S0}^{TC} and R_{I0}^{TC} are the respective initial concentrations.

At $x = 0$, i.e., at the left boundary of the systemic plasma, both the liposome-encapsulated drug and free drug are eliminated through body clearance. These can be mathematically described as follows:

$$-D_L^S \frac{\partial C_L^S}{\partial x} = k_{cl}^L C_L^S \quad \text{and} \quad -D_F^S \frac{\partial C_F^S}{\partial x} = k_{cl}^F C_F^S,$$

where k_{cl}^L and k_{cl}^F are the clearance rate constants of liposomal and free drug respectively, in the systemic plasma. At $x = n1$, i.e., at the interface where both the liposomal drug and free drug enter into the tumour compartment from the systemic plasma, the following interface conditions are taken into consideration. Flux continuity must be assigned at the interface. Therefore,

$$\gamma_1 C_L^S - D_L^S \frac{\partial C_L^S}{\partial x} = \gamma_3 C_L^{TP} - D_L^{TP} \frac{\partial C_L^{TP}}{\partial x},$$

Moreover, at the interface, concentration jump may occur due to different drug partitioning between systemic plasma and tumour compartment. Such complexities are addressed through a suitable mass transfer coefficients [P_q, $q = 1,2,3,4$]. Thus, the following conditions are assigned:

$$\begin{aligned}
-D_F^S \frac{\partial C_F^S}{\partial x} &= P_1 (C_F^{TP} - C_F^S), \qquad \text{at } x = n1,\\
-D_L^{TP} \frac{\partial C_L^{TP}}{\partial x} &= P_2 (C_L^S - C_L^{TP}), \qquad \text{at } x = n1,\\
-D_L^{TIF} \frac{\partial C_L^{TIF}}{\partial x} &= P_3 (C_L^S - C_L^{TIF}), \qquad \text{at } x = n1,\\
-D_F^{TIF} \frac{\partial C_F^{TIF}}{\partial x} &= P_4 (C_F^S - C_F^{TIF}), \qquad \text{at } x = n1,
\end{aligned}$$

Furthermore, since the bound drug is not eligible to emerge out of the tumour compartment, so a no-flux condition may be implied.

$$\gamma_6 C_B^{TIF} - D_B^{TIF} \frac{\partial C_B^{TIF}}{\partial x} = 0, \qquad \text{at } x = n1.$$

At $x = n2$, i.e., the extreme right boundary of the tumour compartment, certain no-flux conditions are considered as the liposome-encapsulated drug and bound drugs are unable to emerge out of the tumour. Hence, the following boundary conditions are taken into account:

$$\begin{aligned}
\gamma_3 C_L^{TP} - D_L^{TP} \frac{\partial C_L^{TP}}{\partial x} &= 0, \qquad \text{at } x = n2,\\
\gamma_4 C_L^{TIF} - D_L^{TIF} \frac{\partial C_L^{TIF}}{\partial x} &= 0, \qquad \text{at } x = n2,\\
\gamma_6 C_B^{TIF} - D_B^{TIF} \frac{\partial C_B^{TIF}}{\partial x} &= 0, \qquad \text{at } x = n2.
\end{aligned}$$

Moreover, due to interaction between C_F^{TIF} and R_S^{TC}, there is feeble possibility of the existence of C_F^{TIF}

at the extreme right boundary at $x = n2$. Hence, $C_F^{TIF} = 0$ at $x = n2$.

7.2.4 Nondimensionalization

In the process of converting the equations to simple forms so that simulations can be done in a systematic approach, all the variables and parameters are nondimensionalized. Hence, the parameters and variables are nondimensionalized in the following way:

$$\overline{C_j^i} = \frac{C_j^i}{M}, \quad i = S,TP,TIF,TC, \quad j = L,F,B,P,BS,BI,FI, \quad \overline{R_k^{TC}} = \frac{R_k^{TC}}{M}, \quad k = S,I,$$

$$\bar{x} = \frac{x}{n2}, \quad \bar{t} = \frac{D_L^S\, t}{n2^2}, \quad \overline{nl} = \frac{nl}{n2}, \quad l = 1,2, \quad \overline{D_m^n} = \frac{D_m^n}{D_L^S}, \quad m = L,F,B, \quad n = S,TP,TIF,$$

$$\overline{F_v} = \frac{F_v\, n2^2}{D_L^S}, \quad \overline{P_o\, \frac{S}{V}} = \frac{P_o\, \frac{S}{V}\, n2^2}{D_L^S}, \quad o = l,fe,be, \quad \overline{k_{rel}} = \frac{k_{rel}\, n2^2}{D_L^S}, \quad \overline{k_{cl}^L} = \frac{k_{cl}^L\, n2}{D_L^S}, \quad \overline{k_{cl}^F} = \frac{k_{cl}^F\, n2}{D_L^S},$$

$$Pe_p = \frac{\gamma_p\, n2}{D_L^S}, \quad p = 1,2,3,4,5,6, \quad Q_q = \frac{P_q\, n2}{D_L^S}, \quad q = 1,2,3,4, \quad \overline{P_0^a} = \frac{P_0^a}{M}, \quad a = TP,TIF,$$

$$\overline{R_b^{TC}} = \frac{R_b^{TC}}{M}, \quad b = S0,I0, \quad Da_0 = \frac{k_a\, n2^2\, P_0^{TIF}}{D_L^S}, \quad Da_1 = \frac{k_a\, n2^2\, P_0^{TP}}{D_L^S}, \quad Da_2 = \frac{k_f\, n2^2\, R_{S0}^{TC}}{D_L^S},$$

$$Da_3 = \frac{k_f'\, n2^2\, R_{I0}^{TC}}{D_L^S}, \quad \alpha = \frac{k_d}{k_a}, \quad \beta = \frac{k_r}{k_f}, \quad \delta = \frac{k_r'}{k_f'}, \quad Bp_0 = \frac{P_0^{TIF}}{\alpha}, \quad Bp_1 = \frac{P_0^{TP}}{\alpha},$$

$$Bp_2 = \frac{R_{S0}^{TC}}{\beta}, \quad Bp_3 = \frac{R_{I0}^{TC}}{\delta}, \quad \overline{k_c} = \frac{k_c\, n2^2}{D_L^S}, \quad c = 1,e_1,t,x,syn,e,hr,hl.$$

Dimensionless equations

The bars are omitted from all the dimensionless parameters and variables for the sake of convenience. The following equations are in nondimensionalized illustration:

$$\frac{\partial C_L^S}{\partial t} = \frac{\partial^2 C_L^S}{\partial x^2} - Pe_1 \frac{\partial C_L^S}{\partial x} - k_1 C_L^S, \tag{7.2.20}$$

$$\frac{\partial C_F^S}{\partial t} = D_F^S \frac{\partial^2 C_F^S}{\partial x^2} - Pe_2 \frac{\partial C_F^S}{\partial x} + k_1 C_L^S, \tag{7.2.21}$$

$$\frac{\partial C_L^{TP}}{\partial t} = D_L^{TP} \frac{\partial^2 C_L^{TP}}{\partial x^2} - Pe_3 \frac{\partial C_L^{TP}}{\partial x} - F_{lp} - k_{rel} C_L^{TP}, \tag{7.2.22}$$

$$\frac{\partial C_L^{TIF}}{\partial t} = D_L^{TIF} \frac{\partial^2 C_L^{TIF}}{\partial x^2} - Pe_4 \frac{\partial C_L^{TIF}}{\partial x} + F_{lp} - k_{rel} C_L^{TIF}, \tag{7.2.23}$$

$$\frac{\partial C_F^{TIF}}{\partial t} = D_F^{TIF} \frac{\partial^2 C_F^{TIF}}{\partial x^2} - Pe_5 \frac{\partial C_F^{TIF}}{\partial x} + F_{fp} + k_{rel} C_L^{TIF} + \frac{Da_0}{Bp_0} C_B^{TIF} - \frac{Da_0}{P_0^{TIF}} C_F^{TIF} C_P^{TIF}$$

$$- \frac{Da_2}{R_{S0}^{TC}} R_S^{TC} C_F^{TIF} + \frac{Da_2}{Bp_2} C_{BS}^{TC}, \tag{7.2.24}$$

$$\frac{\partial C_P^{TIF}}{\partial t} = \frac{Da_0}{Bp_0} C_B^{TIF} - \frac{Da_0}{P_0^{TIF}} C_F^{TIF} C_P^{TIF}, \tag{7.2.25}$$

$$\frac{\partial C_B^{TIF}}{\partial t} = D_B^{TIF} \frac{\partial^2 C_B^{TIF}}{\partial x^2} - Pe_6 \frac{\partial C_B^{TIF}}{\partial x} - \frac{Da_0}{Bp_0} C_B^{TIF} + \frac{Da_0}{P_0^{TIF}} C_F^{TIF} C_P^{TIF} + F_{be}, \tag{7.2.26}$$

$$\frac{\partial C_F^{TP}}{\partial t} = k_{rel} C_L^{TP} - v^{TP} F_{fp} - ke_1 C_F^{TP} - \frac{Da_1}{P_0^{TP}} C_F^{TP} C_P^{TP} + \frac{Da_1}{Bp_1} C_B^{TP}, \tag{7.2.27}$$

$$\frac{\partial C_P^{TP}}{\partial t} = -\frac{Da_1}{P_0^{TP}} C_F^{TP} C_P^{TP} + \frac{Da_1}{Bp_1} C_B^{TP}, \tag{7.2.28}$$

$$\frac{\partial C_B^{TP}}{\partial t} = -v^{TP} F_{be} + \frac{Da_1}{P_0^{TP}} C_F^{TP} C_P^{TP} - \frac{Da_1}{Bp_1} C_B^{TP}, \tag{7.2.29}$$

$$\frac{\partial R_S^{TC}}{\partial t} = -\frac{Da_2}{R_{S0}^{TC}} R_S^{TC} C_F^{TIF} + \frac{Da_2}{Bp_2} C_{BS}^{TC} - k_t R_S^{TC} + k_x R_I^{TC} + k_{syn} R_S^{TC}, \tag{7.2.30}$$

$$\frac{\partial C_{BS}^{TC}}{\partial t} = \frac{Da_2}{R_{S0}^{TC}} R_S^{TC} C_F^{TIF} - \frac{Da_2}{Bp_2} C_{BS}^{TC} - k_e C_{BS}^{TC} + k_x C_{BI}^{TC}, \tag{7.2.31}$$

$$\frac{\partial C_{BI}^{TC}}{\partial t} = k_e C_{BS}^{TC} + \frac{Da_3}{R_{I0}^{TC}} R_I^{TC} C_{FI}^{TC} - \frac{Da_3}{Bp_3} C_{BI}^{TC} - (k_{hr} + k_x) C_{BI}^{TC}, \tag{7.2.32}$$

$$\frac{\partial C_{FI}^{TC}}{\partial t} = -\frac{Da_3}{R_{I0}^{TC}} R_I^{TC} C_{FI}^{TC} + \frac{Da_3}{Bp_3} C_{BI}^{TC} - k_{hl} C_{FI}^{TC}, \tag{7.2.33}$$

$$\frac{\partial R_I^{TC}}{\partial t} = -\frac{Da_3}{R_{I0}^{TC}} R_I^{TC} C_{FI}^{TC} + \frac{Da_3}{Bp_3} C_{BI}^{TC} + k_t R_S^{TC} - (k_{hr} + k_x) R_I^{TC}. \tag{7.2.34}$$

Dimensionless initial, interface and boundary conditions

$$C_L^S(x,0) = 1, \quad C_F^S(x,0) = 0, \quad C_L^{TP}(x,0) = 0, \quad C_L^{TIF}(x,0) = 0, \quad C_F^{TIF}(x,0) = 0,$$

$$C_P^{TIF}(x,0) = P_0^{TIF}, \quad C_B^{TIF}(x,0) = 0, \quad C_F^{TP}(x,0) = 0, \quad C_P^{TP}(x,0) = P_0^{TP}, \quad C_B^{TP}(x,0) = 0,$$

$$R_S^{TC}(x,0) = R_{S0}^{TC}, \quad C_{BS}^{TC}(x,0) = 0, \quad C_{BI}^{TC}(x,0) = 0, \quad C_{FI}^{TC}(x,0) = 0, \quad R_I^{TC}(x,0) = R_{I0}^{TC},$$

$$-\frac{\partial C_L^S}{\partial x} = k_{cl}^L C_L^S \quad \text{and} \quad -D_F^S \frac{\partial C_F^S}{\partial x} = k_{cl}^F C_F^S, \qquad \text{at } x = 0,$$

$$Pe_1 C_L^S - D_L^S \frac{\partial C_L^S}{\partial x} = Pe_3 C_L^{TP} - D_L^{TP} \frac{\partial C_L^{TP}}{\partial x}, \qquad \text{at } x = n1,$$

$$-D_F^S \frac{\partial C_F^S}{\partial x} = Q_1 (C_F^{TP} - C_F^S), \qquad \text{at } x = n1,$$

$$-D_L^{TP} \frac{\partial C_L^{TP}}{\partial x} = Q_2 (C_L^S - C_L^{TP}), \qquad \text{at } x = n1,$$

$$-D_L^{TIF} \frac{\partial C_L^{TIF}}{\partial x} = Q_3 (C_L^S - C_L^{TIF}), \qquad \text{at } x = n1,$$

$$-D_F^{TIF} \frac{\partial C_F^{TIF}}{\partial x} = Q_4 (C_F^S - C_F^{TIF}), \qquad \text{at } x = n1,$$

$$Pe_6 C_B^{TIF} - D_B^{TIF} \frac{\partial C_B^{TIF}}{\partial x} = 0, \qquad \text{at } x = n1,$$

$$Pe_3\, C_L^{TP} - D_L^{TP}\, \frac{\partial C_L^{TP}}{\partial x} = 0, \qquad \text{at } x = n2,$$

$$Pe_4\, C_L^{TIF} - D_L^{TIF}\, \frac{\partial C_L^{TIF}}{\partial x} = 0, \qquad \text{at } x = n2,$$

$$Pe_6\, C_B^{TIF} - D_B^{TIF}\, \frac{\partial C_B^{TIF}}{\partial x} = 0, \qquad \text{at } x = n2,$$

$$C_F^{TIF} = 0, \qquad \text{at } x = n2.$$

7.3 Numerical solution

The system of nondimensional nonlinear partial differential equations (7.2.20) - (7.2.34) are numerically solved using method of finite differences. All the space derivative terms present in the model are approximated by second order accurate three-point central difference formula at the internal nodes. The reaction terms are approximated at each of the nodal points. A vital characteristic of layered geometry is the implementation of conditions like, flux continuity and concentration jump at the interface which is the common boundary between the two layers. It is supposed that only one grid-point is available on the left boundary ($x = 0$), the interface ($x = n1$) and the right boundary ($x = n2$) for spatial discretization in case of clearance, flux continuity and jump concentration conditions. At the interface and boundaries, all the spatial derivatives are approximated with the help of one-sided finite difference formula. After spatial discretization, the advocated system of partial differential equations reduces to a system of ordinary differential equations. The new system thus formed is solved through fourth order explicit Runge-Kutta method. The spatial grid length Δx and the temporal one Δt are chosen in such a way that the numerical scheme converges. Since the proposed model is a generalized one, the model parameters may vary on the basis of different types of anti-cancer drugs. In the computational point of view, fixed model parameters are obtained from available literature. The model parameters along with their dimensional numerical values are tabulated in Tables 7.1 - 7.2.

7.4 Model validation

Site-targeted chemotherapy is a complicated process, specially for low molecular weight cytostatics like Doxorubicin (DOX). In the recent past, approaches are adopted in order to improve the thermosensitive liposome formulation. It is established through research that incorporation of pegylated lipids affects the drug release kinetics of liposome in addition to prolonging the circulation time of them [44, 82, 100]. Lokerse et al. [88] conducted an experimental research in order to improve further the formulation of thermosensitive liposomes through variation of their lipid composition. They prepared four formulations for thermosensitive liposomes by changing DPPC / DSPC (1,2-dipalmitoyl-sn-glycerophosphocholine / 1,2-distearoyl-sn- glycerophosphocholine) ratio. For all formulated liposomes, fluorometry was utilized to measure their stability at 37°C and the release kinetics at 42°C. The intraliposomal buffers ammonium sulphate or citrate were used to compare DOX loading efficiency, stability and release kinetics. The materials used and the methods applied for the preparation of liposomes, for liposome radiolabeling and the measurement of liposomal release kinetics are discussed in details in [88]. The main goal of the present study is to validate the aptness of the advocated model by

directly comparing with experimental results based on liposomal drug delivery. Since all the relevant model parameter values are not available, several articles are consulted and the parameter values are kept within pharmacological range of the order of magnitudes. All the model parameters are enlisted in Tables 7.1 - 7.2. In the experimental article of Lokerse et al. [88], Fig. 3(A) (TSL80A 42°C) depicts the time release profile of liposomal formulation TSL80A at 42°C when $(NH_4)_2SO_4$ was used for DOX loading.

Table 7.1: Parameter values

	Values	Ref.		Values	Ref.
σ_T	0.82	[8, 9, 10, 47]	σ_l	0.95	[156]
$\sigma_{d(free)}$	0.15	[47, 149]	$\sigma_{d(bound)}$	0.82	[47, 149]
π_v	2666 Pa	[8, 9, 10, 47]	π_i	2000 Pa	[8, 9, 10, 47]
P_l	$3.42*10^{-7}$ cm/s	[155, 151]	P_{be}	$7.8*10^{-7} cm/s$	[47, 152]
P_{fe}	$3*10^{-4}$ cm/s	[47, 152]	k_{rel}	0.0078 s^{-1}	[156]
p_v	2080 Pa	[8, 9, 10, 47]	S/V	200 cm^{-1}	[8, 9, 10, 47]
K_v	$2.1*10^{-9} cm/Pa.s$	[8, 9, 10, 47]	v^{TP}	0.07452	[46]
k_{cl}^F	$1.1*10^{-3}$ s^{-1}	[46]	k_{cl}^L	$2.228*10^{-4} s^{-1}$	[46]
k_{hl}	$1.67*10^{-4}$ s^{-1}	[79]	k_{hr}	$3.67*10^{-5} s^{-1}$	[79]

The experimental set-up of thermosensitive liposomes is perused and matched with drug release percentage-time profile (here, non-dimensionalised parameters are used) obtained from the present proposed mathematical model (Fig. 7.2). It is noteworthy that the experimental data matched up well with the present theoretical results, which bespeaks the potency of the advocated model. Thus, the aimed objective of the present study is accomplished. The model solution overestimates the release with time compared to the experimental findings at the initial stage. As time elapses, there is very good agreement between estimation and observation. It can be observed from Fig 7.2 that there is slight disagreement between theoretical result of the present study and that of the experiment [88]. The reason behind such small deviation could be that the present mathematical model involves various complex physical phenomena, right from liposomal drug release to its lysosomal degradation in the tumour intracellular compartment, whereas the experiment [88] only focussed on liposomes with different lipid formulations and their corresponding drug release kinetics.

Table 7.2: Parameter values

	Values	Ref.		Values	Ref.
k_e	$2.75 * 10^{-3}\ s^{-1}$	[140]	k_x	$9.67 * 10^{-4}\ s^{-1}$	[79]
k_t	$5 * 10^{-4}\ s^{-1}$	[79]	ke_1	$1.1 * 10^{-3}\ s^{-1}$	[46]
$n1$	$10^{-3}\ cm$	—	k_r	$2 * 10^{-2}\ s^{-1}$	[41, 143]
k_r'	$2 * 10^{-2}\ s^{-1}$	[41, 143]	k_d	$10^{3}\ s^{-1}$	[106]
k_f	$10^{7}\ (mol\ cm^{-3}\ s)^{-1}$	[79]	k_a	$10^{7}\ (mol\ cm^{-3}\ s)^{-1}$	[79]
k_f'	$2 * 10^{6} (mol\ cm^{-3}\ s)^{-1}$	[79]	$P_i,\ i = 1-4$	$10^{-7} - 10^{-6}\ cm/s$	[11]
$\gamma_j,\ j = 1-6$	$10^{-4} - 10^{-3}\ cm/s$	[156]	$D_p,\ p = L,F,B$	$10^{-8} - 10^{-6}\ cm^2/s$	[30, 34, 66, 126]
k_1	$10^{-5}\ s^{-1}$	[63]	$n2$	$10^{-2}\ cm$	—

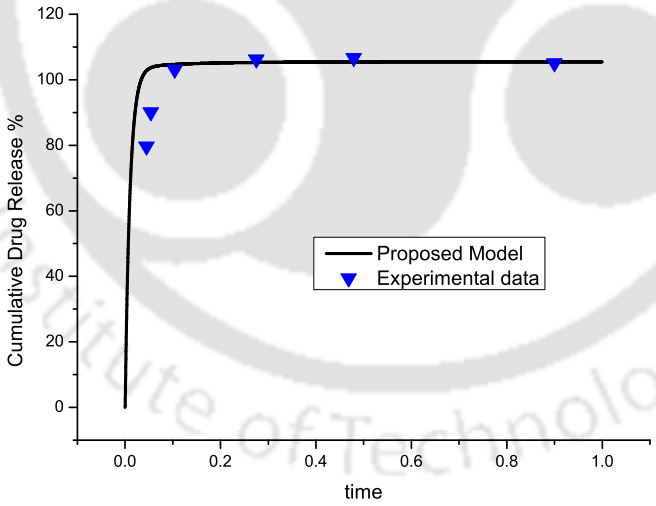

Figure 7.2: Comparison of the present results with experimental data [88].

7.5 Results and discussion

The purpose of the present study on modelling of liposomal drug release system and subsequent drug transport to the tumour cells via complex pathways is to characterize the pharmacokinetic aspects behind the physical, biochemical and physiological processes of the problem. This characterization

is done through a systematic quantitative analysis on the basis of model parameters given in Tables 7.1 - 7.2. Graphical representations of concentration profiles of the liposomal drug in its various embodiments are illustrated in Figs. 7.3 - 7.6. Moreover, influences of various model parameters on different metamorphosed forms of liposomal drug concentrations are elucidated through Figs. 7.7 - 7.14 so that one may look through the underlying physical phenomena in details. The time-variant concentration profiles are plotted at $x = 0.0012\ cm$ in the systemic plasma and $x = 0.003\ cm$ in the tumour compartment respectively. However, one may keep in mind that all graphical portrayals are demonstrated with respect to dimensionless variables and parameters.

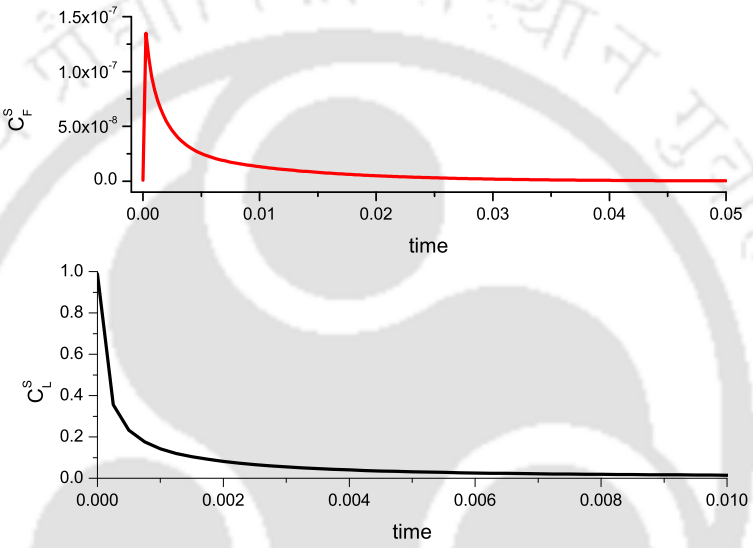

Figure 7.3: Time variant concentration profiles of C_F^S and C_L^S.

Figure 7.3 represents the time-variant concentration profiles of C_F^S and C_L^S i.e free drug and liposome-encapsulated drug in the systemic plasma respectively. Free drug in the systemic plasma is formed as an outcome of drug release from the liposome-encapsulated drug. Thus, initially C_F^S reaches the peak and slowly gets declined due to its transfer to the tumour plasma. Some fraction of C_F^S gets cleared away by a body clearance system. Furthermore, systemic plasma is the location where liposomes are injected. Hence, liposome-encapsulated drug depletes from its maximum concentration quite promptly due to the release of free drug, entering of the liposomal drug into the tumour plasma and ultimately due to liposomal drug clearance through the body clearance phenomenon. Though from the graph, it seems that C_L^S degrades away in very small time, but in actuality, C_L^S has a non-null concentration for a longer time with lower order of magnitude. These types of graphical representations depict the fate of liposomal drug delivery, which is a major tool to combat cancer in a way that the drug reaches the targeted tumour in least time duration.

Figure 7.4 depicts the collage of time-variant profiles of bound drug (C_B^{TP}), free drug (C_F^{TP}) and liposomal drug (C_L^{TP}) concentrations in tumour plasma along with liposomal drug (C_L^{TIF}) concentration in the

tumour interstitial fluid. Figure 7.4 (c) illustrates the variation of liposome-encapsulated drug (C_L^{TP}) concentration with time in the tumour plasma. The increase in its concentration at the onset is due to the diffusion of liposomal drug from the systemic plasma, and its decline is the outcome of drug release as free form and the net loss of liposomes due to the transcapillary drug exchange between tumour sub-compartments. Figure 7.4 (d) describes the variation of liposome-encapsulated drug concentration (C_L^{TIF}) with time in the tumour interstitial fluid. Exchange of liposomal drug occurs between plasma and interstitial fluid of tumour compartment. The increase in its concentration is due to diffusion of C_L^S and net gain of liposomes due to transcapillary drug exchange. The downturn of the profile is due to release of free drug from the encapsulation of liposomes. Moreover, it should be observed that the order of magnitude of C_L^{TIF} is less as compared to C_L^{TP}. This depicts that interstitial fluid contains major fraction of free drug (C_F^{TIF}), which is good for drug targeting to the tumour cells as only free drugs can enter into the tumour intracellular compartment. Another profile displayed in Fig. 7.4 (b) depicts the variation of free drug (C_F^{TP}) with time in the tumour plasma. The increase in concentration is due to the release rate of liposomes and seepage of free drug from systemic plasma to tumour plasma. The profile downturn is the outcome of integrated processes like transcapillary exchange of free drug between tumour plasma and interstitial fluid, binding with tumour plasma proteins and plasma clearance. Lastly, Fig. 7.4 (a) in this panel, illustrates the variation of bound drug (C_B^{TP}) with time in the tumour plasma. The graphical pattern of C_B^{TP} is almost analogous to the previous forms, depicting the transcapillary exchange of bound drug in between tumour sub-compartments and coupled effect of formation of free drug-protein complex along with the dissociation of the complex.

Figure 7.5 delineates the time-variant concentration profiles of free (C_F^{TIF}) and bound (C_B^{TIF}) drug in the tumour interstitial fluid respectively. The contour of C_F^{TIF} attains its peak due to release of drug from liposomes and free drug crossing the capillary wall into the interstitial fluid, while it declines sharply because of its association with proteins and tumour cell surface receptors. On the other hand, the contour of C_B^{TIF} attains its peak as an outcome of its interaction with free drug and transcapillary exchange of bound drug into the interstitial fluid from the tumour plasma. With time, C_B^{TIF} contour also declines quickly due to the dissociation of free drug-protein complex in the tumour interstitial fluid.

Figure 7.6 illustrates the time-variant concentration profiles of free drug-tumour cell surface receptor complex, i.e. bound drug at tumour cell surface (C_{BS}^{TC}), internalized bound drug (C_{BI}^{TC}) and internalized free drug (C_{FI}^{TC}) in the tumour cell compartment. Before elucidating the nature of the respective contours, one may illumine up the misty realms of a cancerous tumour cell in order to better understand the underlying physiological phenomena and its corresponding mathematical interpretation in the form of graphical embodiments. In cancerous tumour cell, cell surface receptors undergo certain changes, like increase or decrease in the number of surface receptors in comparison to normal cell and structural changes so that receptors do not interact with the respective ligands. The distribution of receptors in malignant cell gets modified resulting in the alteration of cell agglutination behaviour [6]. In the present study, it is assumed that the tumour cell has reduced number of cell surface and internalized receptors. This is the reason behind the low ordered magnitude of different drug forms in tumour cell.

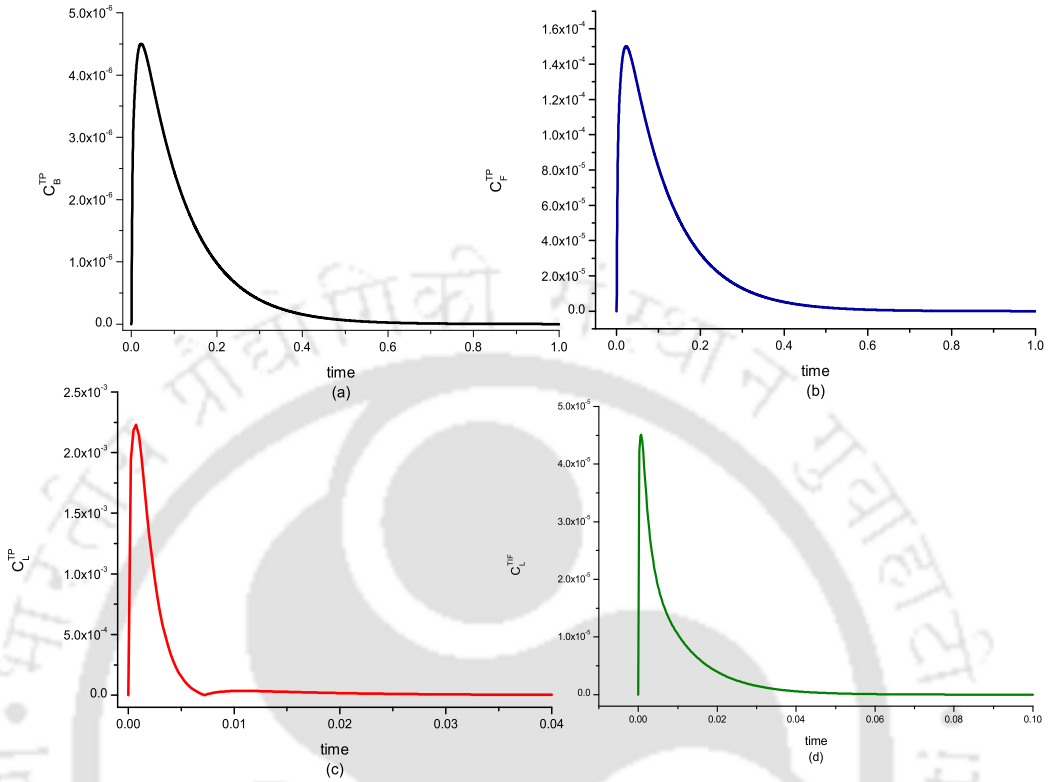

Figure 7.4: Time variant concentration profiles of C_B^{TP}, C_F^{TP}, C_L^{TP} and C_L^{TIF}.

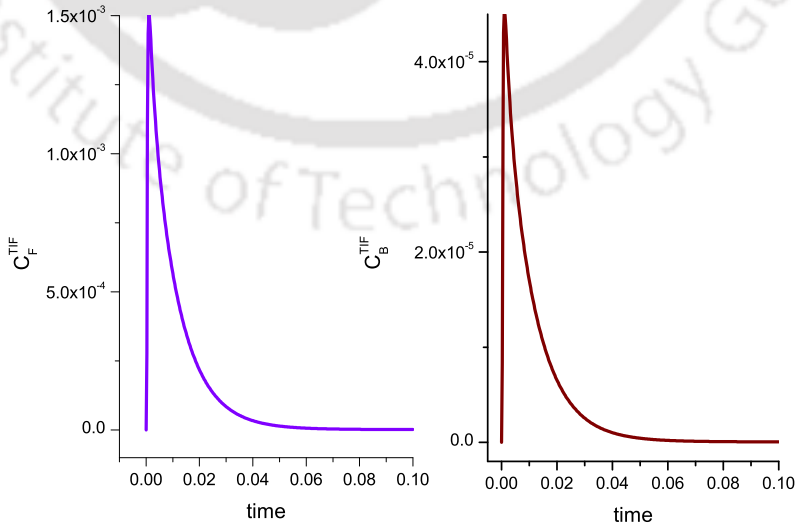

Figure 7.5: Time variant concentration profiles of C_F^{TIF} and C_B^{TIF}.

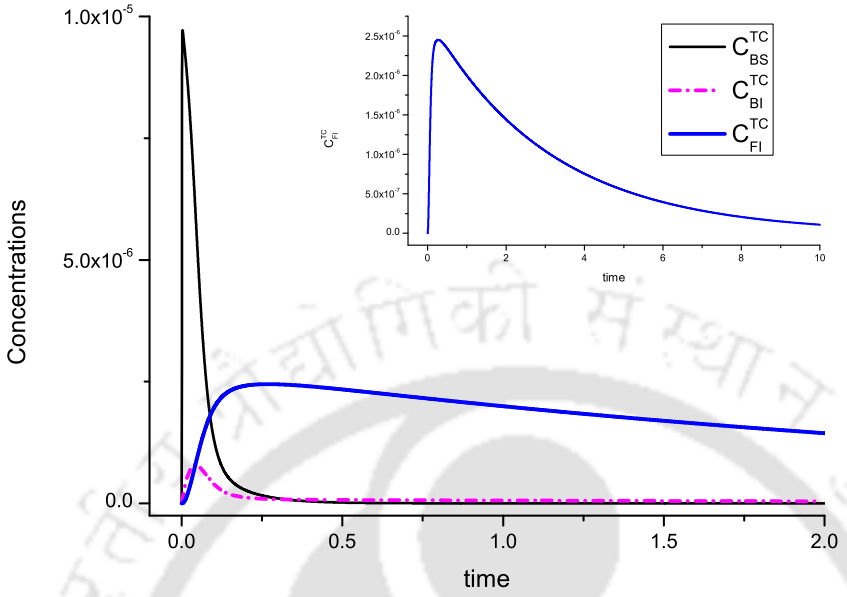

Figure 7.6: Time variant concentration profiles of C_{BS}^{TC}, C_{BI}^{TC} and C_{FI}^{TC}.

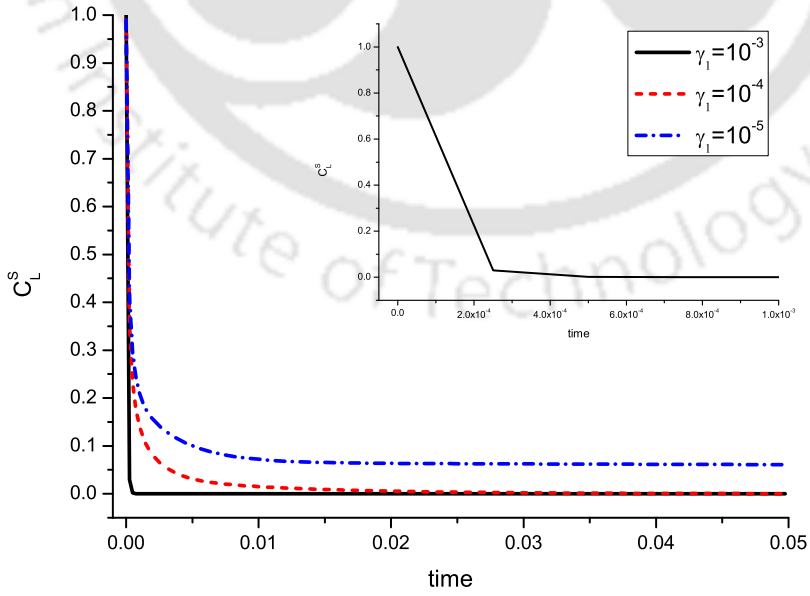

Figure 7.7: Time variant concentration profiles of C_L^S for different γ_1.

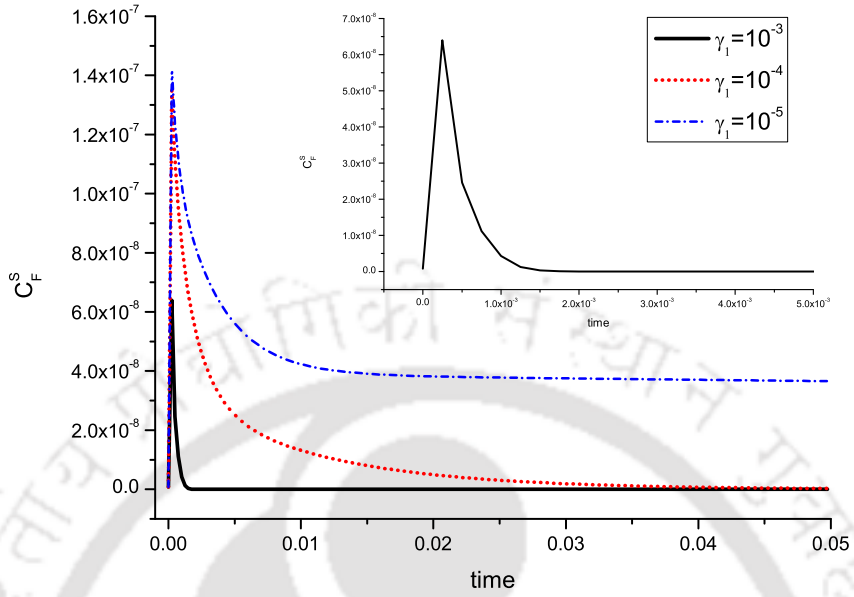

Figure 7.8: Time variant concentration profiles of C_F^S for different γ_1.

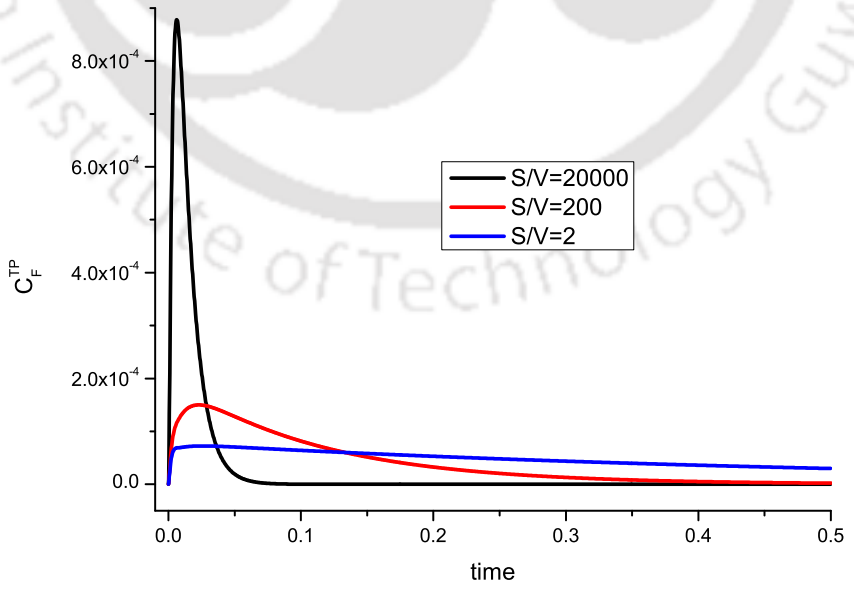

Figure 7.9: Time variant concentration profiles of C_F^{TP} for different S/V.

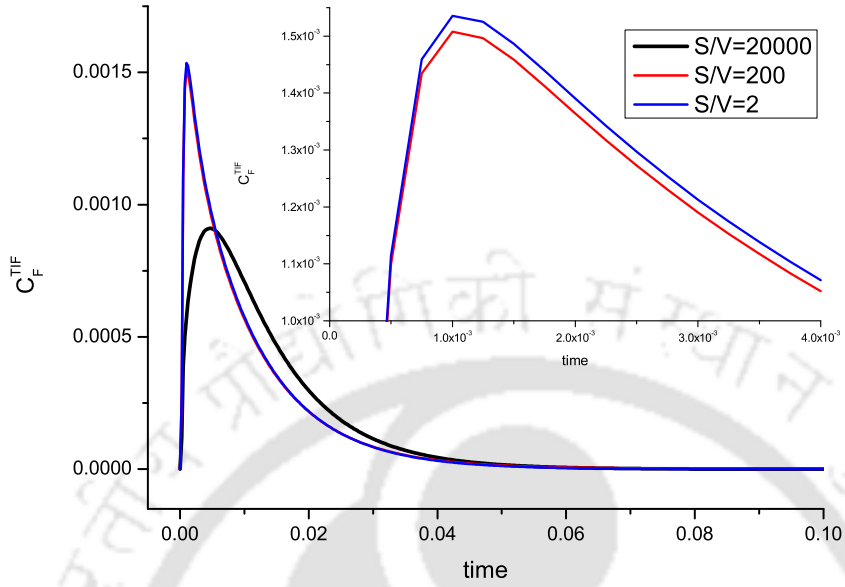

Figure 7.10: Time variant concentration profiles of C_F^{TIF} for different S/V.

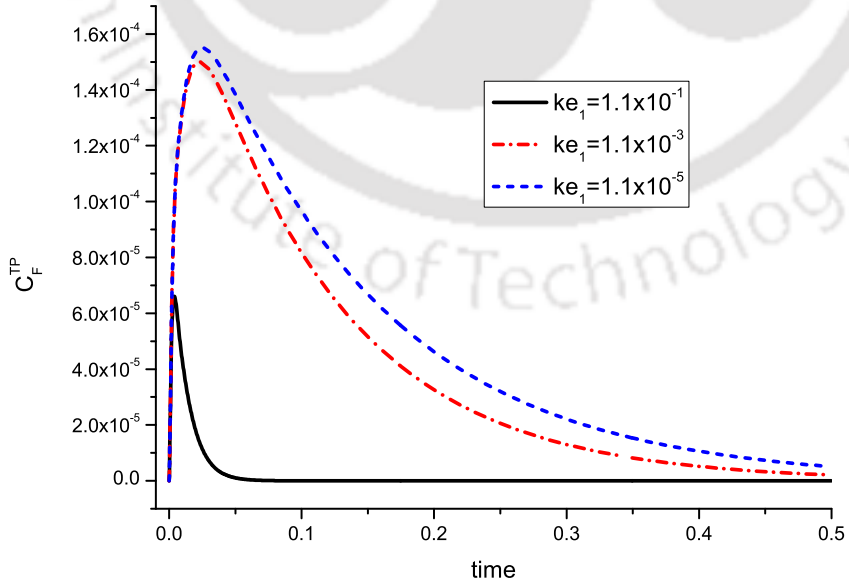

Figure 7.11: Time variant concentration profiles of C_F^{TP} for different ke_1.

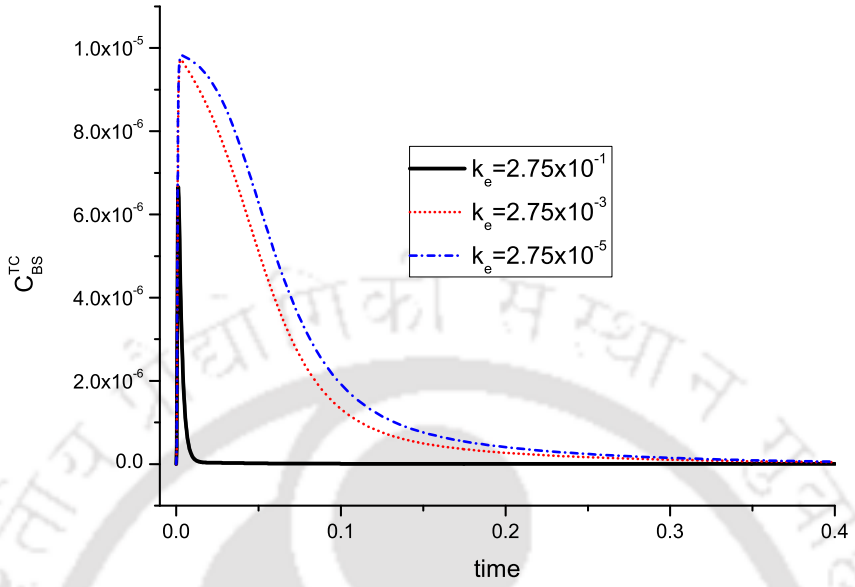

Figure 7.12: Time variant concentration profiles of C_{BS}^{TC} for different k_e.

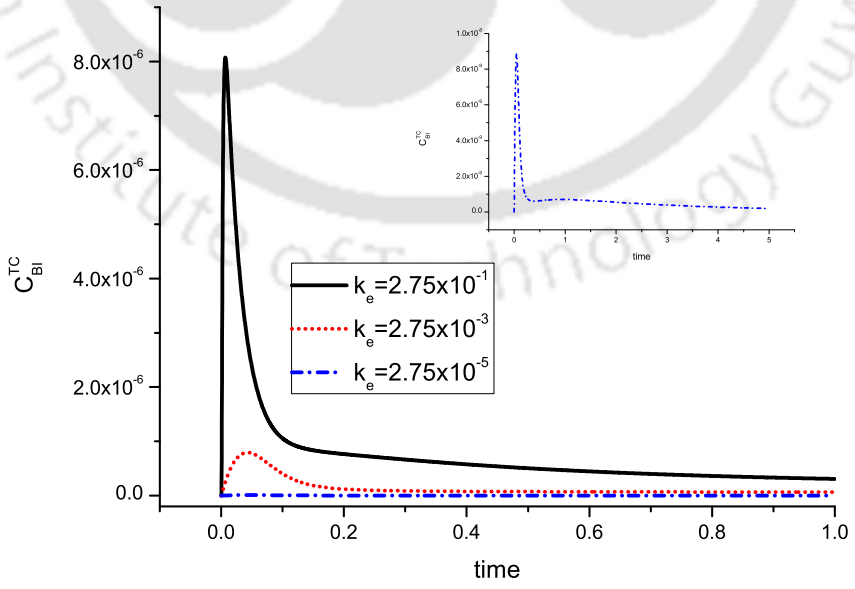

Figure 7.13: Time variant concentration profiles of C_{BI}^{TC} for different k_e.

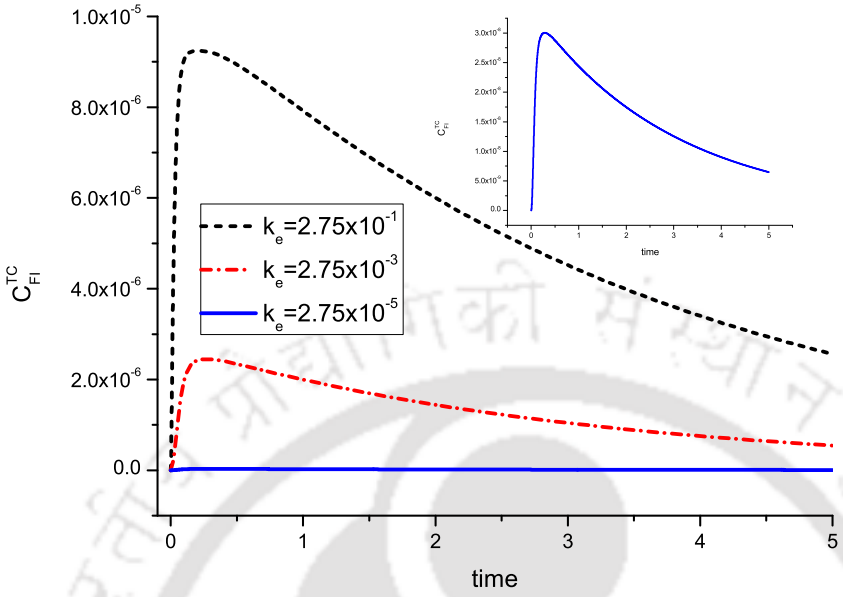

Figure 7.14: Time variant concentration profiles of C_{FI}^{TC} for different k_e.

As it is known that free drug of interstitial fluid interacts with the cell surface receptors to form cell surface bound drug, the peak of cell surface bound drug is maximum in comparison to its other counterparts originated from cell surface bound drug. Moreover, one may observe that internalized free drug, though less in magnitude, has an asymptotic trend against time. This depicts that the intracellular domain of a tumour is having a controlled and non-interrupted sustained medication that enhances therapeutic efficacy of the drug. The inset plot depicts the contour of C_{FI}^{TC} for increased time duration which sheds light on the mentioned claim about therapeutic efficacy.

The mechanism of transportation of the liposome-encapsulated drug to the target tumour cell in a time duration is discussed so far. For the purpose of portrayal of the influence of model parameters on the upshots of the model, a parametric variation is carried out. A series of illustrations are presented with various model parameters, which are made to vary from their respective base values. This study indicates that though there is general conception that drug concentrations in the intracellular domain of tumour compartment are the variables of primary interest since they are responsible for tumour cell survival, but one may understand that the free drug has reached the target cells only through systemic plasma, tumour plasma and tumour interstitial fluid, hence, influence of model parameters on various drug embodiments in systemic plasma, tumour plasma and tumour interstitial fluid are equally significant.

Figures 7.7 & 7.8 represent the changes in time-variant concentration profiles of C_L^S and C_F^S for variation in the magnitude of advection (γ_1). In Fig. 7.7, it may be observed that increased value of γ_1 leads to quick decline of concentration contour of C_L^S from loaded concentration. If the advection process

slows down, the concentration profile after sloping down attains a steady state like condition. The reason behind such behaviour is that, the concentration profile of C_L^S descends from its peak due to release of free drug from the encapsulation of liposomes and transfer of liposomal drug into the tumour compartment. When advection process becomes faster, liposome-encapsulated drug moves towards the interface more quickly so that a higher concentration is formed at the interface for the liposomal drug to enter into the tumour. On the other hand, if advection process slows down, the drug flux into the tumour compartment also becomes low and hence the corresponding contour gets an asymptotic nature. In Fig. 7.8, one may observe significant variation in the concentration profile of C_F^S with change in γ_1 though they are not directly related. Since, liposome-encapsulated drug enters into the tumour compartment faster with the increase in γ_1 , liposomes have less opportunity to release free drug (C_F^S) into the systemic plasma. Hence, the concentration of C_F^S gets reduced. For smaller value of γ_1, free drug concentration is having behaviour analogous to that shown in Fig. 7.7, which is quite obvious.

Figures 7.9 & 7.10 depict the influence of S/V i.e. blood vessels' surface area per unit volume of tumour tissue with respect to free drug concentration in tumour plasma and tumour interstitial fluid (i.e. C_F^{TP} and C_F^{TIF}). Neoplasms (abnormal growth in body tissue, characteristic of cancer) need a functioning vascular network so that oxygen and other nutrients are made available to the tumour in addition to the removal of toxic wastes. Vascular network can be obtained through the incorporation of existing host blood vessels and newly generated networks of microvessels by the tumour in order to cope up with their continued growth and development, by neovascularization [31, 145]. Thus, S/V is of vital importance. In Fig. 7.9, on increasing the blood vessels' surface area, more free drug can enter from tumour interstitial fluid and surrounding medium and hence the concentration profile of C_F^{TP} attains a higher peak, whereas based on the concentration gradient, drug voids out quickly showing a steep decline in the respective contour. On the other hand, in Fig. 7.10, a reverse phenomenon is observed as exchange of free drug occurs simultaneously based on concentration gradient.

Figures 7.11 represents the change in time-variant concentration profile for free drug in the tumour plasma (C_F^{TP}) with the variation of plasma clearance rate (ke_1). As the magnitude of the parameter increases (decreases) from the baseline value, the concentration peak value gets descended (ascended), which is self-explanatory. It may be noted that when ke_1 increases from the baseline value, reduction of the peak concentration becomes more in comparison with the rest. This is because when the plasma clearance is much higher, the drug is expelled out before it settles down completely in the tumour plasma.

Lastly, Figs. 7.12 - 7.14 deal with the variation of time-variant concentration profiles for cell surface bound drug (C_{BS}^{TC}), internalized bound drug (C_{BI}^{TC}) and internalized free drug (C_{FI}^{TC}) in the tumour cell compartment with respect to changes in internalization rate (k_e) of C_{BS}^{TC}. In Fig. 7.12, the plot shows the obvious behaviour of C_{BS}^{TC}, since, when internalization rate increases, transformation of C_{BS}^{TC} to C_{BI}^{TC} gets faster and for decreased value of k_e, the internalization phenomena of C_{BS}^{TC} slows down.

As C_{BI}^{TC} is mainly formed from C_{BS}^{TC}, its contour (Fig. 7.13) behaves reversely for the same variation of

k_e. Though C_{FI}^{TC} is not directly dependent on k_e, yet in Fig 7.14. a significant variation in the contour is observed. This is because C_{FI}^{TC} is formed as a result of dissociation of C_{BI}^{TC}.

Thus, higher concentration of internalized bound drug leads to higher concentration of internalized free drug. Hence, when the internalization rate of cell surface bound drug increases, both internalized bound drug and free drug concentrations enhances. On the other hand, decrease in k_e reduces the concentration of internalized free drug.

7.6 Conclusions

Liposomal drug delivery works for the betterment of bioavailability of therapeutic compound by getting accumulated at diseased sites. Mathematical modelling of such complex physiological and biochemical phenomena is imperative when experimental research speaks about its essence but incompetent to illustrate its full characterization. The current study deals with the mathematical model of drug release from injected liposomes and consequent drug transport into the tumour compartment. The model focuses on the complex endosomal events taking place in the tumour intracellular region so that the drug gets internalized by the process of endocytosis. The study undertaken speaks volumes about its accomplishments. First, the advocated model is more realistic since it takes into account most of the vital biochemical and physiological phenomena participating in liposomal drug delivery. Secondly, nonlinearity in the model deals with the biological complexities in a simplified approach. Thirdly, validation of the model with corresponding experimental findings speaks about the potency, validity and applicability of the model in pharmacokinetic realm. Fourthly, the numerical quantitative analysis is conducted and through graphical portrayals, results illustrate the underlying vital processes in depth. Lastly, model parametric variation is carried out to get an idea about how to optimize the liposomal drug delivery system in order to have maximum therapeutic efficacy. Furthermore, the model acts as a tool to delve deep into the underlying kinetics of drug release and drug transport by comprehending the effects of model parameters that control the pharmacodynamics of liposomal drug delivery. The proposed mathematical model acts as the basis for obtaining a more effective drug delivery system. This mathematical model, by including more complexities, may be modified for any specific tumour-drug interactions.

8 STABILITY ANALYSIS OF DRUG DYNAMICS

This chapter concludes with the stability analysis of drug dynamics model in order to have an overview of the usage of pharmacokinetic mathematical models in the present dissertation.

8.1 Introduction

The process of drug discovery is broadly categorized into two principal steps: choosing the therapeutic target and developing the respective targeting therapeutic agents. Pharmaceutical industry has flourished in the invention and development of drugs and other therapeutic compounds where targeted and structure based drug design have come to its aid. The knowledge of protein potency of drug transformation along with compound selectivity assessment have turned the industry's attention to understand the underlying biological phenomena. It should also be kept in mind that uniformity in drug dosage for a prolonged duration is equally important so that the frequency of repeated drug administration gets reduced. This leads to improved patient compliance. The drug dosage uniformity can only be achieved through controlled release drug delivery. After target identification, the main objective of drug delivery is to modulate the drug-receptor interactions that play a significant role in initiating cellular signalling. Cellular signalling determine the drug efficacy and drug response mechanism.

Most of the researchers till date have focussed their investigation on the mechanism of localised drug release from various types of controlled release drug delivery devices. The works presented in the previous chapters elaborated this approach of study by considering the complete process of drug release from polymeric matrix to drug transport in the biological tissue. The complex interplay between free drug particles with plasma proteins and surface cell receptors along with related endosomal events are well demonstrated with the help of a mathematical model in the current study. The work of concern presents a coupled mathematical model of drug release from polymeric matrix and subsequent drug transport into intracellular domain. This leads to a mixed system of partial and ordinary differential equations along with appropriate set of initial and boundary conditions. The uniqueness in the present

study lies in the fact that considering the dynamics of the proposed mathematical model of drug release from local drug delivery device and subsequent drug transport, a local stability analysis is performed, which is carried out probably for the first time till date as per our knowledge. Rattanakul and Lenbury [117] though studied stability analysis for controlled drug release from matrix system without taking into account the drug transport phenomenon, but detailed analysis was not done and furthermore the drug release model was not advanced. It is a well accepted fact that a normal and healthy physiological system is stable. When the system gets diseased, it shows some unstable behaviour which would again turn into stable state when appropriate medication is provided. Moreover, a little variation in drug dose or small physiological changes is expected not to lead to an unstable system. Thus, stability analysis as done in the present study contributes to a better understanding of the underlying biochemical processes that govern the drug transport to the biological cells. Additionally, study of stability analysis describes the potency of a mathematical model to be realistic enough to formulate drug kinetics.

8.2 Model development

The advocated mathematical model consists of two phases: drug release and drug transport. The drug release phase is dominated by polymeric matrix, which acts as the reservoir of therapeutic compound. The polymeric matrix is having an impermeable backing. The drug transport phase is dominated by the free drug-plasma protein interaction, free drug-receptor interaction and other endosomal events. The detailed drug release mechanism in the polymeric matrix phase is provided in the previous chapters.

At the initial stage, the drug is in solid form (C_L) encapsulated within the polymeric matrix (e.g. in crystalline form) at its loaded concentration. Since it is in bound state, the drug cannot squeeze out of the polymeric matrix. With elapsed time, biofluid enters into the polymeric matrix and transforms the loaded drug crystals into free state (C_0) through solubilisation process, eligible to diffuse out of the matrix. The rate of drug transfer from solid state to free state depends on the difference between C_L and C_0 as well. Moreover, a fraction of solid drug ($\beta_0\ C_L$) is transformed into its free state while through a recrystallisation process, another fraction of free drug ($\delta_0\ C_0$) is returned back to its bound state. Simultaneously, a part of free drug diffuses out of the polymeric matrix.

The diffused out free drug disperses in the surrounding medium, i.e. plasma and interstitial fluid, as C_1 depends on the free drug concentration gradient between polymeric matrix boundary and surrounding medium. The plasma proteins (P) interact with free drug (C_1) to form free drug-plasma protein complex (C_{1P}). While moving in the interstitial fluid, C_1 interacts with the cell surface receptors (R_s) to form free drug-receptor complex (C_{bs}) in the cell surface. These cell surface receptors are continuously synthesized by the golgi bodies. R_s and C_{bs} get internalized into the intracellular region. The internalized free drug-receptor complex (C_{bi}) dissociates to form intracellular free drug (C_{1i}). This internalized free drug C_{1i} interacts with the internalized receptors to again form C_{bi}. Internalized receptors and internalized free drug-receptor complex either recycle back to the cell surface or undergo lysosomal degradation. The internalized free drug along with other internalized forms get degraded in the lysosomes. The detailed mechanism right from drug release to drug transport can be conceptual-

ized and visualized through the given schematic portrayal in the form of Fig. 8.1.

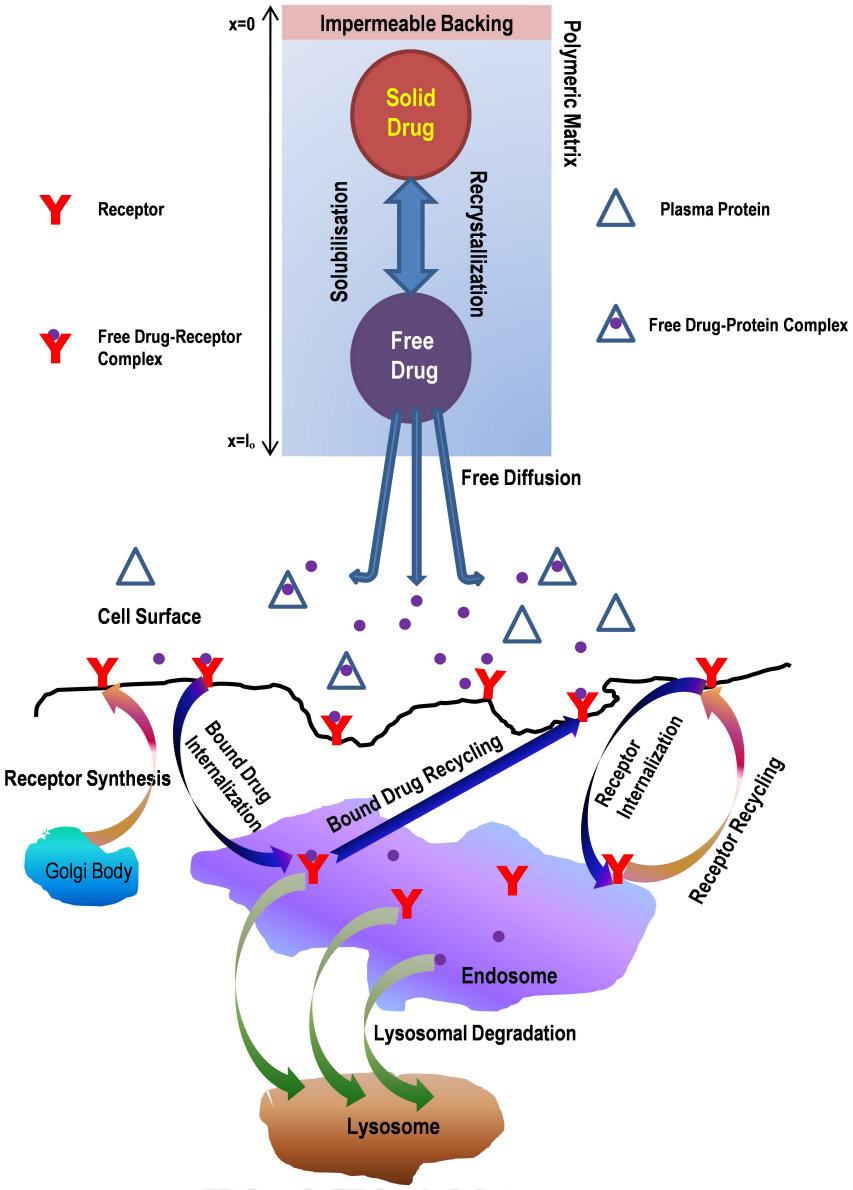

Figure 8.1: Schematic diagram

8.3 Mathematical formulation

Modelling drug dynamics in the polymeric matrix

Initially, the embedded drug in the polymeric matrix transforms into free drug, to be mobile enough to ooze out of the matrix. Thus, accumulation of solid drug and free drug at any instant in the polymeric matrix depend on solubilisation of solid drug, free drug diffusion, dissociation rate of solid drug, recrystallisation rate of free drug and their concentration difference. Thus, the governing equations

describing the dynamics of drug release in the polymeric matrix phase are

$$\frac{\partial C_L}{\partial t} = -\alpha_0(\Phi_0\, C_L - C_0) - k_m(C_{lim} - C_0) - \beta_0\, C_L + \delta_0\, C_0, \quad x \in (0, l_0), \tag{8.3.1}$$

$$\frac{\partial C_0}{\partial t} = D_0 \frac{\partial^2 C_0}{\partial x^2} + \alpha_0(\Phi_0\, C_L - C_0) + k_m(C_{lim} - C_0) + \beta_0\, C_L - \delta_0\, C_0, \quad x \in (0, l_0), \tag{8.3.2}$$

where $\Phi_0 (= \frac{k\varepsilon_0}{1-\varepsilon_0})$ is the ratio of accessible void volume to solid volume, C_L denotes available molar concentration of solid drug, C_0 is the available molar concentration of free drug, k stands for partition coefficient, ε_0 denotes polymeric matrix porosity, l_0 is the length of the polymeric matrix, k_m is mass transfer coefficient, C_{lim} stands for drug solubilisation limit, β_0 is the dissociation rate constant, δ_0 is the association rate constant, α_0 denotes solid-liquid mass transfer coefficient and D_0 is the diffusion coefficient of free drug in the matrix.

Initially, the therapeutic compound is available only in solid state in the polymeric matrix. Therefore, the initial conditions are as follows:
$C_L(x,0) =$M, $C_0(x,0) = 0$, where M is the maximum value of loaded solid drug concentration.
No mass flux can pass to exterior environment due to the presence of impermeable backing and hence no flux condition arises. At $x = 0$, $D_0 \frac{\partial C_0}{\partial x} = 0$.
Lastly, at the boundary of the polymeric matrix, a flux condition is assigned, i.e at $x = l_0$,
$-D_0 \frac{\partial C_0}{\partial x} = P_1 C_0$, where P_1 is a mass transfer coefficient.

Modelling intracellular drug dynamics

After the free drug diffused out of the polymeric matrix, it gets distributed through the plasma and interstitial fluid where it interacts with plasma proteins and cell surface receptors. The process proceeds with drug internalization and finally undergoes lysosomal degradation. Thus, accumulation of free drug in plasma and in interstitial fluid depends on its interaction with plasma proteins, cell surface receptors, difference of free drug concentrations in polymeric matrix boundary and in encompassing medium, as well as dissociation of the complexes formed due to interaction. Accumulation of plasma proteins and free drug-plasma protein complex at any instant depends on association of free drug and plasma proteins as well as the dissociation of the free drug-plasma protein complex. Accumulation of cell surface receptor at any instant depends on its interaction with free drug, dissociation of the free drug-cell surface receptor complex. Cell surface receptor accumulation also depends on its internalization, synthesis rate in the Golgi body, and recycling rate of the internalized receptors. Moreover, accumulation of cell surface bound drug i.e. free drug-cell surface receptor complex at any instant depends on the corresponding interaction between free drug and cell surface receptors and dissociation of the respective complex, internalization of the complex and its recycling back. Lastly, accumulation of internalized bound drug i.e. internalized cell surface bound drug, internalized free drug and internalized receptors at any instant depend on the internalization of cell surface bound drug, association of internalized free drug and internalized receptors, dissociation of internalized bound drug, recycling rate of internalized receptors and internalized bound drug in addition to their lysosomal degradation.

Thus, the corresponding equations governing the intracellular drug dynamics are as follows:

$$\frac{dC_1}{dt} = -k_{+1}\, C_1 P + k_{-1}\, C_{1P} - k_f\, R_s\, C_1 + k_r\, C_{bs} + k_p[C_0\Big|_{x=l_0} - C_1], \tag{8.3.3}$$

$$\frac{dP}{dt} = -k_{+1}\, C_1 P + k_{-1}\, C_{1P}, \tag{8.3.4}$$

$$\frac{dC_{1P}}{dt} = k_{+1}\, C_1 P - k_{-1}\, C_{1P}, \tag{8.3.5}$$

$$\frac{dR_s}{dt} = -k_f\, R_s\, C_1 + k_r\, C_{bs} - k_t\, R_s + k_x\, R_i + k_{syn}\, R_s, \tag{8.3.6}$$

$$\frac{dC_{bs}}{dt} = k_f\, R_s\, C_1 - (k_r + k_e)\, C_{bs} + k_x\, C_{bi}, \tag{8.3.7}$$

$$\frac{dC_{bi}}{dt} = k_e\, C_{bs} + k_f^{'}\, R_i\, C_{1i} - k_r^{'}\, C_{bi} - (k_{hr} + k_x)\, C_{bi}, \tag{8.3.8}$$

$$\frac{dC_{1i}}{dt} = -k_f^{'}\, R_i\, C_{1i} + k_r^{'}\, C_{bi} - k_{hl}\, C_{1i}, \tag{8.3.9}$$

$$\frac{dR_i}{dt} = -k_f^{'}\, R_i\, C_{1i} + k_r^{'}\, C_{bi} + k_t\, R_s - (k_{hr} + k_x)\, R_i. \tag{8.3.10}$$

where C_1 is the concentration of free drug present in plasma and interstitial fluid, P is the concentration of plasma proteins, C_{1P} is the concentration of protein-free drug complex, R_s is the concentration of receptors at the cell surface, C_{bs} is the concentration of free drug-cell surface receptor complex, that is, cell surface bound drug, C_{bi} is the internalized C_{bs}, that is, internalized bound drug concentration, C_{1i} is the free drug concentration due to dissociation of C_{bi}, that is, internalized free drug concentration, R_i is the concentration of internalized receptors, k_{+1} is the association rate constant due to interaction between plasma proteins and free drug, k_{-1} is the dissociation rate constant denoting breakdown of protein-free drug complex, k_f is the association rate constant due to interaction between cell surface receptors and free drug, k_r is the dissociation rate constant denoting breakdown of cell surface receptor-free drug complex, k_e is the endocytosis rate constant, k_t is the constitutive internalization rate constant, k_{hr} is the receptor degradation rate constant, k_{hl} is the drug degradation rate constant, $k_f^{'}$ is the association rate constant due to interaction between internalized receptors and internalized free drug, $k_r^{'}$ is the dissociation rate constant denoting breakdown of internalized bound drug complex, k_x is the receptor recycling rate constant, k_{syn} depicts the receptor synthesis rate and $k_p = \frac{PS}{V}$, in which PS represents permeability-surface area product and V represents intracellular volume. Initially, there is no availability of free drug in the plasma and interstitial fluid. So, there is no chance of availability of other drug forms at that initial time. Therefore, at time $t = 0$, $C_1(0) = 0$, $P(0) = P_0$, $R_s(0) = R_{s0}$, $C_{1P}(0) = 0$, $R_i(0) = R_{i0}$, $C_{bs}(0) = 0$, $C_{bi}(0) = 0$ and $C_{1i}(0) = 0$. Moreover, due to conservation law, $P + C_{1P} = P_0$. P_0, R_{s0} and R_{i0} represent the initial concentrations of proteins, cell surface and internalized receptors respectively. Thus, the modified system of equations depicting drug transport is the following.

$$\frac{dC_1}{dt} = -k_{+1}\, C_1[P_0 - C_{1P}] + k_{-1}\, C_{1P} - k_f\, R_s\, C_1 + k_r\, C_{bs} + k_p[C_0\Big|_{x=l_0} - C_1], \tag{8.3.11}$$

$$\frac{dC_{1P}}{dt} = k_{+1}\, C_1[P_0 - C_{1P}] - k_{-1}\, C_{1P}, \tag{8.3.12}$$
$$\frac{dR_s}{dt} = -k_f\, R_s\, C_1 + k_r\, C_{bs} - k_t\, R_s + k_x\, R_i + k_{syn}\, R_s, \tag{8.3.13}$$
$$\frac{dC_{bs}}{dt} = k_f\, R_s\, C_1 - (k_r + k_e)\, C_{bs} + k_x\, C_{bi}, \tag{8.3.14}$$
$$\frac{dC_{bi}}{dt} = k_e\, C_{bs} + k_f^{'}\, R_i\, C_{1i} - k_r^{'}\, C_{bi} - (k_{hr} + k_x)\, C_{bi}, \tag{8.3.15}$$
$$\frac{dC_{1i}}{dt} = -k_f^{'}\, R_i\, C_{1i} + k_r^{'}\, C_{bi} - k_{hl}\, C_{1i}, \tag{8.3.16}$$
$$\frac{dR_i}{dt} = -k_f^{'}\, R_i\, C_{1i} + k_r^{'}\, C_{bi} + k_t\, R_s - (k_{hr} + k_x)\, R_i. \tag{8.3.17}$$

8.3.1 Dimensionless equations

All the variables and parameters are now made dimensionless in order to make simplified computations in the following way:

$$\bar{x} = \frac{x}{l_0}, \quad \bar{t} = \frac{D_0\, t}{l_0^2}, \quad \overline{l_0} = 1, \quad \gamma = \frac{D_0}{D_0}, \quad \overline{C_j} = \frac{C_j}{M}, j = L, 0, lim, 1, bs, bi, 1i, \quad \overline{C_{1P}} = \frac{C_{1P}}{P_0},$$
$$\overline{P_0} = \frac{P_0}{M}, \quad \overline{R_{s0}} = \frac{R_{s0}}{M}, \quad \overline{R_{s0}} = \frac{R_{s0}}{M}, \quad \overline{\beta_0} = \frac{\beta_0\, l_0^2}{D_0}, \quad \overline{\alpha_0} = \frac{\alpha_0\, l_0^2}{D_0}, \quad \overline{\delta_0} = \frac{\delta_0\, l_0^2}{D_0}, \quad \overline{k_m} = \frac{k_m\, l_0^2}{D_0},$$
$$\overline{P_1} = \frac{P_1\, l_0}{D_1}, \quad \overline{k_i} = \frac{k_i\, l_0^2}{D_0}, i = p, t, x, syn, e, hr, hl, \quad Da_0 = \frac{k_{+1}\, l_0^2\, P_0}{D_0}, \quad Da_1 = \frac{k_f\, l_0^2\, R_{s0}}{D_0},$$
$$Da_2 = \frac{k_f^{'}\, l_0^2\, R_{i0}}{D_0}, \quad K_{d0} = \frac{k_{-1}}{k_{+1}}, \quad K_{d1} = \frac{k_r}{k_f}, \quad K_{d2} = \frac{k_r^{'}}{k_f^{'}}, \quad Bp_0 = \frac{P_0}{K_{d0}}, \quad Bp_1 = \frac{R_{s0}}{K_{d1}},$$
$$Bp_2 = \frac{R_{i0}}{K_{d2}}.$$

Bars over the parameters are omitted for convenience, so the aforementioned equations in their dimensionless form are as follows:

$$\frac{\partial C_L}{\partial t} = -\alpha_0(\Phi_0\, C_L - C_0) - k_m(C_{lim} - C_0) - \beta_0\, C_L + \delta_0\, C_0, \qquad x \in (0,1), \tag{8.3.18}$$
$$\frac{\partial C_0}{\partial t} = \gamma\frac{\partial^2 C_0}{\partial x^2} + \alpha_0(\Phi_0\, C_L - C_0) + k_m(C_{lim} - C_0) + \beta_0\, C_L - \delta_0\, C_0, \qquad x \in (0,1), \tag{8.3.19}$$
$$\frac{dC_1}{dt} = -Da_0\, C_1[1 - C_{1P}] + \frac{Da_0}{Bp_0}\, C_{1P} - \frac{Da_1}{R_{s0}}\, R_s\, C_1 + \frac{Da_1}{Bp_1}\, C_{bs} + k_p\, [C_0\big|_{x=1} - C_1], \tag{8.3.20}$$
$$\frac{dC_{1P}}{dt} = Da_0\, C_1[1 - C_{1P}] - \frac{Da_0}{Bp_0}\, C_{1P}, \tag{8.3.21}$$
$$\frac{dR_s}{dt} = -\frac{Da_1}{R_{s0}}\, R_s\, C_1 + \frac{Da_1}{Bp_1}\, C_{bs} - k_t\, R_s + k_x\, R_i + k_{syn}\, R_s, \tag{8.3.22}$$
$$\frac{dC_{bs}}{dt} = \frac{Da_1}{R_{s0}}\, R_s\, C_1 - \frac{Da_1}{Bp_1}\, C_{bs} - k_e\, C_{bs} + k_x\, C_{bi}, \tag{8.3.23}$$
$$\frac{dC_{bi}}{dt} = k_e\, C_{bs} + \frac{Da_2}{R_{i0}}\, R_i\, C_{1i} - \frac{Da_2}{Bp_2}\, C_{bi} - (k_{hr} + k_x)\, C_{bi}, \tag{8.3.24}$$

$$\frac{dC_{1i}}{dt} = -\frac{Da_2}{R_{i0}} R_i C_{1i} + \frac{Da_2}{Bp_2} C_{bi} - k_{hl} C_{1i}, \tag{8.3.25}$$

$$\frac{dR_i}{dt} = -\frac{Da_2}{R_{i0}} R_i C_{1i} + \frac{Da_2}{Bp_2} C_{bi} + k_t R_s - (k_{hr} + k_x) R_i. \tag{8.3.26}$$

The initial, interface and boundary conditions in dimensionless approach are the following:

$$C_L(x,0) = 1, \quad C_0(x,0) = 0, \quad C_1(0) = 0, \quad R_s(0) = R_{s0}, \quad C_{1P}(0) = 0, \quad R_i(0) = R_{i0},$$

$$C_{bs}(0) = 0, \quad C_{bi}(0) = 0, \quad C_{1i}(0) = 0, \quad -\gamma \frac{\partial C_0}{\partial x}\Big|_{x=1} = P_1 C_0, \quad \text{and} \quad \frac{\partial C_0}{\partial x}\Big|_{x=0} = 0.$$

The governing partial differential equations are solved with the help of separation of variables procedure. The free drug in the polymeric matrix is as follows:

$$C_0 = (e^{-m_1 t} - e^{-m_2 t}) \cos(ax), \quad \text{where,} \quad m_1 = \frac{B_1 - \sqrt{B_1^2 + 4B_2}}{2}, \quad m_2 = \frac{B_1 + \sqrt{B_1^2 + 4B_2}}{2},$$

$$B_1 = \alpha_0(\Phi_0 + 1) + k_m + \beta_0 + \delta_0 - \lambda\gamma, \quad B_2 = \lambda\gamma(\alpha_0\Phi_0 + \beta_0), \quad a = \sqrt{\frac{P_1}{\gamma l_0}}, \quad \lambda = -a^2$$

The non-autonomous system of equations (8.3.20) - (8.3.26) is transformed into autonomous system by considering $x_1 = e^{-t}$ and renaming the other variables as $x_2 = C_1$, $x_3 = C_{1P}$, $x_4 = R_s$, $x_5 = C_{bs}$, $x_6 = C_{bi}$, $x_7 = C_{1i}$ and $x_8 = R_i$. The autonomous system of equations is represented as follows:

$$\frac{dx_1}{dt} = -x_1, \tag{8.3.27}$$

$$\frac{dx_2}{dt} = -Da_0 x_2[1 - x_3] + \frac{Da_0}{Bp_0} x_3 - \frac{Da_1}{R_{s0}} x_4 x_2 + \frac{Da_1}{Bp_1} x_5 + k_p [(x_1^{m_1} - x_1^{m_2}) \cos(a l_0) - x_2], \tag{8.3.28}$$

$$\frac{dx_3}{dt} = Da_0 x_2[1 - x_3] - \frac{Da_0}{Bp_0} x_3, \tag{8.3.29}$$

$$\frac{dx_4}{dt} = -\frac{Da_1}{R_{s0}} x_4 x_2 + \frac{Da_1}{Bp_1} x_5 - k_t x_4 + k_x x_8 + k_{syn} x_4, \tag{8.3.30}$$

$$\frac{dx_5}{dt} = \frac{Da_1}{R_{s0}} x_4 x_2 - \frac{Da_1}{Bp_1} x_5 - k_e x_5 + k_x x_6, \tag{8.3.31}$$

$$\frac{dx_6}{dt} = k_e x_5 + \frac{Da_2}{R_{i0}} x_7 x_8 - \frac{Da_2}{Bp_2} x_6 - (k_{hr} + k_x) x_6, \tag{8.3.32}$$

$$\frac{dx_7}{dt} = -\frac{Da_2}{R_{i0}} x_7 x_8 + \frac{Da_2}{Bp_2} x_6 - k_{hl} x_7, \tag{8.3.33}$$

$$\frac{dx_8}{dt} = -\frac{Da_2}{R_{i0}} x_7 x_8 + \frac{Da_2}{Bp_2} x_6 + k_t x_4 - (k_{hr} + k_x) x_8. \tag{8.3.34}$$

The corresponding initial conditions are $x_1(0) = 1$, $x_2(0) = x_3(0) = x_5(0) = x_6(0) = x_7(0) = 0$, $x_4(0) = R_{s0}$ and $x_8(0) = R_{i0}$.

8.3.2 Boundedness of the system

The boundedness of the concerned system stated by equations (8.3.27) - (8.3.34) is confirmed by the following proposition. One may observe that the right hand sides of the system (8.3.27) - (8.3.34) are smooth functions of the corresponding variables in the positive quadrant $\mathscr{D}$=$\{(x_1, x_2, x_3, x_4, x_5, x_6, x_7, x_8) : x_1 > 0, x_2 > 0, x_3 > 0, x_4 > 0, x_5 > 0, x_6 > 0, x_7 > 0, x_8 > 0\}$. Hence, solution of the system exists. Therefore, the following statement can be proposed.

Proposition 1. *All the solutions of (8.3.27) - (8.3.34) starting in $\mathscr{D}$ are bounded with ultimate bound.*

Proof. It is known that $x_1 = e^{-t}$, which is bounded. This implies $x_1 \leqslant M$, for a constant finite $M > 0$.
Let us define a function
$\chi_1 = x_4 + x_5 + \frac{1}{\eta_1}x_6 + \frac{1}{\eta_2}x_7 + \frac{1}{\eta_3}x_8$, where, $\eta_1 > 0, \eta_2 > 0$ and $\eta_3 > 0$.

Its time derivative along the solutions of (8.3.30) - (8.3.34) is

$$\begin{aligned}\frac{d\chi_1}{dt} &= \frac{dx_4}{dt} + \frac{dx_5}{dt} + \frac{1}{\eta_1}\frac{dx_6}{dt} + \frac{1}{\eta_2}\frac{dx_7}{dt} + \frac{1}{\eta_3}\frac{dx_8}{dt} \\ &\leqslant \left(k_{syn} - k_t + \frac{k_t}{\eta_3}\right)x_4 + \left(\frac{1}{\eta_1} - 1\right)x_5 + \left(k_x + \frac{1}{\eta_2}\frac{Da_2}{Bp_2} - \frac{k_{hr}+k_x}{\eta_1}\right)x_6 - \left(\frac{k_{hl}}{\eta_2}\right)x_7 \\ &\quad + \left(k_x - \frac{k_{hr}+k_x}{\eta_3}\right)x_8 \\ &= a_4\, x_4 + a_5\, x_5 + a_6\, x_6 + a_7\, x_7 + a_8\, x_8\end{aligned}$$

where $a_4 = k_{syn} - k_t + \frac{k_t}{\eta_3}$, $a_5 = \frac{1}{\eta_1} - 1$, $a_6 = k_x + \frac{1}{\eta_2}\frac{Da_2}{Bp_2} - \frac{k_{hr}+k_x}{\eta_1}$, $a_7 = -\frac{k_{hl}}{\eta_2}$ and $a_8 = k_x - \frac{k_{hr}+k_x}{\eta_3}$.
Let $\mu_m = \max(a_4, a_5, a_6, a_7, a_8)$. Therefore,
$\frac{d\chi_1}{dt} \leqslant \mu_m\, \chi_1 \Rightarrow \frac{d\chi_1}{\chi_1} \leqslant \mu_m\, dt$,
$\Rightarrow\ \chi_1(t) \leqslant C\, e^{\mu_m\, t} \leqslant C$ (a positive integration constant), provided $\mu_m < 0$.

Thus, individually, x_4, x_5, x_6, x_7 and x_8 are bounded.
Let us define another function
$\chi_2 = \frac{1}{\eta_4}\, x_2 + x_3$, where $\eta_4 > 0$.

Its time derivative along the solutions of (8.3.28) - (8.3.29) is

$$\begin{aligned}\frac{d\chi_2}{dt} &= \frac{1}{\eta_4}\frac{dx_2}{dt} + \frac{dx_3}{dt} \\ &\leqslant M - \left(-Da_0 + \frac{Da_0}{\eta_4} + \frac{C\, Da_1}{R_{s0}} + \frac{k_p}{\eta_4}\right)x_2 - \left(1 - \frac{1}{\eta_4}\right)\frac{Da_0}{Bp_0}\, x_3 \\ &\leqslant M - a_2\, x_2 - a_3\, x_3, \text{ where, } a_2 = -Da_0 + \frac{Da_0}{\eta_4} + \frac{C\, Da_1}{R_{s0}} + \frac{k_p}{\eta_4},\ a_3 = 1 - \frac{1}{\eta_4}, \\ &\leqslant M - \mu_n\, \chi_2, \text{ where, } \mu_n = \min(a_2, a_3),\end{aligned}$$

$$\Rightarrow \frac{d\chi_2}{dt} + \mu_n \chi_2 \leqslant M$$
$$\Rightarrow \chi_2 \leqslant \frac{M}{\mu_n} + \left(\chi_2(0) - \frac{M}{\mu_n}\right) e^{-\mu_n t}$$
$$\therefore \quad \limsup_{t\to\infty} \chi_2(t) \leqslant \frac{M}{\mu_n}, \text{ which is independent of the initial condition.}$$

Thus, individually, x_2 and x_3 are bounded. Hence, the solutions of the system (8.3.27) - (8.3.34) that initiate from $\mathscr{D}$ are bounded. □

8.3.3 Stability analysis

Because of nonlinearity of the system (8.3.27) - (8.3.34), it is not an easy task to calculate the location of equilibrium points analytically. Hence, with the help of MAPLE software, four equilibrium points are found, out of which only one equilibrium point $E_1(0,0,0,0,0,0,0,0)$ is feasible.

Theorem 8.3.1. *The system represented by (8.3.27) - (8.3.34) is locally asymptotically stable.*

Proof. In order to prove that the system is locally stable, the corresponding linearised system is taken into account. The Jacobian matrix at the equilibrium point E_1 is as follows:

$$V_1 = \begin{bmatrix}
-1 & 0 & 0 & 0 & 0 & 0 & 0 & 0 \\
0 & -(Da_0 + k_p) & \frac{Da_0}{Bp_0} & 0 & \frac{Da_1}{Bp_1} & 0 & 0 & 0 \\
0 & Da_0 & -\frac{Da_0}{Bp_0} & 0 & 0 & 0 & 0 & 0 \\
0 & 0 & 0 & -(k_t - k_{syn}) & \frac{Da_1}{Bp_1} & 0 & 0 & k_x \\
0 & 0 & 0 & 0 & -(\frac{Da_1}{Bp_1} + k_e) & k_x & 0 & 0 \\
0 & 0 & 0 & 0 & k_e & -(\frac{Da_2}{Bp_2} + k_{hr} + k_x) & 0 & 0 \\
0 & 0 & 0 & 0 & 0 & \frac{Da_2}{Bp_2} & -k_{hl} & 0 \\
0 & 0 & 0 & k_t & 0 & \frac{Da_2}{Bp_2} & 0 & -(k_{hr} + k_x)
\end{bmatrix}$$

The characteristic polynomial of V_1 may be represented as

$$\lambda^8 + J_7\lambda^7 + J_6\lambda^6 + J_5\lambda^5 + J_4\lambda^4 + J_3\lambda^3 + J_2\lambda^2 + J_1\lambda + J_0 = 0, \tag{8.3.35}$$

where λ denotes the eigenvalues. The $J_i's,\ i = 0,1,2,3,4,5,6,7$ have got their expressions provided in Appendix 8.7.1. By Routh-Hurwitz criterion, the eigenvalues $\lambda_i,\ i = 1,2,3,4,5,6,7,8$ which are the solutions of equation (8.3.35) have negative real parts and hence the equilibrium point E_1 is locally

asymptotically stable. Moreover, numerically using MAPLE it is confirmed that the eigenvalues are negative and real. □

Table 8.1: Simulated values of the model parameters

Parameters	Values	References
D_0	$4.9 * 10^{-8}\ cm^2\ s^{-1}$	[79]
P_1	$10^{-5}\ cm\ s^{-1}$	–
k	1	[11]
ε_0	0.25	[11]
α_0	$7.5 * 10^{-4}\ s^{-1}$	Estimated from [96]
k_m	$5.6 * 10^{-5}\ s^{-1}$	[18]
β_0	$10^{-4} s^{-1}$	[113]
δ_0	$10^{-4} s^{-1}$	[113]
M	$10^{-6} mol\ \ cm^{-3}$	Estimated from [106, 107]
l_0	$0.01 cm$	Estimated from [113]
C_{lim}	$2.79 * 10^{-5}\ mol\ cm^{-3}$	[18]
k_{hl}	$1.67 * 10^{-4}\ s^{-1}$	[79]
k_{hr}	$3.67 * 10^{-4}\ s^{-1}$	[79]
k_e	$2.75 * 10^{-3}\ s^{-1}$	[140]
k_x	$9.67 * 10^{-4}\ s^{-1}$	[79]
k_t	$5 * 10^{-4}\ s^{-1}$	[79]
k_r	$10^{-2}\ s^{-1}$	[107]
$k_r^{'}$	$10^{-2}\ s^{-1}$	[107]
k_{-1}	$10^{3}\ s^{-1}$	[106, 107]
k_f	$10^{5}\ (mol\ cm^{-3}\ s)^{-1}$	[79, 106]
k_{+1}	$10^{5}\ (mol\ cm^{-3}\ s)^{-1}$	[79, 106]
$k_f^{'}$	$10^{5} (mol\ cm^{-3}\ s)^{-1}$	[79, 106]
k_p	$2.7 * 10^{-2}\ s^{-1}$	–
P_0	$3 * 10^{-6}\ mol\ cm^{-3}$	Estimated from [107]
R_{s0}	$10^{-9}\ mol\ cm^{-3}$	Estimated from [106]
R_{i0}	$10^{-10}\ mol\ cm^{-3}$	Estimated from [106]

8.4 Reduced order model

In order to understand the dynamics of drug transport to the biological tissue in depth, the model is simplified using quasi-steady-state approximations (QSSA) (cf.[89], [83]) for the cell surface receptor (x_4) and cell surface bound drug (x_5) concentrations along with internalized receptor (x_8) concentration. In order to streamline the system of ordinary differential equations and to deal with higher dimensional

model, a mathematical approach, namely, QSSA is used. QSSA is a standard procedure in order to study reaction kinetics, where some compounds exist for a shorter time period with respect to others or some species are less significant in comparison to others. There are specific reasons behind choosing the above-mentioned concentrations. Firstly, as the present problem is dedicated to study the behaviour of drugs, hence detailed study of receptors' concentration is not vital in this study. Secondly, processes regarding formation of the cell surface bound drug and its decay occur in a shorter time scale in comparison to the time-scales required for other phenomena. So, these concentrations are approximated under the said assumption. Hence, equations (8.3.30), (8.3.31) and (8.3.34) become

$$x_4 = \frac{e_1\, x_6\, x_7 + e_2\, x_2\, x_6\, x_7 + e_3\, x_2\, x_6 + e_4\, x_6}{b_1\, x_2\, x_7 + b_2\, x_2 + b_3\, x_7 + b_4}, \tag{8.4.1}$$

$$x_5 = \frac{g_1\, x_6\, x_7 + g_2\, x_2\, x_6\, x_7 + g_3\, x_2\, x_6 + g_4\, x_6}{b_1\, x_2\, x_7 + b_2\, x_2 + b_3\, x_7 + b_4}, \tag{8.4.2}$$

$$x_8 = \frac{c_1\, x_6 + c_2\, x_2\, x_6}{b_1\, x_2\, x_7 + b_2\, x_2 + b_3\, x_7 + b_4}. \tag{8.4.3}$$

The parameters associated with the above equations are described in details in Appendix 8.7.2. Substituting equations (8.4.1), (8.4.2) and (8.4.3) in equations (8.3.27) - (8.3.29) and (8.3.32) - (8.3.33), the modified equations are as follows:

$$\frac{dx_1}{dt} = -x_1, \tag{8.4.4}$$

$$\frac{dx_2}{dt} = -Da_0\, x_2[1 - x_3] + \frac{Da_0}{Bp_0}\, x_3 - \frac{Da_1}{R_{s0}}\, x_2 \left[\frac{e_1\, x_6\, x_7 + e_2\, x_2\, x_6\, x_7 + e_3\, x_2\, x_6 + e_4\, x_6}{b_1\, x_2\, x_7 + b_2\, x_2 + b_3\, x_7 + b_4}\right]$$
$$+ \frac{Da_1}{Bp_1} \left[\frac{g_1\, x_6\, x_7 + g_2\, x_2\, x_6\, x_7 + g_3\, x_2\, x_6 + g_4\, x_6}{b_1\, x_2\, x_7 + b_2\, x_2 + b_3\, x_7 + b_4}\right] + k_p\, [(x_1^{m_1} - x_1^{m_2})\, \cos(a\, l_0) - x_2], \tag{8.4.5}$$

$$\frac{dx_3}{dt} = Da_0\, x_2[1 - x_3] - \frac{Da_0}{Bp_0}\, x_3, \tag{8.4.6}$$

$$\frac{dx_6}{dt} = k_e \left[\frac{g_1\, x_6\, x_7 + g_2\, x_2\, x_6\, x_7 + g_3\, x_2\, x_6 + g_4\, x_6}{b_1\, x_2\, x_7 + b_2\, x_2 + b_3\, x_7 + b_4}\right] - \frac{Da_2}{Bp_2}\, x_6 - (k_{hr} + k_x)\, x_6$$
$$+ \frac{Da_2}{R_{i0}}\, x_7 \left[\frac{c_1\, x_6 + c_2\, x_2\, x_6}{b_1\, x_2\, x_7 + b_2\, x_2 + b_3\, x_7 + b_4}\right], \tag{8.4.7}$$

$$\frac{dx_7}{dt} = -\frac{Da_2}{R_{i0}}\, x_7 \left[\frac{c_1\, x_6 + c_2\, x_2\, x_6}{b_1\, x_2\, x_7 + b_2\, x_2 + b_3\, x_7 + b_4}\right] + \frac{Da_2}{Bp_2}\, x_6 - k_{hl}\, x_7. \tag{8.4.8}$$

All the parameters are provided in Appendix 8.7.2.

8.4.1 Boundedness of the system

Boundedness of the independent variables of the system (8.4.4) - (8.4.8) are similar to those corresponding to the full model represented by (8.3.27) - (8.3.34).

8.4.2 Stability analysis

Analogous to the location of equilibrium of the full model, reduced order model is also having a single feasible equilibrium point $E_2 = (0,0,0,0,0)$.

Theorem 8.4.1. *The reduced system represented by (8.4.4) - (8.4.8) is locally asymptotically stable.*

Proof. In order to prove that the system is locally stable, the corresponding linearised system is taken into account. The Jacobian matrix at the equilibrium point E_2 is as follows:

$$V_2 = \begin{bmatrix} -1 & 0 & 0 & 0 & 0 \\ 0 & -(Da_0 + k_p) & \frac{Da_0}{Bp_0} & \frac{Da_1\ g_1}{Bp_1\ b_4} & 0 \\ 0 & Da_0 & -\frac{Da_0}{Bp_0} & 0 & 0 \\ 0 & 0 & 0 & \left(\frac{k_e\ g_4}{b_4} - \frac{Da_2}{Bp_2} - k_{hr} - k_x\right) & 0 \\ 0 & 0 & 0 & \frac{Da_2}{Bp_2} & -k_{hl} \end{bmatrix}$$

The characteristic polynomial of V_2 can be represented as

$$(-1-\bar{\lambda})\left(\frac{k_e\ g_4}{b_4} - \frac{Da_2}{Bp_2} - k_{hr} - k_x - \bar{\lambda}\right)(-k_{hl}-\bar{\lambda})\left[\bar{\lambda}^2 + \left(\frac{Da_0}{Bp_0} + Da_0 + k_p\right)\bar{\lambda} + k_p\frac{Da_0}{Bp_0}\right] = 0, \tag{8.4.9}$$

where $\bar{\lambda}$ denotes the eigenvalues of V_2.
The calculated values of $\bar{\lambda}'s$ are $-2.10202560495347 * 10^6$, -53.4970465321676, -1, -0.34080 and -22.704870. Since they are all negative and real, the concerned system is locally asymptotically stable. □

8.5 Numerical simulation and discussion

A systematic quantitative analysis is accomplished for the local drug delivery based on the model parameters provided in Table 8.1 with the objective of characterizing the pharmacokinetic aspects in more details. Graphical representations of drug concentration in its different embodiments are well

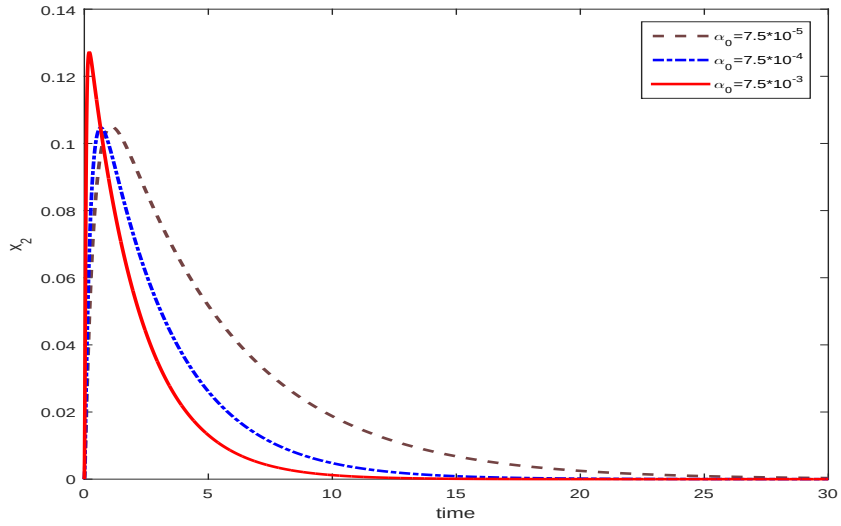

Figure 8.2: Time variant x_2 profile for different α_0

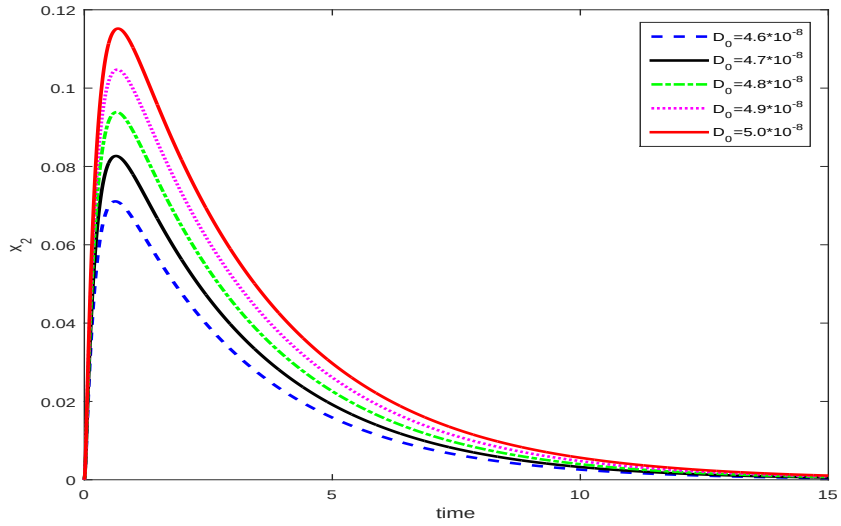

Figure 8.3: Time variant x_2 profile for different D_0

illustrated in Figs. 8.2 - 8.22 so that the underlying governing physical phenomena get elucidated. Figures 8.2 - 8.10 depict the sensitized impact of some vital model parameters through time variant drug concentration profiles of the original full model system (8.3.27) - (8.3.34). As the outcomes of the present dynamic model are all bounded, one may reckon that the original system and its reduced version (8.4.4) - (8.4.8) govern a rich dynamics including their individual stability, both three- and two-dimensional projections of the phase portraits for stability of several subsystems of the reduced model. The system of equations is solved numerically by variable order method with the help of MATLAB software to obtain several apposite findings. The usage of all tabular values of the model parame-

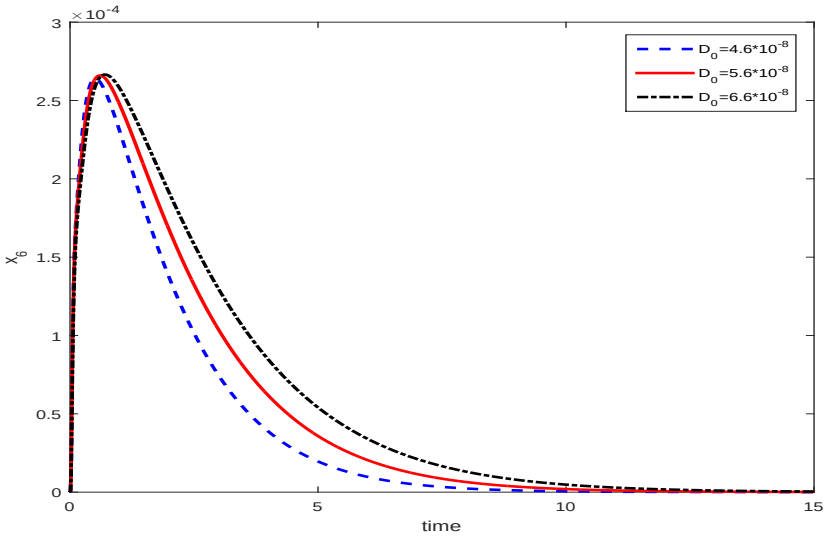

Figure 8.4: Time variant x_6 profile for different D_0

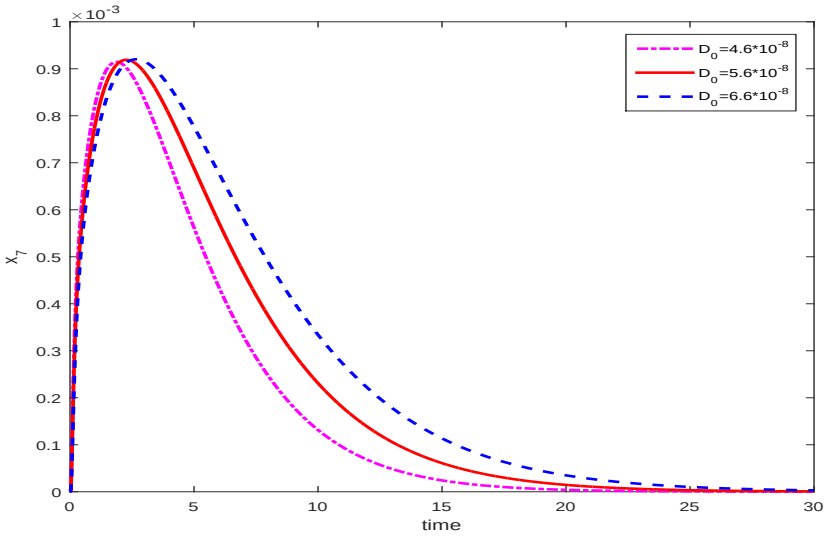

Figure 8.5: Time variant x_7 profile for different D_0

ters yields zero equilibrium positions both for the original system and its reduced one. This indicates precise consistency of the reduced model with the quasi-steady-state theory. Here, 'zero equilibrium position' rightly signifies that the entire process of drug release is deactivated at some instant when the system needs no more medication in terms of either drug administration or its interaction with the receptors. It emerges that the Jacobian matrices corresponding to both the original and the reduced model systems at their respective equilibrium positions possess all real negative eigenvalues and hence both the systems are stable. Due to vastness of the present original dynamical system, attention is focussed on the stability of several subsystems of the reduced model with the inclusion of phase por-

traits as well. The reduced system of equations comprises five variables. Though analytically, it is already proved that the reduced system is stable, yet it is impossible to have five dimensional graphical representation. Hence, in order to have an idea of stability graphically, Figs. 8.11 - 8.15 depict the three-dimensional projection of phase portraits of several subsystems, whereas Figs. 8.16 - 8.22 depict the two-dimensional projection of phase portraits of several subsystems arising from the reduced model system. Moreover, subsystems are formed considering three or two variables at a time out of five variables of the reduced system just to visualize their stability graphically.

Figure 8.2 reveals the influence of α_0 on free drug (x_2) present in plasma and interstitial fluid with time. As α_0 denotes the solid-liquid mass transfer coefficient, it helps in solid drug dissolution phenomenon in the polymeric matrix. Thus, when α_0 gets increased, solid drug is quickly transformed into free drug in the polymeric matrix. Since x_2 is directly proportional to the free drug of the polymeric matrix (which is evident from equation 8.3.20 since $x_2 = C_1$), so its peak reaches its zenith very quickly when α_0 is much increased. Moreover, it may also be observed that when α_0 increases from $7.5 * 10^{-5}$ to $7.5 * 10^{-4}$, the peak height remains the same and it only shifts towards left. This behaviour depicts that higher concentration of free drug is formed only when α_0 is increased beyond a certain threshold value, otherwise only rate of free drug transformation from solid drug is enhanced.

Figures 8.3 - 8.5 show the influence of diffusion coefficient D_0 on free drug in plasma and interstitial fluid (x_2), internalized bound drug (x_6) and internalized free drug (x_7) respectively over a stipulated time period. The impact of diffusivity (D_0) of free drug in the polymeric matrix is visible in Fig. 8.3 as its slight variation affects the concentration profiles. When D_0 gets increased, concentration of x_2 enhances steadily as expected since increased diffusivity leads to faster oozing out of free drug (C_0) from the polymeric matrix. Figures 8.4 & 8.5 manifest notable concentration (x_6 and x_7) profile deviations with perturbation of D_0. The range of D_0 values considered are different in different plots in order to get a clearer view of the corresponding profile variations. In Fig. 8.4, one may observe that variation in x_6 is directly proportional to D_0. This is due to the fact that internalized bound drug (x_6) is formed from cell surface bound drug (x_5), which is the outcome of free drug-cell surface receptor interaction. Thus, in case of higher diffusivity, internalized bound drug declines slowly in accordance with the increment of free drug in plasma and interstitial fluid. However, in Fig. 8.5, a similar attitude is shown by the concentration profile of internalized free drug (x_7) as x_7 is dependent on x_6. It is interesting to note that the profile peaks in Figs. 8.4 & 8.5 remain the same even with the increment of D_0. The reason behind this behaviour is that even though increased diffusivity gives rise to increased concentration of free drug, only a fraction of free drug is available for the cell surface receptors to interact. Furthermore, saturation of receptors is also a cause for such attitude of the respective concentration profiles in Figs. 8.4 & 8.5.

Figures 8.6 & 8.7 show the influence of endocytosis rate constant (k_e) on cell surface bound drug (x_5) and internalized bound drug (x_6) respectively over a stipulated time period. In Fig. 8.6, it is observed that with increasing k_e, the concentration profile of cell surface bound drug declines drastically. This is due to the fact that the increased endocytosis rate constant accelerates the internalization of cell

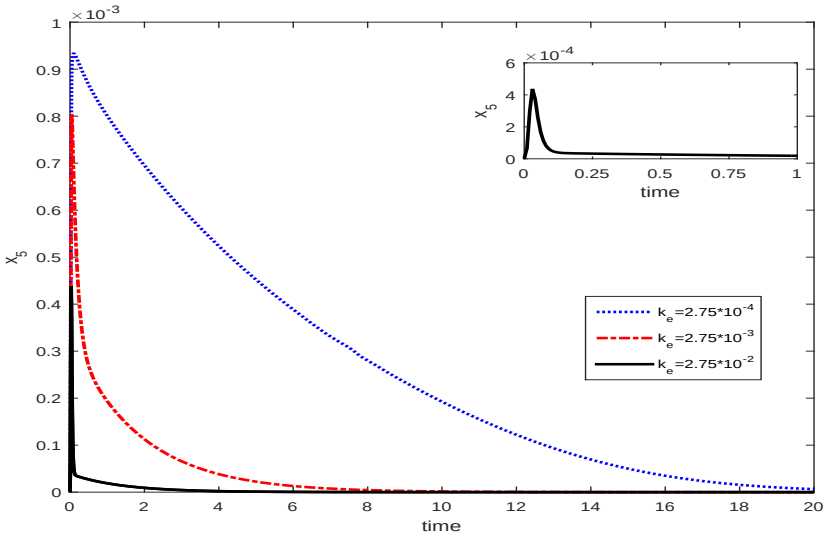

Figure 8.6: Time variant x_5 profile for different k_e

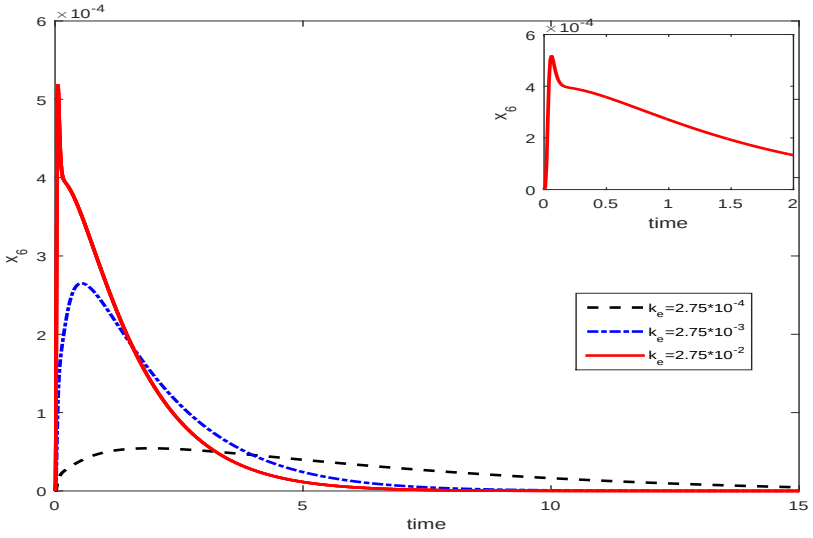

Figure 8.7: Time variant x_6 profile for different k_e

surface bound drug into the intracellular domain. On the other hand, in Fig. 8.7, a reverse attitude is visualized since enhanced endocytosis rate tends to increase the internalized bound drug concentration. The blurred areas in the main plots can be visualized clearly in the inset plots.

Figures 8.8, 8.9 & 8.10 present the influence of the recycling rate constant (k_x) on cell surface bound drug (x_5), internalized bound drug (x_6) and internalized free drug (x_7) respectively over a stipulated time period. In Fig. 8.8, the concentration profile of cell surface bound drug (x_5) increases as expected, with increasing rate of recycling rate constant. With increased recycling rate, the internalised bound drug (x_6) recycles back to the cell surface faster, thus increasing the cell surface bound drug concen-

tration. In Fig. 8.9, it may be visualized that when the recycling rate of x_6 is increased, the peak of the concentration profile decreases. This behaviour is quite natural as more fraction of x_6 is getting recycled back to the cell surface. It is worthy to observe that when k_x is increased beyond a threshold value, the concentration peak lowers but the rate of its decline becomes sluggish. This is because when the recycling rate is increased much, a smaller fraction of internalized bound drug remains to undergo lysosomal degradation but endocytosis of cell surface bound drug continues. In Fig. 8.10, it is observed that internalized free drug is directly proportional to the recycling rate though they are not directly interdependent. The reason behind this behaviour is that increased recycling rate leads to faster recycling back of internalized bound drug as well as internalized receptors to the cell surface. Thus, the internalized free drug cannot interact with the internalized receptors to form internalized bound drug though free drug is constantly being formed from the dissociation of internalized bound drug.

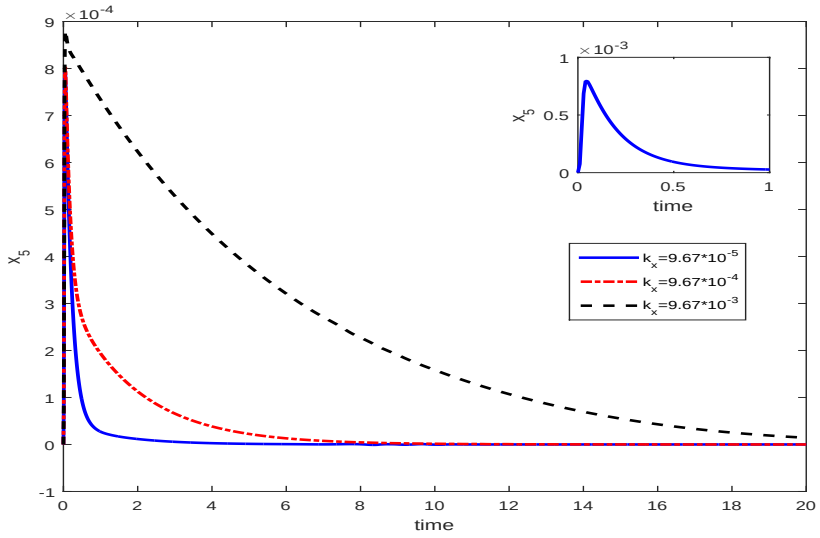

Figure 8.8: Time variant x_5 profile for different k_x

As there are certain limitations to perform an in-depth study on the entire original system under investigation, it is focused on the reduced model having sufficient consistency. For the purpose of investigating the stability criterion of the reduced system, an attempt is made to explore the stability of its various subsystems in three-dimensional spaces namely, (x_2, x_6, x_7), (x_3, x_6, x_7), (x_1, x_2, x_6), (x_1, x_2, x_7) and (x_1, x_6, x_7), which are exhibited in Figs. 8.11 - 8.15 respectively. It is evident from these diagrams that the equilibrium position of the system under study is asymptotically stable in view of the choice of different initial positions. All the trajectories emanate from their respective starting positions eventually approach the equilibrium position following the arrowed flow directions irrespective of the choice of their starting positions. This goes well with realistic physiological systems where small changes in medication dose or receptors concentration do not destabilize the system. Hence, both the advocated mathematical model and its corresponding real biological system can complement each other through the study of stability analysis. This validates the authenticity of the proposed mathematical

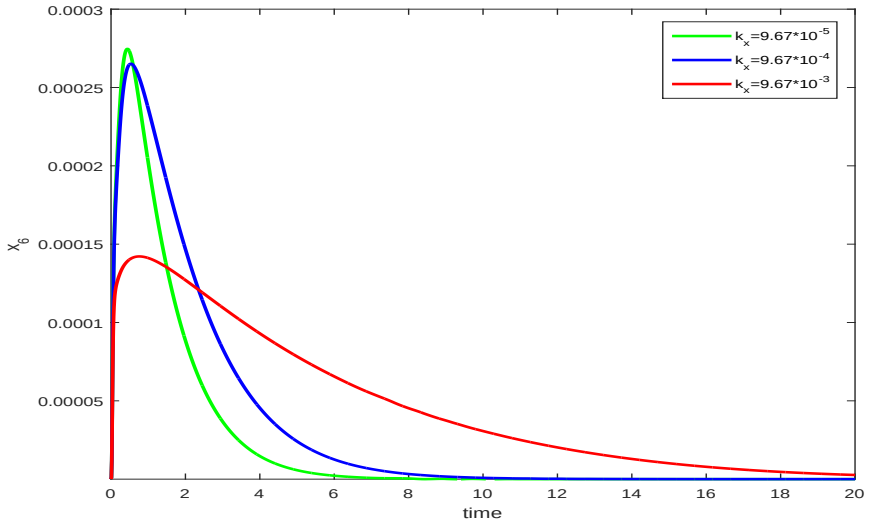

Figure 8.9: Time variant x_6 profile for different k_x

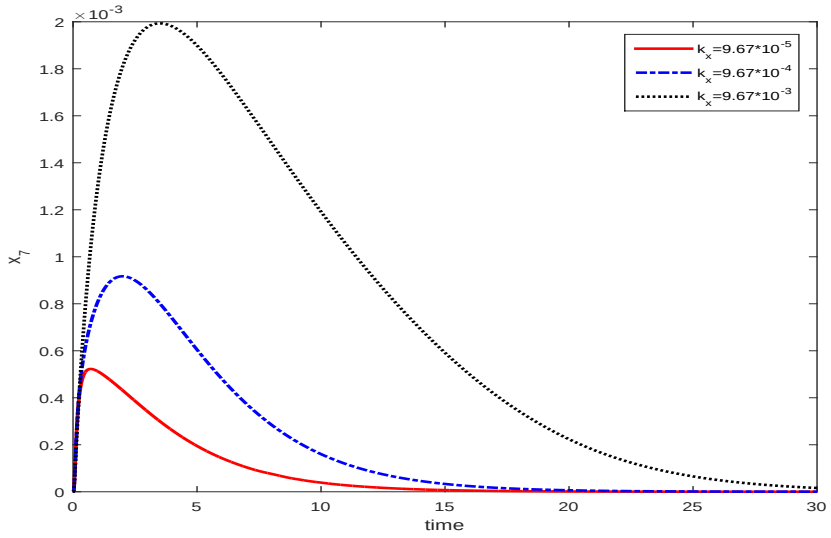

Figure 8.10: Time variant x_7 profile for different k_x

model. Figures 8.11 - 8.12 admit of two three dimensional frameworks demonstrating phase portraits corresponding to four different subspaces comprising free drug in plasma and interstitial fluid (x_2), protein-free drug complex (x_3), internalized bound drug (x_6) and internalized free drug (x_7). The frame of Fig. 8.11 marks the performance of the interplay between free drug in plasma and interstitial fluid with internalized bound drug and free drug dissociated from internalized bound drug through trajectories commencing from initial positions and approaching the equilibrium position with time irrespective of the choice of starting positions. Similar framework consisting of the dynamics of protein-free drug complex, internalized bound drug and internalized free drug is presented in Fig. 8.12 for different

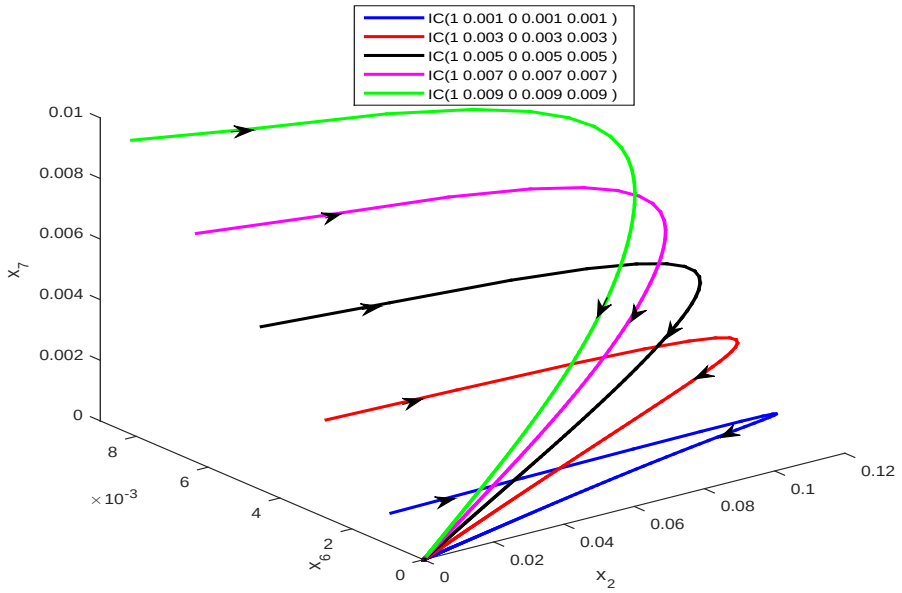

Figure 8.11: 3D projection of subsystem (x_2, x_6, x_7)

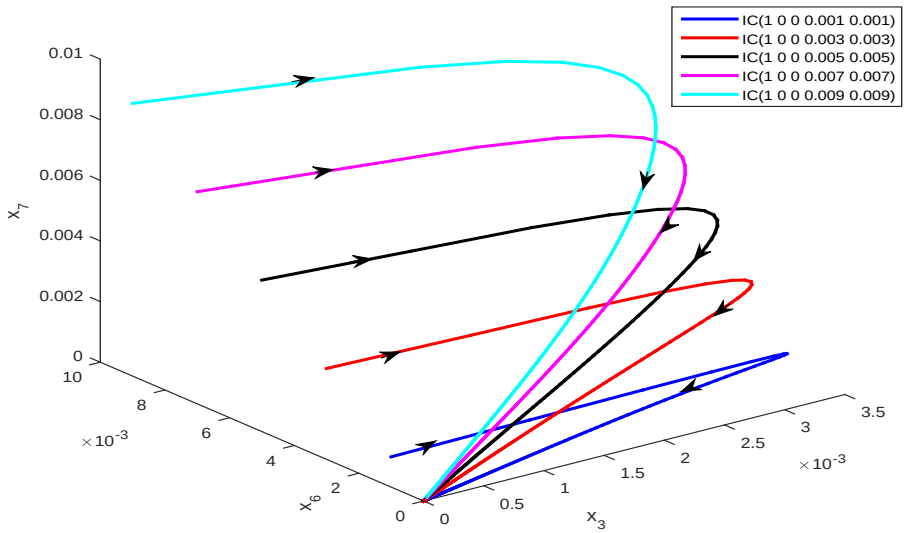

Figure 8.12: 3D projection of subsystem (x_3, x_6, x_7)

initial positions so as to examine the stability of the subsystem. Three more subsystems are displayed in Figs. 8.13 - 8.15 corresponding to four different subspaces, where the stability of the respective subsystems are ensured following similar approach. The essence of all the trajectories of these frames reveals that all the designated subsystems derived from the reduced model system are stable which

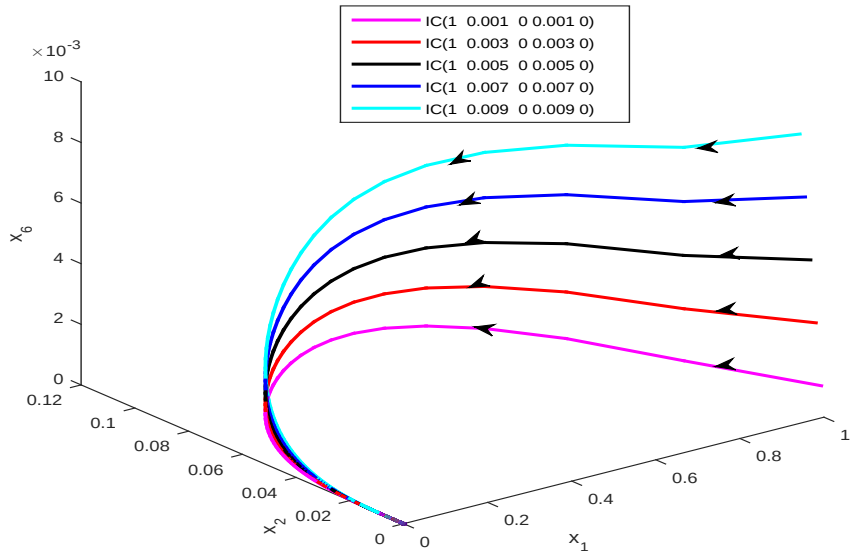

Figure 8.13: 3D projection of subsystem (x_1, x_2, x_6)

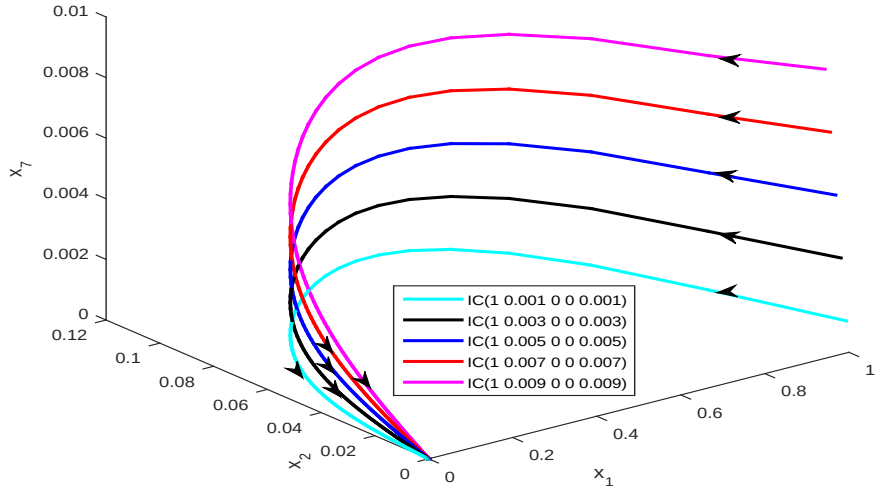

Figure 8.14: 3D projection of subsystem (x_1, x_2, x_7)

motivates towards further investigation of the model of relevance.

Finally, the projections of two dimensional phase portraits corresponding to all different subspaces of the reduced model system are displayed in the concluding graphical representations Figs. 8.16 -

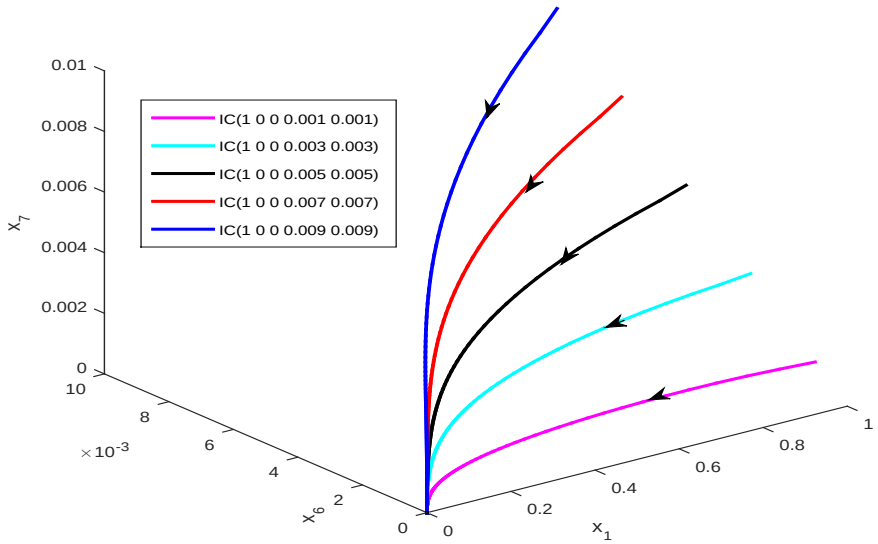

Figure 8.15: 3D projection of subsystem (x_1, x_6, x_7)

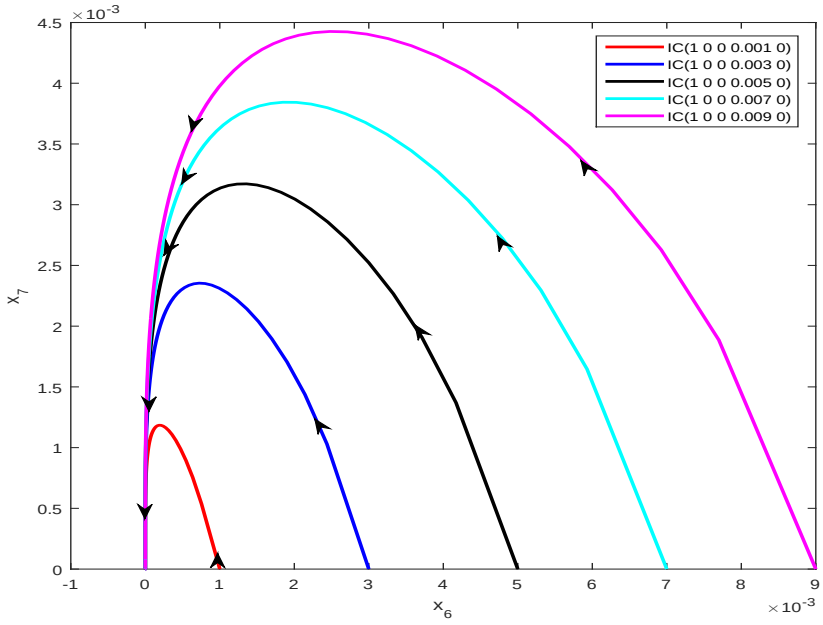

Figure 8.16: (x_6, x_7) phase portrait

8.22 as another measure of stability of the present dynamical system. An attempt is made to plot the phase planes corresponding to (x_6 , x_7), (x_1 , x_6), (x_1 , x_7), (x_2 , x_7), (x_2 , x_6), (x_3 , x_6) and (x_3 , x_7) subspaces in the respective figures. There are seven distinct panels arising from several subsystems of the reduced model in two dimensional subspaces out of all five spaces of the model. All the panels

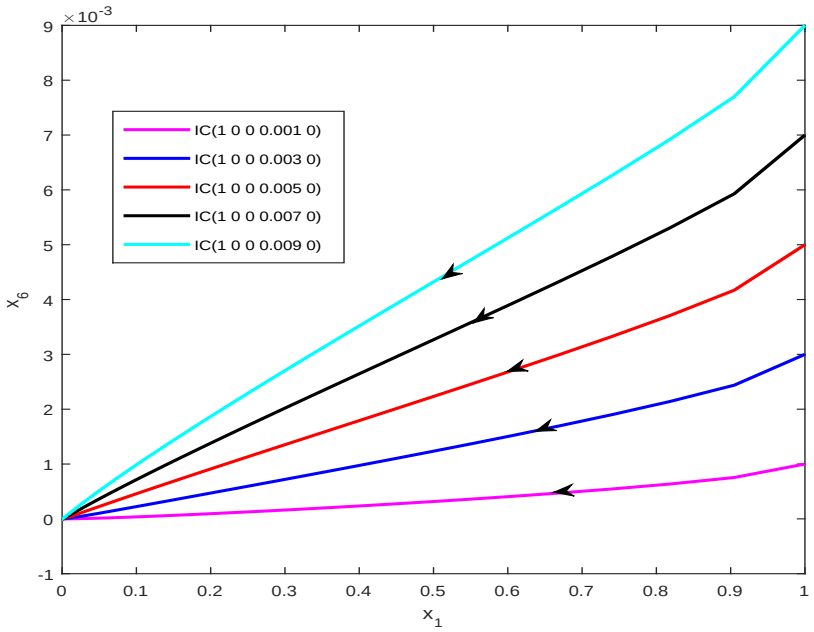

Figure 8.17: (x_1, x_6) phase portrait

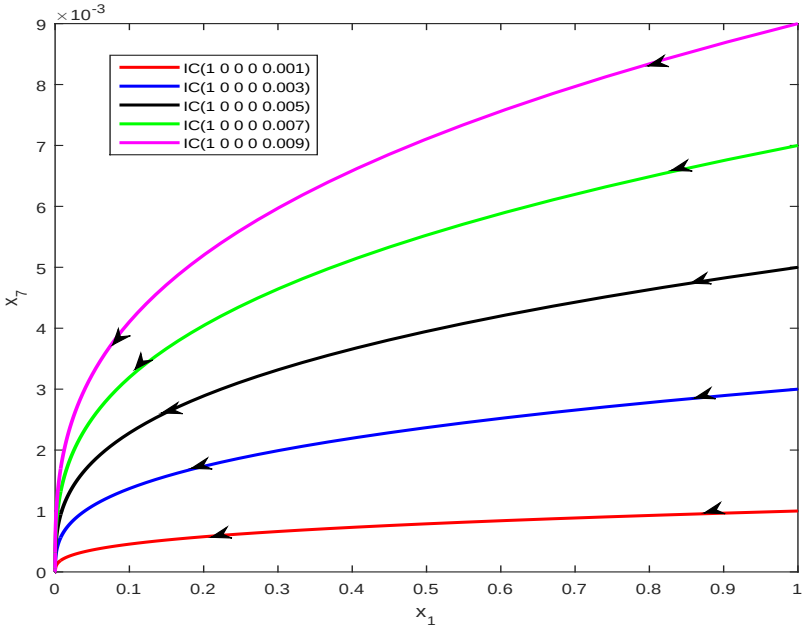

Figure 8.18: (x_1, x_7) phase portrait

have a common feature that various trajectories of the panel bear a tendency to move along the directed pathway towards equilibrium point irrespective of their starting positions. This phenomenon further ensures the stability of the dynamic drug release model under consideration.

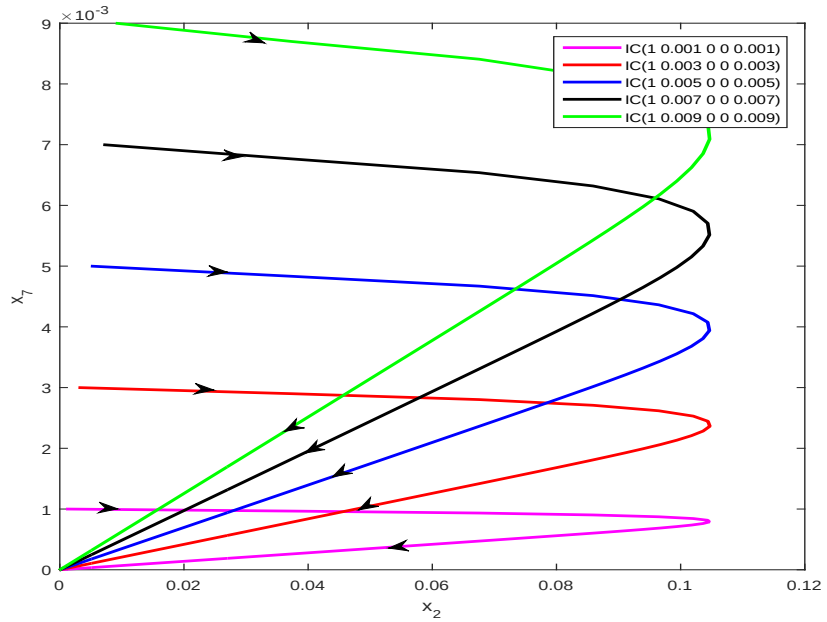

Figure 8.19: (x_2, x_7) phase portrait

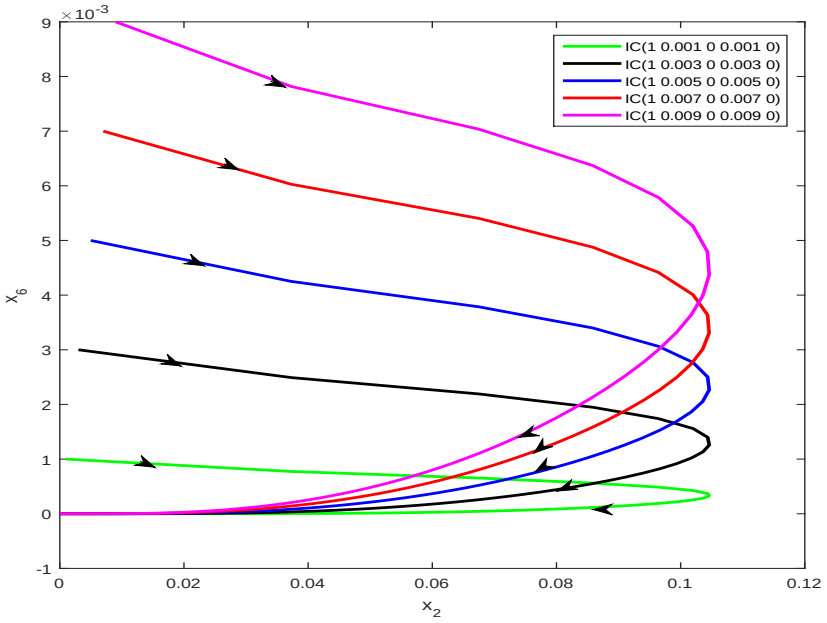

Figure 8.20: (x_2, x_6) phase portrait

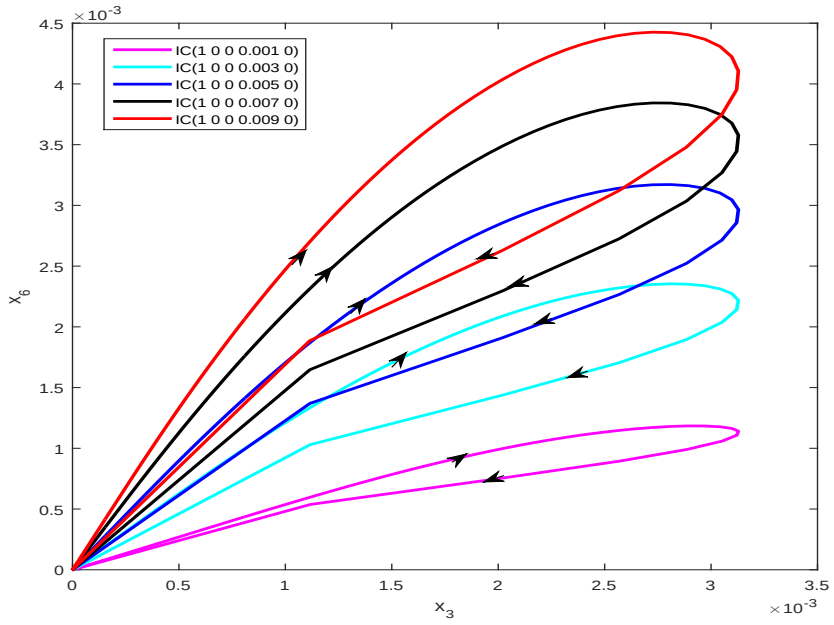

Figure 8.21: (x_3, x_6) phase portrait

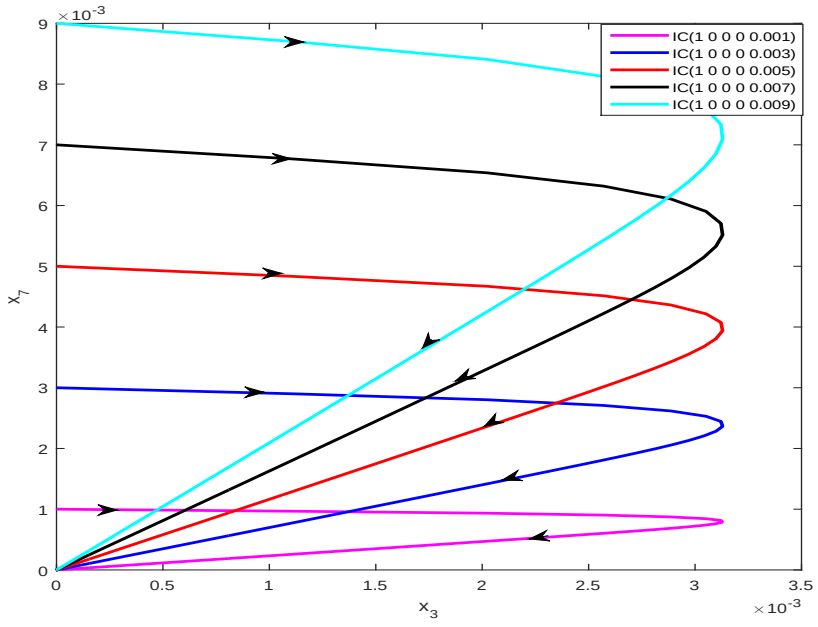

Figure 8.22: (x_3, x_7) phase portrait

8.6 Conclusions

Controlled release local drug delivery betters the bioavailability of drug distribution. Experimental research mostly illustrates the importance of controlled release in local drug delivery, however, to

demonstrate its full characterization, mathematical modelling and corresponding mathematical analysis of such systems are imperative. The present study deals with the establishment of a mathematical prognostic model for drug release from a polymeric matrix and subsequent intracellular drug transport. The model focuses on the complex endosomal events in addition to the drug release mechanism. The model is formulated as a mixed system of partial and ordinary differential equations in association with a set of initial and boundary conditions. The study undertaken is of adequate merit on several counts. First, the propounded model is realistic as it takes into consideration the vital biochemical, physical and physiological phenomena participating in local drug delivery from polymeric matrix. Secondly, nonlinearity in the model deals with the biological complexities. Thirdly, both analytical and numerical methods are adopted to solve the system of governing equations. As the model is vast, it becomes inconvenient to proceed with a detailed study and, therefore, a reduced model system is derived based on Quasi Steady State Approximation (QSSA) theory. Both analytical and numerical studies are carried out for local stability analysis of the full as well as reduced model systems. Fourthly, the novelty of the current work undertaken lies in the stability analysis, which is not illumined till date as per the knowledge of the present authors. Fifthly, the complex characteristics of several subsystems of the reduced model are also investigated through the graphical portrayals of three-dimensional projection of subsystems and phase portraits. Lastly, the responsiveness of drug dynamics to the model parameters is demonstrated through graphical representations, which determines the applicability of the drug administration in treating the patients at large. The advocated mathematical model acts as the basis for obtaining a more advanced drug delivery system. This is because study of stability analysis bridges the gap between the mathematical and physiological systems of drug kinetics more effectively. The behaviour shown by the proposed mathematical model is analogous to the real biochemical and physiological system, which focusses on the necessity of such analysis. Furthermore, this study can be updated with the incorporation of global stability analysis.

8.7 Appendix

8.7.1 Coefficients of the characteristic equation (8.3.35)

$$J_0 = k_{hl}(F_3 - E_4 - I_6), \quad J_1 = [(F_3 - E_4 - I_6)(1 + k_{hl}) - k_{hl}(I_5 + E_3 - F_2)],$$
$$J_2 = [-I_6 - E_4 + F_3 - (1 + k_{hl})(I_5 + E_3 - F_2) - k_{hl}(I_4 + E_2 - F_1)],$$
$$J_3 = [-I_5 - E_3 + F_2 - (1 + k_{hl})(I_4 + E_2 - F_1) - k_{hl}(I_3 + E_1)],$$
$$J_4 = [-I_4 - E_2 + F_1 - (1 + k_{hl})(I_3 + E_1) - k_{hl}\, I_2],$$
$$J_5 = [-I_3 - E_1 - (1 + k_{hl})\, I_2 - k_{hl}\, I_1], \quad J_6 = [-I_2 - (1 + k_{hl})\, I_1 + k_{hl}], \quad J_7 = 1 + k_{hl} - I_1.$$

$$I_1 = G_1 - H_1, \quad I_2 = G_2 + G_1\, H_1 - H_2, \quad I_3 = H_1\, G_2 + H_2\, G_1 - H_3, \quad I_4 = H_2\, G_2 + H_3\, G_1 - H_4,$$
$$I_5 = H_3\, G_2 + H_4\, G_1, \quad I_6 = H_4\, G_2.$$

$$H_1 = C_1 + A_1, \quad H_2 = C_1 + A_1\, C_1 + A_2, \quad H_3 = A_1\, C_3 + A_2\, C_1, \quad H_4 = A_2\, C_3.$$

$$G_1 = k_{syn} - k_t - k_{hr} - k_x, \quad G_2 = (k_{syn} - k_t)(k_{hr} + k_x).$$

$$F_1 = \frac{Da_0^2}{Bp_0} k_x\, k_t, \quad F_2 = D_1\, \frac{Da_0^2}{Bp_0} k_x\, k_t, \quad F_3 = D_3\, \frac{Da_0^2}{Bp_0} k_x\, k_t.$$

$$E_1 = k_x\, k_e\, \frac{Da_2}{Bp_2}, \quad E_2 = k_x\, k_e\, \frac{Da_2}{Bp_2} \left(\frac{Da_1}{Bp_1} + k_e + C_1\right) - k_x^2\, k_e\, k_t,$$

$$E_3 = k_x\, k_e\, \frac{Da_2}{Bp_2} \left[C_1 \left(\frac{Da_1}{Bp_1} + k_e\right) + C_2\right] - C_1\, k_x^2\, k_e\, k_t, \quad E_4 = C_2\, k_x\, k_e \left[\frac{Da_2}{Bp_2} \left(\frac{Da_1}{Bp_1} + k_e\right) - k_x\, k_t\right]$$

$$D_1 = \frac{Da_1}{Bp_1} + \frac{Da_2}{Bp_2} + k_e + k_{hr} + k_x, \quad D_2 = \left(\frac{Da_1}{Bp_1} + k_e\right) \left(\frac{Da_2}{Bp_2} + k_{hr} + k_x\right), \quad D_3 = D_2 - k_e\, k_x.$$

$$C_1 = \frac{Da_0}{Bp_0} + Da_0 + k_p, \quad C_2 = \frac{Da_0^2}{Bp_0} + Da_0\, k_p, \quad C_3 = \frac{Da_0}{Bp_0}\, k_p.$$

$$A_1 = \frac{Da_1}{Bp_1} + \frac{Da_2}{Bp_2} + k_e + k_{hr} + k_x, \quad A_2 = \left(\frac{Da_1}{Bp_1} + k_e\right) \left(\frac{Da_2}{Bp_2} + k_{hr}\right) + \frac{Da_1}{Bp_1}\, k_x.$$

8.7.2 Parameters used in the reduced model

$$b_1 = \frac{Da_1\, Da_2}{R_{s0}\, R_{i0}\, k_t}, \quad b_2 = \frac{Da_1\, (k_x + k_{hr})}{R_{s0}\, k_t}, \quad b_3 = \left(\frac{k_t - k_{syn}}{k_e\, k_t}\right) \left(\frac{Da_1}{Bp_1} + k_e\right) \frac{Da_2}{R_{i0}},$$

$$b_4 = \left\{\frac{(k_t - k_{syn})}{k_e k_t} (k_{hr} + k_x) - \frac{k_x}{k_e}\right\} \left(\frac{Da_1}{Bp_1} + k_e\right)$$

$$c_1 = \left[\left\langle \frac{k_x}{k_e} - \frac{Da_2}{Bp_2} \left(\frac{k_{syn} - k_t}{k_e\, k_t}\right)\right\rangle \left(\frac{Da_1}{Bp_1} + k_e\right) - k_x\right], \quad c_2 = \frac{Da_1\, Da_2}{k_t\, Bp_2\, R_{s0}},$$

$$d_1 = \frac{c_1\, Da_2}{k_t\, R_{i0}}, \quad d_2 = \frac{c_2\, Da_2}{k_t\, R_{i0}}, \quad d_3 = \frac{c_2\, (k_{hr} + k_x)}{k_t}, \quad d_4 = \frac{c_1\, (k_{hr} + k_x)}{k_t}, \quad d_5 = -\frac{Da_2}{Bp_2\, k_t},$$

$$d_6 = d_5\, b_1, \quad d_7 = d_5\, b_2, \quad d_8 = d_5\, b_3, \quad d_9 = d_5\, b_4, \quad e_1 = d_1 + d_8, \quad e_2 = d_2 + d_6,$$

$$e_3 = d_3 + d_7, \quad e_4 = d_4 + d_9, \quad f_1 = \frac{c_1\, Da_2}{R_{i0}} \left(\frac{k_{syn} - k_t}{k_e\, k_t}\right), \quad f_2 = \frac{c_2\, Da_2}{R_{i0}} \left(\frac{k_{syn} - k_t}{k_e\, k_t}\right),$$

$$f_3 = c_1 \left\{\frac{(k_{syn} - k_t)}{k_e k_t} (k_{hr} + k_x) + \frac{k_x}{k_e}\right\}, \quad f_4 = c_2 \left\{\frac{(k_{syn} - k_t)}{k_e k_t} (k_{hr} + k_x) + \frac{k_x}{k_e}\right\},$$

$$f_5 = \left[\frac{k_x}{k_e} - \frac{Da_2}{Bp_2} \left(\frac{k_{syn} - k_t}{k_e\, k_t}\right)\right], \quad f_6 = f_5\, b_1, \quad f_7 = f_5\, b_2, \quad f_8 = f_5\, b_3, \quad f_9 = f_5\, b_4,$$

$$g_1 = f_1 + f_8, \quad g_2 = f_2 + f_6, \quad g_3 = f_4 + f_7, \quad g_4 = f_3 + f_9.$$

9 CONCLUSIONS

I know one thing: that I know nothing (The Socratic paradox)

Socrates

The entire work undertaken in the present dissertation is the general characterisation of drug concentration in its different states through various processes of solubilisation, recrystallisation, diffusion, advection, plasma clearance, protein-drug interactions, transcapillary exchange of drugs, interplay between free drug particles with surface and internalized cell receptors along with related endosomal events including lysosomal degradation. The use of mathematical models of such complex physiological and biochemical phenomena is imperative because of their competence to illustrate complete characterisation unlike experimental findings having obvious limitations.

The present study ventured demonstrates its merits and upgradations. The significant influence of estimated parameters on the drug concentrations establishes the strong fact that by altering the parameters, various means of drug release control can be achieved according to the patient's needs. Various conclusions can be drawn from the dynamical models' behaviour, such as drug diffusion and drug assimilation in the tissue are inversely proportional to the drug binding. It is worth noting that as the drug needs much longer time in the tissue to get absorbed completely, its effect will certainly persist for a long time before the same drug is administered subsequently.

The useful comparison of almost all the models highlighted in the present dissertation with the relevant experimental investigations carried out in the recent past by several researchers, reveals the validity as well as reliability of the mathematical models undertaken in the domain of pharmacokinetics. The inclusion of local sensitivity analysis subject to variations of the various model parameters claims better understanding of the model characteristics so as to pose challenges to the applicability of drug administration for treatment of patients at large through pharmacotherapy. Special emphasis is laid on the

introduction of the influence of both biodegradable and biodurable polymeric matrices on drug release to the biological tissues. One may also highlight the difference in drug release rates corresponding to biodegradable and biodurable polymers, which may help in their respective applications in controlled release drug delivery systems. On the other hand, the study of liposomal drug delivery to solid tumour with the incorporation of complex endosomal events taking place in tumour cell, generates a clearer view of the detailed process of drug delivery right from the systemic plasma to the tumour intracellular domain. The proposed mathematical modelling and its numerical simulations of such complex physiological processes depict the understanding of the underlying physical and biochemical processes and various hindrances offered by physiological barriers in the path of drug transport to the cancerous tumour cells, in more details. Thus, it helps the pharmaceutical and bioengineering scientists to evolve liposomal drug delivery systems along with other nanotechnologies in order to optimize their design and drug dosage forms.

All the studies mentioned are confined to dynamic mathematical models of drug release and drug transport for the characterization of drug kinetics in pharmacotherapy. The study concludes with the stability of such dynamical models for the purpose of examining potentiality to generate appropriate predictive results for drug delivery. The analytical and numerical approaches reveal the stability of equilibrium position of the dynamical system so as to assure the applicability of the models undertaken.

Detailed impact for each of the mathematical models developed in the thesis on pharmacokinetics may be stated categorically as follows.

The impact of the first two models reveals that as the drug needs prolonged time in the tissue to get absorbed completely, its effect will certainly persist for a long time before the same drug is re-administered in order to elude toxicity. Hence proper care needs to be exercised for sustaining specific time-gap before re-dispensation. Local sensitivity analysis performed in third model possesses its own impact in a way that the sensitivity of drug concentration to the model parameters poses challenges to the applicability of drug administration for treatment of patients at large through pharmacotherapy. The fourth model also helps to comprehend the potential impacts of various model parameters of significance that control the therapeutic efficacy of the drug delivery system. Furthermore, the fifth comprehensive model bears the impact on better understanding of the drug release and transport by comprehending the effects of model parameters controlling the pharmacodynamics of liposomal drug delivery. Its significant impact enacts as a basis for obtaining a more effective drug delivery system for cancer therapy. Finally, the concluding mathematical model bridges the gap between the mathematical and physiological systems of drug kinetics more effectively by means of stability analysis. Its impact is also significant in the aspect of studying dynamic stability of the models representing drug release phenomena in pharmacokinetics.

For readers' ease, a comprehensive schematic diagram that connects all different mathematical models described in the dissertation is provided in the next page.

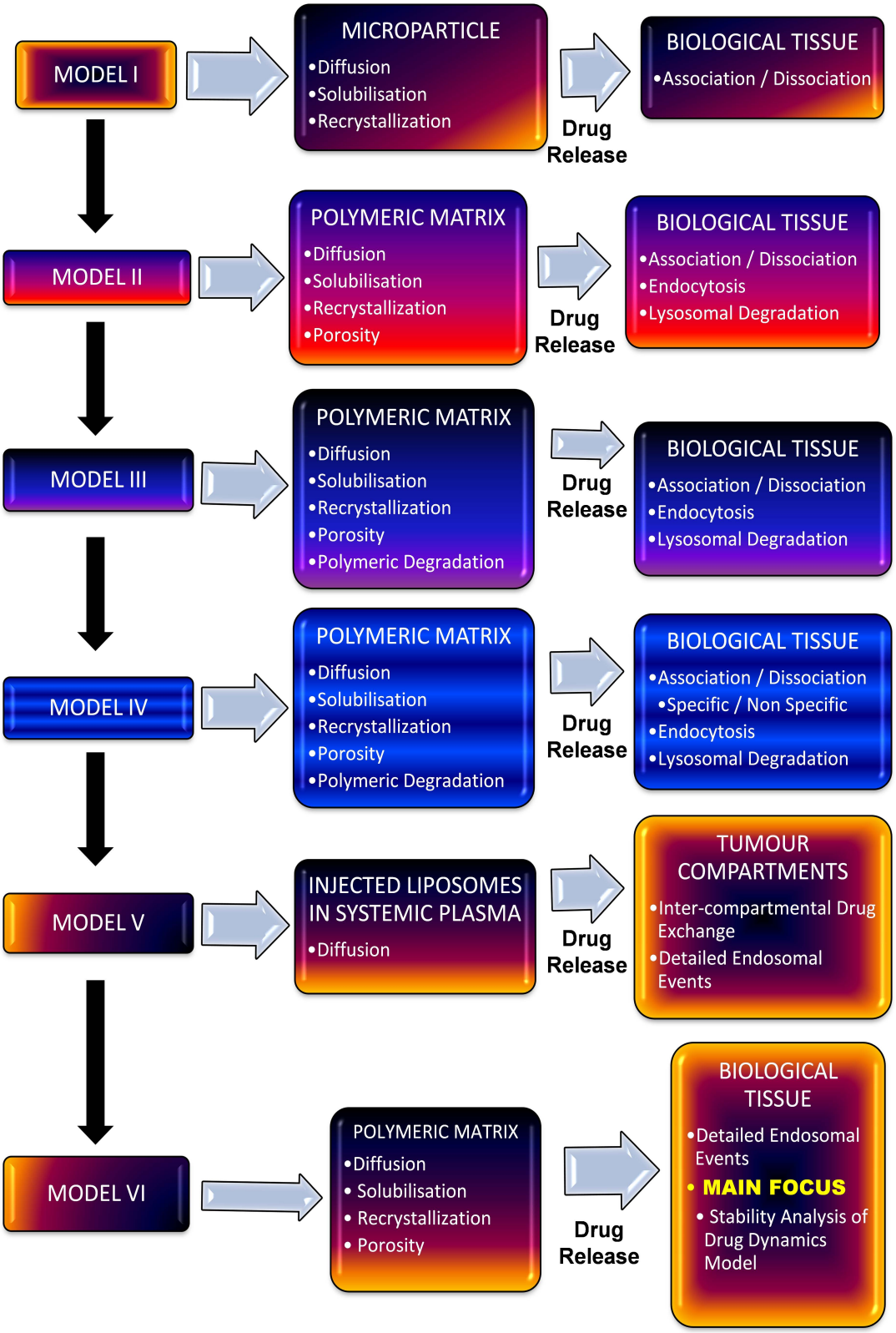

Figure 9.1: Comprehensive schematic diagram connecting all mathematical models

10 FUTURE SCOPE

Prediction is very difficult, especially about the future.

Niels Bohr

New horizons in biomedical research are unlatched due to the availability of unprecedented and rapidly growing amount of data at the molecular, physiological and clinical platforms with respect to *in vitro*, *in vivo* and biomedical investigations. Mathematical modelling as discussed earlier, plays an indispensable role in the generation of predictive hypotheses and in providing significant insights into the mechanism of complex physiological activity due to multi-etiological diseases and corresponding drug action using multilevel data sets.

This dissertation mainly focuses on a combination of mathematical, physiological and pharmacological insight through the process of controlled release drug delivery from a local drug delivery device to the diseased biological tissue. The present thesis manifests the advancement and development of mathematical models from basic to complex and more realistic ones. These investigations can be elaborated and extended in various directions in near future. Some of such possible future directions in this field of research are provided below.

- **Mathematical modelling of probabilistic aspects of receptor-drug interaction**
  Till now it is considered that interaction between drug particles and cell receptors along with other endosomal events are essentially biochemical phenomena, where rate constants symbolising various kinetic events are supposed to be the properties of involved molecular components. Some physical features such as, multivalency of receptors / drugs along with probabilistic effects of binding and other endsomal events also influence the kinetic rate constants. These physical phenomena may be mathematically modelled.

- **Mathematical modelling of signal transduction as a result of drug action**
  Mere interaction of drug particles with cell receptors does not lead to cellular response to drug. Receptors transmit biochemical signals leading to cellular behavioural response. Mathematical modelling of signal transduction would link the cellular response timing, nature and extent with drug dose.

- **Mathematical modelling for treating heterogeneity in the pharmaceutical processes**
  Many physiological reactions and biochemical processes show structural heterogeneity. Moreover, drug particles may have diverse kinetic behaviour depending on their characteristics variation such as variability of chemical composition, molecular weight and hepatic clearance, which may be denoted as functional heterogeneity. Fractals help to understand and describe such structural and functional heterogeneity. Mathematical modelling using fractals would be an interesting task to cope up with biological variabilities.

- **Mathematical modelling of complex pharmacodynamic studies**
  The present dissertation considers " what the body does to the drug", that is, pharmacokinetic study. It is high time to take into account " what the drug does to the body", that is, the pharmacodynamic study which in general deals with drug efficacy and toxicity. Such investigations through mathematical modelling would complement pharmacokinetic investigations for forecasting drug responses in clinical trials.

11 GLOSSARY

Autocatalytic effect: Effect due to the catalytic action of one of the reaction species.

Cardiomyopathy: It refers to the disease of heart muscles.

Endosomal events: An endosome is a membrane-bound compartment inside cells. Endosomal events refer to various processes taking place in the pathway of drugs or molecules internalized from the cell membrane all the way to lysosomes for degradation, or they can be recycled back to the cell membrane. Molecules or drugs transported to endosomes either continue to lysosomes or recycle back.

Endothelial cells: Cells that line the interior surface of blood vessels and lymphatic vessels.

Enhanced permeability and retention (EPR) effect: It is a concept that certain molecules of particular sizes, for example, liposomes and nanoparticles have the tendency to accumulate in tumour tissues in comparison to normal tissues.

Hyperthermia: Elevated body temperature due to the failure of body thermoregulation.

Immunoglobulin: A protein produced by plasma cells and lymphocytes which plays an essential role in the body's immune system. It act as an antibody which is produced in the body in response to and counteracting a specific antigen (a toxin or foreign substance).

Inferior fornix of the conjunctiva: It denotes the loose arching folds which connects the conjunctival membrane lining the inside of the lower eyelid with the conjunctival membrane covering the eyeball.

Interstitium: An interstitial space between tissue or organ.

In vitro: Experimental study using the whole living organism.

In vivo: Technique of conducting a study in the controlled environment, outside of a living organism.

Lumen: Inside of a tubular structure such as artery or intestine.

Lymphatics: They are channels analogous to blood vessels that do not carry blood, but transport tissue fluid (called lymph) in the body.

Lysosomal degradation: It refers to uptake of proteins and internalized drugs by lysosomes. Lysosome is an cell organelle which contains degradative enzymes enclosed in a membrane.

Monomers: Molecules that form the basic units for polymers.

Nasal drug delivery: Drug delivery through the nasal route in order to overcome drug degradation in the gastrointestinal tract as in the case of oral drug administration.

Number-average molecular weight: It is equal to $\frac{\Sigma((W_i)\ (MW)_i)}{\Sigma(X_i)}$, where W_i is the weight fraction of each size fraction of the polymer, X_i is the number of molecules in each size fraction and $(MW)_i$ represents the mean molecular weight of the size fraction.

Oligomers: Compounds in-between a monomer and a polymer having composed of few monomer units.

Ophthalmic matrices: Polymeric matrices used to heal eye related diseases.

Parenteral drug delivery: Drug delivery through injection by subcutaneous, intra-muscular, intravenous and intra-arterial routes.

Pulmonary drug delivery: Drug delivery to the lungs.

Restenosis: It is the recurrence of stenosis, a narrowing of the blood vessel, after corrective surgery leading to restricted blood flow.

Reticuloendothelial system: It is a part of the immune system consisting of mainly liver, spleen, bone marrow and lymph nodes.

Stent: It is a metal or plastic tube implanted into the lumen of an anatomic vessel or duct in order to keep the passage clear for blood flow or other biofluids.

Stratum corneum: It refers to the outermost layer of the skin.

Therapeutic window: Therapeutic window is the dose range that produces therapeutic response without causing any toxic side effects.

Thermal ablation: Damage of body tissues due to extreme hyperthermia (elevated tissue temperature) or hypohermia (depressed tissue temperature).

Transcytosis: It is a type of transcellular transport through which various macromolecules enter into the intracellular domain.

Transdermal drug delivery: Drug delivery through the skin for therapeutic use.

Transmucosal drug delivery: Drug delivery through the mucosal surfaces since mucous membranes lubricates all internal passages and orifices of the living body.

Vasculature: The blood vessels or the arrangement of blood vessels in an organ or part of the body.

Weight-average molecular weight: It is equal to $\frac{\Sigma((W_i)\ (MW)_i)}{\Sigma(W_i)}$, where W_i is the weight fraction of each size fraction of the polymer and $(MW)_i$ represents the mean molecular weight of the size fraction.

12 NOMENCLATURE

Symbols

C_0 : concentration of free drug in the polymeric matrix

C_1 : free drug concentration present in biological tissue (sometimes, particularly specified as plasma and interstitial fluid)

C_{1P} : protein-free drug complex concentration

C_{1i} :concentration of free drug due to dissociation of C_{bi}, that is, internalized free drug

C_{BI}^{TC} : internalized bound drug concentration in tumour cell compartment

C_{BS}^{TC} : cell surface bound drug concentration in tumour cell compartment

C_B^Z, $Z = TP, TIF$: bound drug concentration in tumour plasma and tumour interstitial fluid respectively

C_{FI}^{TC} : internalised free drug concentration in tumour cell compartment

C_F^Y, $Y = S, TP, TIF$: free drug concentration in systemic plasma, tumour plasma and tumour interstitial fluid respectively

C_L : concentration of solid drug in the polymeric matrix

C_L^X, $X = S, TP, TIF$: liposome-encapsulated drug concentration in systemic plasma, tumour plasma and tumour interstitial fluid respectively

C_M : concentration of monomers

C_P^W, $W = TP, TIF$: protein concentration in tumour plasma and tumour interstitial fluid respectively

C_{b1} : concentration of available binding sites on extracellular matrix (ECM)

C_{b2} :concentration of available specific binding receptors (SR)

C_{bi} : concentration of internalized C_{bs}, that is, internalized bound drug

C_{bs} : concentration of free drug-surface receptor complex, that is, cell surface bound drug

C_i : concentration of oligomers, i depicts the length of the oligomer

C_{int} : concentration of internalized drug particles

C_{lim} : drug solubilisation limit

C_n : concentration of polymers, n depicts the length of the polymer

D_0 : diffusion coefficient of free drug in the polymeric matrix

D_1 : diffusion coefficient of free drug in the biological tissue

$D_I^J,\ I = L,F,B\ \&\ J = S,TIF,TP$: diffusion coefficients of liposomal, free and bound drug in systemic plasma, tumour interstitial fluid and tumour plasma respectively

D_M : effective diffusivity of monomers

D_i : effective diffusivity of oligomers

D_l : diffusivity in liquid-filled pores

D_s : diffusivity in the polymer phase

D_{s0} : initial diffusivity of the solid polymeric phase

K_{cl} : tissue-capillary clearance per unit area

K_v : hydraulic conductivity of the wall of blood vessels

M : initial solid drug concentration

M_w : average molecular weight of the polymer

P : concentration of plasma proteins

P_0 : initial concentration of proteins

$P_i, i = 1-4$: mass transfer coefficient

$P_k,\ k = l, fe, be$: denotes the vasculature wall permeability to liposomes, free drug particles and bound drug particles respectively

$Pe_m,\ m = l, f, b$: transcapillary Péclet numbers

R_I^{TC} : internalized receptor concentration in tumour cell compartment

R_S^{TC} : cell surface receptor concentration in tumour cell compartment

R_i : concentration of internalized receptors

R_{i0} : initial concentration of internalized receptors

R_s : concentration of receptors at the cell surface

R_{s0} : initial concentration of cell surface receptors

S/V : blood vessels' surface area per unit volume of tumour tissue

$X_{n,0}$: initial number average degree of polymerization

b_1 : concentration of drug bound to ECM sites

b_2 : concentration of drug bound to specific binding receptors

k : partition coefficient

k_{+1} : association rate constant

k_{-1} : dissociation rate constant

k_1 : drug release rate constant from liposomes at the systemic plasma

k_1^f : association rate constant

k_1^r : dissociation rate constant

k_2^f : association rate constant

k_2^r : dissociation rate constant

k_a : association rate constant

k_{cl}^F : clearance rate constant of free drug in the systemic plasma

k_{cl}^L : clearance rate constant of liposomal drug in the systemic plasma

k_d : dissociation rate constant

k_{dd} : degradation rate constant corresponding to number-average molecular weight change

k_e : internalization / endocytosis rate constant

k_f : association rate constant

$k_f^{'}$: association rate constant

k_{hl} : lysosomal degradation rate constant

k_{hr} : lysosomal degradation rate constant

k_i : internalization rate coefficient

k_{i1} : internalization rate constant for b_1

k_{i2} : internalization rate constant for b_2

k_{id} : degradation rate constant in the lysosome

k_m : mass transfer coefficient

k_n : rate of dissolution

k_r : dissociation rate constant

$k_r^{'}$: dissociation rate constant

k_{rel} : drug release rate constant from liposomes in the tumour compartment

k_{syn} : receptor synthesis rate

k_t : constitutive internalization rate constant

k_x : receptor recycling rate constant

ke_1 : plasma clearance rate

l_0 : length of the polymeric matrix

p_i : pressure of interstitial fluid

p_v : pressure of blood vessels

v^{TP} : volume fraction of tumour plasma

x_p : horizontal coating thickness

Greek Letters

ϕ : porosity

ε: porosity of the biological tissue

τ : tortuosity of its pore path in the biological

δ_0 : association rate constant

β_0 : dissociation rate constant

ε_0 : polymeric matrix porosity

Φ_0 : ratio of accessible void volume to solid volume

α_0 : solid-liquid mass transfer coefficient

ϕ_i : initial porosity

π_i : osmotic pressure of interstitial fluid

$\sigma_j,\ j = T,d,l$: average osmotic reflection coefficients for plasma proteins, free / bound drug particles and liposomal drug particles respectively

$\gamma_p,\ p = 1-6$: magnitudes of advection

π_v : osmotic pressure of plasma

Abbreviations

CARS: Coherent anti-Stokes Raman scattering

DNA: Deoxyribonucleic acid

DOX: Doxorubicin – An anti-cancer drug

ECM: Extracellular matrix

EPR: Enhanced permeability and retention

FDA: Food and drug administration

HIFU: High intensity focused ultrasound

HPLC: High performance liquid chromatography

HPMC: Hydroxypropyl methylcellulose

PLGA: Poly (lactide-co-glycolide)

BIBLIOGRAPHY

[1] A. W. ADAMSON AND A. P. GAST, *Physical chemistry of surfaces*, Wiley-Interscience: New York, Chichester, Weinheim, Brisbane, Singapore, Toronto, chapter X (1997).

[2] A. A. AIMETTI, A. J. MACHEN, AND K. S. ANSETH, *Poly (ethylene glycol) hydrogels formed by thiol-ene photopolymerization for enzyme-responsive protein delivery*, Biomaterials, 30 (2009), pp. 6048 – 6054.

[3] A. ARGEMÍ, J. L. ELLIS, J. SAURINA, AND D. L. TOMASKO, *Development of a polymeric patch impregnated with naproxen as a model of transdermal sustained release system*, J Pharm Sci, 100 (2011), pp. 992 – 1000.

[4] C. E. ASTETE AND C. M. SABLIOV, *Synthesis and characterization of PLGA nanoparticles*, J Biomater Sci Polym Ed, 17 (2006), pp. 247– 289.

[5] R. AVTAR AND D. TANDON, *Modeling the drug transport in the anterior segment of the eye*, Euro J Pharm Sci, 35 (2008), pp. 175 – 182.

[6] A. L. BABA AND C. CÂTOI, *Comparative oncology*, Bucharest: The Publishing House of the Romanian Academy (2007).

[7] R. P. BATYCKY, J. HANES, R. LANGER, AND D. A. EDWARDS, *A theoretical model of erosion and macromolecular drug release from biodegrading microspheres*, J Pharm Sci, 86 (12) (1997), pp. 1464 – 1477.

[8] L. BAXTER AND R. JAIN, *Transport of fluid and macromolecules in tumors. I. role of interstitial pressure and convection*, Microvas Research, 37 (1) (1989), pp. 77 – 104.

[9] L. BAXTER AND R. JAIN, *Transport of fluid and macromolecules in tumors. II. role of heterogeneous perfusion and lymphatics*, Microvas Research, 40 (2) (1990), pp. 246 – 263.

[10] ——, *Transport of fluid and macromolecules in tumors. III. role of binding and metabolism*, Microvas Research, 41 (1) (1991), pp. 5 – 23.

[11] S. BECKER AND A. KUZNETSOV, *Transport in biological media*, Academic Press, Elsevier (2013).

[12] G. BONACUCINA, M. CESPI, AND G. F. PALMIERI, *Evaluation of dissolution kinetics of hydrophilic polymers by use of acoustic spectroscopy*, Int J Pharm, 377 (2009), pp. 153 – 158.

[13] N. I. BORDER AND P. E. BUCHWALD, *Ophthalmic drug design based on the metabolic activity of the eye: soft drugs and chemical delivery systems*, AAPS Journal, 7 (2005), pp. 820 – 833.

[14] B. V. D. BOSSCHE AND C. V. DE WIELE, *Receptor imaging in oncology by means of nuclear medicine: current status*, J Clin Oncol, 22 (2004), pp. 3593 – 3607.

[15] Y. BOUCHER AND R. JAIN, *Microvascular pressure is the principal driving force for interstitial hypertension in solid tumors: implications for vascular collapse*, Cancer Research, 52 (18) (1992), pp. 5110 – 5114.

[16] F. BOZSAK, J. M. CHOMAZ, AND A. I. BARAKAT, *Modeling the transport of drugs eluted from stents: physical phenomena driving drug distribution in the arterial wall*, Biomech Model Mechanobiol, 13 (2014), pp. 327–347.

[17] M. S. BRETCHER, *Fibroblasts on the move*, J Cell Biology, 106 (1988), pp. 235 – 237.

[18] T. CASALINI, F. ROSSI, S. LAZZARI, G. PERALE, AND M. MASI, *Mathematical modeling of PLGA microparticles: from polymer degradation to drug release*, Mol Pharmaceutics, 11 (2014), pp. 4036 – 4048.

[19] J. J. CASTELLOT, K. WONG, B. HERMAN, R. L. HOOVER, D. F. ALBERTINI, T. C. WRIGHT, B. L. CALEB, AND M. J. KARNOVSKY, *Binding and internalization of heparin by vascular smooth muscle cells*, J Cell Physiol, 124 (1) (1985), pp. 13 – 20.

[20] A. CHARLIER, B. LECLERC, AND G. COUARRAZE, *Release of mifepristone from biodegradable matrices: experimental and theoretical evaluations*, Int J Pharm, 200 (2000), pp. 115 –120.

[21] D. S. COHEN AND T. ERNEUX, *Free boundary problems in controlled release pharmaceuticals. I: Diffusion in glassy polymers*, SIAM J Appl Math, 48 (1988), pp. 1451 – 1465.

[22] ——, *Free boundary problems in controlled release pharmaceuticals. II: Swelling-controlled release*, SIAM J Appl Math, 48 (1988), pp. 1466 – 1474.

[23] P. COLOMBO, R. BETTINI, P. L. CATELLANI, P. SANTI, AND N. A. PEPPAS, *Drug volume fraction profile in the gel phase and drug release kinetics in hydroxypropylmethyl cellulose matrices containing a soluble drug*, Euro J Pharm Sci, 9 (1999), pp. 33 – 40.

[24] B. M. O. CONNELL AND M. T. WALSH, *Demonstrating the influence of compression on artery wall mass transport*, Ann Biomed Eng, 38 (4) (2010), pp. 1354 – 1366.

[25] U. CONTE, P. COLOMBO, A. GAZZANIGA, M. E. SANGALLI, AND A. L. MANNA, *Swelling-activated drug delivery systems*, Biomaterials, 9 (6) (1988), pp. 489 – 493.

[26] U. CONTE, L. MAGGI, AND A. L. MANNA, *Compressed barrier layers for constant drug release from swellable matrix tablets*, S T P Pharma Sci, 4 (1994), pp. 107 – 113.

[27] M. A. COSTA AND D. I. SIMON, *Molecular basis of restenosis and drug-eluting stents*, Circulation, 111 (2005), pp. 2257 – 2273.

[28] M. CRANE, N. HURLEY, L. CRANE, A. M. HEALY, O. I. CORRIGAN, K. GALLAGHER, AND L. G. MCCARTHY, *Simulation of the USP drug delivery problem using CFD: experimental, numerical and mathematical aspects*, Simul Model Pract & Theory, 12 (2) (2004), pp. 147 – 158.

[29] J. CRANK, *The mathematics of diffusion*, Clarendon Press: Oxford, second edition (1975).

[30] W. M. DEEN, *Hindered transport of large molecules in liquid-filled pores*, AIChE J, 33 (9) (1987), pp. 1409 – 1425.

[31] J. DENEKAMP, *Angiogenesis, neovascular proliferation and vascular pathophysiology as targets for cancer therapy*, Br J Radiol, 66 (1993), pp. 181 – 196.

[32] J. F. DEUX, A. MEDDAHI-PELLE, A. F. L. BLANCHE, L. J. FELDMAN, S. C. JOUAULT, F. BREE, F. BOUDGHÉNE, J. B. MICHEL, AND D. LETOURNEUR, *Low molecular weight fucoidan prevents neointimal hyperplasia in rabbit iliac artery in-stent restenosis mode*, Arterioscler Thromb Vasc Biol, 22 (10) (2002), pp. 1604 – 1609.

[33] R. DORATI, I. GENTA, C. COLONNA, T. MODENA, F. PAVANETTO, P. PERUGINI, AND B. CONTI, *Investigation of the degradation behavior of poly (ethylene glycol-co-d,l-lactide) copolymer*, Polym Degradation Stability, 92 (2007), pp. 1660 – 1668.

[34] S. EIKENBERRY, *A tumor cord model for doxorubicin delivery and dose optimization in solid tumors*, Theor Biol Med Model, 6 (1) (2009), p. article 16.

[35] N. FAISANT, J. SIEPMANN, AND J. P. BENOIT, *PLGA-based microparticles: elucidation of mechanisms and a new, simple mathematical model quantifying drug release*, Eur J Pharm Sci, 15 (4) (2002), pp. 355 – 366.

[36] G. M. FERRON, W. D. CONWAY, AND W. J. JUSKO, *Lipophilic benzamide and anilide derivatives as high-performance liquid chromatography internal standards: application to sirolimus (rapamycin) determination*, J Chromatogr B: Biomed Sci Appl, 703 (1âĂŞ2) (1997), pp. 243 – 251.

[37] A. FINKELSTEIN, D. MCCLEAN, S. KAR, K. TAKIZAWA, K. VARGHESE, N. BAEK, K. PARK, M. C. FISHBEIN, R. MAKKAR, F. LITVACK, AND N. L. EIGLER, *Local drug delivery via a coronary stent with programmable release pharmacokinetics*, Circulation, 107 (2003), pp. 777 – 784.

[38] L. FORMAGGIA, S. MINISINI, AND P. ZUNINO, *Modeling polymeric controlled drug release and transport phenomena in the arterial tissue*, Math Models Methods Appl Sci, 20 (10) (2010), pp. 1759 – 1786.

[39] H. F. FRASCH AND A. M. BARBERO, *Application of numerical methods for diffusion based modeling of skin permeation*, Adv Drug Deliv Rev, 65 (2) (2013), pp. 208 – 220.

[40] S. FREDENBERG, M. WAHLGREN, M. RESLOW, AND A. AXELSSON, *The mechanisms of drug release in poly (lactic-co-glycolic acid)-based drug delivery systems – a review*, Int J Pharm, 415 (2011), pp. 34 – 52.

[41] A. FRENCH, D. TADAKI, S. NIYOGI, AND D. LAUFFENBURGER, *Intracellular trafficking of epidermal growth factor family ligands is directly influenced by the pH sensitivity of the receptor / ligand interaction*, J Biol Chem, 270 (1995), pp. 4334 – 4340.

[42] G. FRENNING, *Theoretical investigation of drug release from planar matrix systems: effects of a finite dissolution rate*, J Control Release, 92 (2003), pp. 331 – 339.

[43] J. C. FU, C. HAGEMEIR, D. L. MOYER, AND E. NG, *A unified mathematical model for diffusion from drug-polymer composite tablets*, J Biomed Mater Res, 10 (1976), pp. 743 – 758.

[44] M. H. GABER, K. HONG, S. K. HUANG, AND D. PAPAHADJOPOULOS, *Thermosensitive sterically stabilized liposomes: formulation and in vitro studies on mechanism of doxorubicin release by bovine serum and human plasma*, Pharm Res, 12 (10) (1995), pp. 1407 – 1416.

[45] A. GASSELHUBER, M. DREHER, A. NEGUSSIE, B. WOOD, F. RATTAY, AND D. HAEMMERICH, *Mathematical spatio-temporal model of drug delivery from low temperature sensitive liposomes during radiofrequency tumour ablation*, Int J Hyperth, 26 (5) (2010), pp. 499 – 513.

[46] A. GASSELHUBER, M. DREHER, A. PARTANEN, P. YARMOLENKO, D. WOODS, B. WOOD, AND D. HAEMMERICH, *Targeted drug delivery by high intensity focused ultrasound mediated hyperthermia combined with temperature-sensitive liposomes: computational modelling and preliminary in vivo validation*, Int J Hyperth, 28 (4) (2012), pp. 337 – 348.

[47] Y. M. F. GOH, H. L. KONG, AND C. H. WANG, *Simulation of the delivery of doxorubicin to hepatoma*, Pharm Research, 18 (6) (2001), pp. 761 – 770.

[48] S. GOODMAN, A. GILMAN, L. BRUNTON, J. LAZO, AND K. PARKER, *Goodman & Gilman's the pharmacological basis of therapeutics*, McGraw-Hill, New York (2005).

[49] T. T. GOODMAN, J. CHEN, K. MATVEEV, AND S. H. PUN, *Spatio-temporal modeling of nanoparticle delivery to multicellular tumor spheroids*, Biotechnol Bioeng, 101 (2) (2008), pp. 388 – 399.

[50] A. GÖPFERICH, *Mechanisms of polymer degradation and erosion*, Biomaterials, 17 (1996), pp. 103 – 114.

[51] M. GRASSI, I. COLOMBO, AND R. LAPASIN, *Drug release from an ensemble of swellable crosslinked polymer particles*, J Control Release, 68 (2000), pp. 97 – 113.

[52] M. GRASSI, G. GRASSI, R. LAPASIN, AND I. COLOMBO, *Understanding drug release and absorption mechanisms: a physical and mathematical approach*, CRC Press, Boca Raton, FL (2008).

[53] M. GRASSI, R. LAPASIN, AND S. PRICL, *Modeling of drug release from a swellable matrix*, Chem Eng Comm, 169 (1998), pp. 79 – 109.

[54] D. HANAHAN AND R. A. WEINBERG, *The hallmarks of cancer*, Cell, 100 (2000), pp. 57 – 70.

[55] H. HARA, M. NAKAMURA, J. C. PALMAZ, AND R. S. SCHWARTZ, *Role of stent design and coatings on restenosis and thrombosis*, Adv Drug Deliv Rev, 58 (2006), pp. 377 – 386.

[56] H. HARASHIMA, M. TSUCHIHASHI, S. IIDA, H. DOI, AND H. KIWADA, *Pharmacokinetic / pharmacodynamic modeling of antitumor agents encapsulated into liposomes*, Adv Drug Deliv Rev, 40 (1-2) (1999), pp. 39 – 61.

[57] J. HELLER, *Controlled release of biologically active compounds from bioerodible polymers*, Biomaterials, 1 (1980), pp. 51 – 57.

[58] B. HENDRIKS, J. REYNOLDS, S. KLINZ, E. GERETTI, H. LEE, S. LEONARD, D. GADDY, C. ESPELIN, U. NIELSEN, AND T. WICKHAM, *Multiscale kinetic modeling of liposomal doxorubicin delivery quantifies the role of tumor and drug-specific parameters in local delivery to tumors*, CPT: Pharmacomet Syst Pharmacol, 1 (2012), p. e15.

[59] R. I. HICKSON, S. I. BARRY, G. N. MERCEER, AND H. S. SIDHU, *Finite differences schemes for multi-layer diffusion*, Math Comput Model, 54 (2011), pp. 210 – 220.

[60] T. HIGUCHI, *Rate of release of medicaments from ointment bases containing drugs in suspensions*, J Pharm Sci, 50 (1961), pp. 874 – 875.

[61] ——, *Mechanisms of sustained action mediation. theoretical analysis of rate of release of solid drugs dispersed in solid matrices*, J Pharm Sci, 52 (1963), pp. 1145 – 1149.

[62] A. W. HIXSON AND J. H. CROWELL, *Dependence of reaction velocity upon surface and agitation*, Ind Eng Chem, 23 (1931), pp. 923 – 931.

[63] M. HOSSANN, T. WANG, M. WIGGENHORN, R. SCHMIDT, A. ZENGERLE, G. WINTER, H. EIBL, M. PELLER, M. REISER, R. ISSELS, AND L. H. LINDNER., *Size of thermosensitive liposomes influences content release*, J Control Release, 147 (2010), pp. 436 – 443.

[64] E. HULME, *Receptor-ligand interactions: a practical approach*, Oxford: IRL Press (1992).

[65] K. K. JAIN, *Gene therapy: technologies, markets and companies*, Jain PharmaBiotech Publications, Basel (2014), pp. 1 – 665.

[66] R. JAIN, *Transport of molecules in the tumour interstitium: a review*, Cancer Research, 47 (12) (1987), pp. 3039 – 3051.

[67] S. JANG, M. WIENTJES, D. LU, AND J. AU, *Drug delivery and transport to solid tumours*, Pharm Res, 20 (9) (2003), pp. 1337 – 1350.

[68] R. T. C. JU, P. R. NIXON, AND M. V. PATEL, *Drug release from hydrophilic matrices. 1. new scaling laws for predicting polymer and drug release based on the polymer disentanglement concentration and the diffusion layer*, J Pharm Sci, 84 (1995), pp. 1455 – 1463.

[69] ——, *Diffusion coefficients of polymer chains in the diffusion layer adjacent to a swollen hydrophilic matrix*, J Pharm Sci, 86 (1997), pp. 1293 – 1298.

[70] R. T. C. JU, P. R. NIXON, M. V. PATEL, AND D. TONG, *Drug release from hydrophilic matrices. 1. a mathematical model based on the polymer disentanglement concentration and the diffusion layer*, J Pharm Sci, 84 (1995), pp. 1464 – 1477.

[71] Y. KAKIZAWA, R. NISHIO, T. HIRANO, Y. KOSHI, M. NUKIWA, M. KOIWA, J. MICHIZOE, AND N. IDA, *Controlled release of protein drugs from newly developed amphiphilic polymer-based microparticles composed of nanoparticles*, J Control Release, 142 (2010), pp. 8 – 13.

[72] E. KANG, J. ROBINSON, K. PARK, AND J. X. CHENG, *Paclitaxel distribution in poly (ethylene glycol) / poly (lactide-co-glycolic acid) blends and its release visualized by coherent anti-Stokes raman scattering microscopy*, J Control Release, 122 (3) (2007), pp. 261 – 268.

[73] S. KARLSSON AND A. C. ALBERTSSON, *Techniques and mechanisms of polymer degradation.*, Degradable polymers: principles and applications. London: Chapman & Hall (1995).

[74] J. L. KATZ, C. G. AMBROSE, C. MCMILLIN, AND P. SPENCER, *Orthopedic biomaterials*, Encyclopedia of biomaterials and biomedical engineering, New York: Marcel Dekker (2004).

[75] S. W. KIM, J. H. KIM, O. JEON, I. C. KWON, AND K. PARK, *Engineered polymers for advanced drug delivery*, Eur J Pharm Biopharm, 71 (2009), pp. 420 – 430.

[76] D. KLOSE, F. SIEPMANN, K. ELKHARRAZ, AND J. SIEPMANN, *PLGA-based drug delivery systems: importance of the type of drug and device geometry*, Int J Pharm, 354 (2008), pp. 95 –103.

[77] B. C. KUENEN, L. ROSEN, E. F. SMIT, M. R. N. PARSON, M. LEVI, R. RUIJTER, H. HUISMAN, M. A. KEDDE, P. NOORDHUIS, W. J. F. VAN DER VIJGH, G. J. PETERS, G. F. CROPP, P. SCIGALLA, K. HOEKMAN, H. M. PINEDO, AND G. GIACCONE, *Dose-finding and pharmacokinetic study of cisplatin, gemcitabine, and SU5416 in patients with solid tumors*, J Clin Onco, 20 (6) (2002), pp. 1657 – 1667.

[78] R. LANGER, *New methods of drug delivery*, Science, 249 (1990), pp. 1527–1533.

[79] D. A. LAUFFENBURGER AND J. J. LINDERMAN, *Receptors: models for binding, trafficking and signalling*, Oxford University Press, New York (1993).

[80] P. I. LEE, *Controlled release systems: fabrication technology*, D. Hsieh, ed.; CRC Press: Boca Raton II (1987), p. 61.

[81] D. D. LEWIS, *Controlled release of bioactive agents from lactide / glycolide polymers*, Biodegradable polymers as drug delivery systems. New York: Marcel Dekker (1990).

[82] L. LI, L. M. T. TEN HAGEN, D. SCHIPPER, T. M. WIJNBERG, G. C. VAN RHOON, A. M. M. EGGERMONT, L. H. LINDNER, AND G. A. KONING, *Triggered content release from optimized stealth thermosensitive liposomes using mild hyperthermia*, J Control Release, 143 (2) (2010), pp. 274 – 279.

[83] X. LI AND J. X. XU, *A mathematical prognosis model for pancreatic cancer patients receiving immunotherapy*, J Theor Biol, 406 (2016), pp. 42 – 51.

[84] L. E. LIMBIRD, *Cell surface receptors: a short course on theory and methods*, Boston: Martinus Nijhoff Publishing (1986).

[85] W. D. LINDNER, J. E. MOCKEL, AND B. C. LIPPOLD, *Controlled release of drugs from hydrocolloid embeddings*, Pharmazie, 51 (1996), pp. 263 – 272.

[86] C. LIU AND X. XU, *A systematic study of temperature sensitive liposomal delivery of doxorubicin using a mathematical model*, Comp Biol Med, 60 (2015), pp. 107 – 116.

[87] X. LIU, P. KRUGER, H. MAIBACH, P. COLDITZ, AND M. ROBERTS, *Using skin for drug delivery and diagnosis in the critically ill*, Adv Drug Deliv Rev, 77 (2014), pp. 40–49.

[88] W. J. M. LOKERSE, E. C. KNEEPKENS, T. L. TEN HAGEN, A. EGGERMONT, H. GRULL, AND G. A. KONING, *In depth study on thermosensitive liposomes: optimizing formulations for tumor specific therapy and in vitro to in vivo relations*, Biomaterials, 82 (2016), pp. 138 – 150.

[89] Y. LOUZOUN, C. XUE, G. B. LESINSKI, AND A. FRIEDMAN, *A mathematical model for pancreatic cancer growth and treatments*, J Theor Biol, 351 (2014), pp. 74 – 82.

[90] X. LU, J. YANG, J. B. ZHAO, H. GREGERSEN, AND G. S. KESSAB, *Shear modulus of porcine coronary artery: contributions of media and adventia*, Am J Physiol Heart Circ Physiol, 285 (2003), pp. H1966 – H1975.

[91] W. H. MAISEL, *Unanswered questions — drug-eluting stents and the risk of late thrombosis*, New Eng J Med, 356 (2007), pp. 981 – 984.

[92] Y. MALAM, M. LOIZIDOU, AND A. SEIFALIAN, *Liposomes and nanoparticles: nanosized vehicles for drug delivery in cancer*, Trends Pharmacol Sci, 30 (11) (2009), pp. 592 – 599.

[93] R. MANITZ, W. LUCHT, K. STREHMEL, R. WEINER, AND R. NEUBERT, *On mathematical modeling of dermal and transdermal drug delivery*, J Pharm Sci, 87 (1998), pp. 873 – 879.

[94] C. MANOHARAN AND J. SINGH, *Evaluation of polyanhydride microspheres for basal insulin delivery: effect of copolymer composition and zinc salt on encapsulation, in vitro release, stability, in vivo absorption and bioactivity in diabetic rats*, J Pharm Sci, 98 (2009), pp. 4237 – 4250.

[95] F. R. MAXFIELD, J. SCHLESSINGER, Y. SHECHTER, I. PASTAN, AND M. C. WILLINGHAM, *Collection of insulin, EGF and alpha2-macroglobulin in the same patches on the surface of cultured fibroblasts and common internalization*, Cell, 14 (1978), pp. 805 – 810.

[96] S. MCGINTY AND G. PONTRELLI, *On the influence of solid - liquid mass transfer in the modelling of drug release from stents*, J Coupled Syst Multiscale Dyn, 3 (1) (2015), pp. 47 – 56.

[97] B. A. MILLER-CHOU AND J. L. KOENING, *A review of polymer dissolution*, Prog Polym Sci, 28 (2003), pp. 1223 –1270.

[98] S. MUKHERJEE, R. GHOSH, AND F. MAXFIELD, *Endocytosis*, Physiol Rev, 77 (1997), pp. 759 – 803.

[99] B. NARASIMHAN, *Mathematical models describing polymer dissolution: consequences for drug delivery*, Adv Drug Deliv Rev, 48 (2001), pp. 195 – 210.

[100] D. NEEDHAM, J. PARK, A. WRIGHT, AND J. TONG, *Materials characterization of the low temperature sensitive liposome (LTSL): effects of lipid composition (lysolipid and DSPE-PEG2000) on the thermal transition and release of doxorubicin*, Faraday Discuss, 161 (2013), pp. 515 – 534.

[101] A. NOYES AND W. WHITNEY, *The rate solution of solid substances in their own solutions*, J Am Chem Soc, 19 (1897), pp. 930 – 934.

[102] A. PADALKAR, S. SHAHI, AND M. THUBE, *Microparticles: an approach for the betterment of drug delivery system*, Int J Pharma Reseach & Develop, 3 (1) (2011), pp. 99 – 115.

[103] C. J. PAN, J. J. TANG, Y. J. WENG, J. WANG, AND N. HUANG, *Preparation and in vitro release profiles of drug-eluting controlled biodegradable polymer coating stents*, Colloids Surf B: Biointerfaces, 73 (2009), pp. 199 – 206.

[104] E. S. PARK, M. MANIAR, AND J. C. SHAH, *Biodegradable polyanhydride devices of cefazolin sodium, bupivacaine, and taxol for local drug delivery: preparation, and kinetics and mechanism of in vitro release*, J Control Release, 52 (1998), pp. 179 – 189.

[105] K. PARK, W. S. W. SHALABY, AND H. PARK, *Biodegradable hydrogels for drug delivery*, Technomic publishing company, Lancaster (1993), p. 189.

[106] L. A. PELETIER, N. BENSON, AND P. H. GRAAF, *Impact of plasma-protein binding on receptor occupancy: an analytical description*, J Theor Biol, 256 (2009), pp. 253 – 262.

[107] L. A. PELETIER, N. BENSON, AND P. H. VANDER GRAAF, *Impact of protein binding on receptor occupancy: a two-compartment model*, J Theor Biol, 265 (2010), pp. 657 – 671.

[108] N. A. PEPPAS, *Analysis of fickian and non-fickian drug release from polymers*, Pharm Acta Helv, 60 (1985), pp. 110 – 111.

[109] N. A. PEPPAS, R. GURNY, E. DOELKER, AND P. BURI, *Modelling of drug diffusion through swellable polymeric systems*, J Membr Sci, 7 (1980), pp. 241 – 253.

[110] N. A. PEPPAS AND R. W. KORSMEYER, *Dynamically swelling hydrogels in controlled release applications*, Hydrogels in Medicine and Pharmacy, Vol. 3, CRC Press, Boca Raton (1986), pp. 109–136.

[111] N. A. PEPPAS AND C. T. REINHART, *Solute diffusion in swollen membranes. part I. a new theory*, J Mem Sci, 15 (1983), pp. 275 – 287.

[112] O. PILLAI AND R. PANCHAGNULA, *Polymers in drug delivery*, Curr Opin Chem Biol, 5 (2001), pp. 447– 451.

[113] G. PONTRELLI AND F. MONTE, *A two-layer model for transdermal drug delivery and percutaneous absoption*, Math Biosci, 257 (2014), pp. 96 – 103.

[114] M. R. PRAUSNITZ AND R. LANGER, *Transdermal drug delivery*, Nat Biotech, 26 (2008), pp. 1261 – 1268.

[115] S. A. QURESHI, *In Vitro-In Vivo correlation (IVIVC) and determining drug concentrations in blood from dissolution testing âĂŞ a simple and practical approach*, The Open Drug Deliv J, 4 (2010), pp. 38 – 47.

[116] C. RAMAN, C. BERKLAND, K. KIM, AND D. W. PACK, *Modeling small-molecule release from plg microspheres: effects of polymer degradation and nonuniform drug distribution*, J Control Release, 103 (1) (2005), pp. 149 – 158.

[117] C. RATTANAKUL AND Y. LENBURY, *Stability analysis and analytical solution of a nonlinear model for controlled drug release: travelling wave fronts*, Int J Math Comp Simul, 6 (3) (2012), pp. 351 – 359.

[118] C. T. REINHART AND N. A. PEPPAS, *Solute diffusion in swollen membranes. part II. influence of crosslinking on diffusive properties*, J Mem Sci, 18 (1984), pp. 227 – 239.

[119] J. E. RIM, P. M. PINSKY, AND W. W. VAN OSDOL, *Multiscale modeling framework of transdermal drug delivery*, Ann Biomed Eng, 37 (2009), pp. 1217 – 1229.

[120] S. N. ROTHSTEIN, W. J. FEDERSPIEL, AND S. R. A. LITTLE, *A unified mathematical model for the prediction of controlled release from surface and bulk eroding polymer matrices*, Biomaterials, 30 (8) (2009), pp. 1657 – 1664.

[121] C. SACKETT AND B. NARASIMHAN, *Mathematical modeling of polymer erosion: consequences for drug delivery*, Int J Pharmaceut, 418 (2011), pp. 104 – 114.

[122] D. K. SAHANA, G. MITTAL, V. BHARDWAJ, AND M. N. V. R. KUMAR, *PLGA nanoparticles for oral delivery of hydrophobic drugs: influence of organic solvent on nanoparticle formation and release behavior in vitro and in vivo using estradiol as a model drug*, J Pharm Sci, 97 (2008), pp. 1530 – 1542.

[123] M. S. SALAHUDEEN AND P. S. NISHTALA, *An overview of pharmacodynamic modelling, ligand-binding approach and its application in clinical practice*, Saudi Pharm J, 25 (2) (2017), pp. 165 – 175.

[124] E. SALTIEL AND W. MCGUIRE, *Doxorubicin (Adriamycin) cardiomyopathy. A critical review*, West J Med, 139 (3) (1983), pp. 332 – 341.

[125] W. M. SALTZMAN, *Drug delivery: engineerig principles for drug therapy*, Oxford University Press (2001).

[126] W. M. SALTZMAN AND M. L. RADOMSKY, *Drugs released from polymers: diffusion and elimination in brain tissue*, Chem Eng Sci, 46 (10) (1991), pp. 2429 – 2444.

[127] J. SIEPMANN, K. ELKHARRAZ, F. SIEPMANN, AND D. KLOSE, *How autocatalysis accelerates drug release from PLGA-based microparticles: a quantitative treatment*, Biomacromolecules, 6 (2005), pp. 2312 – 2319.

[128] J. SIEPMANN, N. FAISANT, AND J. BENOIT, *A new mathematical model quantifying drug release from bioerodible microparticles using monte carlo simulations*, Pharm Res, 19 (12) (2002), pp. 1885 – 1893.

[129] J. SIEPMANN AND A. GÖPFERICH, *Mathematical modeling of bioerodible, polymeric drug delivery systems*, Adv Drug Deliv Rev, 48 (2001), pp. 229 – 247.

[130] J. SIEPMANN AND N. A. PEPPAS, *Hydrophilic matrices for controlled drug delivery: an improved mathematical model to predict the resulting drug release kinetics (the âĂŸsequential layerâĂŹ model)*, Pharm Res, 17 (2000), pp. 1290 – 1298.

[131] ——, *Modeling of drug release from delivery systems based on hydroxypropyl methylcellulose (HPMC)*, Adv Drug Deliv Rev, 48 (2001), pp. 139 – 157.

[132] J. SIEPMANN AND F. SIEPMANN, *Mathematical modeling of drug delivery*, Int J Pharm, 364 (2) (2008), pp. 328 – 243.

[133] P. K. SINGAL AND N. ILISKOVIC, *Doxorubicin-induced cardiomyopathy*, The New Eng J Med, 339 (13) (1998), pp. 900 – 905.

[134] L. SINGH, V. KUMAR, AND B. D. RATNER, *Generation of porous microcellular 85 / 15 poly (dl-lactide-co-glycolide) foams for biomedical applications*, Biomaterials, 25 (2004), pp. 2611–2617.

[135] M. P. SINGH, J. A. LUMPKIN, AND J. ROSENBLATT, *Mathematical modeling of drug release from hydrogel matrices via a diffusion coupled with desorption mechanism*, J Control Release, 32 (1994), pp. 17 – 25.

[136] ——, *Effect of electrostatic interactions on polylysine release rates from collagen matrices and comparison with model predictions*, J Control Release, 35 (1995), pp. 165 – 179.

[137] M. P. SINGH, J. STEFKO, J. A. LUMPKIN, AND J. ROSENBLATT, *The effect of electrostatic charge interactions on release rates of gentamicin from collagen matrices*, J Pharm Research, 12 (8) (1995), pp. 1205 – 1210.

[138] J. E. SOUSA, P. W. SERRUYS, AND M. A. COSTA, *New frontiers in cardiology, drug-eluting stents: Part I*, Circulation, 107 (2003), pp. 2274 – 2279.

[139] ——, *New frontiers in cardiology, drug-eluting stents: Part II*, Circulation, 107 (2003), pp. 2382 – 2389.

[140] C. STARBUCK AND D. A. LAUFFENBURGER, *Mathematical model for the effects of epidermal growth factor receptor trafficking dynamics on fibroblast proliferation responses*, Biotechnol Prog, 2 (1992), pp. 132 – 143.

[141] T. TA AND T. PORTER, *Thermosensitive liposomes for localised delivery and triggered release of chemotherapy*, J Control Release, 169 (1-2) (2013), pp. 112–125.

[142] A. TZAFRIRI, A. GROOTHUIS, G. S. PRICE, AND E. EDELMAN, *Stent elution rate determines drug deposition and receptor-mediated effects*, J Control Release, 161 (2012), pp. 918 – 926.

[143] A. R. TZAFRIRI AND E. R. EDELMAN, *Endosomal receptor kinetics determine the stability of intracellular growth factor signalling complexes*, Biochem, 402 (2007), pp. 537 – 549.

[144] A. R. TZAFRIRI, A. D. LEVIN, AND E. R. EDELMAN, *Diffusion-limited binding explains binary dose response for local arterial and tumour drug delivery*, Cell Prolif, 42 (3) (2009), pp. 348 – 363.

[145] P. VAUPEL, F. KALLINOWSKI, AND P. OKUNIEFF, *Blood flow, oxygen and nutrient supply, and metabolic microenvironment of human tumors: a review*, Cancer Res., 49 (1989), pp. 6449 – 6465.

[146] X. T. WANG, S. S. VENKATRAMAN, F. Y. C. BOEY, J. S. C. LOO, AND L. P. TAN, *Controlled release of sirolimus from a multilayered PLGA stent matrix*, Biomaterials, 27 (2006), pp. 5588 – 5595.

[147] J. M. WEILER, E. M. SPARROW, AND R. RAMAZANI, *Mass transfer by advection and diffusion from a drug-eluting stent*, Int J Heat Mass Trans, 55 (2012), pp. 1 – 7.

[148] J. WEINSTEIN, R. MAGIN, M. YATVIN, AND D. ZAHARKO, *Liposomes and local hyperthermia: selective delivery of methotrexate to heated tumors*, Science, 204 (1979), pp. 188 – 191.

[149] M. B. WOLF, P. D. WATSON, AND D. R. C. SCOTT, *integral-mass balance method for determination of solvent drag reflection coefficient*, Amer J Physiol, 253 (1) (1987), pp. H194 – H204.

[150] T. C. WOODS AND A. R. MARKS, *Drug-eluting stents*, Annu Rev Med, 55 (2004), pp. 169 – 178.

[151] N. Z. WU, D. DA, T. L. RUDOLL, D. NEEDHAM, A. R. WHORTON, AND M. W. DEWHIRST, *Increased microvascular permeability contributes to preferential accumulation of stealth liposomes in tumor tissue*, Cancer Research, 53 (16) (1993), pp. 3765 – 3770.

[152] N. Z. WU, B. KLITZMAN, G. ROSNER, D. NEEDHAM, AND M. W. DEWHIRST, *Measurement of material extravasation in microvascular networks using fluorescence video-microscopy,âĂİ*, Microvas Research, 46 (2) (1993), pp. 231 – 253.

[153] T. XI, R. GAO, B. XU, L. CHEN, T. LUO, J. LIU, Y. WEI, AND S. ZHONG, *In vitro and in vivo changes to PLGA / sirolimus coating on drug eluting stents*, Biomaterials, 31 (2010), pp. 5151 – 5158.

[154] M. YATVIN, J. WEINSTEIN, W. DENNIS, AND R. BLUMENTHAL, *Design of liposomes for enhanced local release of drugs by hyperthermia*, Science, 202 (1978), pp. 1290 – 1293.

[155] F. YUAN, M. LEUNIG, S. K. HUANG, D. A. BERK, D. PAPAHAD-JOPOULOS, AND R. K. JAIN, *Microvascular permeability and interstitial penetration of sterically stabilized (stealth) liposomes in a human tumor xenograft*, Cancer Research, 54 (13) (1994), pp. 3352 – 3356.

[156] W. ZHAN AND X. XU, *A mathematical model for thermosensitive liposomal delivery of doxorubicin to solid tumour*, J Drug Deliv, 2013 (2013), pp. 1 – 13.

[157] X. ZHU AND R. D. BRAATZ, *Modeling and analysis of drug-eluting stents with biodegradable PLGA coating: consequences on intravascular drug delivery*, J Biomech Eng, 136 (11) (2014), pp. 111004 – 1 – 111004 – 10.

[158] ——, *A mechanistic model of drug release in PLGA biodegradable stent coatings coupled with polymer degradation and erosion*, J Biomed Mater Res Part A, 103A (2015), pp. 2269 – 2279.

[159] S. H. ZIGMOND, *Consequences of chemotactic peptide receptor modulation for leukocyte orientation*, J Cell Biol, 88 (1981), pp. 644 – 647.

BIODATA

If you call failures experiments, you can put them in your resume and claim them as achievements.

Mason Cooley

Recent Past Status

Senior Research Fellow of Department of Mathematics, Indian Institute of Technology Guwahati, Guwahati 781039, India.

Current Status

July 25, 2018 - till date: Assistant Professor, Faculty of Science and Technology at the ICFAI University Tripura, Agartala 799210, India.

Education

- 2011–2013: **Master of Science** (Mathematics and Computing)
  Indian School Of Mines (IIT (ISM) Dhanbad), Dhanbad, Jharkhand, India.
- 2008–2011: **Bachelor of Science** (Honours in Mathematics)
  M. U. C Women's College, The University of Burdwan, Burdwan, West Bengal, India

List of Publications

1. **Koyel Chakravarty** and D.C. Dalal. **A two-phase model of drug release from microparticle with combined effects of solubilisation and recrystallisation.** *Mathematical Biosciences*, 272 (2016) 24–33.
2. **Koyel Chakravarty** and D.C. Dalal. **A two-layer mathematical modelling of drug delivery to biological tissues.** *Journal of Physics: Conference Series*, 759 (2016) 012023.
3. **Koyel Chakravarty** and D.C. Dalal. **An analytical study of drug release to biological tissues through endocytosis.** *Int. J. Dynam. Control*, 6 (2018) 167–178.

4. **Koyel Chakravarty** and D.C. Dalal. **An analytical study of drug release kinetics from a degradable polymeric matrix.** *Int. J. Biomath*, 11 (1) (2018) 1850011 (23 pages).

5. **Koyel Chakravarty** and D.C. Dalal. **A Nonlinear Mathematical Model of Drug Delivery from Polymeric Matrix** *Bulletin of Mathematical Biology*, https://doi.org/10.1007/s11538-018-0519-y (2018).

6. **Koyel Chakravarty** and D.C. Dalal. **Mathematical modelling of liposomal drug release to tumour** *Mathematical Biosciences*, 306 (2018) 82–96.

List of Communicated Articles

1. **Koyel Chakravarty** and D.C. Dalal. **Stability analysis of drug dynamics model: A mathematical approach**.

Conferences / Workshops Attended

1. December 2-5, 2015: XXVII IUPAP Conference on Computational Physics CCP 2015, IIT Guwahati, Guwahati, Assam, India. **Poster presented: A Two-Layer Mathematical Modelling of Drug Delivery to Biological Tissues.**

2. February 19-20, 2016: NBHM Regional Workshop On Research And Opportunities, *Indian Women & Mathematics*, IIT Guwahati, Guwahati, Assam, India. **Poster presented: Pharmacokinetic Mathematical Modelling.**

3. July 10-12, 2016: International Conference on Recent Advances in Mathematics and Their Applications ICRAMTA-2016, Dept. of Mathematics, University of Rajasthan, Jaipur, India. **Talk on: Mathematical Modelling of Drug Release: Polymer Degradation to Drug Transport.**

4. October 5-7, 2017: World Congress on Pharmaceutical Sciences (WCPS), Goa, India. **Talk on: Mathematical Modelling of Polymeric Drug Delivery.**

5. December 4-6, 2017: 5th International Conference on Complex Dynamical Systems and Applications (CDSA 2017), IIT Guwahati, Guwahati 781039, India. **Poster presented: Mathematical Modeling of Liposomal Drug Delivery.**

INDEX